# Microbial diversity and biogeochemical processes in the Deilmann tailings management facility, Key Lake, Saskatchewan

A Thesis Submitted to the College of Graduate Studies and Research in Partial Fulfillment of the Requirements for the Degree of Doctor of Philosophy in Applied Microbiology in the Department of Food and Bioproduct Sciences, University of Saskatchewan, Saskatoon.

**By**

**VIORICA FLORICA BONDICI**

© Copyright Viorica F Bondici, August, 2015

All rights reserved

**PERMISSION TO USE**

In presenting this thesis in partial fulfillment of the requirements for a Postgraduate degree from the University of Saskatchewan, I agree that the Libraries of this University may make it freely available for inspection. I further agree that permission for copying of this thesis in any manner, in whole or in part, for scholarly purposes may be granted by the professor or professors who supervised my thesis work or, in their absence, by the Head of the Department or the Dean of the College in which my thesis work was done. It is understood that any copying or publication or use of this thesis or parts thereof for financial gain shall not be allowed without my written permission. It is also understood that due recognition shall be given to me and to the University of Saskatchewan in any scholarly use which may be made of any material in my thesis.

Requests for permission to copy or to make other use of material in this thesis in whole or part should be addressed to:

Head of the Department of Food and Bioproduct Sciences

University of Saskatchewan

Saskatoon, Saskatchewan, S7N 5A8

Canada

**ABSTRACT**

The Deilmann Tailings Management Facility (DTMF) at Key Lake in northern Saskatchewan, Canada, is an active deposition site for uranium tailings and it has been in operation since 1996. In terms of geochemical stability of the tailings, a ferrihydrite secondary phase is utilized for the sequestration of contaminants, such as As, Ni, Mo, and Se, under alkaline and highly oxic conditions. Arsenic is highly abundant in the DTMF tailings and the principal environmental concern is the possibility for leaching of ferrihydrite-attached As into the surrounding environment. Microorganisms can proliferate in a broad range of habitats and their activities are key factors in determining fate and transport of contaminants in various environments.

This thesis attempts to obtain insights into the biogeochemical processes that may occur during the early phase of the DTMF's history that could potentially become significant over extended periods of time that run from 100's to 1000's of years. Hence, a primary focus was to characterize microbial diversity and extrapolate their potential functional roles as well as their potential to chemically alter the Eh and ferrihydrite, which are the primary controlling conditions within the DTMF tailings and in the mineral secondary phase, respectively. To achieve these goals, two molecular techniques (clone library construction and Ion Torrent sequencing), a range of conventional culture-based techniques, metabolic assays addressing metabolic transformation and resistance to metals/metalloids, microscopic technique (Confocal Laser Scanning Microscope), spectroscopic analyses (Scanning Transmission X-ray Microscope) and bench-scale microcosm assays were carried out.

Culture-dependent and -independent methods revealed that the most prevalent microbial groups in the water column, tailings mass and at the tailings-water interface affiliated into phyla (e.g., *Proteobacteria*, *Actinobacteria, Firmicutes* and *Bacteriodetes)* that have previously been detected at uranium-, heavy metal- and complex hydrocarbon-contaminated sites. Phylotypes closely related to well-characterized sulfate-, thiosulfate- and iron-reducing bacteria (e.g., *Desulfosporosinus*, *Dethiobacter*, *Geoalkalibacter*, *Ralstonia*, *Georgfuchsia*) were also detected at low frequency, with the exception of the tailings-water interface where sequences closely related to *Desulfosporosinus* were abundant. The readily culturable heterotrophs (e.g., *Pseudomonas*, *Arthrobacter*, *Massilia*, *Hydrogenophaga*, *Polaromonas*, *Bacillus*) retrieved from the tailings exhibited reducing/oxidizing capabilities as well as high tolerance to metal/metalloids. Bench scale microcosm assays showed that heterotrophs native to the DTMF site could not only reduce ferrihydrite but could also create highly reducing (< -300 mV) conditions within the tailings amenable to strict anaerobic bacteria such as *Desulfosporosinus.* STXM image analyses confirmed the presence of reduced iron in close proximity to bacterial cells in biofilm grown *in situ* and in microcosm tailings, strongly suggesting that ferrihydrite served as electron acceptor during microbial processes. Reduced iron detected *in situ* also indicated that microscale iron reduction could occur even though macroscale DTMF chemistry remained oxidizing.

Overall, the nature of microbial community present in the DMTF system strongly indicated that complex hydrocarbons (e.g., kerosene) discharged into the tailings during processing could potentially support microbial processes that involve Fe and S cycling and that this process could become significant over extended period of times, contributing to arsenic escape into the environment.

**AKNOWLEDGEMENTS**

Pursuing Ph.D. has its enjoyable and challenging moments. It is like climbing a high mountain peak, some sections of the route are easy and some are hard. My journey to the final destination was accompanied with enjoyment, moments of satisfaction, hardship and sometimes frustration. I would like to express my gratitude and say many thanks to those who were there for me, who provided guidance and coached me to get to my final destination.

First of all, I would like to thank my supervisors, Drs. Darren Korber and John Lawrence, who guided me and built confidence over the years. Dr. Korber, I would like to thank you for giving me this opportunity, providing me a stimulating environment where I could grow, being available anytime for discussions, being patient and supportive. You and Dr. Lawrence, taught me science, shared ideas, assisted me to find solutions to problems and guided me to see the big picture. I was always inspired with your knowledge and experience. Your impact has been powerful by helping me to become a scientist.

I wish to thank my advisory committee members Dr. Janet Hill, Dr. Vladimir Vujanovic and Dr. Xiao Qiu. I wish to extend my special thanks to Dr. Janet Hill for her valuable assistance and help with my research project. I would like to thank Dr. Robert Tyler and Dr. George Khachatourians (past Chair) who served as the graduate chairs during my research program. I appreciate Dr. Gideon Wolfaardt for his valuable suggestions and comments throughout my research.

I would like to thank George Swerhone for all the help and technical assistance. You were always ready to help me and highly supportive. I greately appreciate Dr. Jay Dynes for his help with the synchrotron data acquisition and analyses. Many thanks to my colleagues and friends Prabha, Tara, Huda, Maria, Sasha, Natasha, Daphne and Jeff, you all created a memorable atmosphere in the lab. I truly appreciate those times talking about technical failure /success, plans, values, or goals.

I am very grateful to my brother, Alex Bondici, your encouragement and constant support have been my strength. Your ambition and persistence have always been a true example to me. I would like to thank my partner, Jason Benderski, who was very understanding and supportive at the end of this journey.

Last but not least, I would like to thank my parents for the many sacrifices they made for me. Your untiring support always strengthened my dedication to academia. To my regret my father did not live to share this moment with me, but I know he would have been very proud of me.

This thesis is dedicated to

***The memory of my father***

**TABLE OF CONTENTS**

**LIST OF TABLES**

**LIST OF FIGURES**

## LIST OF ABREVIATIONS

| | |
|---|---|
| **BLAST** | Basic Local Alignment Tool |
| **CLS** | Canadian Light Source |
| **CLSM** | Confocal Laser Scanning Microscopy |
| **DGGE** | Denaturing Gradient Gel Electrophoresis |
| **DO** | Dissolved Oxygen |
| **DTMF** | Deilmann Tailings Management Facility |
| **EDX** | Energy Dispersive X-ray Spectroscopy (EDX) |
| **EMBL** | European Molecular Biology Laboratory |
| **LINAC** | Linear Accelerator |
| **MID** | Multiplex Identifier |
| **MPN** | Most Probable Number |
| **NARMS** | National Antimicrobial Resistance Monitoring System |
| **NEXAFS** | Near-edge X-ray Absorption Fine Structure |
| **NGS** | Next Generation Sequencing |
| **ORP** | Oxidation Reduction Potential |
| **PCR** | Polymerase Chain Reaction |
| **PGM** | Personal Genome Machine |
| **RDP** | Ribosomal Database Project |
| **SEM** | Scanning Electron Microscopy |
| **SPSS** | Statistical Package for the Social Science |
| **SRB** | Sulfate Reducing Bacteria |
| **STXM** | Scanning Transmission Microscopy |
| **T-RFLP** | Terminal Restriction Fragment Length Polymorphism |
| **TDS** | Total Dissolved Solids |
| **UMT** | Uranium mill tailings |
| **XANES** | X-ray Absorption Near-edge Structure |

# 1 INTRODUCTION AND LITERATURE REVIEW

## 1.1 Uranium mill tailings (UMT) and deposition sites

Uranium mill tailings are low activity radioactive waste generated in high volume from ore mining and milling (Landa *et al*. 2004). Uranium mining has generated an estimated volume of one billion tons of tailings from more than 4000 mines worldwide (IAEA, 2004). The history of uranium mining can be divided into two main time periods, the so called "uranium rush" periods, that were dictated by different uses of uranium (IAEA, 2004). The first rush occurred during the mid-1940s to mid-1960s at which time uranium was mined to ensure feedstock uranium for the development of military nuclear weapons; however, in the mid-1970s, concerns over the oil supply for the World's energy needs and the proposed use of nuclear power led to a second rush period (IAEA, 2004). Indeed, each of these booms was followed by an increase of uranium prices and extensive exploitation of uranium resources to meet the high demand. However, these periods resulted in a legacy of thousands of abandoned mines and millions of tons of UMT waste (IAEA, 2004; Fettus and McKinzie, 2012).

Today, UMT wastes are deposited into tailings management facilities (e.g., mined-out pits) to ensure long-term containment; however, this wasn't always the practice (Natural Resources Canada, 2012). Before 1950, UMT was not considered a hazardous and problematic waste (Waggitt, 1994). There was only a gradual realization of the risk levels associated with uranium mining during the uranium rush periods. Initially, the focus was on workers' health and safety, especially those persons who were in immediate contact with the ore and processing streams. This was a driving force to improve safety practices; however, only in recent times have concerns arisen regarding the impacts of UMT on public health and the surrounding natural environment (IAEA, 2004). For example, in the United States legal and regulatory frameworks

to address the impacts of uranium mining were only initiated in the late 1970s. Consequently, the relatively late regulations and ineffective controls have left behind damaged and contaminated environments posing risks to human health (Fettus and McKinzie, 2012).

Uranium mill tailings are an environmental concern mainly because this waste is radioactive, contains a wide range of toxic contaminants, can produce acid mine drainage, and is leachable and erodible under various conditions (IAEA, 2004). Past practices for UMT disposal included the following: no containment, topographic depressions, custom-built ring-dykes, underground mines, low embankments, mined-out pits, valleys, and deep lakes or rivers (IAEA, 2004). Contaminants or hazardous elements can slowly be released from deposition sites over long periods of time or in large amounts over short periods of time. Contamination of surrounding areas by UMT has been continuously detected (IAEA, 1997). Slow release of contaminants into subsurface sediments and groundwater may occur through seepage from unlined tailings impoundments (Frost, 1998). This type of release may also occur through erosion of the dry form of UMT in uncovered tailings resulting in contaminant transport by wind (Sevcik, 2003). Release of large quantities of contaminants may also occur during accidental dam failure (IAEA, 1997). A recent catastrophic dam failure occurred in 2014, where approximately 10 billion litres of wastewater and 5 billion kilogram of tailings waste escaped into the environment at the Imperial Metals' Mount Polley mine waste management site, British Columbia, Canada (MiningWatch Canada, 2014).

The continuous detection of contaminants associated with UMT in aquatic and soil systems have been the source of much environmental concern (Pyle *et al*. 2002; Akob *et al*., 2007). The potentially adverse effects of UMT required attempts to improve tailings management practices to such an extent that uranium tailings should be isolated from the

environment for indefinite periods, on the order of thousands of years (Frost, 1998; IAEA, 2004). This involves a number of engineering steps and processes at multiple levels, such as containment, tailings preparation, dewatering, surface treatment, decant water treatment, seepage control, and application of coverings (IAEA, 2004). Containment involves implementation of liners to prevent groundwater inflow and tailings pore-water escape (IAEA, 2004). Since some radioactive elements have a long half-life the use of synthetic linings alone has proven to be only a temporary solution to prevent contaminant migration. In contrast, the employment of natural geologically impervious barriers for the retention of heavy metals is preferred (Al-Hashimi *et al*., 1995). Once uranium is extracted from the acidic solution the tailings are neutralized taking into consideration the wide solubility spectra (e.g., stability increase with alkalinity) of the associated contaminants prior to disposal (IAEA, 2004; Gomez *et al*., 2013). Addition of chemical binders (e.g., cement) to the tailings is also practiced to significantly reduce permeability. To consolidate tailings material and reduce seepage into the groundwater, dewatering is widely used either before the tailings are discharged or in waste deposition sites using under-drainage or evaporation techniques (IAEA, 2004). Before the final covering, the UMT are deposited subaqueously or stabilized with chemical agents to prevent dust generation and transportation of contaminants (IAEA, 2004). After decommissioning, soil capping is a common practice for containment (Gavrilescu *et al*., 2009).

### 1.1.1 Elements associated with uranium tailings

In general, the composition of tailings is highly dependent on the composition of the ore and the extraction process utilized. The extraction of uranium from ores generally involves grinding, chemical processing to dissolve the uranium, followed by several washing and purification steps. Uranium operations mainly employ sulphuric acid ($H_2SO_4$) as the leaching

agent, except in the case of high carbonate-content ores, which are preferably leached with $Na_2CO_3$. For *in situ* uranium extraction, ferric iron solutions are generally used (Abdelouas, 2006). Once uranium is extracted, the raffinate solution (see below), which contains contaminants that were solubilized along with uranium during the leaching process, is neutralised and mixed with ground rock, forming the UMT waste (Abdelouas, 2006).

During the leaching process various elements of concern are liberated from the ore, including As, Ni, $U^{235/238}$, Mo, Fe, Mg, V, Ba, Cr, $Ra^{226}$, $Po^{210}$, and $Th^{230}$ (Donahue, 2000; Martin *et al*., 2003). In general, the chemical composition of the tailings corresponds with the mineralogy of the ore (Abdelouas, 2006). Therefore, the composition of ores from different geographical locations may vary determining the most abundant elements of concern present in the UMT (Abdelouas, 2006). For example, the As concentration in the tailings deposited at Rabbit Lake, Canada, is higher, reaching 5640 μg/g (Donahue, 2000) in comparison to the As (120.6 μg/g) content in the UMTs deposited at Ecarpiere, France (Somot *et al*., 1997).

The oxidation state, and hence, the solubility or mobility of the redox-sensitive metals in the tailings is generally governed by the pH, Eh, and buffering capacity of the environment. These factors are highly controlled during processing, neutralization and deposition. In general, there are two solid mineral phases in the tailings; primary and secondary minerals (Abdelouas, 2006). The primary mineral phases resist the leaching process and mainly include the silicate minerals, such as quartz, feldspars, and clay. The secondary phases are formed from the leached ore species and include reagents added during the neutralization process (Abdelouas, 2006).

Ferrihydrite is widespread in natural environments including, soil, clay, sediments, and water either as a partial coating on minerals or as discrete colloids (Pierce and Moore, 1981).

Ferrihydrite is formed by the hydrolysis of ferric iron under oxidizing conditions (Eggleton and Fitzpatrick, 1988; Hamzaoui *et al*., 2002). In some uranium mining operations, ferrihydrite is the dominant secondary phase mineral formed during the neutralization process (Moldovan *et al*., 2003; Shaw *et al*., 2011). Due to its high surface area and reactivity it is considered an important adsorbent of various cations and anions in natural systems (Jambor and Dutrizac, 1998). Changes in the environmental parameter, pH appears to control the absorption-desorption capacity of ferrihydrite with various metal ions (Jambor and Dutrizac, 1998).

Since ferrihydrite exhibits adsorptive ability, it may serve as a dominant sink for various elements, such as As, Se, Mo, Ni, in iron-rich uranium tailings under oxic conditions (Moldovan *et al*., 2003; Moldovan and Hendry, 2005; Shaw *et al*., 2011). The trace metal profiles of the water-tailings interface at UMT, Elliot Lake, Ontario, Canada also revealed the adsorptive ability of ferrihydrite given that As mobility was congruent with ferrihydrite redox cycling (Martin *et al*., 2003). Selective leaching trials have also shown that Fe oxidation state is an important factor in complexation with $^{226}$Ra and Ba in uranium tailings (Landa *et al*., 2001). Under reducing conditions, reductive dissolution of ferrihydrite may occur releasing adsorbed oxyanions from the surface of the ferrihydrite (Morin and Calas, 2006). Thus, positive Eh and alkaline pH are essential during metallurgical processing or in tailings management systems to maintain stable ferrihydrite, which further controls mobility of other elements forming insoluble complexes. Similarly, manganese oxyhydroxides are important secondary phases, which also can adsorb radionuclides, metals and metalloids, and in particular, arsenic (Chao and Theobald, 1976).

Hydrotalcites are secondary phase minerals that consist of di- and trivalent metals and an interlayer anion. These compounds exhibit high adsorption capacity for elements of concern associated with uranium tailings (Gomez *et al*., 2013; Gomez *et al*., 2014). Primary phase

minerals can also act as sinks for contaminants. For example, clay minerals can retain Ba and Sr cations. However, abundant clay within the tailings prevents the formation of insoluble alkaline earth sulphates and $Ra^{226}$ co-precipitation as $Ba(Ra)SO_4$, leading to an increase of soluble $Ra^{226}$ (Lottermoser, 2007).

Overall, secondary mineral phases, such as ferrihydrite, manganese oxyhydroxides and hydrotalcites found in some uranium tailings can serve as important adsorbents of contaminants under strong oxic and alkaline conditions; therefore, processes that can affect these stablizing conditions are of great interest.

### 1.1.2 Deilmann Tailings Management Facility

The Key Lake uranium milling operation is a major supplier of uranium for the global nuclear industry (Natural Resources Canada, 2004). Uranium production at this milling operation commenced in 1983 and by the end of October 2009, more than 375 million pounds of uranium had been produced (Cameco, 2009). Initially, ores were obtained from Gartner and Deilmann pits but since 1999 ore from the McArthur River mine has been processed at this site (Cameco, 2009). Since the ore from the McArthur River has a very high uranium concentration, it is blended with low-grade ores and waste rock. This process generates millions of tonnes of uranium tailings, which are deposited approximately 4 km east of the milling operation in the Deilmann tailings management facility (DTMF). The DTMF is a mined-out pit, with an elongated shape 1300 m long, 600 m wide and 170 m deep. Tailings deposition commenced in 1996 in the East part of the pit and ore mining from the West part of this pit was completed in 1999 (Figure 1.1) (Cameco, 2009).

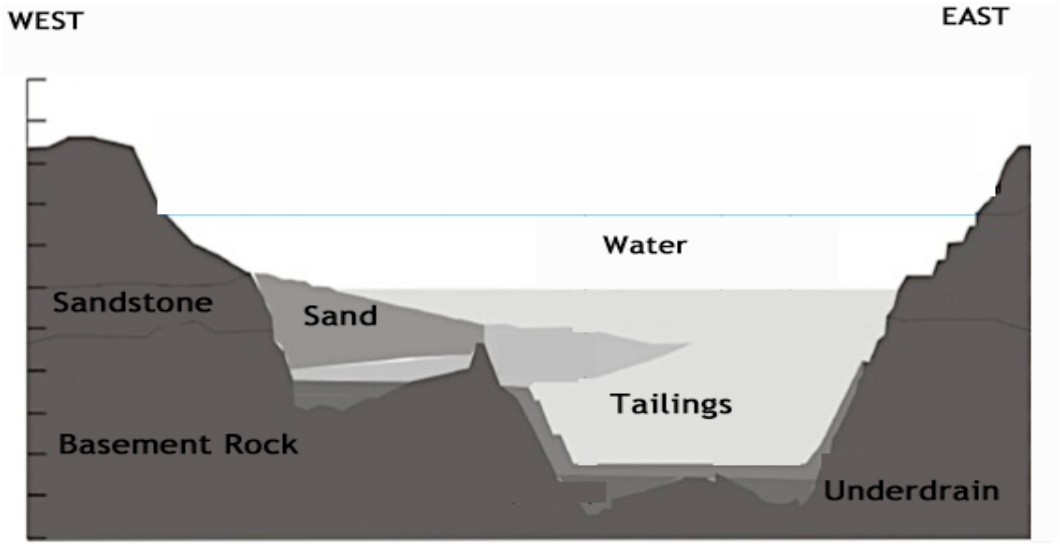


**Figure 1.1** Schematic cross section of the Deilmann tailings management facility (Shaw *et al*., 2001).

In order to isolate uranium tailings at the DTMF from the surrounding environment, geotechnical, hydrogeological and geochemical factors were taken into consideration when the facility was designed. The facility is located at the southern rim of the Athabasca Basin, which is part of a tectonically stable continental plate with low risk of seismic activity. The basement rock and sandstones of the mined-out pit serve as a natural impermeable barrier, preventing contaminant escape from the tailings (Cameco, 2010). To facilitate tailings consolidation, the base and side of the DTMF include drains to remove pore-water from the tailings and groundwater from the surrounding area, respectively (Azam *et al*., 2014). Currently, the dewatering wells around the pit ensure an inward hydraulic gradient towards the pit and direct groundwater flow (Cameco, 2010; Azam *et al*., 2014). By securing consolidation of the tailings body, it is expected that upon decommissioning, the regional groundwater will take a path around the pit, minimizing the hydraulic gradient between the tailings and groundwater (Azam *et al*., 2014). To determine consolidation behaviour of the DTMF tailings, geotechnical data from

drilling programmes conducted in 1999, 2004/2005, 2008 and 2009 have recently been analysed (Azam *et al*., 2014). It has been shown that the water content decreased within the tailings body, with a water content range 100-250% close to the tailings surface and 60-80 % at the base of the DTMF. Interestingly, a relatively low water content range (20-30%) was measured at a location where sloughed sand had intruded into the tailings depth profile. At the base of the DTMF, a sand layer serves as a drain, contributing to faster consolidation of tailings (Azam *et al*., 2014). Furthermore, as expected, a linear increase of effective stress (vertical stress minus the pore water pressure) was detected; 0 kPa at the surface of the tailings and around 600 kPa at the deepest parts of the DTMF (Azam *et al*., 2014). This indicates that, over time, the tailings have gone through a significant consolidation under its own weight.

In addition to the geotechnical and hydrogeological engineering programs, measures have also been taken to ensure geochemical stability of the tailings before deposition into the management facility. This essential process follows these steps: i) to extract U from the ore, a $H_2SO_4$ leaching process is utilized, ii) from the acid, leachate U is obtained using an organic solvent (e.g., amide) extraction method, and iii) the organics are separated by using an ammonium sulphate solution (Cameco, 2010; Shaw *et al*., 2011) producing U and a waste solution termed “raffinate”. The raffinate solution is then subjected to a series of neutralization-precipitation processes, where the pH is increased stepwise from 1.0, 3.5, 6.5 and to 9.2 (Shaw *et al*., 2011; Gomez *et al*., 2013).

From the final neutralization tank the mixture is thickened by adding flocculants (e.g., polyacrylamides) and in the final step, before discharge, the pH is increased to 10.5 using lime. During this series of treatments the contaminants are removed from the aqueous phase and are precipitated as secondary mineral phases (Shaw *et al*., 2011; Gomez *et al*., 2013). Geochemical

studies have shown that mineralogical controls in the tailings are dominated mainly by ferrihydrite and hydrotalcite mineral phases, which adsorb/co-precipitate elements of concern (EOCs) (Moldovan and Hendry, 2005; Shaw *et al*., 2011; Gomez *et al*., 2013). The tailings also contain clay, silicate gangue minerals, oxides and gypsum precipitates (Shaw *et al*., 2011). Component map image analyses have shown that gypsum nodule precipitates are surrounded by a metallic ring consisting of ferrihydrite, onto which EOCs, such as As and Ni, are adsorbed. The center of the nodule precipitate is mainly composed of gypsum/lime (Essilfie-Dughan *et al*., 2011). Large masses of Mg-Al hydrotalcite mineral phases also form during the raffinate neutralization process at pH >6.7 (Gomez *et al*., 2013). Similar to ferrihydrite, Mg-Al hydrotalcite plays a role in controlling the solubility of EOCs in the tailings. It has been suggested that during the raffinate neutralization process, ferrihydrite adsorbs the majority of the EOCs and hydrotalcites take up the remainder. Furthermore, it has been proposed that in the DTMF tailings a dual-phase (ferrihydrite-hydrotalcite) system potentially controls the EOCs under oxic conditions (Gomez *et al*., 2013).

## 1.2 Potential factors influencing microbial diversity associated with uranium-contaminated environments

Numerous studies have attempted to characterize microbial communities associated with uranium-contaminated environments using DNA sequence based analyses (Radeva and Selenska-Pobell, 2005; Michalsen *et al*., 2007). The harsh uranium extraction processes, geochemical composition and varied geographical origins contribute greatly to the generation of diverse and extreme geochemical conditions at uranium tailings-contaminated sites (Radeva and Selenska-Pobell, 2005; Michalsen *et al*., 2007; Moreels *et al*., 2008). Various studies conducted to determine microbial community composition in uranium-contaminated environments

demonstrated that bacterial diversity is most likely to be site-specific (Radeva and Selenska-Pobell, 2005). However, geochemical variables such as type, level of co-contaminants or pH associated with uranium-contaminated sites could be considered as the factors determining community composition (Michalsen *et al*., 2007).

In addition, bioremediation studies have consistently proven that microbial community composition and function are also greatly affected by environmental factors, such as availability of electron donors and acceptors (Xu *et al*., 2010). Introduction of suitable carbon sources can be used to stimulate indigenous bacteria of interest at sites co-contaminated with heavy metals, metalloids, nitrate, and radionucleotides (Moreels *et al*., 2008). This stimulatory process may initiate a conversion from a microaerophilic environment to an anoxic condition (Moreels *et al.*, 2008). Such shifts in environmental conditions would also be expected to influence resident microbial community composition as well.

### 1.3 Microbial communities associated with uranium-contaminated sites

With the advent of understanding the pivotal role of microbial activity in geochemical cycles along with the fact that these processes can have either detrimental (bioleaching) or beneficial (bioremediation) effects, investigations of microbial community composition at contaminated sites has increasingly been of interest. Numerous studies have pointed out the importance of linking microbial diversity and geochemical data of contaminated sites to identify the functional potential along with the abundance of key bacterial populations involved in bio-transformations (Fields *et al*., 2005; Gadd, 2010; Lloyd and Gadd, 2011; Cho *et al*., 2012; Williams *et al*., 2013). Furthermore, by using this approach, researchers have been able to define factors that may limit microbial community diversity and their *in situ* activity (Cho *et al*., 2012).

In general, combinations of low pH and high concentration of heavy metals, metalloids and radionuclides characterize the subsurface of uranium-contaminated sites around the world (Abdelouas, 2006; Akob *et al*., 2007). Bacterial community structural analyses of uranium-contaminated ground water from the Field Research Centre (FRC) at Oak Ridge, Tennessee, showed that bacterial diversity decreased with increasing nitrate and heavy metals concentration (Fields *et al*., 2005; Cho *et al*., 2012). Furthermore, novel sequences, at both, the genus- and species-level were recovered equally from clone libraries at these contaminated sites (Fields *et al*., 2005). Relatively high concentrations of contaminants in uranium-contaminated groundwater at the Oak Ridge FRC site apparently selected for bacterial species capable of using various electron acceptors, such as uranium (*Shewanella* and *Pseudomonas*), nitrate (*Pseudomonas*, *Rhodanobacter* and *Xanthomonas*) and iron (*Stenotrophomonas*) (Cho *et al*., 2012). Similarly, bacterial lineages adapted to low-nutrient, nitrate reduction and metal resistance, including as *Sphingomonas*, *Acidovorax*, *Acinetobacter*, *Alcaligenes*, and *Ralstonia*, were detected in Oak Ridge FRC uranium-contaminated subsurface sediments (Akob *et al*., 2007). Studies have shown that members of the *Ralstonia* group tend to be resistant to metals; for example, Cu, Ni, Cd, Zn, and were also able to reduce Fe (III) (Mergeay *et al*., 2003; Lin *et al*., 2007).

Since the discovery that microbial reduction of highly soluble U (VI) to the less soluble U (IV) was a promising bioremediation strategy, several bacterial species with U-reducing capabilities have been recovered and documented at uranium-contaminated sites (Lovley *et al*., 1991; Lloyd and Gadd, 2011; Williams *et al*., 2013). The rationale of this process is to promote the growth and activity of indigenous microorganisms which are capable of reducing U (VI) to U (IV) by adding organic electron donors (Holmes *et al*., 2002; Vrionis *et al*., 2005; Radeva and Selenska-Pobell, 2005; Suzuki and Suko, 2006; Akob *et al*., 2007). In order to design an

appropriate uranium bioremediation strategy, molecular techniques are applied to characterize and obtain phylogenetic profiles of uranium-contaminated subsurface communities (Holmes *et al*., 2002; Vrionis *et al*., 2005). Most of these bacteria are anaerobes and able to utilize other elements as electron acceptors, most notably Fe (III), which is one of the most abundant elements in subsurface settings (Lovley *et al*., 2011; Williams *et al*., 2013) and in uranium tailings (Abdelouas, 2006). At uranium waste management sites where the ferrihydrite mineral phase serves as adsorbent of contaminants the presence of a microbial community with iron reducing potential can be considered as a great concern.

Microorganisms from different physiological groups are capable of dissimilatory reduction of radionuclides; for example, mesophilic iron-reducing, mesophilic sulphate-reducing and fermentative bacteria, as well as alkaliphilic and acidotolerant microorganisms (Mohapatra *et al*., 2010). Specific members of these groups include *Shewanella putrefaciens*, *Geobacter metallireducens*, *Desulfovibrio desulfuricans*, *Desulfotomaculum reducens*, and *Clostridium spp.* (Lovley and Phillips, 1991; Elias *et al*., 2003; Petrie *et al*., 2003; Suzuki and Suko, 2006). Recently, other uranium-reducing bacteria, such as *Pseudomonas spp*., *Pantoea* sp., and *Enterobacter spp*., have been isolated from uranium mine sites (Chabalala and Chirwa, 2010; Williams *et al*., 2013).

Selective pressures are considered to effectively reduce microbial diversity; however, the surviving taxa associated with uranium-contaminated complexes exhibit considerable adaptive properties. This was demonstrated in a biofilm study carried out using water samples taken from the highly alkaline overlying water body of the uranium tailings management site at Rabbit Lake, Canada (Wolfaardt *et al*., 2008). Even though the pH varied between 7 and 10 in the flow cell system, little change was detected in microorganism survival (Wolfaardt *et al*., 2008).

Microorganisms cultivated from the Field Research Centre acidic subsurface sediments were closely related to *Anaeromyxobacter*, *Paenibacillus*, *Brevibacillus*, as well as spore-forming bacterial groups, further indicates that the extreme conditions associated with uranium waste sites select for microorganisms that can survive and proliferate in this type of environment (Petrie *et al*., 2003). In a column experiment where uranium contaminated sediment was subjected to a carbon source, phylogenetic analysis revealed that the microbial community changed from heavy metal-sensitive to metal-resistant nitrate and sulphate reducing microorganisms (Moreels *et al*., 2008). It is important to note that the presence of heavy metal resistance genes and horizontal gene transfer within the endogenous microbial population could be considered critical for this occurrence (Moreels *et al*., 2008).

### 1.4 Biogeochemical redox processes

Microorganisms can influence the redox state of elements, hence their mobility, toxicity or bioavailability via the oxidation of labile organic carbon or inorganic compounds coupled to the reduction of electron acceptors, including humic substances, iron-bearing minerals, transition metals, metalloids, and actinides (Borch *et al*., 2010). Throughout the Earth's history, biogeochemical processes have contributed to a global redox gradient where the surface environment is oxidizing and the subsurface environment is rich in reduced biogenic products, such as organic matter, sulphide minerals and methane (Borch *et al*., 2010). Dynamic redox gradients can also occur in time and space dependent upon the chemical composition, the potential of redox couples and the microbial-activity present at that particular site (Borch *et al*., 2010). The fact that microbial-activity is dictated by a redox ladder in aquifers was first proposed by Champ *et al*. (1979). Oxidation potential measurements at Chalk River suggested that the groundwater flows through multiple redox zones progressing towards a less energetically

favourable zone, where electron transfer yields less energy. As expected, mobility and concentration of the multivalent metals and metalloids would also vary in each zone (Champ *et al.,* 1979). Similarly, a thermodynamic redox ladder operates in other subsurface settings, such as marine sediments, soil (Bethke *et al*., 2011) or potentially in tailings environments.

In subsurface environments, microbial energy sources are organic matter or reduced compounds (Mn (II), Fe (II), ammonia or sulphide) and the predominant electron acceptors are, in order from most oxidized to most reduced, $O_2$, $NO_3^-$, Mn (IV), Fe (III), $SO_4^{-2}$ and $CO_2$ (Lovley and Chapelle, 1995). Oxygen has the highest electron affinity, and thus microbial metabolism coupled with the reduction of $O_2$ will yield the most energy for microbial growth. An anaerobic respiration that is similar to aerobic metabolism is denitrification where nitrate is used as an electron acceptor (Lovley and Chapelle, 1995). Some nitrate reducing bacteria, such as *Paracoccus denitrificans*, exhibit respiratory flexibility, modulating expression of different terminal oxido-reductases in the presence of various $O_2$ tensions and are able to switch to $NO_3^-$ when $O_2$ is absent (Richardson, 2000). Once $O_2$/$NO_3^-$ are depleted from a system, and if Fe (III) is available, Fe (III)-reducing microorganisms will proliferate (Lovley and Chapelle, 1995). As initially suggested by Champ *et al*. (1979), specific microbial processes within distinct redox zones are determined by potential thermodynamic yields; however, other factors such as physiological controls on microbial metabolism and competition for electron acceptors also contribute to the specific bacterial activity distribution (Lovley and Chapelle, 1995). Furthermore, in terms of phase formation, many can be well explained based on thermodynamics, however, some are the result of kinetic pathways of biotic origin (Zachara *et al*., 2002). For example, biogenic Fe (II) supply can modify the predicted iron phase purely based on the thermodynamic stability of a system at a given time point.

### 1.4.1 Phase transformation of iron(hydr)oxides

Iron minerals are ubiquitous in soils and sediments and play an important role in the geochemistry of surface and subsurface environments (Stumm and Sulzberger, 1991; Borch *et al*., 2010; Pallud *et al*., 2010). The importance of the Fe (II)-Fe (III) redox pair in global geochemical cycling of elements was well underlined in an earlier study (Stumm and Sulzberger, 1991) and has the following features: i) a relatively high proportion ($3.5 \times 10^{12}$ moles)/year of Fe of the total amount ($17 \times 10^{20}$ moles) found in sedimentary rocks go through redox change from oxidized to reduced and vice versa. In order for iron species to become oxidized or reduced, the iron cycle must be linked to other reductant and oxidant electron transfer mediators; ii) iron oxide, oxyhydroxide and hydroxide phases (collectively called iron(hydr)oxides) due to their relatively large specific surface area and chemical reactivity are considered as potent sorbants and repositories for other chemical species. This adsorption potential contributes to the interdependence of the iron cycle with the redox cycle of other elements such as, heavy metals, metalloids and oxyanions (Stumm and Sulzberger, 1991).

There is a wide range of iron(hydr)oxide secondary minerals with different crystallinities and reactivities that exist in natural environments. Goethite and hematite secondary phases are the dominant form of iron(hydr)oxide in solids and sediments on a total mass basis (Schwertmann and Taylor, 1989). Ferrihydrite, although a short-lived phase, is considered to be the most bioavailable iron-phase for bacterial reduction, hence, having a profound impact on metal biogeochemical cycling (Lovley *et al*., 1991). In general, the process of dissimilatory iron reduction solubilizes poorly crystalline iron(hydr)oxides to $Fe(II)_{aq}$ or converts them to Fe (II)-containing secondary phases (Zachara *et al*., 2002). Ferrihydrites are considered an intermediate structural phase between amorphous and partly crystalline forms (Zachara *et al*., 2002).

Under oxidizing conditions, ferrihydrites are thermodynamically unstable in comparison to the secondary crystalline iron(hydr)oxides. There are several factors, such as pH, presence of inorganic/organic ionic species and temperature that control the rate and extent of phase transformation. Since ferrihydrites are thermodynamically unstable, they go through phase transformation, primarily to goethite and hematite, during the aging process at constant room temperature (Zachara *et al*., 2002). It has previously been shown that pH has a significant effect on the formation of goethite and hematite from ferrihydrite, where the proportion and crystallinity of these phases varies with pH (Shwertmann and Murad, 1983; Jambor and Dutrizac, 1998). It was shown that hematite preferentially forms at pH 7 and 8, whereas the maximum goethite formation occurs at pH 4 and pH 12. Furthermore, the two secondary phases are formed through two competitive processes, the goethite crystal is formed from dissolved monovalent Fe (III) ions generated through ferrihydrite dissolution, and hematite from internal dehydration and rearrangement. Hence, goethite would form when the concentration of Fe (III) ion, which is in equilibrium with ferrihydrite, increases, whereas hematite would be favoured as the concentration of Fe (III) ion decreases (Shwertmann and Murad, 1983).

Adsorption and co-precipitation with silica, organic matter, trace metal cations or metalloids delay the crystallization process of ferrihydite to goethite and hematite (Jambor and Dutrizac, 1998; Zachara *et al*., 2002). The crystallinity of ferrihydrite determines the ability of effective adsorption of elements (e.g., arsenic); therefore, the least-crystalline 2-line ferrihydrite has a higher sorption affinity than the 6-line ferrihydrite (Swash and Monhemius, 1995). Each exhibits different X-ray diffraction pattern, the least crystalline 2-line ferrihydrite has two peaks in the other hand the more crystalline 6-line ferrihydrite has 6 broad peaks (Kukkadapu *et al*., 2003). Adsorption of elements onto ferrihydrite occurs commonly through a co-precipitation

process, because it blocks crystallization itself, ensuring the existence of specific surface areas on ferrihydrite (Waychunas *et al*., 1993).

The primary driving force for phase transformation under anaerobic conditions is the thermodynamic instability of ferrihydrites, the same as under aerobic conditions. Reductive transformation of ferrihydrite strongly depends on the concentration of Fe $(II)_{aq}$ and similar phases that form under both biotic and abiotic conditions (Zachara *et al*., 2002). Basically, the microbial reduction of ferrihydrite is a coupled biotic-abiotic process, where dissimilatory Fe-reducing bacteria serve as Fe (II) supplier and Fe (II) further catalyzes reductive dissolution of ferrihydrite and subsequently, crystallization (Hansel *et al*., 2003; Pallud *et al*., 2010). Reaction of Fe (II) with ferrihydrites yields more thermodynamically stable phases, such as goethite (α-FeOOH), lepidocrocite (γ-FeOOH), and magnetite ($Fe^{III}Fe^{II}O_4$) (Zachara *et al*., 2002; Hansel *et al*., 2003; Borch *et al*., 2007).

Formation of these mineral phases primarily depends on the Fe (II) concentration, electron donor/ferrihydrite ratio and the presence of complexing ligands (e.g., organic material) (Zachara *et al*., 2002; Hansel *et al*., 2003). In a biotic column experiment it was shown that both phases, goethite and magnetite, would form if the produced Fe (II) concentrations were greater than 0.5 mmol Fe(II)/g ferrihydrite; however, at lower concentrations only the goethite phase transformation would occur (Hansel *et al*., 2003). Similarly, when the concentration of electron donor/ferrihydrite is relatively high, which is related to increased iron reducing bacteria activity and Fe (II), ferrihydrite is bio-transformed to magnetite (Zachara *et al*., 2002). Despite the fact that defined chemical conditions determine the phase type to be formed, in the natural environments there are mixtures of products. Microenvironments with chemical gradients may contribute to simultaneous formation of different phases (Zachara *et al*., 2002).

### 1.4.2 Arsenic mobilization

Since solubility, mobility, bioavailability and toxicity of arsenic depend on its oxidation state, there have been numerous studies carried out on As speciation and behaviour under various conditions and in the presence of different mineral phases (Masscheleyn *et al*., 1991; Burnol *et al*., 2007; Erbs *et al*., 2010; Muehe *et al*., 2013). The two major oxidation states of arsenic found in natural environments are trivalent arsenite (As(III)) and pentavalent arsenate (As(V)). Both exhibit different sorption and toxicity properties, where the reduced form is considered potentially more mobile and toxic (Masscheleyn *et al*., 1991; Smedley and Kinniburgh, 2002; Chatain *et al*., 2005). Their redox state can be changed chemically or due to bacterial activity (Masscheleyn *et al*., 1991). A microbially mediated methylated form of arsenic has also been reported to occur in environmental settings (Brannon, 1987; Masscheleyn *et al*., 1991).

Arsenic speciation, transformation and solubility are greatly influenced by redox potential and pH in subsurface environments (Masscheleyn *et al*., 1991). The predicted effects of these chemical parameters are illustrated in Figure 1.2 adapted from Masscheleyn *et al*. (1991). As the Eh-pH diagram indicates that there are four thermodynamically dominant arsenic species: $H_2AsO_4^-$, $HAsO_4^{2-}$, $H_3AsO_3$, As(s). At high redox potentials and lower pH values, the dominant As species is $H_2AsO_4^-$. The dominant species at alkaline pH is still As (V) in the $HAsO_4^{2-}$ form over a wide redox range, including negative Eh conditions. Arsenic (III) is the predominant form under reducing conditions even at higher pH ranges (7.5 and 8.5). Elemental As(s) is thermodynamically stable at relatively low Eh levels (-100 and -300).

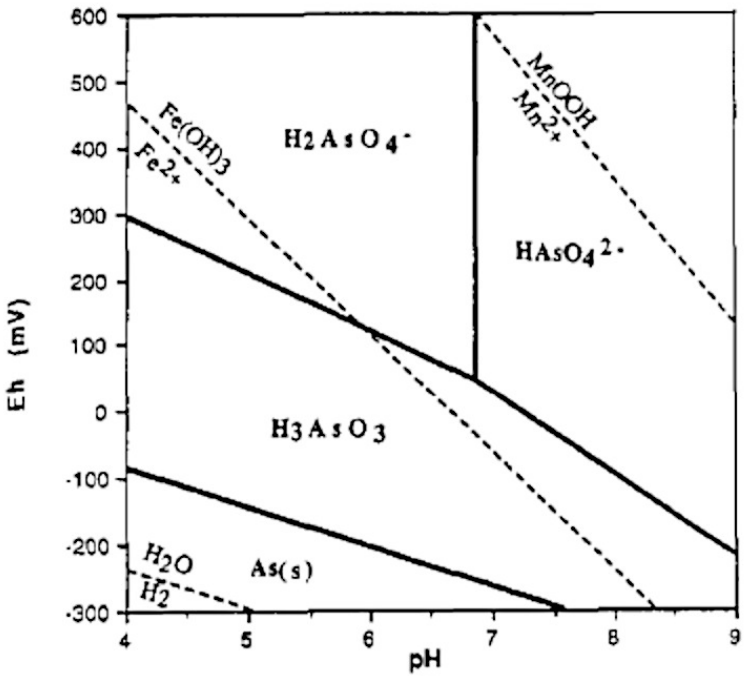


**Figure 1.2** Stability Eh-pH diagram of Arsenic
(Masscheleyn *et al*., 1991)

High concentrations of arsenic occur in groundwater and subsurface systems around the world, most notably in South Asia (West Bengal, Bangladesh), and have generated interest in understanding mechanisms that potentially control the arsenic geochemical cycle (Smedley and Kinniburgh, 2002). Despite numerous and extensive investigations of contaminated sites, understanding of the exact processes controlling arsenic release is still an ongoing investigation (Islam *et al*., 2005; Burnol *et al*., 2007; Borch *et al*., 2010). The main mechanisms proposed to explain arsenic mobility include reductive dissolution of the iron(hydr)oxides, direct microbial reduction of As (V), and competition of solutes for sorption sites (Dixit and Hering, 2003).

It is well documented that iron oxides play an important role in controlling the arsenic cycle through adsorption and co-precipitation reactions (Zachara *et al*., 2002). The correlation

between the development of reducing conditions and the simultaneous presence of dissolved As and Fe (II) have led to the widely accepted hypothesis that reductive dissolution of arsenic bearing iron(hydr)oxides results in the liberation of the attached arsenic (Masscheleyn *et al*., 1991; Islam *et al*., 2004; Burnol *et al*., 2007; Sutton *et al*., 2009). Reductive dissolution experiments have demonstrated that ferrihydrites that were precipitated with and without arsenic had similar reaction rates, reaction mechanism and activation energy. Furthermore, it has also been shown that arsenic can be released through reductive dissolution of ferrihydrite regardless of whether arsenic was adsorbed to or co-precipitated with ferrihydrite (Erbs *et al*., 2010).

In addition to the fact that both biotic and abiotic processes play important roles in iron-associated arsenic mobilization in contaminated natural environments, the defining role of microbial activity in the redox-transformation and ultimately mobility of arsenic is widely acknowledged (Masscheleyn *et al*., 1991; Islam *et al*., 2005). Through a series of microcosm-based experiments using arsenic rich natural sediments, it was shown that in the presence of electron donors an increase of Fe (III) reduction as well as arsenic release could be detected (Islam *et al*., 2004). Since the highest As (III) concentrations were detected only after Fe (II) concentrations reached a maximum in the sediment phase, Islam *et al*. (2005) stated that the reduction of Fe (III) and appearance of As (III) is a decoupled process in contaminated sediments stimulated with an electron donor. The order of the reduction sequence can be rationalized, in general, in terms of the higher oxidation/reduction potential of the Fe (III)/Fe (II) couple in comparison to As (V)/As (III) (Islam *et al*., 2004). Free energy required for the reduction of As (V) to As (III) is estimated to be between the values required for the reduction of Fe (III) and $SO_4$ (Sadiq, 1990; Lee *et al*., 2009). Therefore, decoupling of the reduction of Fe (III) and appearance of As (III) indicates that the constituent microbial community respiratory pathways

may change in accordance with the available electron acceptors (Islam *et al*., 2005). Co-occurrence of As (V) in the solid phase and As (III) in the aqueous phase indicates preferential adsorption of As (V) onto ferrihydrite. Furthermore, it was speculated from the fact that the predominant form of arsenic in the solid phase was As (V), before and after the incubation, that not all As (V) in the solid was bioavailable (Islam *et al*., 2004). It has recently been noted that despite the fact that arsenic can be released from ferrihydrite regardless of its attached form, arsenate release is substantially greater when arsenic is attached primarily to the surface, rather being co-precipitated with ferrihydrite (Erbs *et al*., 2010).

Other incubation batch experiments of arsenic-bearing ferrihydrite have shown that kinetics of reductive dissolution may occur in two phases (Burnol *et al*., 2007). During the first phase, an increase in Fe $(II)_{aq}$ is accompanied by an increase in bacterial growth and decrease of Eh. In the second phase, the $Fe(II)_{aq}$ concentration remains stable or even decreases. Arsenic release and reduction occurring in the second phase supports the idea of the decoupling process proposed by Islam et al. (2004). Similarly, it was concluded that once Eh decreases due to bio-reduction of arsenic-bearing ferrihydrite, As (V) can become an alternative electron acceptor for bacterial respiration. However, it is important to note that reductive dissolution of arsenic bearing Fe minerals may not result in arsenic release under all circumstances, confounding our understanding of processes controlling arsenic retention (Herbel *et al*., 2006; Tufano and Fendorf, 2008; Muehe *et al*., 2013). While As (V) binds strongly to most of the solids in the natural environment, including clay minerals, iron, manganese, and aluminium oxides (Gupta *et al*., 1978), As (III) can also bind effectively to iron(hydr)oxide phases (Dixit and Hering, 2003; Turfano and Fendorf, 2008). As suggested by Dixit and Hering (2004), the generalization that As (III) is more mobile than As (V) is oversimplified when iron is present. In fact, the well-accepted

paradigm that iron dissolution results in arsenic release has previously been questioned (Herbel *et al*., 2006).

Some microcosm based studies which investigated arsenic behaviour during the microbial formation of secondary iron(hydr)oxide phases using both chemically synthesized arsenic-bearing iron(hydr)oxide (Herbel *et al*., 2006; Tufano and Fendorf, 2008) and natural arsenic-bearing contaminated sediment (Islam *et al*., 2005) showed that reductive dissolution of arsenic-bearing iron(hydr)oxide and reductively induced phase transformation can actually result in arsenic retention. Batch-desorption and -transport experiments using ferrihydrite-coated sand indicated that less arsenic was released into the effluent in systems containing iron reducing bacteria than from an abiotic system (Herbel and Fenford, 2006). Seemingly, the release of both arsenic species, As (V) and As (III), diminished during recrystallization of ferrihydrite induced by biogenic Fe (II). Iron oxide phase transformation simply would not result in affinity decrease for As (III) (Dixit and Hering, 2003).

The retention process was explained by the recognition that the duration of reductive dissolution ultimately determines the fate of arsenic; prolonged iron reduction and dissolution eventually will result in arsenic release (Turfano and Fendorf, 2008). It was identified that As (III) goes through three sequential competing processes: i) desorption enhanced by chemical disequilibrium during pore water flow through; ii) adsorption onto the transforming iron phase; iii) release from the recrystallized iron phase (Turfano and Fendorf, 2008). Basically, arsenic desorption in the first period of the elution is the result of weak binding of As (III) to the surface of ferrihydrite. Retention during the second phase is due to incorporation of arsenic into the forming iron phase, such as magnetite, and once the sorption sites are depleted by the Fe (II) generated from iron(hydr)oxide reductive dissolution then arsenic desorption occurs (Turfano

and Fendorf, 2008). Therefore, in natural iron and arsenic-rich systems, microbial activity can lead to temporal arsenic retention; however, prolonged reductive dissolution would likely lead to complete depletion of the sorbent phase, resulting in arsenic mobilization (Turfano and Fendorf, 2008; Borch *et al*., 2010).

Most of the studies investigating arsenic mobilization and retention on Fe (III) minerals used abiogenic type iron(hydr)oxides. However, in nature biogenic Fe (III) minerals originating from Fe (II)-oxidizing bacteria are also present and they have different properties (Muehe *et al*., 2013). In a recent study it was demonstrated that the mobility of arsenic loaded onto biogenic Fe (III) minerals was different from the abiogenic counterpart during microbial iron reduction (Muehe *et al*., 2013). It was found that biotic reduction of As (III)-bearing biogenic Fe (III) minerals released more arsenic than the abiotic one. It was suggested that bio-minerals contain cell-derived organic matter and during iron reduction the released As (III) may complex with the organic matter, preventing re-adsorption to the newly formed iron phase.

Direct microbial reduction of As (V) has received significant attention because this mechanism has been implicated in arsenic release (Islam *et al*., 2005). Two types of microbial As (V)- reducing mechanisms have been identified: detoxification and dissimilation (Tamaki and Frankenberger, 1992). Since As (V) is a structural analogue of phosphate, it readily enters the bacterial cell via phosphate uptake protein and interferes with protein synthesis (Tamaki and Frankenberger, 1992). Some microorganisms confer resistance through an arsenic resistance system (ars) (Lee *et al*., 2009), which reduces As (V) under both aerobic and anaerobic conditions. Furthermore, some anaerobic bacteria are able to obtain energy employing As (V) as an electron acceptor (Lee *et al*., 2009). Dissimilatory As (V)-reducing microorganisms possessing a conserved respiratory arsenate reductase gene (*arrA*) are phylogenetically diverse,

and include *Crysiogenese*, *Bacillus*, *Citrobacter*, *Sulfurospirillum*, *Desulfomicrobium*, *Shewanella*, *Sulfurihydrogenibium* species (Kraft and Macy, 1998; Lear *et al*., 2007). It has been suggested that in iron-rich environments, microorganisms capable of As (V) reduction may initially be sustained through respiration using Fe (III) and once the condition becomes thermodynamically favourable, As (V) is used as an electron acceptor (Islam *et al*., 2004; Islam *et al*., 2005).

Anoxic incubation experiments of samples contaminated with As have indicated that in the presence of electron donors (e.g., acetate), the microbial community composition becomes dominated by Fe (III) reducers Geobacteraceae (van Geen *et al*., 2004; Chatain *et al*., 2005). It is important to note that an increased prevalence and activity of dissimilatory As (V)-respiring microorganisms have been also detected when both organic matter and relatively high concentration of As (V) were added to an environmental sample (Lear *et al*., 2007). Molecular analysis of the As (V)-amended sediment indicated a decrease in microbial community diversity. The combined treatment seemed to select for microorganisms related to *Rhizobium*, *Acidovorax temperans* and Comamonadaceae, which are believed to be tolerant to relatively high concentrations of arsenic and able to respire and reduce As (V). Lear *et al*. (2007) indicated that these microorganisms are initially present in low numbers in arsenic-contaminated environments until favourable conditions reappear.

Based on the biogeochemical basis for As mobilization, bioremediation techniques have been developed for the removal of arsenic from contaminated environments. In a study carried out by Vaxevanidou *et al*. (2008), a combined chemical and biological treatment approach was employed to remove As from contaminated soil. Due to the fact that iron oxide is the major sink of As, the reductive dissolution of soil iron oxide was targeted with *Desulfuromonas palmitates*,

which is able to use Fe (III) as a terminal electron acceptor during respiration. The experiment results indicated that effective dissolution of Fe and release of As was accomplished when *D. palmitates* was combined with the presence ethylenediaminetetraacetic acid (EDTA). It was suggested that the produced Fe (II) initially exerted an inhibitory effect on microbial reductive activity due to its sorption on the surface of Fe (III) oxides and bacterial cells. Complexation of Fe (II) with a strong chelating agent was able to prevent this negative effect (Vaxevanidou *et al*., 2008). It has also been suggested that chelators make Fe (III) more bioavailable by dissolving through chelation (Nevin and Lovley, 2002; Vaxevanidou *et al*., 2008).

## 1.5 Profiling microbial population

Microorganisms play an essential role in the regulation of ecosystem processes. Microbially mediated activity in various ecological systems can be viewed as either beneficial (e.g., carbon and nitrogen cycle, symbiotic interactions with plants, organic contaminant degradation) or detrimental, especially in heavy metal-contaminated environments (e.g., leaching of heavy metals in acid mine drainage). To improve their beneficial effects or minimise their negative environmental impacts, the ecological diversity of microorganisms, including microbial community composition and complexity of interaction, are of great interest (Hirsh *et al*., 2010; Fierer and Lennon, 2011). Methods, such as DNA sequence-based techniques to obtain in-depth microbial diversity have advanced over the past several decades providing comprehensive information on the composition of microbial communities.

Exclusive reliance on a single approach, such as DNA-sequence based techniques, to estimate microbial diversity in natural environments has been criticized because it may fail to identify certain microorganisms leading to significant gaps in microbial composition data (Donachie *et al*., 2007). Furthermore, the fact that many cultivated microorganisms are not

detected by sequence-based methods has been explained by potential biases introduced during preparation steps (Donachie *et al.,* 2004) and Polymerase Chain Reaction (PCR) conditions (Hongoh *et al*., 2003) involved in molecular approaches. Either culture-based or culture-independent methods, used independently, could potentially miss significant fractions of microbial biodiversity; hence, a polyphasic approach to describe microbial diversity has been highly recommended (Donchie *et al*., 2007).

### 1.5.1 Culture-based methods used in microbial ecology

Culture-dependent methods have been used for more than a century to study the diversity of bacteria in natural habitats; however, only a small fraction, estimated to be around 1% of the total number of bacteria, can be routinely cultured using laboratory media and cultural methods (Amann *et al*., 1995; Davis *et al*., 2005). Despite the fact that culture-dependent methods are not an ideal approach to estimate microbial diversity when used alone, they can provide essential information regarding potential function of microorganisms in their natural habitat. Furthermore, a comprehensive understanding of microbial physiology requires cultivation of these microorganisms for direct study (Oremland *et al*., 2005).

Various types of media are available for bacterial culturing; however, as Oremland *et al*. (2005) pointed out, conventional enrichment and cultivation techniques are not suitable for many environmental bacteria. Media used for growing pure cultures of bacteria are generally high in soluble carbon; however, in natural environments, organic compounds tend to be scarcely available at steady-state concentrations, hence exposing starved microorganisms from an oligotrophic habitat to high nutrient conditions can be toxic. Improved results can be obtained by simulating, or mimicking, the original natural habitat in question (Zinder and Salyers, 2001).

Therefore, physiochemical factors (e.g. pH, various solutes concentration, temperature) dominating the microbial environment should be always considered.

### 1.5.2 Molecular approaches used in microbial ecology

A primary objective of most microbial ecology studies is to identify the members of a microbial community and to understand their function and activity, such as microbe-microbe interaction and microbes' interaction with their environments (Robinsol *et al*., 2010; Simon and Daniel, 2011). A combination of multi-level methodological approaches, namely DNA-, mRNA- and protein-based analyses, has unprecedented potential to accomplish those objectives (Simon and Daniel, 2011). As reviewed by Robinson *et al*. (2010), the beginning of the microbial ecology era identified bacteria using microscopes, biochemical tests and culture-based techniques. A new era of molecular microbial ecology started once sequencing of RNA-encoding genes was introduced to identify bacterial species (Riesenfeld *et al*., 2004).

Polymerase chain reaction (PCR)-coupled cloning and sequencing of 16S rRNA-encoding genes has been widely used method for the estimation of microbial diversity (Robinson *et al*., 2010) and numerous microbial community compositions from various ecosystems were explored using this molecular approach (Cardenas, *et al*., 2008; Rastogi *et al*., 2010). PCR allows selective amplification of the DNA target sequences, and cloning-systems allow for the separation of PCR amplicons from the heterogeneous gene-pools (Xu, 2006). Community fingerprinting methods, such as terminal restriction fragment length polymorphism (T-RFLP) (Liu *et al*., 1997) and denaturing gradient gel electrophoresis (DGGE) (Muyzer, 1999) were also developed for rapid comparative analyses of microbial communities. Both molecular methods involve gel separation of the amplified heterogeneous amplicons, which are then sequenced

providing comparable estimation of species diversity and quantitative aspects of microbial communities (Robinson *et al*., 2010).

Metagenomics is becoming more widely used for microbial community investigations and it is not dependent on a universal target-gene; instead, the total genomic DNA is used for sequence analyses (Riesenfeld *et al*., 2004; Simon and Daniel, 2011). Basically, this technique allows direct genetic analysis of a mixture of microbial genomes obtained from an environmental sample (Thomas *et al*., 2012). Initially, it was used to clone sheared environmental DNA to screen for new functional activities, such as production of new chemical products (Handelsman *et al*., 1998). Cloning and functional analyses of collective genomes from the environment was subsequently complemented with direct shotgun sequencing of the sheared environmental DNA (Riesenfeld *et al*., 2004; Tyson *et al*., 2004). Tyson et al. (2004) used the metagenomics approach on biofilms from acid mine drainage, and since the sample originated from an extreme environment and contained a low microbial diversity, it was possible to reconstruct near-complete genomes of the microbial species present. Obtaining a whole genome sequence of uncultured bacteria was considered an unprecedented breakthrough. The creation of a functional gene profile allowed Tyson *et al.* (2004) to define ecological role(s) of the microbial community present in the acid mine drainage biofilm. Since metagenomics provides access to both community structure and functional gene profiles, it is considered superior to phylogenetic surveys, which usually employ a universal gene target (Thomas *et al*., 2012; Hazen *et al*., 2013).

### 1.5.3 Microbial genetic markers

For phylogenetic studies of complex microbial communities, the molecular targets of PCR must fulfill the following main criteria in that they must: i) be universal in all forms of life and functionally homologous, ii) be informative (contain variable regions for differentiation

between organisms as well as conserved regions for alignment), and iii) have an available reference database for comparison.

The use of PCR-derived 16S rRNA gene (rDNA) sequences is one of the most common genetic markers used for the study of microbial ecology because it is present in all prokaryotes, contains highly conserved sequence domains interspersed with variable regions, and provides a relatively large region of DNA for comparative and reliable analyses (Case *et al*., 2006; Janda and Abbott, 2007). This gene has been considered as the "gold standard" for bacterial phylogeny and microbial ecology studies; however, it has its potential drawbacks. It has been suggested (Case *et al*., 2006) that multiple heterogeneous copies are typical in bacteria isolated from the environment. This may lead to the detection of multiple ribotypes within a single species. Therefore, 16S rRNA gene-based community analyses may result in an overestimation of microbial diversity when certain molecular tools are employed (Case *et al*., 2006). Despite the fact that 16S rRNA is one of the most widely used molecular techniques, fingerprinting methods and clone library construction are not limited to this gene (Case *et al.,* 1996). Housekeeping genes such as *rpoB* (RNA polymerase beta subunit) and *cpn60* (chaperonin 60 kDa) have been proposed and employed for phylogenetic relationship characterization. It has been suggested that both genes fulfill the criteria of being excellent molecular "chronometers" and some argue that they even surpass the 16S rRNA gene. Comparative studies have demonstrated that these gene sequences exhibit a greater discriminating power when closely related species are compared (Goh *et al*., 1996; Dahllof *et al*., 2000; Hill *et a*l., 2005; Case *et al*., 2006).

Due to its universal nature, the *cpn60* gene has been used as a molecular target in phylogenetic studies and as a tool for the detection and identification of clinical microorganisms (Hill *et al*., 2004). In order to identify pathogens accurately (e.g., coagulase-negative

staphylococci) to the species level in a hospital setting, several molecular methods based on restriction analysis of the 16S rRNA gene had been previously used (Goh *et al*., 1996). To avoid the potential multiple intragenomic copy drawback of 16S rRNA, a highly conserved and single-copy 60 kDa heat shock protein (HSP60) gene, also known as *cpn60*, was proposed by Goh *et al.* (1996) for species identification of *Staphylococcus* and other microorganisms. In this study, *cpn60* gene PCR- amplicon probes were derived from one *Staphylococcus* species and cross-hybridized to genomic DNA from other species. The unsuccessful probing under high-stringency conditions clearly indicated the presence of species-specific variation, which may generally provide discriminatory power (Goh *et al*., 1996). The fact that *cpn60* may be phylogenetically more informative than 16S rRNA was demonstrated in a comparative study where the sequence similarity in 16S rRNA (range 92 to 99%) was found to be considerably higher than in cpn60 (range 74-93%) among 29 different *Staphylococcus* species (Kwock *et al*., 1999). Since the *cpn60* gene is a protein-coding sequence, there exists more variation than in the structural RNA-encoding gene (Hill *et al*., 2004). The ability to amplify the *cpn60* gene from any genomic template with degenerate universal PCR primers allowed the implementation of *cpn60* molecular target advantages over 16S RNA for complex microbial community analyses (Hill *et al*., 2004; Schellenberg *et al*., 2011; Chaban *et al*., 2014;).

It has been also demonstrated that unlike 16S rRNA sequences, *cpn60* sequence identity alone can predict the whole-genome sequence relationships or genome identity (Verbeke *et al*., 2011). Furthermore, evaluation of DNA barcodes for Bacteria has shown that *cpn60* is the preferred barcode with the largest barcode gap (ratio of inter- and intra-specific distances) making species discrimination more robust than 16S rRNA (Links *et al*., 2012). Hence, *cpn60* is

the preferred barcode sequence where identification beyond genus level and detection of novel taxa are desirable (Links *et al*., 2012).

### 1.5.4 Next generation sequencing (NGS) technologies

Automated conventional Sanger sequencing is capable of producing a 1 kb sequence data from a single template and up to 96 different specimens simultaneously. Next generation sequencing can generate hundreds of thousands of sequence reads in parallel in a relatively short period of time (Sokralla *et al*., 2012). These NGS techniques not only increase the depth of sequences by orders of magnitude, but they do not require DNA template separation; hence, eliminating the vector-based cloning step (Robinson *et al*., 2010; Shokralla *et al*., 2012). Phylogenetic surveys using either single gene or metagenomic shotgun methods are typically performed using NGS platforms. Tagging of different DNA samples eliminates the need for cloning (Edwards *et al*., 2006).

Over the past few years, DNA sequencing platforms have developed at a rapid pace with substantial reductions in cost. A series of high-throughput sequencing devices are currently available, mainly differing in terms of what chemistry and detection methods are used (Shokralla *et al*., 2012). The sequencing platforms have been categorized into two major groups; 2$^{nd}$ and 3$^{rd}$ generation sequencing (Glenn, 2011). The 2$^{nd}$ generation platforms require PCR-amplification of the DNA templates before sequencing, whereas 3$^{rd}$ generation platforms sequence DNA templates directly. Second generation platforms include the Roche 454 Genome sequencer, the HiSeq 2000 (Illumina), AB SOLid (Life Technology), and the Ion Personal Genome Machine (Life Technologies). Third generation platforms include the HeliScope (Helicos), PacBio (Pacific Biosciences), and Starlight (Life Technologies) systems (Glenn, 2011). For large-scale biodiversity analyses of environmental samples Roche 454, HiSeq Illumina, and Ion Torrent

sequencing platforms have primarily been used (Shokrala *et al*., 2012); therefore, the main principle of these techniques will be briefly described.

#### 1.5.4.1 Roche 454 sequencer

The Roche 454 sequencer was the first commercial next generation platform, and was introduced in 2005 (Shokrala *et al*., 2010; Glenn, 2011; Liu *et al*., 2012). This technology is a real time sequencing-by-synthesis method, which includes emulsion PCR and pyrosequencing (Siqueira *et al*., 2011). In this approach, genomic DNA samples are fragmented, ligated to adapters, separated into single-stranded sequences and captured on amplification beads. The ligated distinct adapters are priming sites for the subsequent amplification and sequencing (Rothberg and Leamon, 2008). To produce clonal copies of target DNA, each single template attached to a bead is amplified using emulsion PCR. Then, the beads are transferred onto a PicoTiterPlate such that only one bead is positioned in a well, which contains the enzymes and reagents required for the pyrosequencing reaction (Rothberg and Leamon, 2008). Specifically, the reaction mixture consists of a sequencing primer, DNA polymerase, ATP sulfurylase, luciferase, apyrase and single-stranded DNA template. The sequencing stage consists of repetitive cycle of dNTP supplementation where only one type of dNTP is supplied per cycle. When incorporation occurs the pyrophosphate ($pp_i$) is converted to ATP by the enzyme ATP-sulfurylase, and the generated ATP mediates luciferin conversion to oxyluciferin by the enzyme luciferase. The emitted light is detected as peaks and the height of each peak is proportional to the number of ATP molecules, which is further proportional to the number of incorporated nucleotides. The unincorporated dNTP is degraded by the enzyme apyrase (Siqueira *et al*., 2011). The upgraded 454 FLX+ instrument (summer 2011) able to produce sequence reads of 700 bp in length (Glenn, 2012).

#### 1.5.4.2 Illumina sequencer

Illumina sequencing (formerly known as Solexa) was the second commercial next generation sequencing platform and was introduced in 2007 (Glenn, 2011; Shokralla *et al*., 2012). This platform is also a sequencing-by-synthesis method coupled to bridge-PCR amplification on the surface of a flow cell (Shokralla *et al*., 2012). The surface of the flow cells are covered with oligo-sequences, which are complementary to the adaptors attached onto the DNA templates. The oligo-adapter hybridization in the flow cells occurs through active heating and cooling. The captured DNA templates are amplified into small clusters of identical clones through bridge-PCR amplification. These clusters are then sequenced with a method similar to Sanger sequencing, where dye-labelled reversible terminator nucleotides are incorporated by DNA polymerase. This ensures that only one nucleotide is incorporated and its fluorescence measured. A chemical de-blocking treatment removes the blocking dye from 3'-OH end allowing the incorporation of another dye-labelled reversible terminator nucleotide base (Shokralla *et al*., 2012). The updated MiSeq Illumina sequencing platform can produce sequence read lengths between 100-150 bp (Glenn, 2012).

#### 1.5.4.3 Ion Torrent sequencer

The Ion Personal Genome Machine (PGM) platform was first commercialized in late 2010. The sequencing principle is similar to 454 pyrosequencing except the $H^+$ ion is detected in real time rather than after the pyrophosphate reaction chain event (Glenn, 2012). The system has no optical component (e.g., no laser or fluorescence detection system required); instead, field-effect transistor-based sensors directly measure the ions generated during synthesis (Rothberg *et al*., 2011). It is the first sequencing machine that does not require fluorescent dyes and detectors; therefore, it is cheaper and faster (Liu *et al*., 2012). DNA preparation for sequencing is similar to

the steps involved for 454 pyrosequencing; for example, DNA fragmentation, ligation of adapters, attachment onto beads, emulsion PCR amplification of the templates, amplicon-bearing beads loading into individual sensor wells and stepwise addition of each nucleotide base. When nucleotide incorporation occurs a single proton is released from the hydrolysis of the nucleotide triphosphate. The pH change (0.02 pH units per single nucleotide) of the solution is immediately detected by the sensor and converted to voltage and then to digital data over a 4 s period (Rothberg *et al*., 2011).

Since one of the key features of this sequencing platform is speed it has gained favour in the clinical field. One of the first applications of Ion Torrent sequencing was for microbial pathogen identification during the outbreak of an extremely virulent Shiga toxin producing *E. coli* O104:H4 in Germany (2011) (Mellmann *et al.,* 2011). Sequencing the whole genome of the outbreak strain and historical reference strains with Ion Torrent PGM helped to identify why the new strain was pathogenic. Studies involving characterization of microbial diversity have also been carried out using Ion Torrent PGM to confirm that this relatively new sequencing platform is suitable for microbial ecology studies (Whiteley *et al*., 2012; Yergeau *et al*., 2012). These initial studies have confirmed applicability of Ion Torrent sequencing to multiplex microbial communities.

Furthermore, performance comparisons have also been carried out between Ion Torrent and other next generation sequencing platforms commonly used for microbial diversity studies (Yergeau *et al*., 2012; Liu *et al*., 2012; Salipante *et al*., 2014). It was shown that DNA datasets generated by Ion Torrent and 454 pyrosequencing, respectively, were almost the same with exact ecological interpretation (Yergeau *et al*., 2012). An extensive comparison between Ion Torrent and Illumina sequencing platforms, where both methods were used to investigate microbial

diversity of a known and of an unknown naturally occurring microbial community targeting 16S rRNA universal gene sequence was performed by Salipane et al. (2014). In both cases, the identified microbial profile and abundance of most species detected were generally in good agreement; however, there were some cases with significant differences. There were libraries in which one or more microorganisms were under-represented by Ion Torrent sequencing; furthermore, in some cases, certain microorganisms were not detected by the Ion Torrent sequencing platform, but were identified by Illumina and vice versa. It was pointed out under-representation of some species by Ion Torrent sequencing method could be attributed to the failure of synthesizing full-length sequence reads for some microorganisms; however, exclusion of these sequences can be prevented by reducing the threshold read length during the initial filtering process (Salipane *et al*., 2014). It is important to note that discrepancies in bacterial community profiles can result from the selected/available sequencing platforms (Salipane *et al*., 2014), therefore, caution needs to be taken when microbial diversity obtained by different methods are compared.

## 1.6 Imaging techniques

### 1.6.1 Microscopic techniques used in biofilm research

Nutrient limitations and various stress factors in natural environments trigger bacterial communities to form biofilms which consist of bacterial cells and aggregates embedded in complex protective polymeric matrices of variable density with permeable water channels (Caldwell *et al*., 1992; Lawrence *et al*., 1991). Bacterial growth in this form may provide greater tolerance and increased survival. Physicochemical properties of matrix-enclosed microenvironments mainly depend on biofilm structure, limited diffusion and stratified metabolic functions of the biofilm bacterial communities (Costerton *et al*., 1994). Environmental

biofilms are complex structures with well-defined microenvironments of different physicochemical conditions and they play an important role in metal cycling in the environment (Toner *et al*., 2005; Yang *et al*., 2013).

Traditional methods used for biofilm analyses generally relied on disaggregation and subsequent isolation/enumeration of microbial community members. Due to the physical disruption of well-established spatial relationships (which favour survival of the biofilm bacterial community), cultivation-based methods are considered as inadequate approaches to conclude potential viability and activity of bacteria within biofilms (McFeters *et al*., 1995). For a few centuries, light microscopy was the basic standard imaging tool for the analyses of biological samples (Neu *et al*., 2010; Neu and Lawrence, 2014). Important inventions which allowed compositional analyses of samples at higher magnifications and resolution were the scanning and transmission electron microscopes. Another major invention was the scanning tunnelling microscope, which provides three-dimensional topography at higher resolution than the conventional transmission electron microscope, basically at the atomic scale (Binning *et al*., 1982).

Advances in imaging techniques made possible non-invasive analyses of complex structure, composition, or processes of samples in various scientific fields (Neu *et al*., 2010). Confocal laser scanning microscopy (CLSM) has become an essential tool for *in situ* imaging of hydrated microbial biofilm systems (Lawrence *et al*., 1991; Palmer and Sternberg, 1999; Neu *et al*., 2010). Most importantly, CLSM paved the way for three-dimensional optical sectioning of intact biofilm samples and imaging of bacterial cells in the context of their microhabitats (Palmer and Sternberg, 1999). Images derived from each optical section are relatively sharp, because the emitted fluorescence from the sample pass through the dichromatic mirror and only in-focus

fluorescence emitted from the sample are allowed through the detector pinhole aperture whereas out-of-focus light don't contribute to the image (Claxton *et al*., 2005).

Applications of this powerful imaging tool has recently been reviewed and compiled by Neu and Lawrence (2014). A major characteristic of CLSM is the laser lines used for the excitation of fluorochromes enable a variety of simultaneous analyses. In general, three laser lines, at 488, 561, 633 nm are sufficient to cover the range of commonly used fluorochromes, for example, acridine orange (ex/em, 460/650 nm (RNA); ex/em, 500/526 nm (DNA)), 4,6-diamidino-2-phenylindole, dihydrochloride (DAPI) (ex/em, 358/461nm) for nucleic acid staining or fluorescein isothiocyanate (FITC) (ex/em, 494/518 nm), tetramethylrhodamine-5-(6)-isothiocyanate (TRITC) (ex/em, 541-572 nm) used alone or conjugated to other specific probes, such as lectins or oligonucleotides (Neu and Lawrence, 2014). Through CLSM optical sectioning, architectural changes within bacterial biofilms can be monitored (Lawrence *et al*., 1991). This imaging technique also allows extrapolation of useful information from the intrinsic properties of biofilms; for example, from autofluorescent signals detected in tailings water biofilms, it was determined that the phototrophic bacterial community was responsible for carbonate mineral formation and heavy metal co-precipitation (Podda, *et al*., 2000).

Furthermore, specific fluorescent probes may be used to assess biofilm structural composition, biofilm functionality as well as biofilm response to environmental factors (Neu *et al*., 2010). It has previously been observed that exposure of river biofilms to nickel resulted in significant changes in the abundance of exopolymeric substances and composition of the biofilm matrix (Lawrence *et al*., 2004). Potential application of specific fluorescent probes to map metal species within biofilms has recently been reviewed by Hao *et al*. (2013). It has been concluded that even though specific fluorescent probes are available to detect the distribution of certain

metal elements (e.g., Fe, Cu, Ni, Cd, Hg) within biofilms using CLSM, results should be confirmed with other conventional methods, such as electron microscopy in combination with energy-dispersive X-ray spectroscopy (EDX) or Scanning Transmission X-ray Microscopy (STXM), which is also suitable for hydrated sample analyses. Furthermore, it was pointed out that there is a need for highly sensitive and specific CLSM-compatible metal probe development (Hao *et al*., 2013).

### 1.6.2 Synchrotron-based techniques

### 1.6.3 Overview of synchrotron radiation

Initially, synchrotron radiation was considered as an unwanted, but unavoidable, energy loss when the path of accelerated electrons was directed using an electromagnetic field (Willmot, 2011). Electromagnetic theory states that when charged particles are accelerated through a magnetic field, radiation is given off. The emitted radiation occurs perpendicular to the direction of magnetic field and the accelerated electron's direction of travel (Margin, 1998).

The main components of a synchrotron are the electron gun (the electron source), linear accelerator (LINAC), booster ring, and storage ring (Willmot, 2011). These components are briefly described according to Willmot (2011) and the information currently available on the Canadian Light Source (CLS) homepage (http://www.lightsource.ca/education/whatis.php). The electron gun generates the electrons through thermionic emission by applying high voltage electricity through a hot filament (e.g., a tungsten filament is used at the CLS). The electrons are accelerated almost to the speed of light in the LINAC, and then directed into the booster ring where the energy of the electrons is further increased (e.g., from 250 to 2500 MeV at the CLS). The electrons are injected into the storage ring, which maintains them on a closed path using an

array of magnets. The dipole, or bending, magnets force the electrons to change their path and as the charged electrons circulate almost at the velocity of light, synchrotron radiation is emitted tangentially from the bending magnet. Insertion devices, such wigglers and undulators, are used at the straight sections of the storage ring to produce higher intensity, or brilliant, synchrotron radiation. Basically, brilliance gives information of the photon flux distribution and determines the smallest spot onto which an X-ray beam can be focused. The undulator generates the highest brilliance, whereas the wiggler exhibits a wider spectral range than the undulator.

X-rays generated by synchrotron method have several advantages over those generated by sealed X-ray tubes; for example, they exhibit higher flux, are highly directional and parallel, and highly focusable, which allows chemical characterization of elements at very fine resolution. Synchrotron radiation produces a continuum of wavelengths from the ultra-violet to X-ray region of the electromagnetic spectrum and hence allows the selection of the correct wavelength for specific experiments (Margin, 1998; Lachlan *et al*., 2010).

#### 1.6.3.1 X-ray absorption spectroscopy (XAS)

X-ray absorption spectroscopy is a highly specific method that can be used to identify and characterize elements of various phases (George and Pickering, 2007). When X-rays interact with matter, they can be transmitted through the sample, scattered and/or absorbed. The latter occurs when the energy of the X-ray is transferred to an electron, which is then ejected from its shell to a higher energy orbital (MacLean *et al*., 2010). When the incident photon has sufficient energy to eject a core electron to an unoccupied orbit or to the continuum, an abrupt increase in absorption occurs, which are termed absorption “jumps” or “edges” (Cramer and Hodgson, 1979). The absorption edges are named according to the core electrons that are being excited; the K-edge comes from 1s electrons, whereas L-edge originates from 2s or 2p electron excitation.

Electron deficiencies, or hole states, are designated as K, $L_1$, $L_2$, $L_3$, $M_1$ and their corresponding configurations are 1s, 2s, $2p_{1/2}$, $2p_{3/2}$, and 3s, respectively (Kawai, 2000).

The X-ray absorption spectrum can be divided into three regions: the pre-edge region, which indicates where core-electron excitation occurs; the near edge region, called the X-ray Absorption Near-Edge Structure (XANES) or near-edge X-ray absorption fine structure (NEXAFS) and the far edge, called the Extended X-ray Absorption Fine Structure (EXAFS) (MacLean *et al*., 2010). The NEXAFS spectrum ranges from -50 eV below and 100 eV above the absorption edge and provides information about the oxidation state and bonding of an element of interest. The EXAFS spectrum reaches to about 1000 eV above the absorption edge and gives information about chemical characteristics of the absorbing element. The number of and type of the neighbouring atoms affect the amplitude of oscillation in this region of the spectrum (Penner-Hann, 1999; MacLean, 2010). Meaning the more atoms in a particular shell or higher the atomic number of the bound atom, the higher the amplitude of the EXAFS.

#### 1.6.3.2 Scanning Transmission X-ray Microscopy (STXM)

STXM is a powerful imaging tool because it combines chemical speciation of elements derivable from NEXAFS spectra with possible quantification and mapping at a very high spatial resolution (Behrens *et al*., 2012). Undulators used at the CLS STXM beamline produce high brilliance, soft X-rays between 130 and 2500 eV energy range. Because X-rays cannot be focused by glass-lenses, Fresnel zone plates, as diffractive focusing elements, are used to focus the high-flux photons ($10^8$ ph/s) to nm scale resolution (e.g., ~25 nm at the CLS) (Beelen *et al*., 1997; Behrens *et al*., 2012). Transmitted X-ray data can be collected as single images at a specific energy or as sequence of images over a range of energies across the absorption edges.

Spectra can be extracted from individual pixels, enabling redox species to be identified and quantitatively analysed and used for spatial mapping (Willmot, 2011; Behrens *et al*., 2012).

The energy range of a STXM beamline is highly suitable for geo-microbiological research because it contains energy levels matching the K absorption edge of elements (e.g., C, N, O, P), which are constituents of organic matter as well as L-edges of transition elements (Fe, Co, Ni, Co) characteristic of the natural environment (Behrens *et al*., 2012). STXM has increasingly been used in recent years to determine the biochemical composition of bacteria and biofilms (Lawrence *et al*., 2003), as well as to map metal redox species or mineral phases in the context of bacterial biofilms (Toner *et al*., 2005; Dynes *et al*., 2006; Hunter *et al*., 2008; Hitchcock *et al*., 2009). STXM has successfully been shown to be an excellent tool to investigate microbial interactions with metal elements and dissimilatory redox reactions mediated by microbial processes. Toner et al. (2005) mapped Mn species spatially and temporally within bacterial biofilm using this imaging technique. It was shown that $Mn_{aq}$ (II) was taken up from solution and concentrated within biofilm adjacent to the bacterial species in its oxidized forms, such as Mn (III) and Mn (IV).

The range of elements analysed within hydrated microbial biofilm was expanded using soft X-ray STXM-NEXAFS (Dynes *et al*., 2006; Hitchcock *et al*., 2009). Dynes et al. (2006) acquired 2p absorption spectroscopic data for the quantitative mapping of Fe, Mn, and Ni metal elements. To investigate metal distribution in the context of the river biofilm, images were obtained at the C 1s and O 1s edges of the same area. It was observed that Ni and biogenic Mg oxides were grouped together in association with bacterial polysaccharides. They also found that the distribution of Fe redox species within the biofilm was different compared to that of Mn and Ni. More detailed nano-scaled biogeochemistry was investigated using STXM analyses on a

river biofilm treated with Ni (Hitchcock *et al*., 2009). In this study, it was revealed that Ni potentially adsorbed onto biogenic Mn-Fe mineral and was selectively associated with sheaths of filamentous bacteria within a heterogeneous river biofilm matrix. Limitations and possible inaccuracies of chemical extraction-based methods and analytical electron microscopic imaging techniques have also been discussed by Dynes *et al.* (2006). Accordingly, mapping of metal elements in biofilms using chemical processes may be suspect due to metal re-distribution, re-speciation and limited sensitivity or modification of biofilm components. Similarly, sample dehydration and sectioning of biofilm samples that are required for electron microscopy may result in artefacts such as shrinkage and aggregation of particles.

To date, most STXM analyses have been made in 2D, but there has been an increasing interest in performing STXM imaging in 3D projections (Johansson *et al*., 2007; Obst *et al*., 2009). Tomography 3D imaging basically requires the collection of multiple 2D images from a wide range of projection angles. This has been achieved by positioning the samples in a cylindrical capillary, which allows a full 360 turn on a sample stage (Johansson *et al*., 2007). STXM angle-scan spectro-tomographic mapping was successfully used to characterize $CaCO_3$ biomineralization on the surface of a cyanobacterial cell at a spatial resolution <80 nm (Obst *et al*., 2009). From the 3D mapping and 2D spectroscopic analyses of bio-macromolecules and Ca it was extrapolated that nucleation of $CaCO_3$ mineral potentially started from Ca-rich hot spots within the EPS surrounding the bacterial cell. The authors further indicated that the STXM 3D spectro-tomographic method could potentially be used for the investigation of metal sorption to biomolecules within bacterial cells.

In conclusion, the STXM imaging technique is a powerful tool to detect, speciate or quantify a range of elements in the context of biological matter; however, it has been recently

pointed out that STXM should not be used as a single technique or replacement of other methods that could serve complementary information for a given investigation (Behrens *et al*., 2012; Lawrence *et al*., 2014).

## 1.7 Hypotheses

Given the paucity of information available on the distribution, activity and biogeochemical potential of the microbial community in the DTMF, an in-depth characterization of the microbial diversity in the system was undertaken. Two main hypotheses have guided the research conducted in this thesis: 1) labile carbon source and complex hydrocarbons discharged into the tailings support microbial activity in the DTMF, and 2) microbial activity acts as a biocatalyst for the redox-transformation of elements of interest, such as reductive dissolution of iron.

## 1.8 Technical objectives

Research was undertaken to obtain an early insight into the biogeochemical processes that might take place in the DTMF and that likely would become increasingly important over extended periods of time. In order to elucidate microbial processes active in the DTMF, a number of technical objectives were identified, including:

1. To characterize the microbial diversity at three sites in the DTMF: the water column, the tailings-water interface and the tailings body.
2. To deduce the functional and metabolic potential of the microbial community present in the DTMF tailings body.
3. To elucidate the biogeochemical potential of microorganism native to the DTMF site, specifically the potential of microorganisms to alter Eh and ferrihydrite redox state,

which are the primary controlling conditions, and secondary mineral phase, respectively, within the tailings.

4. To taxonomically characterize novel species present in the DTMF that are observed constantly at high frequency.

## 1.9 Organization of thesis

This thesis is organized according to "manuscript-style" option of the College of Graduate Studies and Research.

# 2 BIOGEOCHEMICAL ACTIVITY OF MICROBIAL BIOFILMS IN THE WATER COLUMN OVERLYING URANIUM MINE TAILINGS

This chapter has been published: Bondici, V.F., Khan, H.K., G.D.W. Swerhone, G.D.W., Dynes, J.J., Lawrence, J.R., Yergeau, E., Wolfaardt, G.M., Warner, J., and Korber, D.R. (2014). Biogeochemical activity of microbial biofilms in the water column overlying uranium mine tailings. *J. Appl. Microbiol.* 117, 1079-1094.This chapter is published here with the permission from the copyright owner (Wiley publications).

Author contributions

All authors participated in the design of the experiments and contributed to writing of the manuscript. Preparation of the initial draft of the manuscript, as well as all other data presented in this manuscript, are the work of the thesis author.

## 2.1 Abstract

The aim of this study was to describe microbial diversity, biofilm composition and biogeochemical potential within biofilms in the water overlying uranium tailings characterized by high pH, high metal concentration and low permeability. To estimate microbial diversity in biofilms formed in water columns overlying uranium mine tailings, culture-dependent and culture-independent methods were employed. High-throughput sequencing revealed the presence of 11 phyla; however, the majority of the sequences were affiliated with 4 major lineages *Proteobacteria, Bacteroidetes, Actinobacteria* and *Firmicutes,* as confirmed by culture-based methods. Dominant phylotypes were closely related to methylotrophs (*Methylobacterium*) and bacterial groups able to utilize complex hydrocarbons (*Aquabacterium* and *Dechloromonas*). Microbial diversity in biofilms from the 13 m depth were significantly different that in biofilms from 1 m and 41 m ($p<0.05$). Phylotypes closely related to iron reducing bacteria were identified at each depth; whereas, sulfate, thio-sulfate, sulfite and sulfur reducing bacteria, at low abundance, were only detected at lower depths. Confocal laser scanning microscopy (CLSM) was used to investigate polymer quantity and composition of the biofilm components, and principal component analysis of the CLSM data revealed that the relative abundance of α-L-fucose and N-acetyl-glucosamine/lipopolysaccharide residues separated tailings-water interface biofilms from those from other depths. Reduced (ferrous) iron was detected within all the biofilm samples examined by scanning X-ray transmission microscopy. This study demonstrates the biogeochemical potential of microbial biofilm communities in the water column covering an alkaline uranium tailings body; specifically, the nature of the bacterial groups detected (*Aquabacterium*, *Dechloromonas*) and the presence of reduced iron suggests that complex hydrocarbons are available for bacterial growth and

geochemical change, such as iron reduction, can occur even though the system bulk-phase is predominantly oxic.

## 2.2 Introduction

The nature of uranium tailings waste is considered unique due to low-level radioactivity and elevated concentration of numerous hazardous constituents (Mudd 2000); the risk of contamination of surrounding areas and groundwater by abandoned uranium mine tailings represents a significant environmental concern (Pyle *et al.,* 2002; Akob *et al.,* 2006). Currently, major environmental protection measures at uranium tailings management facilities involve the physical isolation of the uranium waste from the environment by engineered structures. To ensure containment of the tailings, waste liners and coverings have been implemented (Al-Hashimi *et al.,* 1995). In terms of cover, soil capping is a common option for containment after decommissioning (Gavrilescu *et al.,* 2009).

The Deilmann Tailings Management Facility (DTMF) is an active, in-pit deposition site for uranium mine tailings and is located at the southern edge of the Athabasca Basin, Canada. To shield radioactivity and prevent dried or freeze-dried tailings particles being transported by wind, the facility is currently covered with approximately 40 m of water. The depth of the water column varies depending on the season, periodic deposition of tailings and extent of removal of pore water from the base of the system. Geochemical controls and spatial/temporal distribution of elements of concern have previously been investigated within the DTMF tailings (Essilfie-Dughan *et al.,* 2011; Shaw *et al.,* 2011) where it has been shown that highly alkaline and oxic conditions exist throughout the deposited tailings mass. Under these conditions, ferrihydrite adsorbs many heavy metals and oxyanions released during uranium extraction, thus controlling their solubility in, and mobility into, the bulk water phase (Shaw *et al.,* 2011).

It is well-documented that, under certain conditions, microbial processes may result in metal dissolution, metal mobilization or metal immobilization (Francis, 1990). These processes may include oxidation or reduction, attachment to chelators, alteration of environmental pH or Eh, and bio-absorption by the bacterial cell or extracellular polymeric substances (EPS) (Francis, 1990; Lloyd, 2003; Choudhary *et al.,* 2009; Hua *et al.,* 2013). Initial microbial studies of the DTMF indicated that the tailings body and tailings-water interface support the growth of bacterial communities that exhibit metal/metalloid-reducing capabilities with the potential to influence Fe and S biogeochemical cycling (Bondici *et al.,* 2013; Khan *et al.,* 2013). Relatively high bacterial cell counts, i.e., 2.2 X $10^8$ cfu $g^{-1}$ at some depths within the tailings suggest the presence of nutrient-rich zones where the geochemistry may differ from that in the bulk phase (Bondici *et al.,* 2013). Previous studies have also revealed that microscale chemical characteristics can be distinct from the bulk phase environment due to local microbial activity (Nguyen *et al.,* 2012). Therefore, identification or characterization of microscale geochemical conditions is critical to understand geochemical changes that may not be reflected by the chemical measurements carried out on the bulk phase of the system.

Nutrient limitation and other stress factors in natural environments trigger bacterial communities to form polymicrobial structures that consist of bacterial cells and aggregates embedded in complex and protective EPS (Costerton *et al.,* 1995; Flemming and Wingender, 2010). The matrix of the biofilm possesses physical and chemical characteristics that protects bacterial cells and responds to environmental changes (Decho, 2000). Within biofilms, there are matrix-enclosed microenvironments with various physicochemical properties where different geochemical reactions can take place (Costerton *et al.,* 1995; Nguyen *et al.,* 2012). Furthermore, the bacterial cell surface and associated EPS contain ionizable functional groups that allow

binding of various metal elements (Jang *et al.,* 2001; Dong *et al.,* 2000; Warren and Haack, 2001; Hua *et al.,* 2013). Therefore, metal-binding tendencies, along with the dynamic geochemical conditions created within biofilm micro-environments, may significantly impact Fe-binding and microscale speciation within the DTMF.

Most uranium tailings research has involved investigation of microbial community composition and biogeochemical potential in radionuclide-contaminated environments (Anderson *et al.,* 2003; Vrionis *et al.,* 2005; Rastogi *et al.,* 2010). In general, studies that conducted *in situ* measurements at contaminated aquatic sites were, in fact, evaluating *in situ* uranium bioremediation attempts of contaminated groundwater (Anderson *et al.,* 2003; Vrionis *et al.,* 2005). We present the first investigation of the effects of microbial activities on the behavior of metal elements of concern in a water column covering a highly alkaline uranium tailings body at an active tailings management facility. For this purpose, microbial biofilms formed *in situ* on coupons incubated in the DTMF water column were investigated in terms of microbial diversity, structure/composition, metal absorption/interaction as well as microenvironmental effects on the redox state of Fe.

## 2.3 Material and methods

### 2.3.1 *In situ* biofilm development

Four polycarbonate slides (1 cm wide, 11 cm long and 2 mm thick) affixed to holders were vertically suspended in the DTMF water column at 13 m intervals (1, 13, 27, 41 m) for an approximate 3 month interval during the ice free period from May to August, 2011. The holder array was located at the E2 site (Khan *et al.,* 2013), positioned approximately at the center of the DTMF. On retrieval, the coupons were placed in a primary container filled with water obtained

from corresponding depths of the DTMF water column. Samples were stored at 4° C until processing, which took place within 3 days of sample collection.

### 2.3.2 Biofilm chemical analysis

Since the concentrations of metal elements accumulated by the biofilm were expected to be low, one polycarbonate slide per depth was used for inductively coupled plasma-mass spectrometry (ICP-MS) analysis, with the exception of the 27 m depth, where only half of the slide was used because one of the polycarbonate slides became dislodged from the holder. Since our installation in the DTMF was limited to a single array of coupons suspended at the E2 site, only one sample was subjected to ICP-MS analysis. Accordingly, biofilm material on each slide was digested in 3 ml ultrapure 8 N $HNO_3$ and 0.5 ml reagent-grade $H_2O_2$ solution mixture. Aliquots (0.2 ml) of internal standards (Be, Ge, and In) of known concentration were also added to each sample, to a final concentration of 50 ppb. Ten milliliters of Milli-Q water was added to the solution mixture containing the polycarbonate slides after 12 hours shaking, followed by shaking for an additional 4 hours. ICP-MS analyses were carried out using a Perkin Elmer Elan 5000 ICP-MS with the following settings: 1000 W RF power; 10 L $min^{-1}$ cooling gas; 0.8 L $min^{-1}$ intermediate gas; 0.85 L $min^{-1}$ nebulizer gas; B lens setting of 45; P lens setting of 45; E1 lens setting of 25; and S2 lens setting of 45 (Jenner *et al.,* 1990; Longerich *et al.,* 1990; Stefanova *et al.,* 2003).

### 2.3.3 Bacterial cell counts and colony isolation

Prior to removal of biofilm material from whole polycarbonate slides, they were rinsed with pH 8, Tris-EDTA (TE) buffer. The biofilm material was then removed by scraping, re-suspended in TE buffer, and plated, in triplicate, on both Reasoner's 2A (R2A) and 5 % trypticase soy agar (TSA) (Difco media, Franklin Lakes, NJ, USA) followed by incubation under

aerobic conditions at room temperature (22± 2° C) for 15 days, at which time visible colonies were enumerated. Phenotypically distinct colonies were selected for isolation and subsequent 16S rRNA-based identification, as described by Bondici et al. (2013).

### 2.3.4 DNA extraction and Ion Torrent 16S rRNA gene sequencing

Pre-rinsed biofilm material removed from whole coupons were re-suspended in Tris-EDTA buffer and centrifuged for 20 min at 4000 rpm. DNA extraction from the resultant pellets was carried out using the FastDNA SPIN kit (MP Biomedicals, Solon, OH) following the recommended protocol. DNA samples were coded for Ion Torrent sequencing using specific adapter-linked primers (E786F and U926R) (Baker *et al.,* 2003) targeting the V5 region of the 16S rRNA gene (the underlined region of the primer, below, represents the specific gene target-region). The forward primer also contained a key tag and a multiplex identifier (MID) specific to each sample used on the Ion Torrent chip. The sequence of the forward and reverse primers were F5' CCATCTCATCCCTGCGTGTCTCCGACTCAG**MID**GATTAGATACCCTGGTAG and R5'- CCTCTCTATGGGAGTCGGTGATCCGTCAATTCCTTTRAGTTT, respectively. The PCR amplicon preparation, Ion Torrent sequencing, and data processing were carried out according to Bondici et al. (2013). The MIDs used for the DNA samples obtained from the four depths (from the surface) of the tailings water column were as follows: TACTC (1 m), ACGAG (13 m), TCGTC (27 m) and ATCAG (41 m). Biofilm DNA extracts were PCR-amplified in a 50 µl reaction mixture consisting of 1.0 µmol $l^{-1}$ primers, 1.0 U *Taq* polymerase (Invitrogen, Carlsbad, CA, USA), 1.0 µmol $l^{-1}$ $MgCl_2$, 1.0 × PCR buffer (both provided with the Taq polymerase), and 4.0 µmol $l^{-1}$ of deoxyribonucleotide triphosphates (dNTPs). PCR cycling parameters included an initial denaturation at 95°C for 5 min, followed by 40 cycles of denaturation at 95°C for 30 s, annealing at 57°C for 30 s, extension at 72°C for 45 s, and final

extension at 72°C for 10 min. A Qiagen gel purification kit (Qiagen Sciences, Germantown, MD, USA) was used for PCR amplicon purification. The pooled, multiplexed purified products were sequenced using an Ion Torrent Personal Genome Machine (Life Technologies, Carlsbad, CA, USA) at the National Research Council (Montreal, Quebec, Canada). The RDP pipeline Initial Process Tool was used to remove low-quality sequence data. Taxonomic affiliation of the quality sequences was obtained through the RDP classifier with a bootstrap cut-off value of 50%. Lastly, the four sequence libraries were compared using Unifrac analysis based on the phylogeny derived from the GreenGene core data set (Hamady *et al.,* 2010).

### 2.3.5 Biofilm staining and confocal laser scanning microscopy (CLSM) analysis

One whole polycarbonate slide from each water column depth was subjected to CLSM biofilm analysis, except for the sample obtained from 27 m depth, where only one-half a polycarbonate slide was available for study. Biofilm samples were treated with a panel of fluorescent probes and examined using CLSM. Staining was carried out according to Neu et al. (2001), as follows: fluorescently conjugated lectins were dissolved at a concentration of 100 μg $ml^{-1}$ in filter-sterilized (0.2 μm) DTMF water and then 100 μl of lectin-fluor solution was directly applied to biofilm that had colonized the surface of the polycarbonate slide. The samples were incubated for 20 min at room temperature, and then the excess lectin-fluor was rinsed off with sterile water. To avoid desiccation, the stained biofilm samples were flooded with sterile water. To target total bacteria in the biofilms, Syto 9, a membrane-permeant, green fluorescent nucleic acid stain, was used. Algae and photosynthetic bacterial cells were detected by autofluorescence (ex 647, em 680). Diversity in EPS was investigated using the following lectin-fluor conjugates: *Arachis hypogaea*-, *Ulex europaeus*-, *Canavalia ensiformis*-fluorescein isothiocyanate (FITC), wheat germ agglutinin-tetramethyl rhodamine isothiocyanate (TRITC),

and glycine max-Alexa 488. The lectins had the following saccharide specificities; β-D-Gal (1-3)-D-GalNac targeted by *Arachis*; α-L-fucose by *Ulex;* α-D-Man and α-D-Glc by *Canavalia*; D-GalNac by *Glycine;* and N-acetyl-gluscosamine/lipopolysacharide by wheat germ agglutinin (Goldstein and Hayes, 1978; Wolfaardt *et al.,* 1997). Fluorescent lectins were purchased from Sigma-Aldrich (St. Louis, MO, USA).

Biofilm optical thin sections were obtained using a Bio-Rad MRC 1024 Lasersharp fluorescence scanning laser system mounted on a Nikon Microphot SA microscope equipped with either 10 or 40X water-immersible objectives. The images were acquired as a single XY scan or XY series where the sectioning interval was 5 µm. Four coupon subsamples, each 1 cm in length, were used for each fluorescent lectin probe. Images were taken from 5 random regions from each of the 1 $cm^2$ subsamples. The Syto 9 and wheat germ agglutinin-TRITC stains were used in combination during dual-channel optical thin sectioning, due to the well-separated excitation-emission wavelengths of these two fluorophores. The acquired images were processed using NIH Image version 1.61 http://rsb.info.nih.gov/nih-image/download/nih-image.

CLSM image data was then subjected to principle components analysis (PCA) using PRIMER v6 software (PrimerE, Ltd., Lutton, UK). Eigenvalue decomposition analysis was performed on a dataset containing the following variables: photosynthetic bacteria, total bacteria, and five lectins (*Arachis hypogaea*-, *Ulex europaeus*-, *Canavalia ensiformis*-fluorescein isothiocyanate (FITC), wheat germ agglutinin-tetramethyl rhodamine isothiocyanate (TRITC), and glycine max-Alexa 488). The analysis of similarity (ANOSIM) and similarity percentage (SIMPER) tests were also generated to further confirm significance.

### 2.3.6 Scanning Transmission X-ray Microscopy (STXM) and X-ray Fluorescence (XRF)

Metal speciation and distribution in the biofilm were studied using scanning transmission X-ray microscopy (STXM) and X-ray Fluorescence (XRF) at the soft X-ray microspectroscopy (SM) beamline of the Canadian Light Source (CLS). A small volume (1 μL) of biofilm material was carefully removed from a polycarbonate coupon to maintain an intact biofilm and aseptically transferred onto an X-ray transparent silicon nitride window. Biofilm material from three depths (1, 27 and 41 m) was subjected to STXM analyses. X-ray data was collected at the metal's respective 1s, or 2p, absorption edges (Dynes *et al.,* 2006). Stacks of absorption images were thus recorded using the 280-288.2 eV, 720-780eV, 700-730 eV, 1315-1350 eV and 1420-1450 eV photon energy ranges for C, U, Fe, As and Se, respectively, with a 1 ms dwell time/pixel, over a minimum scan area of 4 $\mu m^2$. Recorded images were aligned using Axis2000 software to correct for lateral shifts of the X-ray beam on the area of interest (Hitchcock, 2008; Jacobsen *et al.,* 2000). Once the images were aligned, absorption spectra were obtained by converting transmitted signals to optical density using the incident flux signal through areas on the window absent of biofilm. The major species of interest were mapped by fitting the stack to a linear combination of suitable reference spectra using stack fit (Dynes *et al.,* 2006). Reference spectra were utilized to create the component maps of biomolecules and metal species (Lawrence *et al.,* 2003; Dynes *et al.,* 2006).

Arsenic, one of the main elements of concern in the DTMF system, could not be detected using STXM, therefore additional steps were taken for its detection in an attempt to relate its speciation and mapping to that of Fe (III) reduction by microbial processes. Accordingly, XRF, which has a significantly lower detection limit (by one order of magnitude) in comparison to STXM (Hitchcock *et al.,* 2012), was used. Biofilm samples from the water tailings interface,

where STXM analysis had previously indicated the occurrence of microbial iron reduction, were re-analyzed by collecting X-ray fluorescence spectra. During this process, a larger area was scanned (13 $\mu m^2$), including the area that was previously investigated by STXM. X-ray fluorescence yield was recorded from 1300 eV to 1356 eV, covering the Mg 1s and As 2p edges, while concurrently obtaining the transmitted X-rays (Hitchcock *et al.,* 2012).

## 2.4 Results

### 2.4.1 Accumulated metals and metalloids in biofilm grown *in situ*

In general, the majority of the elements accumulated within the biofilm measured using ICP-MS did not show a specific trend (Table 2.1). Biofilms grown nearest to the tailings interface had relatively lower concentrations of Ca, Mn, and Se; however, V and Mo were approximately 6X and 5X higher, respectively, and Pb 19X higher, in comparison with biofilms from the 1 m depth. Similarly, the concentration of dissolved V and Mo increased and Mn decreased with depth in the water column (Supplemental data, Table 9.1). In the case of Fe, the concentrations measured within the biofilm paralleled that of the dissolved Fe concentration in the water. The Fe concentration measured in 1 $cm^2$ of biofilm recovered from 27 m was only 4 times lower than the dissolved Fe within 1.0 l of tailings water. The highest concentration (1.1 $\mu g/cm^2$) of biofilm-accumulated Fe was measured in biofilms from the 27 m depth, where the pH was ~7; whereas, the lowest concentration of Fe (0.14 $\mu g/cm^2$) was measured in biofilms from the 13 m depth where the pH was ~ 6.2. According to the geochemical characteristics of the water column, the sum of ions (1.3 to 2.6 g/l), pH (6.54 to 9.44) and total alkalinity (4 to 70 mg/l) all increased with depth (Supplemental data, Table 9.1).

**Table 2.1 Concentration (µg) of metal elements in biofilms grown on 1.0 $cm^2$ polycarbonate coupons positioned at 1.0, 13, 27, and 41 m in the DTMF water column.**

| Depth (m) | Mg | Al | Ca | V | Cr | Mn | Fe | As | Se | Mo | Pb | U |
|---|---|---|---|---|---|---|---|---|---|---|---|---|
| **1** | 0.098 | 0.771 | 1.862 | 0.001 | 0.002 | 0.011 | 0.143 | 0.056 | 0.005 | 0.008 | 0.006 | 0.166 |
| **13** | 0.095 | 0.121 | 2.025 | 0.001 | 0.001 | 0.01 | 0.139 | 0.007 | 0.003 | 0.005 | 0.003 | 0.048 |
| **27** | 0.578 | 2.323 | 3.812 | 0.015 | 0.005 | 0.038 | 1.096 | 0.096 | 0.005 | 0.034 | 0.107 | 0.269 |
| **41** | 0.098 | 0.610 | 0.809 | 0.006 | 0.002 | 0.006 | 0.185 | 0.005 | 0.000 | 0.042 | 0.115 | 0.150 |

### 2.4.2 Bacterial cell count and taxonomic affiliation

The total number of culturable cells per $cm^2$ of biofilm material at different depths was all within the same log range: $3.3 \times 10^4$ at 1.0 m depth (top), $3.8 \times 10^4$ at 14 m, $2.4 \times 10^4$ at 27 m and $8.1 \times 10^4$ at 41 m, nearest the tailings/water interface (bottom). Twenty-one morphologically distinct colony types were isolated after 3 subculture passages. Partial sequencing of the 16S rRNA gene (spanning the first three variable regions; ~500 bp) revealed the presence of 16 unique bacterial isolates that affiliated into four phyla: *Actinobacteria*, *Bacteroidetes*, *Proteobacteria* and *Firmicutes* (Figure 2.1). DNA sequences were submitted to the EMBL database. The accession numbers for the partial 16S rRNA gene sequences are LK022086 to LK022101**.**

### 2.4.3 Microbial community structure revealed by Ion Torrent sequencing

After the removal of low-quality and unclassified non-16S rRNA sequences, a total of 24250 high-quality sequence reads were generated using Ion Torrent sequencing, including 5618, 5992, 7206, 5434 sequences representing biofilm DNA libraries obtained from the 1, 13, 27, and 41 m water column depths, respectively.

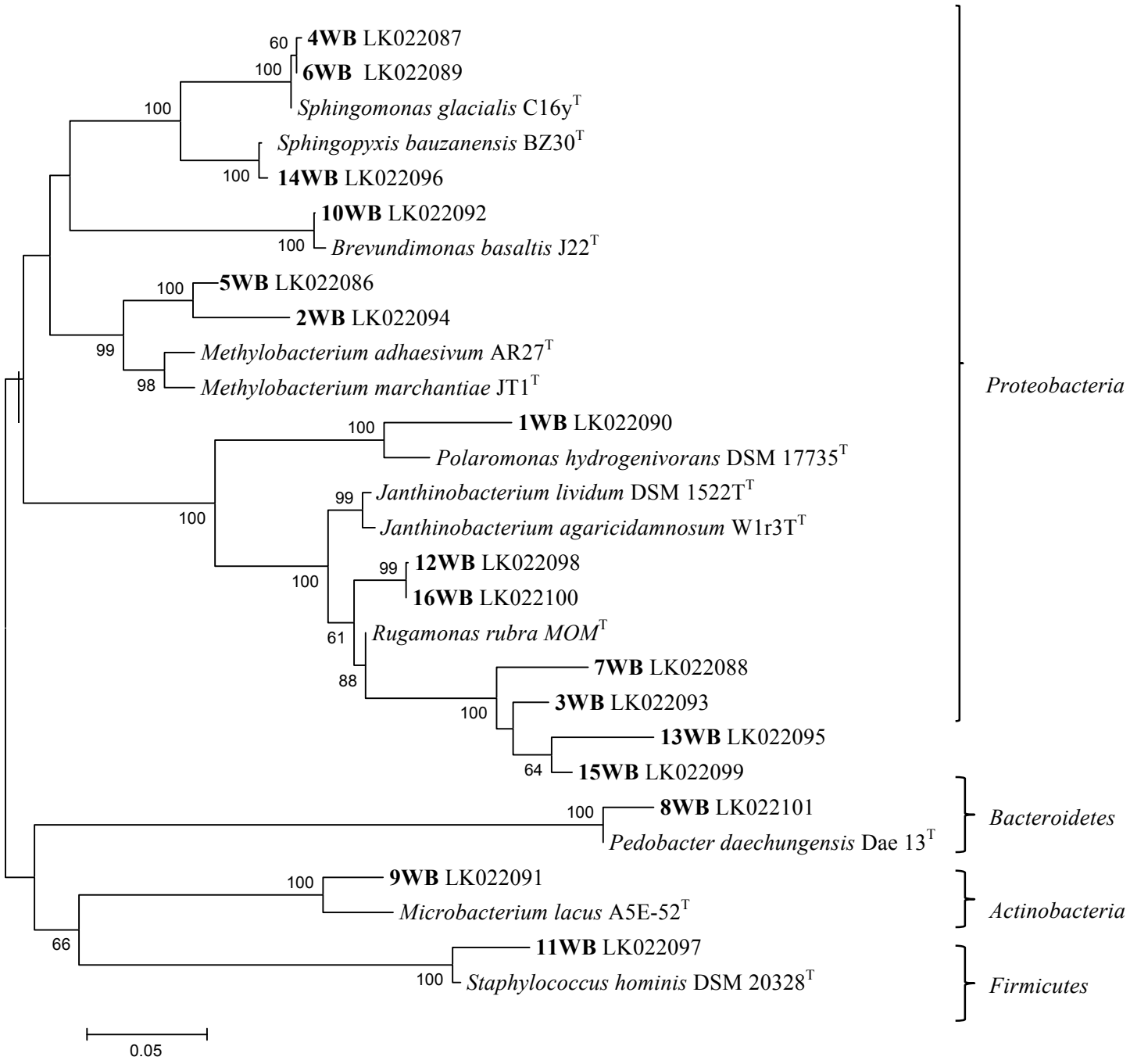


**Figure 2.1 Neighbour-joining phylogenetic tree of 16 distinct bacterial isolate sequences along with corresponding 16S ribosomal reference sequences.**

The evolutionary distances were computed using the Maximum Composite Likelihood method. Bootstrap analysis (1000 replicates) was used to test reliability of the trees and values are indicated at the nodes. The scale bar is equal to 5% sequence variation. Sequence names are indicated by numbers followed by their source, W-water and B-biofilm. Accession numbers are also indicated after the sequence name.

Phylogenetic analysis led to the classification of the total unique sequences of the four libraries into 11 taxonomic groups: *Proteobacteria*, *Planctomycetes*, *Chlorobi*, *Cyanobacteria/Chloroplast*, *Fusobacteria*, *Nitrospira*, *Chlamydiae*, *Acidobacteria*, *Firmicutes*, *Actinobacteria*, and *Bacteroidetes* (Figure 2.2). The sequence reads affiliated into 62, 113, 111 and 75 genera corresponding to depths of 1, 13, 27 and 41 m, respectively. *Proteobacteria* was the most prevalent phylum, accounting for more than 75% of the bacterial community sequence diversity in all of the libraries. The proportion of *Alphaproteobacteria* was highest at the 1 m depth, but then decreased with depth; whereas, the proportion of *Betaproteobacteria* increased with depth. *Bacteroidetes* were the second most-abundant phylum, with the highest proportion of sequences in the biofilms from the 1 m depth. Biofilms from the 13 and 27 m depths contained the highest number of taxonomic groups, and included all 11 identified phyla.

Predominant *Betaproteobacterial* sequences affiliated with the genus *Polaromonas* were detected from each depth, and at the 1.0 m depth represented 39.5% of the total sequences classified to genus level (Figure 2.3). The most abundant *Alphaproteobacteria* sequences belonged to *Methylobacterium,* with 41 and 22.5% abundance seen at the 1.0 and 13 m depths, respectively; however, at the 27 m depth, *Dechloromonas* and *Aquabacterium* respectively contributed to 41.5 and 22.7% of the detected sequence diversity. At the 41 m depth, *Polaromonas,* along with *Acidovorax,* both belonging to the *Betaproteobacteria,* were the most abundant genera (Figure 2.3). It was apparent that biofilms, which developed at 13 and 27 m had the highest diversity in terms of number of genera identified; approximately half of which were shared. Furthermore, the number of different genera from the middle depths was approximately 50% greater than that detected at the top (1 m) and bottom (41 m) depths. A bacterial group known to reduce iron, *Ralstonia,* was also detected in biofilms developed at each depth in the

DTMF. Sulfate reducing bacteria represented by *Desulfosporosinus* and sulfur, thio-sulfate and sulfite reducing bacteria represented by *Desulfitibacter and Dethiobacter* were found only at lower depths.

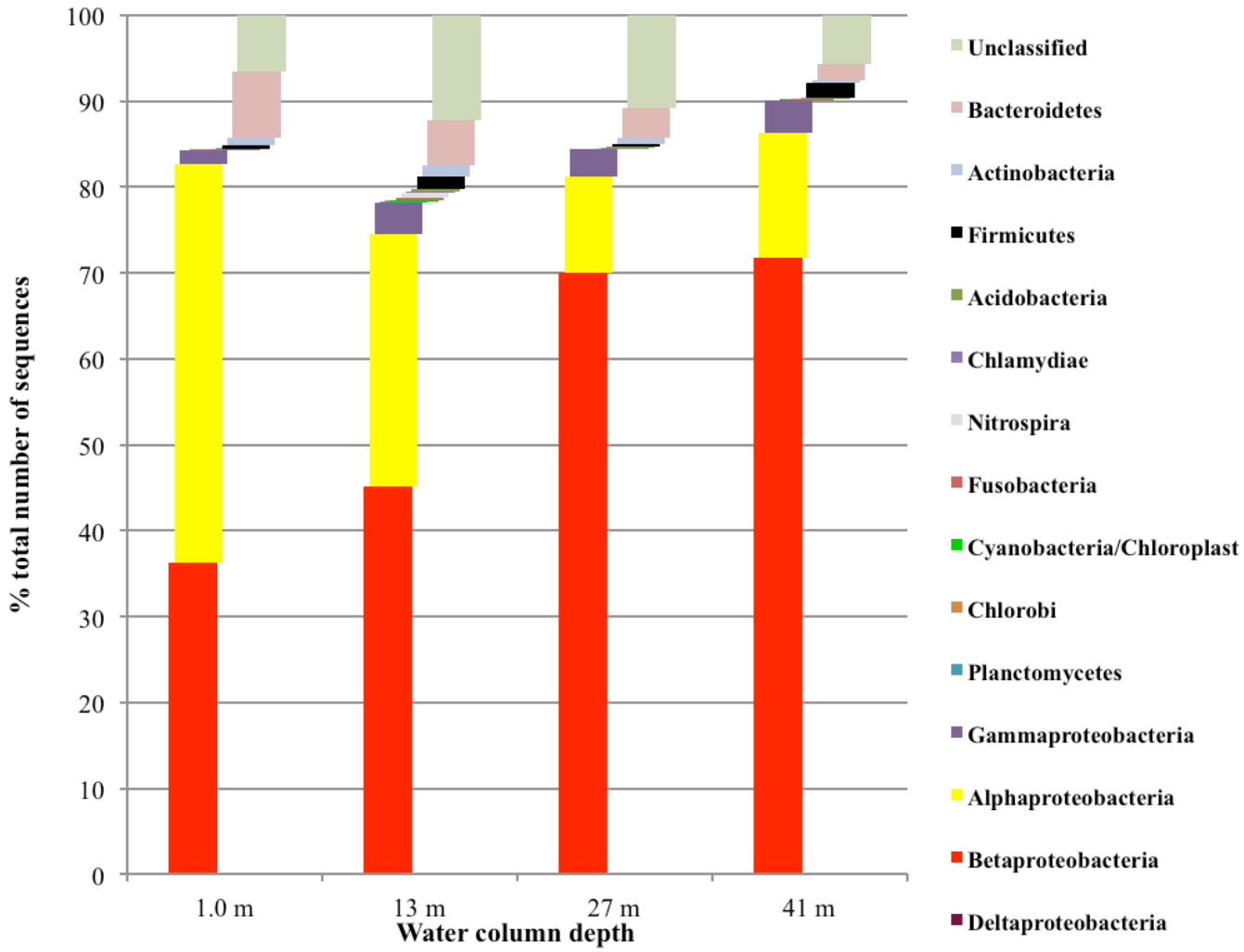


**Figure 2.2 Taxonomic classification of bacterial 16S rRNA partial gene sequences (V5 variable region) obtained by Ion Torrent sequencing technique.**
Each library represents DNA extracts from biofilms grown at 1.0, 13, 27, 41m depth in the DTMF water column.

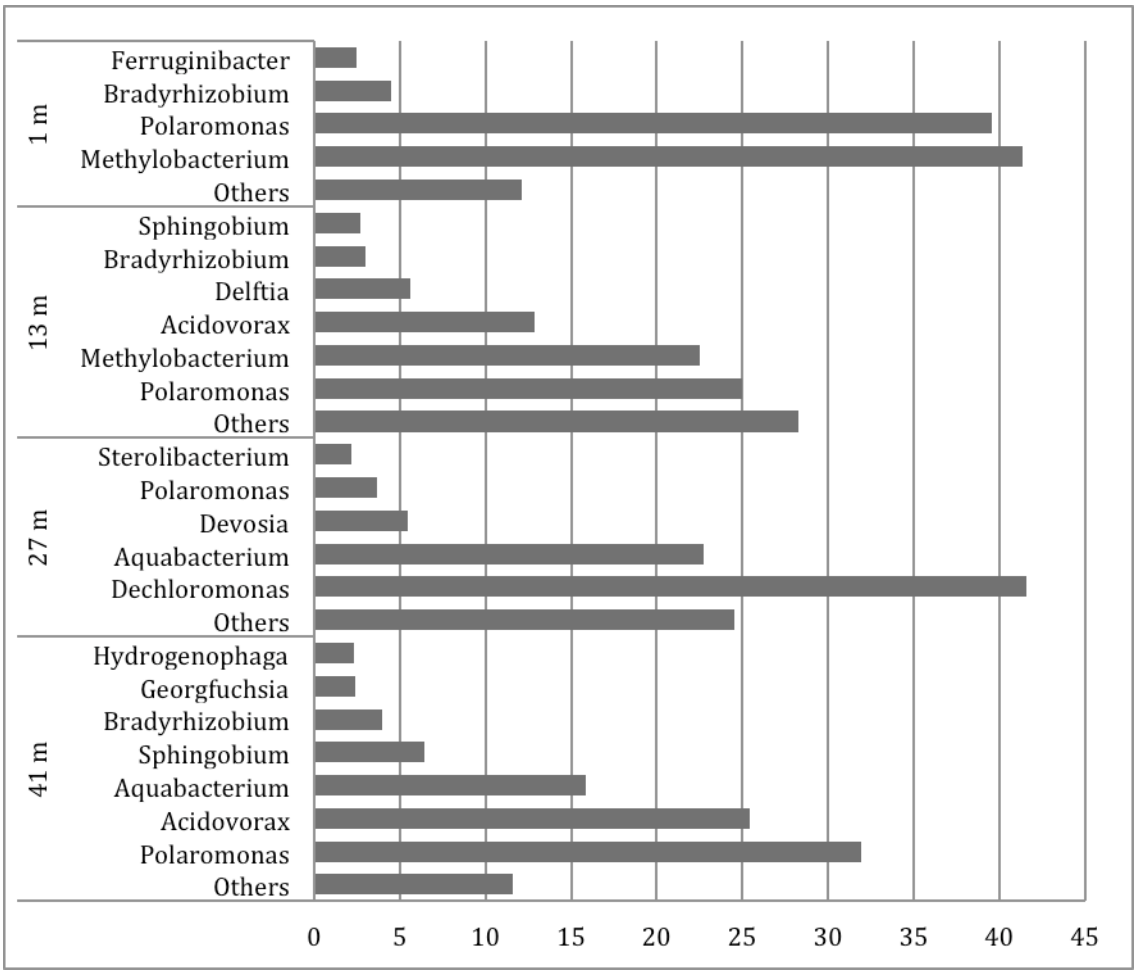


**Figure 2.3 Distribution of the most abundant bacterial genera inhabiting biofilms grown at 1.0, 13, 27, 41 m depths in the DTMF water column overlying the uranium tailings body.** 16S rRNA partial gene sequences obtained by Ion Torrent sequencing technique were used for the classification. Only genera representing higher than 2% of the total sequence reads classified at genus level are shown, the rest are grouped as Others.

Comparison of the phylogenetic composition of the four sequence libraries with Unifrac distance statistical analyses showed that biofilm microbial composition from the 13 m depth was significantly different ($p<0.05$) from the top (1 m) and bottom (41 m) layers (Table 2.2). To further validate the detected dissimilarities of the libraries, the probability of difference between the most abundant taxa in each library was determined using the RDP LIB (Ribosomal database

project library) compare tool. The probability of equal distribution of *Proteobacteria* taxon members was investigated in libraries that showed a significant difference. The obtained significance, $6 \times 10^{-14}$, between libraries from the 13 m and 1.0 and 41 m depths, indicated that differences in frequency of the main taxa members may have also contributed to the observed difference between the libraries. Microbial composition in biofilms recovered from the 27 m depth did not differ significantly from biofilms, which developed at other depths, including 13 m.

**Table 2.2 Statistical significance (p-values) of differences among the bacterial communities of biofilms obtained from DTMF water column using Unifrac distance analyses.**

| **Ion Torrent libraries of biofilms** | **1 m** | **13 m** | **27 m** | **41 m** |
|---|---|---|---|---|
| **1 m** | | <0.05 | >0.1 | >0.1 |
| **13 m** | | | >0.1 | <0.05 |
| **27 m** | | | | <0.1 |

P-test significance was based on 500 permutation and P values were corrected for multiple comparisons (Bonferroni correction).

### 2.4.4 Biofilm composition

Principle component analysis was used to detect components responsible for the largest variations in the biofilm image dataset (Figure 2.4). The highest eigenvalues (3.25 $e^3$ and 931) represented the largest variation in the data and were identified as the first (PC1) and second (PC2) principle components, respectively. The score plot of PC1 and PC2, which accounted for 78.9% (61.3% for PC1 and 17.6% for PC2) of the total variation in the dataset, grouped the biofilms obtained from the 4 depths into 2 major clusters (Figure 2.4). PC1 separated the biofilm samples grown closest to the tailings-water interface from the other biofilm samples; furthermore, a high correlation between PC1 and wheat germ agglutinin/ulex binding (-0.557 and

-0.488) indicated that these variables were responsible for most of the variation. The abundance of bacteria with a high correlation (0.847) with PC2 showed that this variable was responsible for the next largest variation. The presence of photosynthetic bacteria and algal biomass also contributed to the difference having the highest correlation with PC4, which accounted for 6.4% of the total variation. Although the photosynthetic biomass did not differ significantly within the water column ($p<0.328$), the lowest abundance was detected at the tailings-water interface.

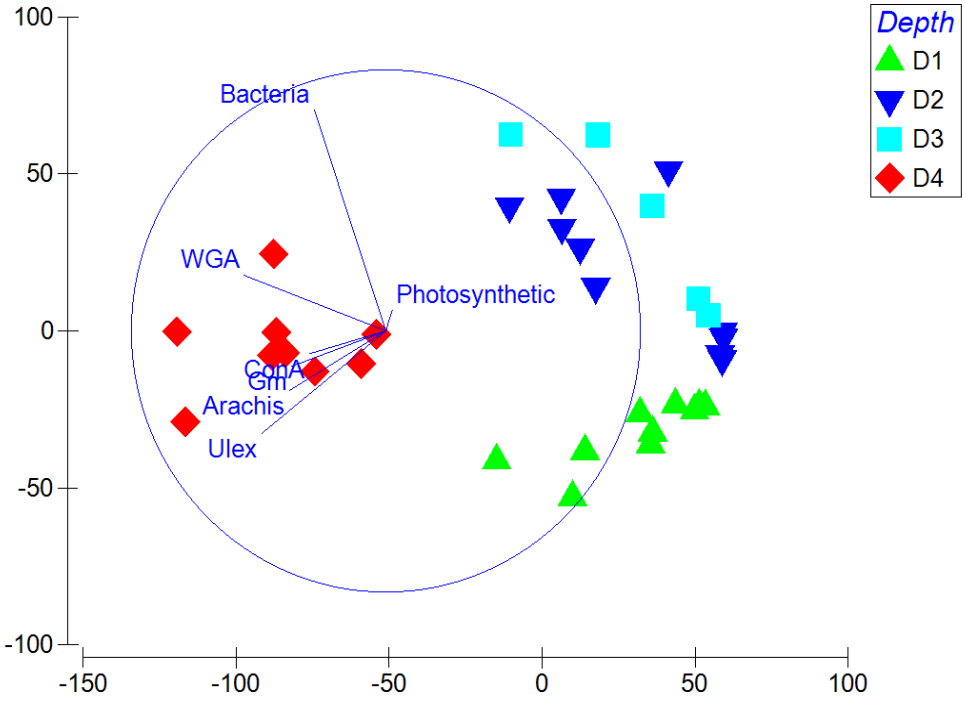


**Figure 2.4 Results of principal components analysis (PCA) of biofilm grown at 1.0, 13, 27, 41 m depths in the DTMF water column analyzed using CSLM.**
Total bacteria were detected using Syto 9 green fluorescent nucleic acid stain.
Various elements of EPS were stained with lectins conjugated with fluorescein isothiocyanate (FITC), tetramethyl rhodamine isothiocyanate (TRITC) or Alexa 488: *Arachis hypogaea*-, *Ulex europaeus*- , *Canavalia ensiformis*-FITC, wheat germ agglutinin-TRITC, and glycine max-Alexa 488. (D- depth; D1- 1.0 m; D2-13 m; D3-27 m; D4-41 m).

ANOSIM (global R = 0.618; number of permutations = 999) also confirmed that the composition of microbial biofilms closest to the tailings-water interface (41 m depth) was significantly different from biofilms grown at the 1.0 m ($p < 0.001$; $R = 0.976$), 13 m ($p < 0.001$; $R = 0.925$) and 27 m depths ($p < 0.001$; $R = 0.998$). Based on SIMPER analysis, which determines variation between and within samples, the abundance of wheat germ agglutinin binding to EPS was again identified as the variable that primarily contributed to the dissimilarity between biofilms obtained from 41 m and biofilms which developed at the other depths in the DTMF water column.

### 2.4.5 STXM mapping of biochemistry and metal speciation in biofilm

Scanning transmission X-ray microscopy was used to map Fe, Se, As, U in the context of the biological components of the biofilms grown *in situ* at three depths (1, 27 and 41 m).The primary elements of concern (Se, As, U) were below the STXM detection limit in all scanned samples; on the other hand, Fe and organic C were identified in every biofilm sample. STXM data obtained from biofilm grown at 41 m is shown for illustration purposes (Figure 2.5). The C 1s absorption image (Figure 2.5A) illustrates the presence of organic carbon in the biofilm sample from the tailings-water interface, wherein a cluster of bacterial cells can be distinguished within the biofilm. Biochemical components (protein, polysaccharides, and lipids) of the biofilm and cells are shown in Figure 2.5-B2. Distribution of Fe (II) and Fe (III) within the biofilm sample were determined at the Fe 2p absorption edge recorded at the same location as for carbon. To obtain the best fitted spectra, iron spectra were extracted from various other regions and compared to Fe (II) and Fe (III) reference spectra. Both valence states showed a double-peaked signal, but with different intensities: the major peak for Fe (II) is at 708.0 eV; whereas, for Fe (III) the major peak is at 709.8 eV.

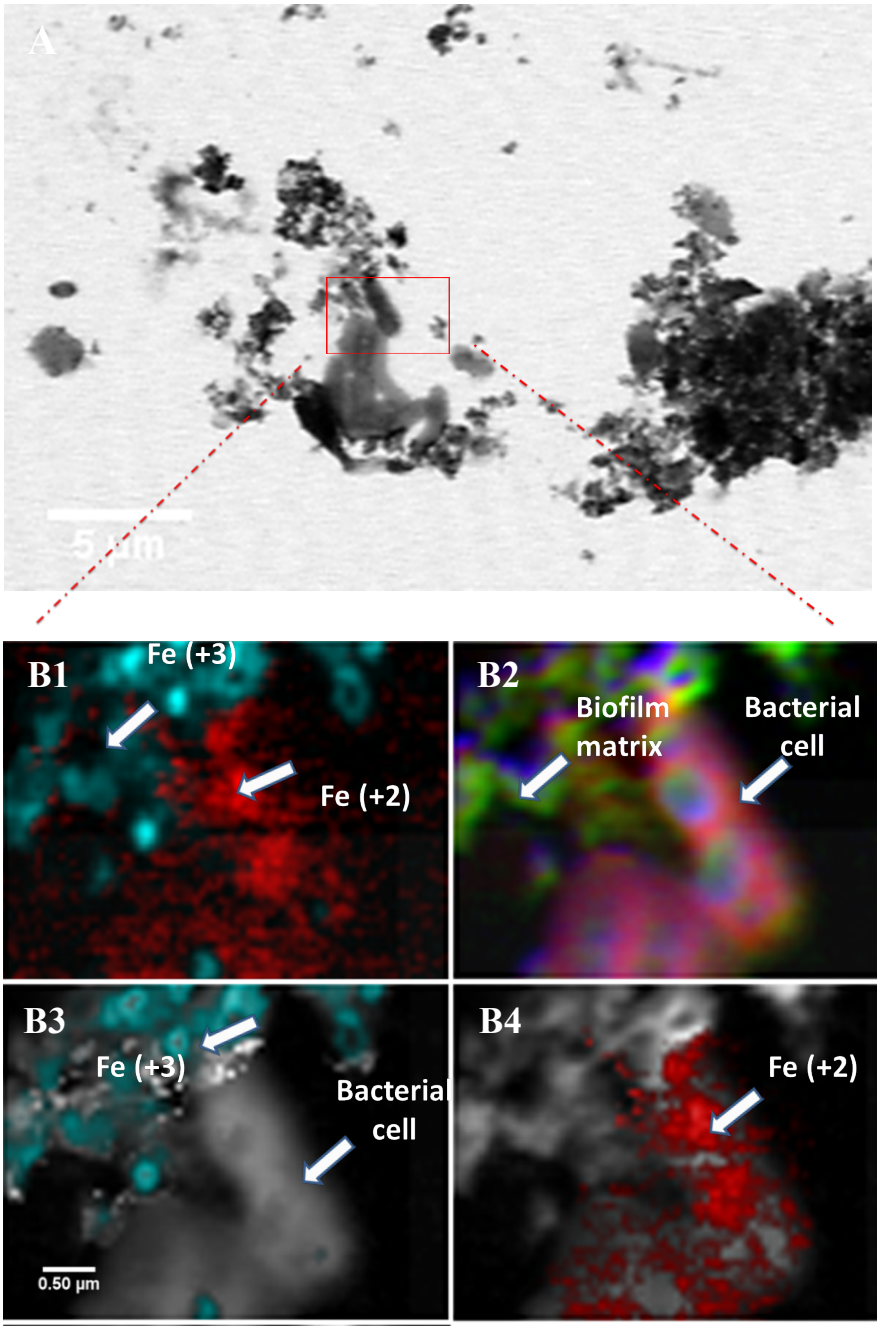


**Figure 2.5 Color coded composite map of C and Fe in the biofilm from the tailings-water interface.**

A) C 1s absorption image representing organic carbon in the biofilm sample. B1) Iron component map derived by fitting an energy sequence of images (stack) of the Fe L2,3-edge (139 images from 699-730 eV, 1 ms/pixel). Colors: cyan= Fe (III); red= Fe (II). B2) Individual carbon component maps by fitting stack of the C K-edge (116 images from 280-320 eV, 1 ms/pixel). Colors: red=protein; blue=lipid; green=polysaccharides. B3) Overlaid composite map of Fe (III) and carbon. B4) Overlaid composite map of Fe (II) and carbon.

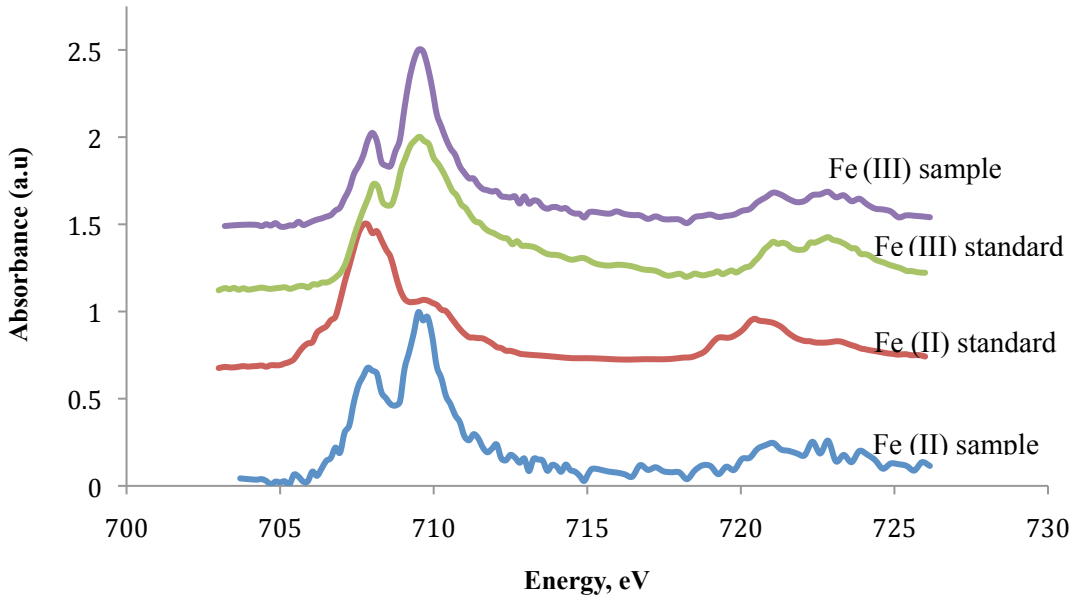


**Figure 2.6 Fe 2p X-ray absorption spectra of $FeCl_2 \cdot 4H_2O$, Fe $Cl_3 \cdot 6H_2O$ standards and Fe (II), Fe (III)-rich location in the biofilm sample grown at the water tailings interface.** (represented in Figure 2.5B1).

Comparison of the obtained Fe (III) spectrum to the reference spectra revealed the presence of Fe (III). From the Fe (II) spectrum, it was apparent that the reduced iron was present in mixed-valence form, having two peaks at 708.0 eV and 709.8 eV that are characteristic of Fe (II) and Fe (III), respectively (Figure 2.6). Iron spectra obtained from biofilm samples from 1 and 27 m also indicated presence of Fe (II) (Supplemental data, Figure 9.2). The iron oxidation state was quantified from the selected region by using curve fitting to the reference spectra of $FeCl_2$ and $FeCl_3$, the results of which showed that approximately 20% of the total iron was Fe (II) in the biofilm grown at 41 m. The iron component map indicated that the reduced form of Fe was mainly located on the surface of the bacterial cells, with a small portion of reduced Fe, along with the oxidized form of Fe, appearing within the biofilm matrix (Figure 2.5). In an attempt to detect arsenic, the more sensitive XRF method was employed but was not successful in detecting

As. Since the Mg 1s absorption edge overlaps with the As 2p edge, at the high Mg concentrations present in the sample it was suspected that possible presence of relatively low concentrations of As (if present at low concentrations) was masked (data not shown).

## 2.5 Discussion

### 2.5.1 Metal element content of biofilms

Uranium mill tailings contain relatively high concentrations of elements of concern (e.g., As, Ni, Mo, Mg, Se, V, Pb, U) that are liberated following the extraction of the uranium ore. In general, it is anticipated that water bodies covering tailings management facilities would, to a certain extent (i.e., most significantly at tailings-water interfaces), reflect the physiochemical characteristics of the deposited uranium tailings. Accordingly, the pH and the total dissolved solutes of the DTMF water were highest near to the tailings-water interface as this is where the chemistry of the water would be most affected by the expulsed pore water (caused by the compression of the tailings mass under its own weight, essentially squeezing water from the pore spaces) from the tailings body. In fact, previous *in situ* pore water measurements obtained from tailings materials from the interface region (~450 m asl) at other boreholes (Shaw *et al.,* 2011) agree with the water chemistry obtained near the tailings-water interface at 41 m. The pH (9.44) of this zone reflected the pH of the deposited tailings; whereas, the pH of the water in the overlying zones was several units lower. Thus, there was a gradual increase of pH with depth from approximately 6.5 to 9.5, as follows: pH ~6.5 (1 m to 16 m); pH ~ 7 (21 m to 26 m); pH ~ 8 at 31 m and pH ~ 9 (36 to 41 m). A relatively acidic zone, with a pH of 6.19, was measured at the 11 m depth. A similar pH profile was observed in August 2010 at three DTMF locations (Khan *et al.,* 2013). Recent measurements (September, 2013) showed pH values of < 6 in the first 25 m and a relatively alkaline pH (8.4) at 28 m; however, a similar pH stratification trend

still remained throughout the water column (data not shown). Since the DTMF is an open system, rainwater may directly enter or drain into the pit from the surroundings, thereby creating a pH gradient due to slow mixing. Similarly, the majority of the metal elements also exhibited a gradient throughout the water column, with increases or decreases in metal concentration corresponding with increases or decreases in pH.

The spatial and temporal distribution of pH within the water column may predict the adsorption potential of the measured soluble species and may also provide insight regarding the biogeochemical potential and buffering capacity of this water system (Jourabchi *et al.,* 2005). Reduced concentrations of dissolved Ni, Mg, Mn, Zn, and Cu at pH ~9 indicated adsorption/co-precipitation of these elements under alkaline conditions (Aziz *et al.,* 2008). Sequestration and solubility control of elements of concern by ferrihydrite (Moldovan *et al.,* 2003; Essilfie-Dughan *et al.,* 2011, 2012; Shaw *et al.,* 2012) and Mg-Al hydrotalcite at alkaline oxic conditions is well-understood in the DTMF system (Gomez *et al.,* 2013). However, increased dissolved concentration of As and Se close to the tailings-water interface, despite alkaline conditions, is probably due to the presence of expulsed pore water at the interface that contains these elements at relatively higher concentrations, possibly in conjunction with saturated complexation sites on the minerals.

Biofilms can be considered as integrative indicators of a system's chemistry due to their constituent properties, such as ionizable functional groups (Ancion *et al.,* 2013). Metal accumulation within biofilms is well-documented (Dong *et al.,* 2000; Warren and Haack, 2001; Dynes *et al.,* 2006; Hitchcock *et al.,* 2009; Hua *et al.,* 2013). The retention of elements is mainly governed by the anionic biopolymers present in the biofilm (various polysaccharides, lipids, lipoproteins, nucleic acids, etc.). Direct absorption of metal elements from the bulk phase also

depends on the pH, solubility and concentration of bioavailable metals (Jang *et al.,* 2001). In general, acidic conditions contribute to the release of bound ions, while alkaline pH favors their chelation and binding (Decho, 2000). At acidic pH, the carboxylates and phosphates are uncharged; conversely, under neutral or alkaline conditions, the number of ionized acidic groups increases and metal cations tend to be adsorbed (Ferris *et al.,* 1989). Therefore, the accumulation of higher concentrations of V, Mo, and Pb by biofilms at lower depths would most likely be due to the effect of the alkaline pH. Interestingly, accumulation of various elements (As, Se, Al, Mg, U) in the biofilm samples grown in upper regions of the DTMF (pH ~6.5) was also detected. In general, especially during the summer, biofilms grown near surface water are exposed to intense UV irradiation. EPS, which play a role in the retention of metal elements, undergo post-secretive modification due to UV irradiation (Kieber *et al.,* 1990; Decho, 2000). As a result, more carboxyl groups become available for cation binding (Kieber *et al.,* 1990). Furthermore, highly structured microenvironments within biofilms may also create local pH differences (favorable to cation or anion binding) due to respiratory activities relative to the bulk phase or macroenvironment (Decho, 2000).

In general, the Fe concentrations sequestered within biofilms varied with depth and paralleled the dissolved Fe in the DTMF water column. Iron precipitation or accumulation within the biofilm matrix surrounding bacterial cells has previously been detected and its modulatory effects on geochemical cycling recognized (Ferris *et al.,* 1989; Boult *et al.,* 1997). Due to protonation/de-protonation processes, other metal/metalloid species can in turn be bound onto the surface of the biofilm via Fe-particle or colloidal bridging (Ferris *et al.,* 1989; Tazaki, 2000). This was considered to be a strong indication that metal flux prediction may not be possible from physical and chemical data of a system alone; thus, information about the biofilm physiology and

ecology is also required (Boult *et al.,* 1997). In the present study, it is suggested that biofilms located in the water column, as well as at the tailings-water interface, play an important role in the accumulation and speciation of various metals.

### 2.5.2 Microbial community composition

Biofilm microbiological diversity analysis was carried out using culture-dependent and culture-independent methods in an attempt to define potential metabolic processes that may take place within the DTMF water column biofilms. The culturable cell counts were relatively low, but likely 10 to 100 × less numerous than actually present in biofilms due to culture biases (Davey and O'Toole, 2000). Cell counts did not differ greatly with depth, suggesting the availability of equal quantities of nutrients throughout the water column; furthermore, photosynthetic and UV inhibition effects were not apparent. The chemical data, and particularly pH, indicated a degree of stratification within the water column, and that minimal mixing occurred in the water covering the uranium tailings. Questions may arise regarding the type of carbon source that may support bacterial growth equally throughout the water column. Given that the DTMF is an open system (Jones *et al.,* 2009) and receives tailings effluent, a variety of potential carbon sources exist. For example, organic compounds of plant origin may be transported by wind from the surrounding area. CLSM investigation revealed that algae were significant components of biofilms formed in the DTMF water column, and may themselves serve as significant sources of carbon and nutrients. More significant are potential sources of carbon substrates resulting from the uranium extraction-milling process, including various solvents (e.g., kerosene, isodecanol, amines) that are subsequently discharged into the tailings (Shaw *et al.,* 2011). Kerosene, an insoluble complex-carbon compound present in the tailings, may migrate to the surface of the water column or stay suspended, attached to colloidal tailings

particles, especially near the tailings water interface. Attachment of bacterial cells onto the surface of tailings particles embedded within the biofilm matrix was observed during CLSM analyses of the biofilm samples grown at the tailings-water interface (Supplemental data, Figure 9.1). The potential role of these various sources of carbon in the context of the DTMF tailings body are not insignificant when one compares the relatively low abundance of the cultivable microbial cells in overlying water biofilms and increasing numbers associated with the tailings-water interface region (~6 logs CFU/ml; Khan *et al.,* 2013) and at specific zones of high cell abundance (up to $2x10^8$ CFU/gr) within the tailings body (Bondici *et al.,* 2013). The tailings body appears largely inhospitable, yet the presence of relatively high bacterial cell counts indicates that the bacterial communities in this system are well-adapted to this harsh environment and may influence metals/metalloids stability.

The major lineages *Proteobacteria, Bacteroidetes, Actinobacteria* and *Firmicutes* were identified using both culture-based and sequencing-based approaches. Of particular importance is that in addition to the readily culturable taxonomic groups, an additional 7 phyla were identified using DNA sequencing methods. These major lineages have previously been described in the DTMF system, including within the tailings body and at the tailings-water interface (Bondici *et al.,* 2013; Khan *et al.,* 2013). Similar bacterial lineages have been detected at other uranium-contaminated waste sites (Vrionis *et al.,* 2005; Akob *et al.,* 2006), where it was shown that some members of these groups were able to grow in low nutrient environments, and in general, were resistant to various heavy metals or able to change the redox state of various elements (Petrie *et al.,* 2003; Akob *et al.,* 2006; Bondici *et al.,* 2013).

Based on the number of genera identified at each depth, biofilms grown at 13 and 27 m were the most microbially diverse, containing over 100 different microbial genera. Reduced

microbial diversity within biofilms grown at the upper water layer (1 m) and tailings-water interface (41 m) could be due to various, and distinct, selective pressures; for example, solar UV radiation at the 1 m depth and elevated total dissolved solutes at the 41 m depth as a consequence of expulsed tailings pore water. However, the fact that the cell counts within biofilms did not change substantially with depth whereas diversity did, indicates that despite additional selective pressure, the (microbial) carrying capacity remained relatively constant with depth. Studies have shown that selective pressures may reduce bacterial diversity; however, the surviving taxa associated with uranium-contaminated tailings exhibit considerable adaptive properties (Wolfaardt *et al.,* 2008; Bondici *et al.,* 2013). Wolfaardt et al. (2008) demonstrated this in a biofilm continuous-flow cell study using microbes recovered from the overlying water of the highly alkaline uranium tailings management facility at Rabbit Lake, Canada. Even though the pH of the water was varied between 7 and 10 in the flow cell system, little change was detected in microbial survival and biofilm formation. Another study by Bondici et al. (2013) similarly showed the adaptative abilities of microorganisms indigenous to uranium waste site in terms of heavy metal resistance and NaCl tolerance. The majority of the 59 representative isolates obtained from the DTMF tailings body exhibited multiple-metal resistance and tolerance to elevated NaCl concentration.

The abundance of sequences closely related to *Methylobacterium* detected in biofilms recovered from the 1 and 14 m depths in the present study was also notable. Members of the genus *Methylobacterium* are methylotrophs, and thus possess the ability to use carbon substrates without C-C bonds, as a source of energy (Christoserdova, 2011). These microorganisms are well-adapted to extreme conditions typified by industrially contaminated environments; they can thrive in the presence of organic pollutants and withstand high concentrations of toxic metal

elements (Marco *et al.,* 2004). The substrates that support methylotrophic activity consist of methane, methanol, methylated amines, or methylated sulfur species (Christoserdova, 2011). High frequencies of phylotypes closely related to *Methylobacterium* in biofilms recovered from the upper layer of the DTMF water column may correlate with the presence of high concentration of residues of various organic chemicals containing methyl groups, along with amines released as a consequence of the uranium milling process (Shaw *et al.,* 2011). Methylated elements such as mono-methyl arsenic have been reported in this system and therefore questions may arise as to whether these microorganisms are able to utilize this particular methylated metalloid as an energy source, thereby influencing its geochemical fate. It has previously been shown that bacterial isolates closely related to *Methylobacterium adhaesivum* obtained from DTMF tailings exhibited iron-reducing potential (Bondici *et al.,* 2013). Therefore, an abundance of this group of bacteria could be important primarily due to their ability to influence biogeochemical cycling of C1 compounds, as well as Fe.

A large number of sequences recovered from biofilms that developed at the 27 m depth were shown to be affiliated with *Aquabacterium* and *Dechloromonas*. Both bacterial groups utilize complex carbon compounds as energy sources (Chakraborty *et al.,* 2005; Jechalke *et al.,* 2013). Sequences affiliated with *Polaromonas* were also relatively abundant in biofilms that formed at all depths. *Polaromonas spp*. have been detected using molecular methods and isolated using culture-based techniques in the current study, as well as from within the DTMF tailings body (Bondici *et al.,* 2013). Important phylotypes that were closely related to well-known iron reducing bacteria, such as *Ralstonia,* were also identified in biofilms found at each depth. These genera have been previously reported at heavy metal- and hydrocarbon-contaminated sites and play an important role in Fe cycling (Rastogi *et al.,* 2011). The presence of *Desulfosporosinus*

*spp*. at lower depth (27 m) is not surprising because this genus was found to be prevalent at the DTMF tailings-water interface (Khan *et al.,* 2013). Members of this bacterial group are spore-forming obligate anaerobes, and in addition to sulfate, they are able to use alternative electron acceptors, such Fe and Mn (Stackebrandt *et al.,*, 2003; Spring and Rosenzweig, 2006). Similarly, *Desulfitibacter* and *Dethiobacter,* found at 41 m, are spore-forming obligate anaerobes capable of growth at high pH and capable of using sulfur, thio-sulfate and sulfite as electron acceptor (Nielsen *et al.,* 2006; Sorokin *et al.,* 2008). Even though the water column is an oxic environment, biofilms may create a suitably anaerobic environment to support the persistence and activity of viable *Desulfosporosinus, Desulfitibacter,* and *Dethiobacter* cells. For example, complex hydrocarbon consumers, which are able to use respiratory or fermentative pathways, are abundant in the biofilms grown throughout the water column and can be expected to create anoxic conditions within the biofilm microenvironment. Hence, these bacterial groups may play important role in the reductive part of the sulfur cycle.

### 2.5.3 Biofilm composition and biogeochemical activity revealed by STXM

Extracellular polymers are recognized as major components of the biofilm matrix whose composition varies with microbial diversity and environmental conditions (Decho, 1990). The carbohydrate fraction of the EPS consists of polysaccharides made up of various mono-sugar derivatives; for example, galacturonic acid, mannose, glucose, arabinose, xylose, galactose, fucose, N-acetyl glucosamine, etc. (Wozniak *et al.,* 2003; Pierre *et al.,* 2012). The composition of the monomers has a great influence on the properties of the biofilm matrix (Lembre *et al.,* 2012). Various fluor-conjugated lectins bind to carbohydrate residues with high specificity (Wozniak *et al.,* 2003; Pierre *et al.,* 2012) and thus this property can be investigated through non-invasive CSLM imaging. Five lectins were selected in this study to target specific EPS residues:

β-D-Gal (1-3)-D-GalNac targeted by *Arachis*; α-L-fucose by *Ulex;* α-D-Man and α-D-Glc by *Canavalia*; D-GalNac by *Glycine;* and N-acetyl-gluscosamine/lipopolysacharide by wheat germ agglutinin (Goldstein and Hayes, 1978; Wolfaardt *et al.,* 1997). CLSM lectin analyses demonstrated that the biofilm grown at the tailings-water interface was significantly different from the biofilms grown in the upper layers of the DTMF water column. Lectin binding tests revealed that fucose and N-acetyl-glucosamine glycoconjugates were abundant in the biofilm present at the bottom of the water column and together likely contributed to the observed difference. Increased amounts of fucose residues have previously been detected in biofilms grown *in vitro* using hydrocarbon-contaminated sediments, where significant correlations were found between fucose abundance and total concentration of petroleum or straight-chain hydrocarbons (Yergeau *et al.,* 2013). Other target structure residues, N-acetyl-glucosamine/lipopolysaccharide, have been related to the presence of Gram-positive (peptidoglycan-containing cells) and Gram-negative bacteria, respectively (Strathman *et al.,* 2002). Since the glycosyl composition of EPS produced by various bacteria is quite diverse and, in addition, most of the biofilm studies involve model microorganisms, it is difficult to correlate the presence or function of specific sugar residues to specific bacterial groups within an environmental biofilm produced by multiple bacterial species. Ion Torrent sequence analysis showed that the microbial community composition from the tailings-water interface was only significantly different from the biofilm community grown at the 14 m depth. This may indicate that differences in biofilm composition may arise from the fact that same bacterial groups may produce different polysaccharides under different physiochemical conditions. However, it is important to note, that even though there were differences in biofilm composition from near the

interface and other depths, the concentration of the accumulated iron within the biofilm varied with the Fe concentration in the water column and was much higher at the interface.

Both oxidized and reduced forms of iron, Fe (III) and Fe (II), were identified within the biofilms grown at 1, 27 and 41 m. Reduced iron (Fe (II)) associated with bacterial cells (Figure 2.5B4) strongly suggests iron-reducing ability of microorganisms present in the DTMF. Furthermore, strict anaerobic conditions were clearly not necessarily for the reduction of Fe (III) within biofilm systems. The fact that the reduced form of iron was mainly located on the surface of the cell provides some insight regarding the type of iron reducing mechanism used and the fact that Fe (III) was reduced biotically, rather than as a consequence of an abiotic process. For example, observing the cluster of cells shown in Figure 2.5 suggests Fe reduction occurs following direct and intimate contact of bacteria with the electron acceptor (Lloyd 2003). Furthermore, these results reveal that reduction likely occurred within the microenvironment surrounding individual biofilm cells or colonies even though the DTMF macroenvironment was oxidizing. The role of microbial activity in biogeochemical cycling of redox-sensitive metal elements associated with uranium tailings and off-site migration of these contaminants are well-documented (Abdelouas *et al.,* 2006; Muscatello *et al.,* 2008). In the DTMF, when ferrihydrite is reduced, it becomes unstable, losing its absorptive property and releasing absorbed contaminants (Shaw *et al.,* 2012). Since the DTMF is an open system, the contaminants (e.g., As, Ni, Se) released due to reductive dissolution may eventually migrate into the surrounding environment.

This study is the first to investigate potential effects of microbial biofilms on the behavior of elements of concern in a water column overlying a highly alkaline uranium tailings body at an active tailings management facility. Microbial communities present within the biofilms grown *in situ* suggests the presence of sufficient nutrients (e.g., complex hydrocarbons and C1

compounds) to sustain a notable microbial community. Furthermore, the existence of distinct microenvironments within the biofilm samples was supported by the fact that strict anaerobic bacteria, such as *Desulfosporosinus, Desulfitibacter and Dethiobacter,* were present, an observation directly supported by the presence of the reduced form of iron, even though the macroenvironmental conditions were oxic. Our results suggest that microbial aggregates such as biofilms are key components of the DTMF that reflect water chemistry variation, type of carbon available for bacterial growth and iron reducing potential in microenvironments. However, it remains unclear as to whether microenvironmental effects translate to macroenvironmental concerns. More work is also required to investigate the effect of microbial activity on specific elements of concern, such as As. Since C1 substrate-utilizing bacterial groups were relatively abundant in the DTMF, it would seemingly be important to determine whether these microorganisms are able to utilize methylated arsenic and to what degree the stability of these elements would be influenced.

## 2.6 Connection to next study

This study demonstrated the biogeochemical potential, such as iron reduction, of microbial biofilm communities present in the water column overlying the DTMF uranium tailings mass. In order to estimate the type of microbial community being incorporated into the tailings, the next study assessed the microbial diversity and metabolic processes present at the water-tailings interface, the next zone of the DTMF, and compared it with nearby non-impacted reference lake.

# 3 BACTERIAL DIVERSITY AND COMPOSITION OF AN ALKALINE MINE TAILINGS-INTERFACE

This chapter has been published: Khan, N.H., Bondici, V.F., Medihala, P.G., Lawrence, J.R., Wolfaardt, G.M., Warner, J. and Korber, D.R. (2013). Bacterial diversity and composition of an alkaline uranium mine tailings-water interface. *J. Microbiol.* 51, 558-569. This chapter is published here with the permission from the copyright owner (Springer publications).

Author contributions

All authors participated in the design of the experiments and contributed to writing of the manuscript. Preparation of the initial draft of the manuscript was prepared by the first author. The author of this thesis contributed to the data analyses and interpretation.

## 3.1 Abstract

The microbial diversity and biogeochemical potential associated with a northern Saskatchewan uranium mine water-tailings interface was examined using culture-dependent and -independent techniques. Morphologically distinct colonies from uranium mine water-tailings and a reference lake, McDonald Lake (MC) obtained using selective and non-selective media were selected for 16S rRNA gene sequencing and identification, revealing that culturable organisms from the uranium tailings interface were dominated by *Firmicutes* and *Betaproteobacteria*; whereas, MC organisms mainly consisted of *Bacteroidetes* and *Gammaproteobacteria*. Ion Torrent (IT) 16S rRNA sequence analysis carried out on extracted DNA from tailings and MC interfaces demonstrated the dominance of *Firmicutes* in both of the systems. Overall, the tailings-water interface environment harbored a distinct bacterial community relative to the MC, reflective of the ambient conditions (e.g., total dissolved solids, pH, salinity, conductivity, heavy metals) dominating the uranium tailings system. Significant correlations among the physicochemical data and the major bacterial groups present in the tailings and MC were also observed. Presence of sulfate reducing bacteria demonstrated by culture dependent analyses and the dominance of *Desulfosporosinus* spp. indicated by Ion Torrent analyses within the tailings-water interface suggests the existence of anaerobic microenvironments along with the potential for reductive metabolic processes.

## 3.2 Introduction

The Athabasca Basin in northern Saskatchewan hosts the largest high-grade uranium mines and deposits in the world, and represents about one third of global annual uranium production. Cameco Corporation operates three mines and a uranium mill at Key Lake (Natural Resources Canada, 2006; Saskatchewan Mining Association, 2010). The tailings from this mill are

deposited within an in-pit tailings management facility (TMF). The potential migration of elements associated with uranium mine tailings, including As, Ni, U, and $^{226}$Ra, present an environmental concern (Akob *et al.*, 2007; Pyle *et al*., 2002). Microbial processes can influence the redox status of heavy metal elements and radionuclides, and consequently their mobility (Selenska-Pobell, 2002). It is expected that upon decommissioning of these in-pit TMFs, the hydraulic gradients between the tailings and the regional ground waters would be small enough that the migration of contaminants would be controlled by diffusion, and not advection, with a minimum flux of heavy metals from the tailings into the regional groundwater system. Geotechnical, hydrogeological, and geochemical considerations have been key factors in the design of the TMFs in the Athabasca Basin; however, the potential for microbial metabolic activity to affect these processes upon decommissioning remains poorly understood. The broad habitat range of microorganisms known to participate in a variety of geochemical transformations suggests that they may play a role in the mobilization and subsequent transport of metal elements from tailing bodies into the surrounding environment (Miller *et al.*, 1987).

The sediment-water interface overlying tailings deposits is a dynamic and complex aquatic environment characterized by steep gradients of oxygen, nutrients, organic matter, and high bacterial abundance, diversity and activity (Herlihy *et al.*, 1985; Mills *et al.*, 1989; Shelobolina *et al.*, 2003). There have been limited studies carried out on the pore-water and sediment of some acidic mine tailings, but examination of the sediment-water interface of an alkaline uranium mine in microbial analyses has not been documented. Furthermore, microbiological studies on acid mine effluent, streams or unsaturated uranium waste piles have focused on U (VI) reduction to the less soluble U (IV) as a bioremediation strategy (Landa *et al.*, 1991; Lovley and Phillips, 1993; Lovley *et al.*, 1992), as well as the effect of microbial activity

on the partitioning of metals between mobile and immobile phases (Miller *et al.*, 1987). These conditions are in sharp contrast to those dominating TMFs in northern Saskatchewan, which are characterized by a high pH ( $\geq$ 9.0) and saturated conditions, and thus the potential effect of microbial activity on the geochemical behaviour of contaminants associated with TMFs is poorly understood. Furthermore, studies from uranium tailings environments in other regions of the world are of limited use in understanding the geochemical controls in Saskatchewan TMFs, since the ore mined and the milling technology used in the contributing mills are unique. The mined ore at the Deilmann Tailings Management Facility (DTMF) frequently contains relatively high amounts of nickel (2%) and arsenic (1.2%), and tailings are deposited in a very alkaline state as a means of precipitating and immobilizing metals dissolved during processing. The potential effects of microbial diversity and activities on the environmental behavior of immobilized metals such as Cu, Fe, Mo, Ni, and Zn, and oxyanions such as As and Se present in porewaters, at the interface between uranium mine tailings and overlying pond water is similarly not well understood.

It has previously been shown that microbial communities with diverse metabolic profiles exist at the Rabbit Lake TMF, a high pH environment, where the elapsed time since deposition of the tailings (>10 years for the deepest samples collected) did not appear to have a measurable impact on microbial numbers or metabolic profiles (Wolfaardt *et al.*, 2008). No information is presently available on the distribution, relative abundance and activity of microorganisms in the DTMF, or any other high-pH TMF from northern regions. Characterization of the organisms present at the tailings-water interface of the DTMF was therefore undertaken, using both culture-dependent and -independent approaches, to obtain benchmark diversity measurements relative to a nearby reference lake.

## 3.3 Materials and methods

### 3.3.1 Sampling sites

The Key Lake uranium processing mill is located 570 kilometers north of Saskatoon, Saskatchewan, Canada, on the southern rim of the uranium-rich Athabasca Basin (coordinates at 57°12′24″N and 105°39′33″W). The Key Lake site was an active mining operation since 1984; however, the last ore was mined from the Deilmann Open Pit in 1997, after which mining operations ceased. Uranium processing of ore from regional mining operations has subsequently resulting in tailings that have been deposited in the excavated Dielmann pit (now known as the Dielmann Tailings Management Facility, or DTMF) since 2000. The DTMF is 1000 m by 600 m, having approximately 60 m of tailings material emplaced under approximately 45 m of water (Bondici *et al*., 2013). Samples were collected from 3 distinct sites of the DTMF, designated as sites D2, D3 and E2. Site D2 was closest from the shoreline; whereas, E2 was located at the center of the DTMF. Site D3 was located in between D2 and E2 (Figure 3.1). The distance between the 3 sampling sites were approximately 200 m. McDonald Lake is located approximately 5 km from the DTMF, but is unaffected by mining operations and therefore was selected as a reference lake (hereafter referred to as MC) for comparative microbial analyses (Figure 3.1). The MC is shallow (average depth 3.0 meters) and surrounded by trees and shrubs. At the time of sampling (August, 2010), an abundance of plant and leaf litter was visible in the littoral zones of the MC.

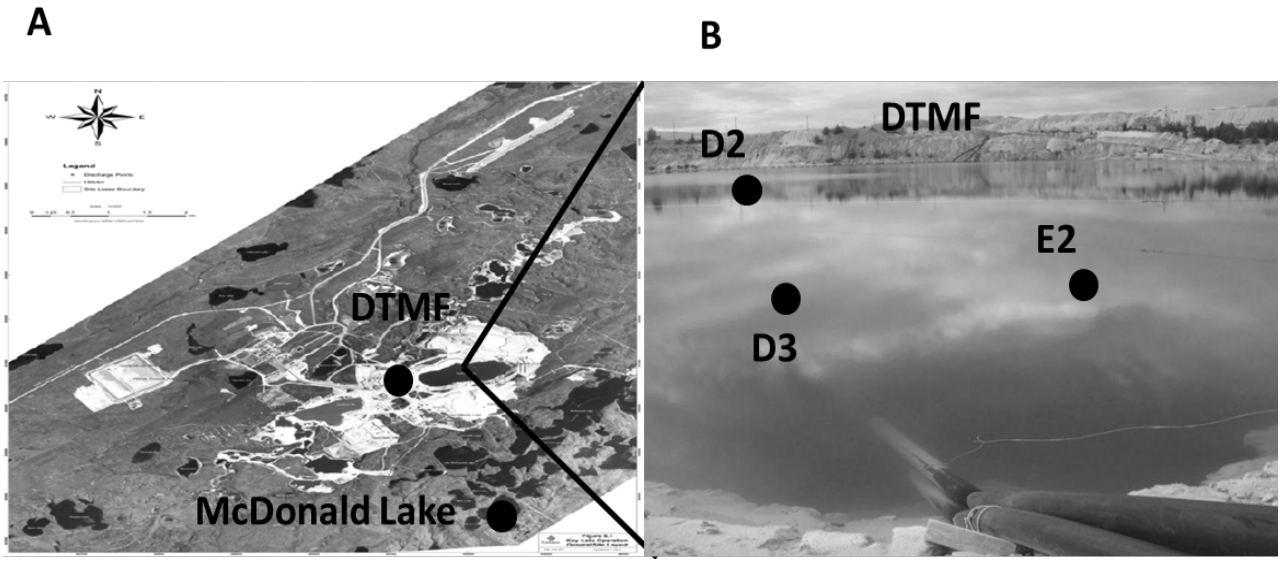


**Figure 3.1 Map and location of the sampling sites at the Key Lake uranium mine site.**
A). Map of the DTMF and MC site. B). D2, D3 and E2 are the sampling locations in the DTMF.

### 3.3.2 Physicochemical properties of the water body and tailings-water interface of the DTMF

A panel of physiochemical parameters was measured at 1 m depth intervals throughout the DTMF water column (from surface to the tailings-water interface) using a Hydrolab (Hydrolab DS5X, Hach, Loveland, CO, USA). Measured parameters included temperature, pH, conductivity, total dissolved solids (TDS), salinity, dissolved oxygen (DO) and oxidation-reduction potential (ORP). In the MC, only pH, conductivity, TDS and salinity data were available.

### 3.3.3 Sampling procedures

Samples for microbiological analysis were collected from the tailings-water interface zone (the first 1 meter of sediment) of the DTMF and MC. In terms of consistency, the DTMF interface samples were a yellowish gelatinous/semisolid; whereas, the MC interface material was clay-like and brown-colored. All interface samples from the DTMF and MC were collected in

August, 2010 using a Van Dorn (SKU 1960-G65) horizontal water sampler (Wildco, Wildlife Supply Company, FL, USA). Tailings-water interface and MC interface samples were collected in duplicate glass bottles which were filled completely with sediment and water to eliminate air headspace. In between sampling events, the sampler and associated equipment were rinsed with sterile deionized water. Counting sulfate reducing bacteria (SRB) via dilution and inoculation of pre-prepared media was initiated on-site to minimize external effects. Samples were processed immediately (described below) for enumeration of total culturable cell counts (within 3-4 hours after collection) in the laboratory on-site at Key Lake. Samples for remaining analyses were maintained at 4°C before processing. All the analyses were carried out within 15 days of collection.

### 3.3.4 Enumeration of total culturable bacteria

Interface samples were serially diluted using sterile physiological saline (0.85% NaCl) and plated on to two types of non-selective agar plates (R2A and TSB; Difco media, Franklin Lakes, NJ, USA). Plates were incubated under aerobic and anaerobic conditions (using an anaerobic glovebox with an $O_2$-free atmosphere consisting of 10% $CO_2$, 80% $N_2$, and 10% $H_2$) at room temperature for 15 days, after which time visible colonies were enumerated. All plating was done in triplicate.

### 3.3.5 Enumeration of SRB

Sulfate reducing bacteria were enumerated using the three-tube, most probable number (MPN) method. Accordingly, a 1 ml sample of homogenized composite interface material was drawn into a sterile 1 ml syringe and transferred to 10 ml vials containing 9 ml of pre-sterilized and pre-reduced Postgate's B semisolid SRB medium (Jain, 1995), and then serially diluted to provide up to $10^{-3}$ dilution for the SRB-MPN determination. The MPN tubes were incubated at

room temperature for 28 days and observed twice a week for a change in color of the medium (formation of a black precipitate) indicative of the presence of SRB. All determinations were performed in triplicate. In parallel, SRB-like organisms were enumerated, in triplicate, using the SaniCheck™ SRB kit (Biosan Laboratories, Inc., Michigan, USA). The inoculated SRB tubes were inspected daily for 5 days, at which time the results were recorded and interpreted following the procedures of the manufacturer. The tubes showing positive counts after 5 days were confirmed to contain only SRB-like organisms in the samples.

### 3.3.6 Isolation of culturable bacteria

After incubation of the interface samples on agar plates at room temperature (~22 ± 2°C) under both aerobic and anaerobic conditions for more than two weeks, unique colonies were picked (based on colony morphology, color, surface texture and pigmentation) and sub-cultured (2x) onto R2A agar plates to isolate individual colonies. A total of 128 colonies were picked, isolated and purified by consecutive subculturing.

### 3.3.7 Identification of culturable bacterial isolates

Isolated bacterial colonies were subjected to DNA extraction using the Qiagen DNA extraction kit (Qiagen, Maryland, USA). Partial 16S rRNA gene polymerase chain reaction (PCR) amplification was performed using the 8F (5'-AGAGTTTGATCCTGGCTCAG-3') and 531R (5'-ACGCTTGCACCCTCCGTATT-3') (Hirkala and Germida, 2004) universal primer sets, yielding ~500 bp PCR product. The final concentration of reagents used for a 50 µl PCR reaction mixture were as follows: 1.0 µM each of the forward and reverse primers, 1.0 U *Taq* polymerase (Invitrogen, Burlington, ON, Canada), 1.0 µM $MgCl_2$, 1.0X PCR buffer, and 4.0 µM of deoxyribonucleotide triphosphates (dNTPs). The PCR assay reaction mixture was adjusted with sterile distilled water to a final volume of 50 µL. The thermal cycling profile was set

according to Hirkala and Germida (2004). For sequencing, the PCR amplicons were purified using the Qiagen purification kit according to the manufacturer's instructions (Qiagen, Germantown, Maryland, USA). Taxonomic identification and clustering of 16S rRNA gene sequences were assigned based on similarities to available strains within the NCBI/GenBank 16S rRNA sequence database using the Basic Local Alignment Search Tool (BLAST) search tool. Sequences of 16S rRNA were verified using the Chromas software program, version 2.32 (Technelysium Pty. Ltd., Brisbane, Australia). The sequence alignments were also edited manually using Chromas. Identification of distinct isolates was based on percent identity where 100% identical sequences were affiliated with the same taxon.

### 3.3.8 Comparative analyses of diversity of culturable bacteria from the DTMF and MC interface region

The identified bacterial isolates were group-defined using the Ribosomal Database Project (RDP release 10). Thirty four unique isolates were subjected to further biocomputational analyses and clustered into the major bacterial groups. Diversity and abundance of the cultural bacterial community were determined by enumerating the number of isolated colonies from the selective and non-selective agar media incubated under aerobic and anaerobic conditions and by calculating their percentage and distribution among various bacterial groups. Genetic diversity among the bacterial isolates was determined by phylogenetic analysis of the 16S rRNA sequences.

### 3.3.9 Phylogenetic analysis

Phylogenetic trees of the aligned unique sequences and their closest 16S rRNA gene matches were constructed by a neighbor joining method (Saitou and Nei, 1987) using MEGA v5

with 1000 bootstrap replicates (Tamura *et al.*, 2011). Closely related bacterial sequence data were selected from the NCBI/GenBank database using BLAST.

### 3.3.10 Nucleotide sequence accession numbers

The 16S rRNA sequences for the isolated bacteria were deposited in the EMBL Nucleotide Sequence Database under the accession numbers HE649225 to HE649270.

### 3.3.11 Ion Torrent analyses

Next-generation sequence analyses were conducted using the Ion Torrent Personal Genome Machine (PGM; Life Technologies, Carlsbad, CA, USA) (Yergeau *et al.*, 2012; Bondici *et al*., 2013). A set of primers specific to the V5 region of the 16S rRNA gene was used for the Ion Torrent sequencing. To these primers, Ion Torrent adapter A (forward) and adapter P1 (reverse) fragments were attached. In addition to the adapters, the target-specific forward primer also included a key tag and a multiplex identifier (MID). The sequence of the primers were F5'-CCA TCT CAT CCC TGC GTG TCT CCGACTCAGMIDGATTAGATACCCTGGTAG and R5'-CCTCTCTATGGGCAGTCGGTGAT CCGTCAATTCCTTTRAGTTT, respectively. The sequencing of 5 base pair MIDs used for each of the samples was as follows: ATCAG (D2), CGTGT (D3), CTCGC (E2) and TGATA (MC). The PCR reactions were carried out in 50 µl volumes containing 2 µl of template DNA, 1.0 µM each primer, 1.0 U *Taq* polymerase (Invitrogen, Carlsbad, CA, USA), 1.0 µM $MgCl_2$, 1.0 X PCR buffer (both provided with the *Taq* polymerase), and 4.0 µM of dNTPs. Cycling conditions involved an initial 5 min denaturing step at 95°C, followed by 40 cycles of 30 s at 95°C, 30 s at 57°C, and 45 s at 72°C, and a final elongation step of 10 min at 72°C. The PCR amplicons were purified using the Qiagen purification kit according to the manufacturer's instructions and quantified using a NanoDrop spectrophotometer. Pooled, key-tagged gene amplicons were sequenced at the Biotechnology

Research Institute (Montreal, Quebec, Canada) using the Ion Torrent PGM and a 314 chip. The sequences retrieved from Ion Torrent analyses were processed using RDP pyrosequencing pipeline tools. Low-quality sequences with lower scores and shorter than 100 bp were removed using the pipeline initial process tool. Hierarchical clustering of sequences was obtained by the RDP classifier with bootstrap cut-off value of 50%.

### 3.3.12 Statistical analyses

Analyses of variance (ANOVA) was used to demonstrate differences among the sample means at $p < 0.05$ using SPSS v17 (Statistical Package for the Social Sciences). The number of culturable bacteria and culture-independent sequence frequencies were used for principal components analyses (PCA) using PRIMER v6 software (PrimerE Ltd., Lutton, UK). Similarity and dissimilarity analyses were carried out using the paired sample t-test and a $p < 0.05$ significance level using SPSS. Correlation among the class-wise sequence data and physicochemical data (TDS, conductivity, salinity and pH) from the DTMF and MC were done using means and standard deviation by bivariate analyses at the $< 0.01$ and $< 0.05$ significance levels.

## 3.4 Results and discussion

### 3.4.1 Physicochemical properties of the water and tailings-water interface

Physicochemical parameters were measured for the DTMF water body at 1 m intervals from the air-water interface to the tailings-water interface for each of the three sampling locations (D2, D3 and E2). Representative physicochemical data is presented for the 1, 20 and 43 m (interface) sampling depths (Table 3.1)

**Table 3.1 Physicochemical properties of the water body and tailings-water interface of DTMF.**

| Sites | Location/ depth | Temp. °C | [1]TDS g $l^{-1}$ | Conduct. µS $cm^{-1}$ | pH | Salinity ppt | [2]ORP mV | [3]DO% Sat. | DO mg $l^{-1}$ |
|---|---|---|---|---|---|---|---|---|---|
| **E2** | 1m | 14.2 | 1.0 | 1531 | 5.9 | 0.78 | 255 | 107.5 | 10.31 |
| **D2** | | 14.2 | 0.9 | 1472 | 6.9 | 0.81 | 204 | 109.4 | 10.49 |
| **D3** | | 14.3 | 1.0 | 1528 | 6.9 | 0.81 | 228 | 108.4 | 10.37 |
| **E2** | 20m | 8.2 | 1.2 | 1815 | 6.1 | 0.97 | 224 | 20.4 | 2.24 |
| **D2** | | 8.1 | 1.2 | 1863 | 6.5 | 0.99 | 193 | 22.1 | 2.43 |
| **D3** | | 8.2 | 1.2 | 1905 | 6.5 | 1.02 | 190 | 20.6 | 2.27 |
| **E2** | Interface (43 m) | 12.2 | 1.6 | 2467 | 10.2 | 1.33 | 118 | 3.2 | 0.32 |
| **D2** | | 10.9 | 1.5 | 2300 | 9.4 | 1.23 | 126 | 1.7 | 0.18 |
| **D3** | | 10.8 | 1.6 | 2571 | 9.2 | 1.38 | 118 | 1.8 | 0.18 |
| **McDonald Lake** | Interface | ND | 0.18 | 21 | 7.0 | 0.00 | ND | ND | ND |

[1]TDS, total dissolved solids

[2]ORP, oxidation-reduction potential, [3]DO, dissolved oxygen.

TDS, conductivity, pH and salinity increased with depth, ranging from 1.0 to 1.6 g $l^{-1}$, 1510 to 2446 µS $cm^{-1}$, 6.6 to 9.6 and 0.8 to 1.4 ppt, respectively. In contrast, redox potential, DO (% saturation) and DO (mg $l^{-1}$) gradually decreased with depth, ranging from 229 to 121 mV, 108 to 2.2 % and 10.39 to 0.23 mg $l^{-1}$, respectively. An exception to this trend existed for temperature, which was highest at the air-water interface (14°C), rapidly decreased to ~8°C at 20 m, and then increased again with depth to 10-12°C at the water-sediment interface (Table 3.1). It is assumed that the variation in temperature was due to solar heating of the upper layers of the DTMF. Physicochemical parameters for DTMF sites D2 and D3 were similar; whereas, E2 was slightly different from D2 and D3 with regard to temperature, pH and DO profiles (Table 4.1). The DTMF tailings body was highly alkaline, with an average pH of ~10. A limited physicochemical data set was available for the MC, where TDS, pH, salinity and conductivity were determined to be 0.18 g $l^{-1}$, 7.0, 21 uS $cm^{-1}$ and 0 ppt, respectively. The average temperature of the DTMF tailings (11.3°C) was considerably higher than the average temperature of Rabbit Lake uranium mine tailings (~0°C) also located in northern Saskatchewan; however, the pH of Rabbit Lake tailings (9.9) determined by Wolfaardt *et al.* (2008) and Moldovan and Hendry (2005) were very similar to the DTMF. The concentration of metal elements within the DTMF pore water and MC water has been described by Shaw et al. (2011) and also compiled from internal company reports (Harm Matthius, Cameco Corporation), respectively. Accordingly, the average concentrations of arsenic, cadmium, iron, manganese, molybdenum, nickel and selenium in DTMF porewater were 2.9100, 0.0026, 0.0086, 0.1396, 13.1484, 0.04495 and 0.0384 mg $L^{-1}$, respectively, and 0.0002, <0.0001, 0.0310, 0.0180, <0.0001, 0.01 and <0.0001 mg $L^{-1}$, respectively, in the MC.

Natural alkaline environments are relatively rare. The best-studied alkaline environments are temperate and subtropical alkaline soda lakes with pH values ranging from 8 to more than 12,

containing large amounts of sodium carbonates in combination with low concentrations of $Mg^{2+}$ and $Ca^{2+}$ (Duckworth *et al.*, 1996; Jones *et al.*, 1998). These extreme conditions are reflected by the adaptation of the microorganisms found in the lakes, many species of which are both alkaliphilic and halophilic, or extremely halotolerant (Ma *et al.*, 2004; Sorokin *et al.*, 2003). The DTMF, with a pH around 10, along with high conductivity, salinity, TDS and low oxygen and ORP, may also be considered a somewhat extreme environment and thus may also contain adapted and metabolically distinct microorganisms.

### 3.4.2 Total culturable bacterial counts

Total culturable bacterial counts from the DTMF sites (ranging from 6.33 to 6.89 $Log_{10}$ CFU $ml^{-1}$) were approximately 0.5 $Log_{10}$ higher than for the MC (6.14 $Log_{10}$ CFU $ml^{-1}$) (Table 3.2). The total bacterial counts from the interface of the DTMF were 1 to 2 $Log_{10}$ higher than previously reported counts on 10% trypticase soy agar (TSA) for the TMF at Rabbit Lake, also a high-pH system (Wolfaardt *et al.*, 2008), indicating that the DTMF interface region is relatively more microbiologically active, based on culturable cell counts. The total bacterial counts from the MC near the DTMF were also 2 $Log_{10}$ higher than the upstream surrounding lakes in the Rabbit Lake area (Wolfaardt *et al.*, 2008). The elevated numbers of bacteria in the DTMF in relation to Rabbit Lake could be linked with greater carbon availability (on average, the DOC available in DTMF was 20 mg $ml^{-1}$ versus < 0.8 mg $g^{-1}$ in the Rabbit Lake region (Wolfaardt *et al.*, 2008) occurring either as a consequence of $UO_2$ processing (requiring chemicals such as kerosene, isodecanol, amines, etc.) or arising naturally (airborne sediment, surface runoff, algal primary production, etc.). Differences in the temperature profiles in the two systems could also provide an entirely reasonable explanation for the elevated numbers the DTMF, as the temperature was almost 10°C higher than in the Rabbit Lake TMF (Wolfaardt *et al.*, 2008).

**Table 3.2 Total culturable bacteria counts in DTMF and McDonald lake.**

| Sites | Counts $Log_{10}$ CFU $ml^{-1}$ (SD)[1] |
|---|---|
| DTMF-D2 | 6.89 (±0.21) |
| DTMF-D3 | 6.59 (±0.09) |
| DTMF-E2 | 6.33 (±0.26) |
| McDonald Lake | 6.14 (±0.0) |
| Rabbit Lake* | 5.17 (±0.0) |

SD[1] = standard deviation
*Data from Wolfaardt *et al.* 2008

### 3.4.3 Culturable bacterial isolates from DTMF and McDonald lake

Following plating of samples from the DTMF and MC, a total of 128 bacterial isolates were recovered, 74 of which were from the DTMF and 54 from the MC. Gene sequence (16S rRNA) analysis was used to determine that of these 128 isolates, 34 were unique (18 were from the DTMF and 16 were from the MC) and that from the four sampling sites (three from DTMF and 1 from MC), each yielded 21 to 32% of the total unique isolates. Pooling the bacterial isolates from both the DTMF and MC revealed the following proportional groupings; *Proteobacteria* (75%), *Firmicutes* (14%), *Bacteroidetes* (7%), and *Actinobacteria* (4%). The DTMF microflora was dominated by *Proteobacteria* isolates (73%), whereas no *Bacteroidetes* were detected. Similarly, *Proteobacteria* was the proportionally dominant culturable phyla in the DTMF tailings waste and Bacteroides was the least frequent (Bondici *et al*., 2013). Twenty-four percent of the DTMF bacterial community consisted of *Firmicutes* and only 3% were *Actinobacteria* (Figure 3.2A). In the MC, the microflora was again dominated by *Proteobacteria* (76%) followed by *Bacteroidetes* (15%). Six and 3% of the total culturable bacterial community from the MC were *Actinobacteria* and *Firmicutes*, respectively (Figure 3.2B). Despite the fact that 75% of the isolates from the DTMF and MC were *Proteobacteria*, there were distinct

differences in *Proteobacteria* composition between the two bacterial communities. For example, the DTMF consisted of mainly *Betaproteobacteria* (58%), often thought to be more dominant in nutrient/carbon rich environments (Ley *et al.*, 2006), followed by *Gammaproteobacteria* (26%) and *Alphaproteobacteria* (16%) (Figure 3.2C). In contrast, the MC was dominated by *Gammaproteobacteria* (72%), followed by *Betaproteobacteria* (22%), and with *Alphaproteobacteria* making up only (4%) of the culturable isolates (Figure 3.2D). Neither of the study sites yielded any culturable *Deltaproteobacteria*. In general, it is noteworthy that the proportionally higher percentage of culturable *Proteobacteria* may reflect the fact that they tend to be much easier to cultivate on agar media than *Firmicutes* (Wagner, 2008), leading to a relatively higher apparent abundance.

The *Betaproteobacteria* includes several groups of aerobic or facultatively anaerobic bacteria with highly versatile degradation capacities, including chemolithotrophic genera and some phototrophs. The observed abundance of *Betaproteobacteria* amongst DTMF isolates is in contrast with previous reports indicating the prevalence of *Gammaproteobacteria* in underground uranium mine gallery of Jaduguda uranium mine, India (Islam and Sar, 2011) and uranium mill tailings in Shiprock, New Mexico, USA (Selenska-Pobell *et al*., 2001; Radeva and Selenska-Pobell, 2005). However, the prevailing conditions in these two sites are significantly different from that of the DTMF at Key Lake in terms of key physicochemical parameters, offering a reasonable explanation for the observed differences. The observed pH and conductivity at the Jaduguda uranium mine site was 6.4 and 200 μS $cm^{-1}$ (Islam and Sar, 2011); whereas, the DTMF interface had an average pH and conductivity of 9.9 and 2446 μS $cm^{-1}$, respectively.

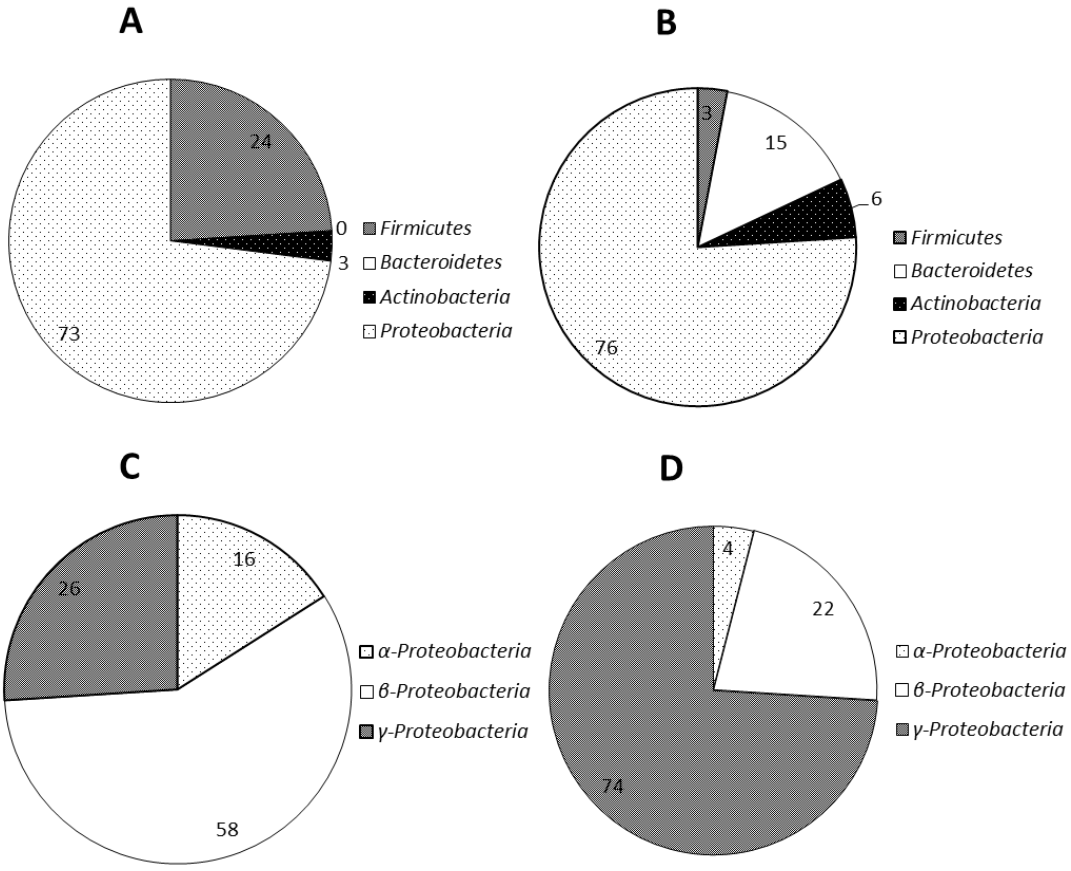


**Figure 3.2 Diversity and distribution of culturable bacteria from the DTMF and MC interface.**
A) distribution of major culturable bacterial groups in DTMF; B) distribution of major culturable bacterial groups in MC; C) distribution of culturable *Proteobacteria* in DTMF and D) distribution of culturable *Proteobacteria* in MC. Percentages of bacterial groups were calculated based on the number of total unique bacterial isolates by culture-based methods.

Similarly, Radeva and Selenska-Pobell (2005) reported the average pH of the Shiprock uranium mill sampling site to be 6.8. Generally, the abundance of alkaline-adapted *Betaproteobacteria* in the DTMF suggests a potential for bioconversion of heavy metals in the DTMF system (Burkhardt *et al.*, 2010; Miller *et al.*, 1987).

The *Alphaproteobacteria* comprise most of the phototrophic genera, but also includes several genera capable of metabolising C1-compounds (single carbon compounds), symbionts of plants and animals, and a group of pathogens. The low frequency or absence of *Alphaproteobacteria* has also been seen in other studies, for example, in soil samples from uranium mill tailings Gittersee/Coschütz in Germany where *Alphaproteobacteria* were not predominant (Selenska-Pobell, 2002).

The *Gammaproteobacteria* consist mainly of human and animal pathogens, and are generally present in eutrophic environments; however, their presence in uranium mine tailings has been indicated by several studies (Moreels *et al.*, 2008; Radeva and Selenska-Pobell, 2005; Selenska-Pobell, 2002). The presence of 75% of the total *Proteobacteria* being *Gammaproteobacteria* in the DTMF is suggestive of possible exposure of the system to animal faecal material, and reflective of the routine use of the DTMF for disposal of human sewage.

*Firmicutes* are one of the most common bacterial groups isolated from extreme environments (Bowers *et al.*, 2009; Dib e al., 2009). Many *Firmicutes* produce endospores which are resistant to unfavourable conditions and might overcome the conditions of high pH, low oxygen, high or low temperatures, high NaCl and elevated heavy metal concentrations associated with industrial activities (Bowers *et al.*, 2009). The prevalence of *Firmicutes* in the DTMF interface zone is consistent with the physicochemical conditions and selective pressure of the DTMF. *Bacteroidetes*, which were predominant in the MC, are widely distributed bacteria mainly found in environments enriched with warm blooded animal feces; thus, an impact of animals and waterfowl activity at the MC sites appears likely. As both the DTMF and MC are open environments in close geographic proximity, we expected to see some similarity in the microbial diversities in both systems. The distinct differences observed in the DTMF

environment, which has been developed recently in comparison to MC, suggests that the physical and chemical conditions indeed impose a significant selective pressure, likely based on the combined effects of elemental toxicity, pH, and salinity. In such an environment, the existence and proliferation of a distinctive bacterial community is not surprising, and accordingly a number of the isolates found in the DTMF interface were determined to be putatively novel species based on their having less than 97% sequence homology to known 16S rRNA sequences. In contrast, the MC contained fewer putative novel species.

A neighbour-joining phylogenetic tree showed clustering of the DTMF and MC bacterial isolates (Figure 3.3), including very distinct clades of *Proteobacteria*, *Actinobacteria*, *Firmicutes* and *Bacteroidetes*. *Proteobacteria* also showed clear subdivisions of *Alpha*, *Beta* and *Gammaproteobacteria*. In most cases, the DTMF isolates separated into a distinct branch of the tree with a higher bootstrap value, further supporting the notion that the DTMF interface represented a distinct environment. The group *Bacteroidetes* was comprised solely of MC isolates and was similar to the cluster formed by *Gammaproteobacteria*, where again most of the isolates originated from the MC. Out of 7 *Gammaproteobacteria*, only 3 came from the DTMF, two of which formed a separate cluster, which were *Acinetobacter* sp. (97% similarity) and *Enhydrobacter* sp. (100% similarity). All other isolates from the MC formed two distinct clades. DTMF isolates D213, D327, D219, E213 and E208 are part of the *Betaproteobacteria* and were distantly related to the MC isolates. The DTMF interface was dominated by special groups of culturable bacteria from the *Betaproteobacteria* and *Firmicutes*; whereas, the *Gammaproteobacteria* and *Bacteroidetes* were dominant in the MC (Figure 3.3).

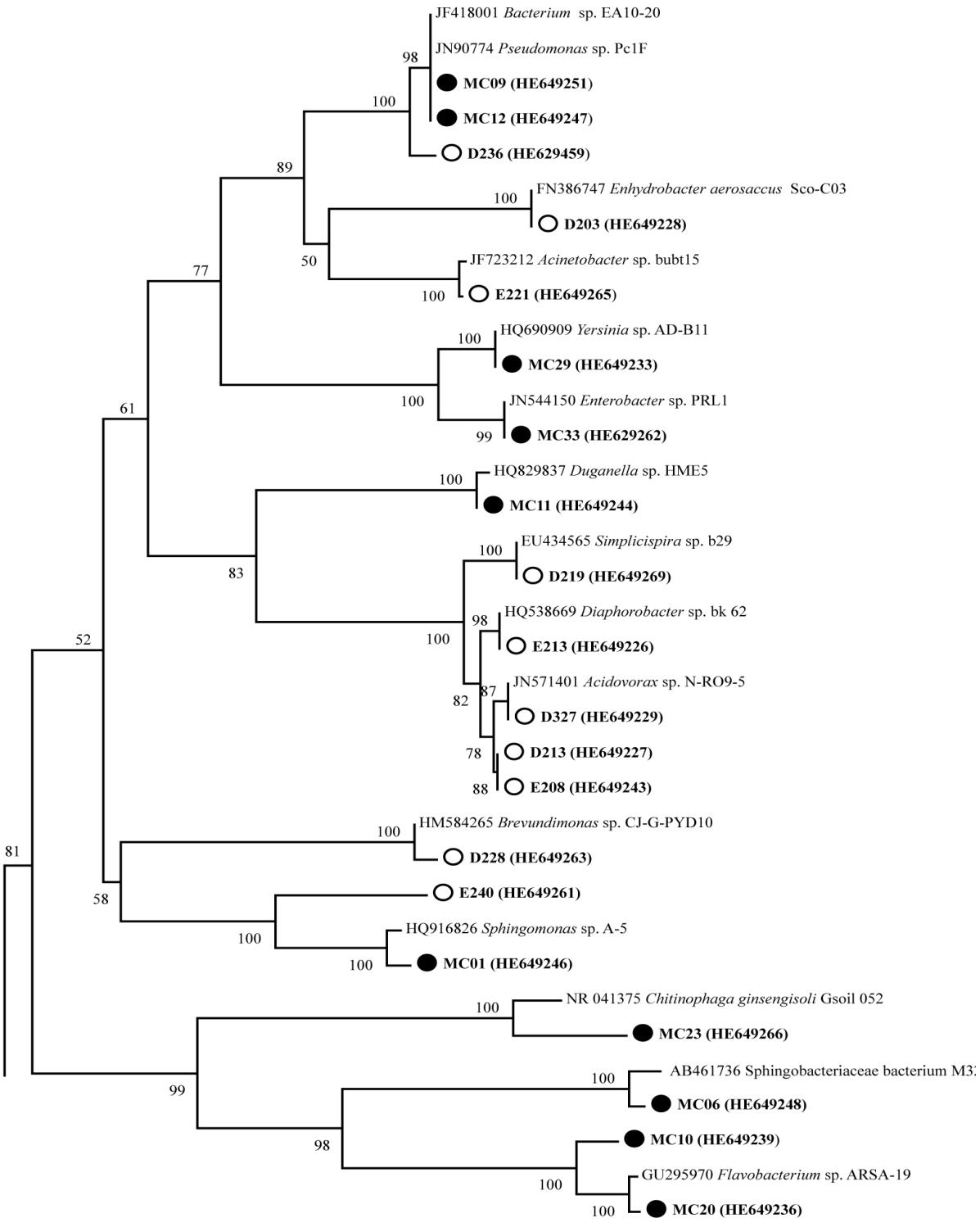


**Figure 3.3 Unrooted Neighbor Joining Tree of the partial 16S rRNA gene sequences.**
The phylogenetic tree was divided into two panels for presentation purposes. A detailed legend is provided next page.

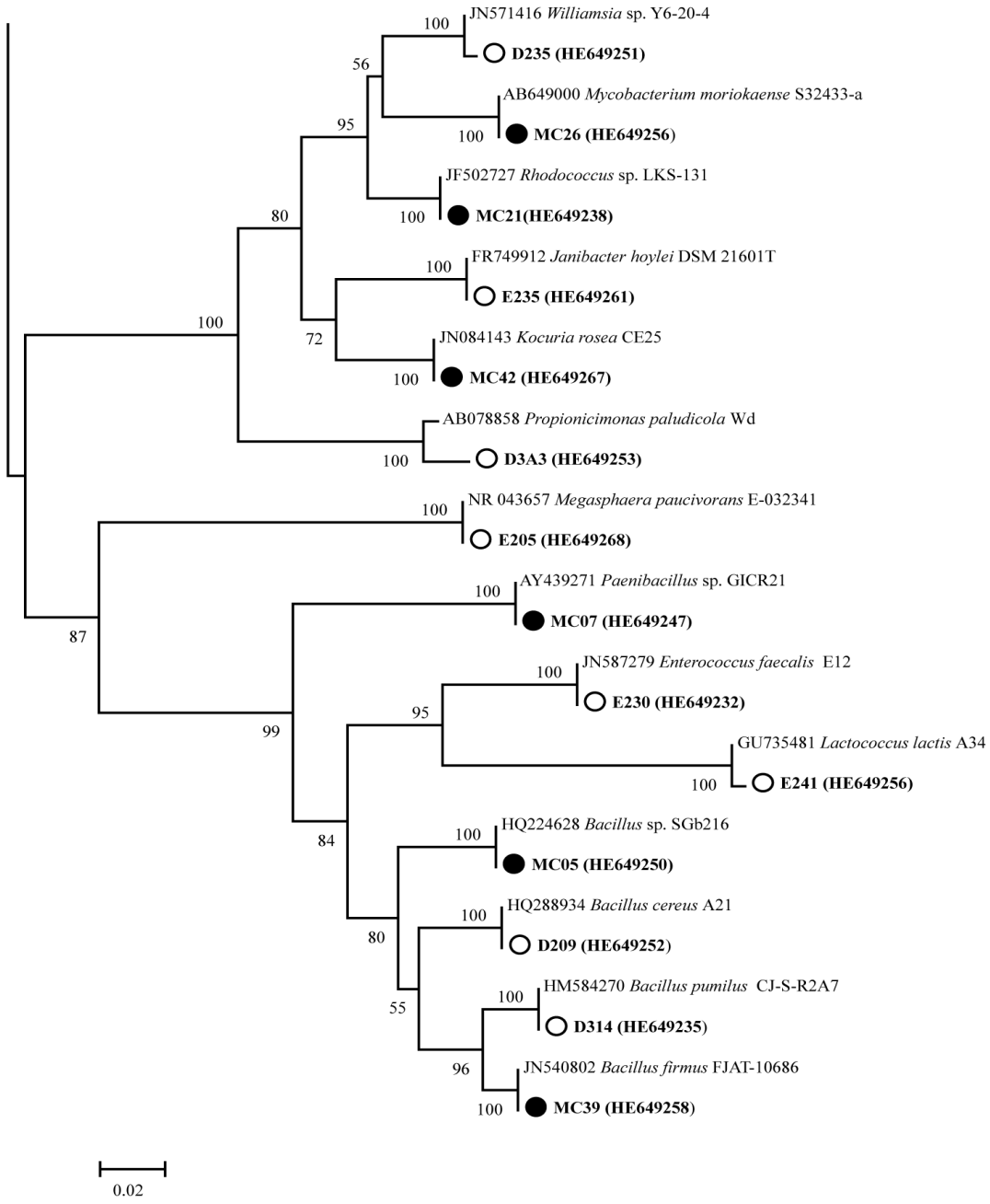


**Figure 3.3 Unrooted Neighbor Joining Tree of the partial 16S rRNA gene sequences.** The phylogenetic tree was divided into two panels for presentation purposes. Sequence data represents diversity and distribution of the culturable bacteria isolated from the DTMF (open circle) and MC (solid black circle) interface along with the closely related 16S rRNA sequence data from the NCBI/GenBank. N-J tree was generated with Kimura 2 correction (Kimura, 1980) for distance calculations. Bootstrap percentages retrieved in 1,000 replications are shown at the nodes. Clusters and bootstrap values that were 50% or greater are indicated. The scale bar (0.02) indicates the number of nucleotide substitutions per site.

The contrasts evident in the respective culturable bacterial communities clearly point to distinct physicochemical properties of the DTMF compared with the MC, and provides some insight into the possible metabolic activities that may be occurring in the DTMF interface zone. A detailed phylogenetic analysis was previously carried out on the bacterial communities in uranium ores and surrounding soils from the Banduhurang open cast uranium mine, India, by 16S rRNA sequence analyses (Islam *et al.*, 2011). The *Gammaproteobacteria* from this study were represented by 7 ribotypes, covering 56−65% of the communities present in ore samples, while showing relatively lower abundance (30%) in association with soils. All ribotypes under the subphylum *Betaproteobacteria* retrieved from ores were affiliated to the order *Burkholderiales* (Islam *et al.*, 2011). In contrast, no *Burkholderia* isolate was recovered in the present study from any of the DTMF interface samples. Among the *Alphaproteobacteria*, *Brevundimonas* spp. (99% similarity) was present in our study and was also observed by Islam *et al.* (2011). Among the *Firmicutes*, Bacilli were common and represented at least 5 unique bacterial isolates from the present study whereas Islam *et al.* (2011) found only one *Bacillus* sp. in their uranium ore sample. Presence and abundance of these isolates at the DTMF water tailings interface were similar to the isolates in the tailings (Bondici *et al*., 2013).

### 3.4.4 SRB counts

Based on the MPN data the MC interface sample contained ~100 times higher SRB counts than the DTMF samples (>700 SRB $ml^{-1}$ for MC versus 23, 6 and 6 SRB $ml^{-1}$ for sampling sites D2, D3 and E2, respectively) (Table 3.3). The SANICHECK™ kit yielded similar low counts of ≤ 10 SRB-like organisms per ml in DTMF and $>10^4$ $ml^{-1}$ in MC. The DTMF SRB counts are similar to the low SRB counts determined from a uranium pit mine in Brazil (Benedetto *et al.*, 2005), and SRB numbers in metal- and radionuclide-contaminated soils in a

former mining area near Ronnenberg, Germany (Sitte *et al.*, 2010). These culture-based findings suggest that the highly oxic chemical state of the ferrihydrite-complexed tailings was not conducive to the recovery and growth of the strictly anaerobic SRB.

**Table 3.3 Total SRB counts in DTMF and MC determined by MPN method and SANICHECK SRB kit.**

| Sites | SRB counts $ml^{-1}$ (MPN) | SRB like organisms counts $ml^{-1}$ (SANICHECK kit) |
|---|---|---|
| **D2** | 23 | $\leq 10^{*}$ |
| **D3** | 6 | $\leq 10$ |
| **E2** | 6 | $\leq 10$ |
| **McDonald Lake** | $>700^{2}$ | $>10^{4}$ |

*Black precipitate was observed after 5 days of incubation thus the counts were considered as ≤ 10 $ml^{-1}$ in accordance with the manufacturer's instructions.
[2]Samples were positive for all 3 dilution tubes.

### 3.4.5 Bacterial diversity in DTMF and MC by Ion Torrent analyses

Using Ion Torrent high-throughput sequence analysis, an estimated 36000 classified sequences were obtained from all four sampling sites. The number of sequences varied from 20 to 28% in E2, MC, D3 and D2 sites, respectively. In the DTMF, 89% of sequences retrieved were *Firmicutes* and 7, 3 and 1% were from *Bacteroidetes*, *Actinobacteria* and *Proteobacteria*, respectively (Figure 3.4A). In contrast, 71% of the sequences from the MC were *Firmicutes* and 23, 3 and 1% were *Bacteroidetes*, *Proteobacteria* and *Actinobacteria* (Figure 3.4B). When the total *Proteobacteria* data were analysed (as they were dominant in culture-based analyses), 58% were found to be *Betaproteobacteria* in the DTMF and 40% were found to be

*Gammaproteobacteria* (Figure 3.4C). In the MC, *Gammaproteobacteria* constituted 85% of the total *Proteobacteria* and only 10% were *Betaproteobacteria* (Figure 3.4D).

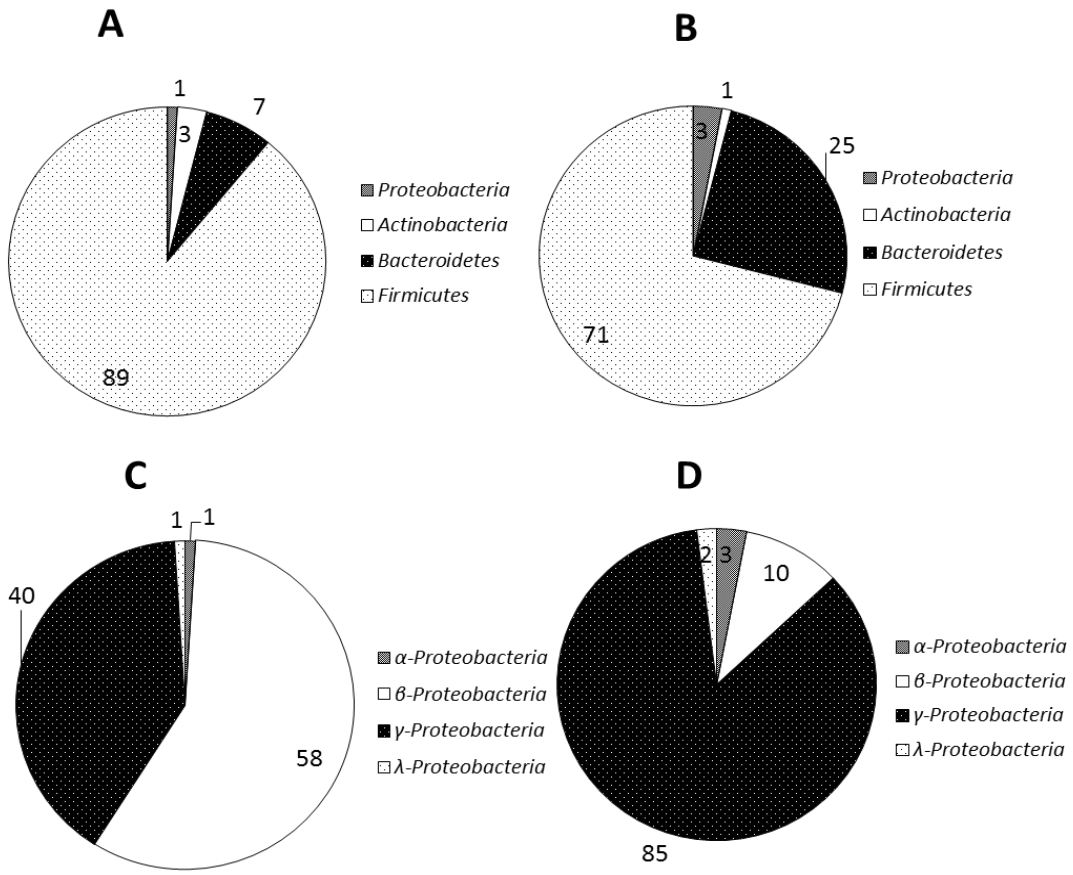


**Figure 3.4 Diversity and distribution of bacteria in DTMF and MC interface revealed by Ion Torrent analyses.**
A) distribution of major bacterial groups in DTMF; B) distribution of major bacterial groups in MC; C) distribution of *Proteobacteria* in DTMF and D) distribution of *Proteobacteria* in MC. Percentage distribution was calculated based on the total number of sequences available in each bacterial group.

*Deltaproteobacteria* (2% of total *Proteobacteria*) was detected in the MC but not in DTMF. The low numbers of *Proteobacterial* sequences found using IT sequencing contrasts

with the high number of culturable *Proteobacteria* isolates. This observation is thought to be reflective of the respective ease and difficulty of culturing *Proteobacteria* and *Firmicutes*, respectively, and reveals the potential to reach erroneous conclusions when either culture-dependent or culture-independent community characterization techniques are used in isolation. A total of 73 genera were identified in both DTMF and MC by IT analyses, of which, 43 were present in DTMF, 37 were present in MC, and 14 were common to both. Five most dominant bacterial genera were selected to observe their abundance in DTMF and MC by calculating their percentage in the total number of sequences (Table 3.4). It was observed that *Desulfosporosinus*, *Dysgonomonas* and *Proteiniclasticum* were the most predominant genera in DTMF of which *Desulfosporosinus* comprised 55.1% of the total sequences. On the other hand MC also showed 20.6% abundance of sequences of *Desulfosporosinus* (Table 3.4). The genus *Desulfosporosinus* from the *Firmicutes* group was the most abundant bacterial genus in both systems.

**Table 3.4 Percentage distribution of 5 dominant bacterial genus in DTMF and MC demonstrated by Ion Torrent analyses.**

| Genus | Class | Percentage in total sequences | |
|---|---|---|---|
| | | DTMF (average) | MC |
| *Anaerovorax* | *Clostridia* | 0 | 6.6 |
| *Buttiauxella* | *Gammaproteobacteria* | 0 | 13.2 |
| *Desulfosporosinus* | *Clostridia* | 55.2 | 20.6 |
| *Dysgonomonas* | *Bacteroidia* | 4.1 | 13.2 |
| *Proteiniclasticum* | *Clostridia* | 16.3 | 0.1 |

Percentage is calculated based on the total number of sequences.

**Table 3.5 Correlation coefficient analyses (two-tailed) among bacterial classes (number of isolates and sequence frequencies) and physicochemical parameters in DTMF and MC.**

APB, *Alphaproteobacteria*; BPB, *Betaproteobacteria*, GPB, *Gammaproteobacteria*; DPB, *Deltaproteobacteria*; SPB, *Sphingobacteria*; BAC, *Bacteroidia*; BCL, *Bacilli*; CLD, *Clostridia*, ACB, *Actinobacteria*; MLC, *Mollicutes* and MMB, *Methanomicrobia*.

| | **Bacterial classes** | | | | | | | | | | |
|---|---|---|---|---|---|---|---|---|---|---|---|
| Factors | APB | BPB | GPB | DPB | SPB | BCD | BCL | CLD | ACB | MCL | MMB |
| TDS | -0.930 | 0.679 | -0.785 | -0.998** | -0.998** | -0.274 | 0.358 | 0.340 | 0.268 | 0.484 | -0.998** |
| Conductivity | -0.936 | 0.612 | -0.763 | -0.996** | -0.996** | -0.238 | 0.388 | 0.309 | 0.305 | 0.498 | -0.996** |
| pH | -0.994** | 0.690 | -0.885 | -0.959* | -0.922 | -0.469 | 0.130 | 0.536 | 0.051 | 0.730 | -0.959* |
| Salinity | -0.937 | 0.611 | -0.763 | -0.996** | -0.992** | -0.239 | 0.387 | 0.310 | 0.304 | 0.501 | -0.996** |

**Correlation is significant at the 0.01 level (2-tailed)*Correlation is significant at the 0.05 level (2-tailed).

Ion Torrent data indicated that the most abundant bacteria in the DTMF and the MC was in fact the SRB, *Desulfosporosinus,* despite the fact that MPN and SANICHECK data suggested that SRB were relatively rare. No other study besides the tailings of this site has yet demonstrated the presence of *Desulfosporosinus* in an alkaline uranium mine impacted site. *Desulfosporosinus* spp. are obligate anaerobes, autotrophs and spore-formers (Stackebrandt *et al*., 2003) capable of consuming short-chain fatty acids as members of consortia that collectively degrade petroleum hydrocarbons (Suzuki *et al.*, 2002). The present work is the first report of *Desulfosporosinus* in an engineered, highly alkaline environmental setting. Members of the genus mainly inhabit industrially impacted soil and sediments, coal mining-impacted lakes and radionuclide-contaminated sediments (Singleton, 1993; Vatsurina *et al.*, 2008). *Desulfosporosinus*-like strains have repeatedly been seen to dominate subsurface bacterial communities associated with radionuclide-contaminated sediment that include the Midnight Mine, Washington (Suzuki *et al.*, 2002), the DOE Field Research Center in Oak Ridge, Tennessee (Shelobolina *et al.*, 2003), and uranium mine tailings in Shiprock, New Mexico (Shelobolina *et al.*, 2003). Since sulfate is present in the DTMF at concentrations ranging from 2 to 3 orders of magnitude greater than that of uranium, sulfate might play a dominant role in *Desulfosporosinus* metabolism. However, it may also be the case that since the DTMF is an "open" system, significant numbers of *Desulfosporosinus* may have entered the system, but then encountered poor conditions for growth and proliferation and thus were in the process of dying off (yet still detectable using DNA-based detection techniques). Additional work is therefore needed to elucidate the potential for SRB like those found in the DTMF to survive, and potentially proliferate, under the metal-rich, oxic conditions prevalent in the tailings.

### 3.4.6 Comparative analyses of bacterial diversity in the DTMF and MC as demonstrated by culture-based and Ion Torrent techniques

The major bacterial communities in the DTMF and MC showed clear differences; seven culturable bacterial classes represented the DTMF and MC (Figure 3.5A), whereas 11 bacterial classes were present in both systems (Figure 3.5B) based on Ion Torrent analyses. *Deltaproteobacteria*, *Bacteroidia*, *Mollicutes* and *Methanomicrobia* were not identified by culture methods (Figure 3.5A) but were identified by the culture-independent approach (Figure 3.5A and 3.5B).

In comparison to culture-based findings, Ion Torrent results were dominated by *Deltaproteobacteria* sequences, possibly due to their slow-growing nature on agar plates (Mitsui *et al*., 1997) and or specific physiological/nutritional requirements that were not met during repetitive subculture in the present study. This kind of contrast amongst culture-dependent and culture-independent analyses is not an uncommon phenomenon in microbial diversity studies (Ellis *et al*., 2003). Among the eleven classes demonstrated by culture-independent analyses, *Deltaroteobacteria* and *Methanomicrobia* were present only in the MC. In contrast, *Mollicutes* were present only in the DTMF (Figure 3.5B). In the DTMF, *Betaproteobacteria*, *Bacilli* and *Clostridia* represented the majority of sequences in comparison to MC where *Bacteroidia* and *Clostridia* were dominant (Figure 3.5B). Principle component analysis (PCA) of the class-wise culturable bacterial isolates (Figure 3.6A) and culture-independent bacterial sequences frequencies (Figure 3.6B) in the DTMF (D2, D3 and E2) and the MC revealed significant differences ($p < 0.01$; $R = 0.737$-$0.831$). Not surprisingly, no significant differences were observed among the three sites of DTMF (D2, D3 and E2) ($p > 0.05$; $R = 0.405$-$0.543$).

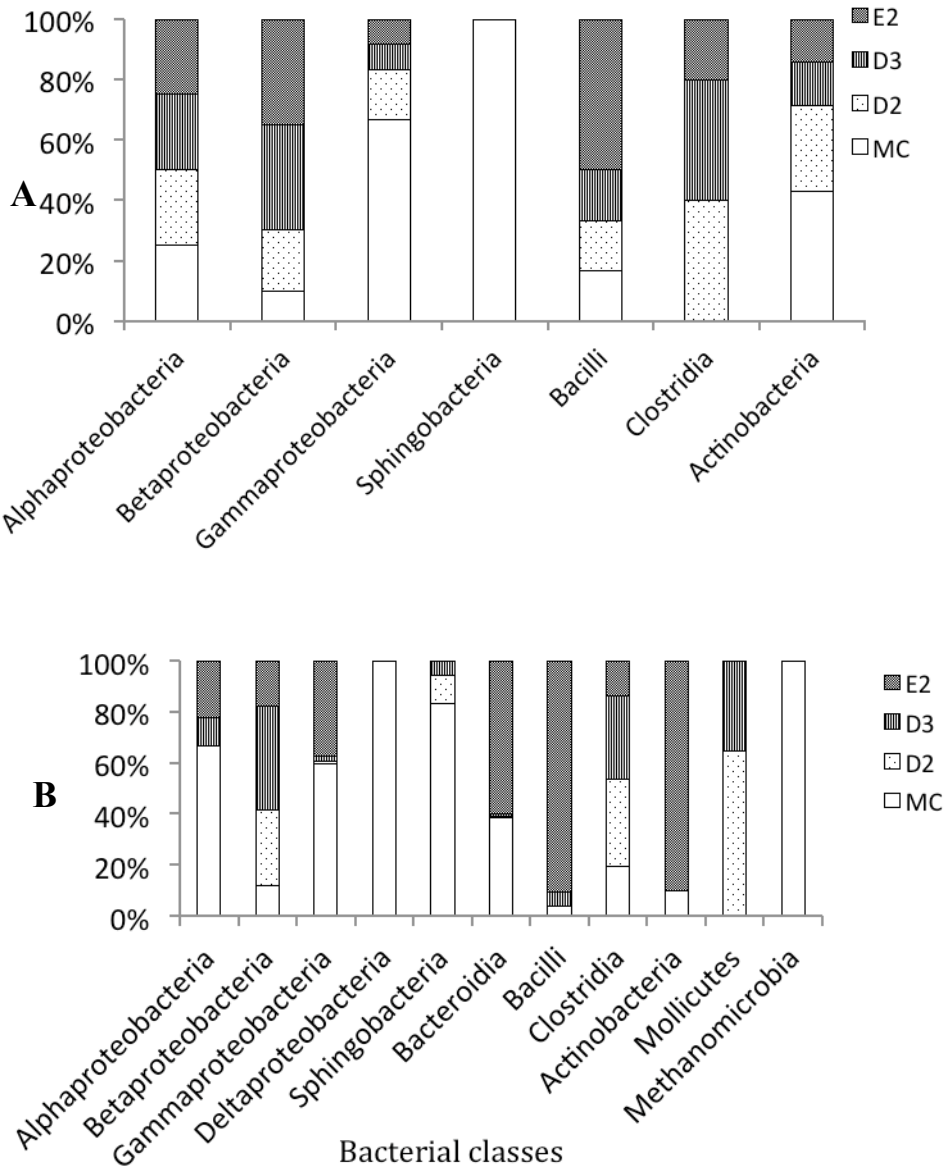


**Figure 3.5 Comparative site-wise community composition and diversity of bacteria for DTMF and MC interface samples**.

D2, D3 and E2 are the DTMF sampling locations; whereas, MC is the MC sampling location. A, diversity of bacteria based on culturable data and B, diversity of bacteria based on culture-independent data by Ion Torrent analyses. Percentage was calculated based on available unique bacterial isolates (A) and number of sequences observed in the DNA sample (B) in each sampling site.

However, the PCA analysis of the data from both culture-based and culture-independent analyses confirmed the presence of a distinctive environmental ecosystem harboring a specialized microbial community in the DTMF (Figure 3.6A, B).

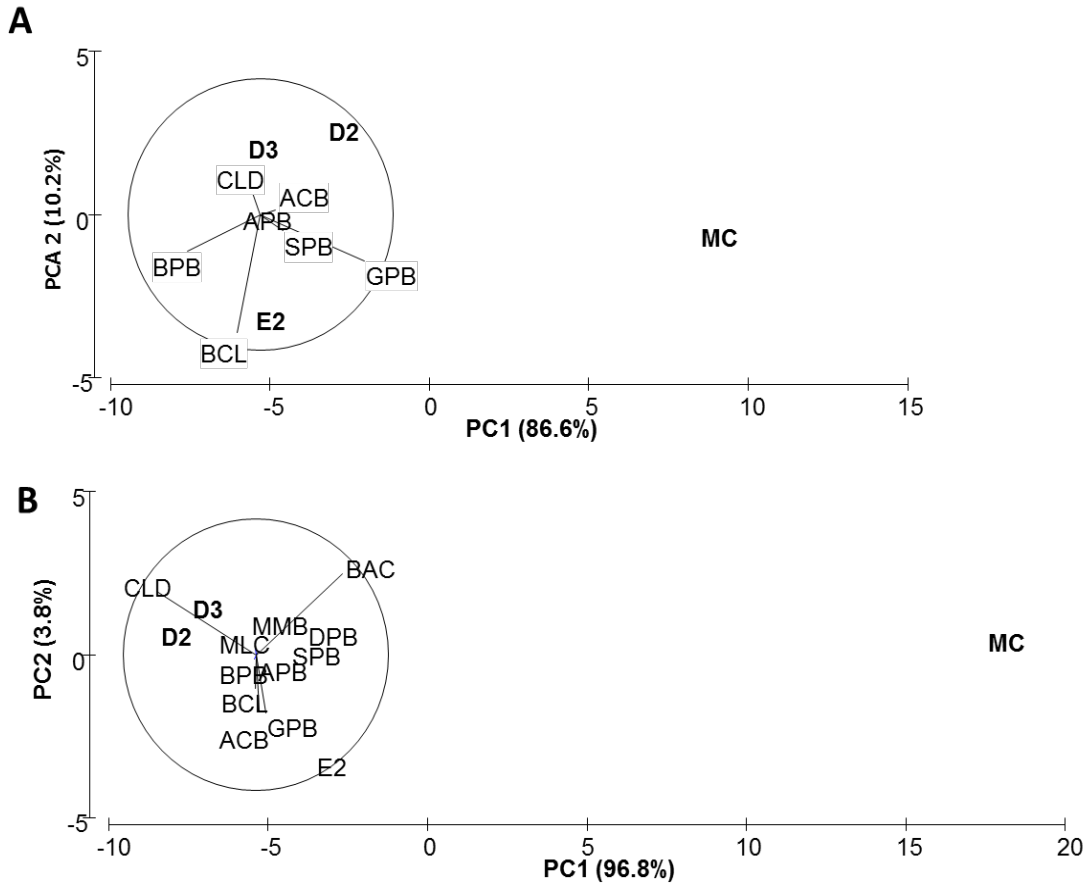


**Figure 3.6 Principal component analysis of the community structure of bacteria based on the number of available sequences of bacterial classes in each sampling location**.
D2, D3 and E2 are the DTMF sampling locations whereas MC is the MC sampling location. A) PCA of the culturable bacterial isolates present in DTMF and MC samples; and B) PCA of the culture-independent sequence analyses of the DNA samples isolated from DTMF and MC interface samples. APB, *Alphaproteobacteria*; BPB, *Betaproteobacteria*, GPB, *Gammaproteobacteria*; DPB, *Deltaproteobacteria*; SPB, *Sphingobacteria*; BAC, *Bacteroidia*; BCL, *Bacilli*; CLD, *Clostridia*, ACB, *Actinobacteria*; MLC, *Mollicutes* and MMB, *Methanomicrobia*.

### 3.4.7 Role of physicochemical parameters on the culture-independent bacterial diversity

A bivariate correlation analysis was carried out among the available sequence frequencies of various bacterial classes and physicochemical parameters in the DTMF and MC. TDS, conductivity, salinity and pH were included in these analyses whereas other parameters (e.g., the concentrations of metal elements) were not included as they were not measured in MC. Table 3.5 showed that the abundance of *Alphaproteobacteria* was negatively correlated with pH ($p < 0.01$). *Deltaproteobacteria* and *Methanomicrobia* were also negatively correlated with pH ($p < 0.05$). *Betaproteobacteria*, *Clostridia* and *Mollicutes* were positively correlated with pH; whereas, *Deltaproteobacteria*, *Sphingobacteria* and *Methanomicrobia* were negatively correlated ($p < 0.01$) with TDS, conductivity and salinity. *Betaproteobacteria*, *Bacilli*, *Clostridia* and *Mollicutes* all showed a positive correlation with TDS, conductivity, pH and salinity. The four tested parameters (which were each individually higher in the DTMF than in the MC) all positively correlated with the dominant bacterial classes in the DTMF (Table 3.5). In contrast, these four parameters negatively correlated with different bacterial clusters in the MC (Table 3.5).

### 3.4.8 Conclusions

The results of this study have identified the presence of specialized groups of bacteria inhabiting the water-tailings interface of the DTMF. Overall, it is evident that the distinctive conditions imposed within the DTMF (e.g., pH, TDS, conductivity, salinity and metal ion concentrations) exert selective pressures on the resident microbial communities. As there are no other reports of the culturable and culture-independent bacterial populations and diversity existing at the interface of alkaline uranium mine tailings, the present study will aid in the understanding of these environments along with potential microbial activities occurring therein. In particular, these findings may help understand the changes in microbiological diversity and

metabolic potential that occur in microbial communities that have been incorporated within the tailings mass for extended periods of time. The potential for the use of metal elements present in the DTMF as electron acceptors by SRB, as well as the activity of heterotrophic microorganisms in general, could influence the chemical stability of the system over long periods, and thus additional study of these effects is warranted.

### 3.5 Connection to next study

This study revealed that members of the microbial community at the water-tailings zone, the primary site where the tailings become incorporated into the tailings body, were closely related to the well-known sulfate reducing bacteria, which primarily utilize sulfate or iron as electron acceptor. The impact of contaminants, on microbial diversity was also evident as the DTMF water-tailings interface harbours a distinct bacterial community from a nearby reference lake. In order to demonstrate that the microbial populations with redox-transforming potential are present within the tailings, the next study characterized the microbial diversity and metabolic potential within the tailings body.

# 4 MICROBIAL COMMUNITIES IN LOW-PERMEABILITY, HIGH pH URANIUM MINE TAILINGS: CHARACTERIZATION AND POTENTIAL EFFECTS

This chapter has been published: Bondici, V.F., Lawrence, J.R., Khan, N.H., Hill, J.E., Yergeau, E., Wolfaardt, G.M., Warner, J. and Korber, D.R. (2013). Microbial communities in low permeability, high pH uranium mine tailings: characterization and potential effects. *J. Appl. Microbiol.* 114, 1671. This chapter is published here with the permission from the copyright owner (Wiley publications).

Author contributions

All authors participated in the design of the experiments and contributed to writing of the manuscript. Preparation of the initial draft of the manuscript, as well as all other data presented in this manuscript, are the work of the thesis author.

## 4.1 Abstract

The aim of this study was to describe the diversity and metabolic potential of microbial communities in uranium mine tailings characterized by high pH, high metal concentration and low permeability. To assess microbial diversity and their potential to influence the geochemistry of uranium mine tailings, aerobic and anaerobic culture-based methods were used in conjunction with next generation sequencing and clone library sequencing targeting two universal bacterial markers (16S rRNA and *cpn60* genes). Growth assays revealed that 69% of the 59 distinct culturable isolates evaluated were multiple-metal resistant, with 15% exhibiting dual-metal hypertolerance. There was a moderately positive correlation coefficient ($R=0.43$, $p < 0.05$) between multiple-metal resistance of the isolates and their enzyme expression profile. Of the isolates tested, 17 reduced amorphous iron, 22 reduced molybdate, and 7 oxidized arsenite. Based on next generation sequencing, tailings-depth was shown to influence bacterial community composition, with the difference in the microbial diversity of the upper (0-20 m) and middle (20-40 m) tailings zones being highly significant ($p < 0.01$) from the lower zone (40-60 m) and the difference in diversity of the upper and middle tailings zone being significant ($p < 0.05$). Phylotypes closely related to well-known sulfate and iron reducing bacteria were identified with low abundance, yet with relatively high diversity. The presence of a population of metabolically diverse, metal-resistant microorganisms within the tailings environment, along with their demonstrated capacity for transforming metal elements, suggests that these organisms have the potential to influence the long term geochemical stability of the tailings. This study was the first investigation of the diversity and functional potential of microorganisms present in low permeability, high pH uranium mine tailings.

## 4.2 Introduction

Mining and processing of uranium are associated with the generation of large quantities of residual materials containing heavy metals (Palmisano and Hazen, 2003). Microorganisms have evolved mechanisms that enable them to expand their habitat range so as to grow in a variety of apparently inhospitable environments. An example of such an environment is the uranium tailings management facility (the Deilmann Tailings Management Facility; DTMF) at Key Lake, northern Saskatchewan, Canada, which is characterized by high pH, high metal concentrations and low permeability. Tailings management facilities have been engineered to stabilize elements of concern (e.g., As, Se, Mo, U, Ra-226), but have only been in operation for several decades. In contrast, the processes that may affect their geochemical evolution and stability will occur over significantly longer periods of time and thus contaminant migration into the natural environment cannot be ruled out (Camus *et al.,* 1999). Since off-site migration of metal contaminants from uranium mine tailings is well documented and a subject of much environmental concern, it is critical to identify factors that may initiate or accelerate these processes (Pyle *et al.,* 2002; Thompson *et al.,* 2005; Abdelouas, 2006; Muscatello *et al.,* 2008). Off-site migration may involve both geochemical and biogeochemical factors; thus, modeling of the stability of tailings waste facilities should consider the possible contribution of both eventualities (Wilkin 2008).

As indicated by Rastogi et al. (2010), various studies have examined microbial community composition in uranium-contaminated environments (Fields *et al.,* 2005; Akob *et al.,* 2006). However, relatively few of these studies have involved actual uranium mining or tailings deposition sites (Wolfaardt *et al.,* 2008; Rastogi *et al.,* 2010; Islam *et al.,* 2011). In general, most uranium tailings are acidic and unsaturated; little microbiological research has been conducted

on high pH, saturated, uranium tailings deposition sites (Wolfaardt *et al.,* 2008) such as the Deilmann Tailings Management Facility (DTMF) located at Key Lake, Saskatchewan. Geochemical studies have been conducted to characterize heavy metal behavior in the DTMF uranium tailings and the results indicate that their long-term stability, in terms of immobilizing metals and oxyanions such as arsenic, selenium, and nickel, is dependent upon maintenance of oxic and alkaline conditions within the deposited tailings mass (Dughan-Essilfie *et al.,* 2011; Shaw *et al.,* 2011).

Microbial processes are important and sometimes even dominant factors in determining the fate and transport of contaminants in various subsurface environments. In general, microbial metabolism or resistance mechanisms result in redox transformation reactions leading to immobilization or increased mobility of the metal/metalloid element (Gadd 2010). Dissimilatory Fe (III) reduction is an important biogeochemical process as it may determine both iron distribution and the fate of iron-associated elements in subsurface systems (Lovley 2006). Evidence suggests that reductive dissolution of ferrihydrite-bound arsenic leads to an elevated concentration of soluble arsenic (Islam *et al.,* 2011). Similarly, arsenic and selenium speciation and mobility can readily be changed through microbial dissimilatory reduction or resistance mechanisms (Stolz *et al.,* 2006). Microbial metabolism may also result in the production of acidic micro-environments, causing a local decrease in pH that may promote metal mobilization if the buffering capacity of the immediate environment is exceeded (Al-Hashimi *et al.,* 1996).

In the DTMF, the ability of ferrihydrite to complex with, and thus control the solubility and mobility of, various heavy metals and metalloids is strongly dependent upon the oxic/alkaline condition of the tailings, which may be influenced by microbial activity. Initial studies have shown that bacteria were present in all core samples (obtained at 1 m intervals over

a 1.0 to 60 m depth profile) throughout the tailings body, with numbers ranging from 2.1 x $10^2$ to 2.2 x $10^8$ cfu $g^{-1}$ wet tailings material (unpublished data). The goal of the present study was to assess the functional and biological diversity of these bacteria in order to develop a better understanding of potential geomicrobiological processes that might occur within the tailings over extended periods of time (on the order of 1,000's of years). Culture-dependent and -independent methods were therefore used to characterize the microbial diversity in the tailings in conjunction with a panel of assays addressing metabolic transformation and resistance to metals to characterize potential functional roles of culturable organisms. This knowledge base will improve our understanding of the microbial ecology of these environments and provide an improved point of reference for microbial effects research on tailings geochemistry, and may also benefit efforts to mitigate the environmental impact of tailings management facilities.

## 4.3 Materials and methods

### 4.3.1 Sampling site

The Key Lake operation is located in the southern region of the Athabasca Basin, Canada, and is an important supplier of uranium ore for the global nuclear industry (Cameco Corporation 2011). Mining commenced in 1983 and the mined-out Deilmann pit became the mill tailings deposition site (DTMF) in 1996. Currently, the Key Lake mill processes uranium ore extracted from the McArthur River mine. Since this ore is of a very high purity (~34% $UO_2$) it is mixed with lower grade ore and waste rock during milling. This process generates millions of tons of uranium tailings that are deposited on top of the original Deilmann tailings. For example, in 2004 more than 30 million tons were produced (Natural Resources Canada 2004). The DTMF is 1000 m by 600 m by 60 m deep and is currently covered with a ~45 m layer of water (Cameco Corporation 2009). The average concentration of various metals along the depth profile of the

tailings sediment has recently been reported (Shaw *et al.,* 2011). In general, the concentration of the various elements in the two tailings zones differ; the lower Deilmann tailings have a higher elemental concentration than the overlying McArthur River tailings (Table 4.1). These differences are attributed to the fact that the Deilmann uranium ore body contained higher concentrations of Ni- and As-bearing sulfides; however, the pH (mean ~10) of the tailings does not vary with depth between the two zones (Shaw *et al.,* 2011).

**Table 4.1 Tailings sediment physiochemical characteristics.**

| Parameter (Mean) | Deilmann tailings (<410 masl) | McArthur tailings (>410 masl) |
|---|---|---|
| pH | ~10 | ~10 |
| T ($^{o}$C) | ~ 10 | ~10 |
| Eh (mV) | 189 | 220 |
| Na (µg/g) | 175 | 35 |
| As | 5.9 x$10^{3}$ | 440 |
| Ni | 6.1 x $10^{3}$ | 551 |
| Se | 17.0 | 3.0 |
| Mo | 183 | 14 |

Adapted from measurements previously reported (Shaw *et al.,* 2011).
Measurements were collected from three borehole locations between 2004 and 2009.
[Metal/metalloids]→ µg $g^{-1}$
Sodium and T → unpublished data
Eh → measured on tailings porewater
Masl→ meter above sea level

A vertical borehole was cored in the DTMF east cell to a depth of 122.6 m from water surface using a sonic track-mounted drill rig placed on a floating barge. Core sampling over the entire tailings depth (~60 m) was conducted using a 75 mm (inner diameter) by 3.1 m long core barrel. Each tailings core brought to the surface was immediately aseptically sub-sampled (using pre-sterilized 10 ml syringes as coring devices) at 1.0 m intervals, with duplicate samples collected at each depth for subsequent aerobic and anaerobic storage (in separate, sterile

Whirlpak™ bags; Fisher Scientific Ltd., Toronto, ON, Canada) and handling. Samples for anaerobic storage and processing were purged with an excess of $O_2$-free nitrogen gas before sealing, on site. The 120 samples (60 each for aerobic and anaerobic conditions) were then stored at 4°C until processing, which was initiated immediately after receiving the shipment. The tailings core material, which was slightly radioactive, was packed in a leak-proof primary container and shipped by truck to the laboratory and analysed within 10 days from the time of sampling.

### 4.3.2 Primary bacterial culture

Approximately 0.2 g (+/-0.01g) of each tailings sample was re-suspended in 1.0 mL of sterile Tris-EDTA (TE) buffer at pH 8. Four types of media were used for primary isolation of aerobic, facultative anaerobic, and potential strictly anaerobic bacteria: 5% Tryptic Soy Agar (TSA), Reasoner's 2A media (R2A), R2A10 (pH 10) containing 18.2 g R2A agar and $Na_2CO_3$ with a final concentration of 0.1mol $l^{-1}$ (Schmidt *et al.,* 2006), and a modified 0.2 % TSA media that contained the major chemical constituents in the tailings pore-water, as determined in 2008. This chemically modified TSA medium was designed to improve the isolation of strains that were highly adapted to *in situ* DTMF conditions and hence difficult to cultivate on standard agar media. To eliminate fungal growth on bacterial plates, cycloheximide (10 mg $l^{-1}$) was added to the media used for initial plating of the tailings samples (Irisawa and Okada 2009).

To enhance the isolation of potential psychrophiles, samples collected for aerobic bacteria isolation were incubated at 5°C for 3 weeks following plating (Gow and Mills 1984). An anaerobic glovebox with an $O_2$-free atmosphere consisting of 10% $CO_2$, 80% $N_2$, and 10% $H_2$ was utilized for the isolation of anaerobic bacteria at room temperature (21±2°C); anaerobic media (the same four media formulations as used for aerobic cultivation) was supplemented with

cysteine as a reducing agent (Meng *et al.,* 2001). Plates were incubated under anaerobic conditions for 3 weeks. The streak plate method was employed to isolate bacterial colonies from the mixed bacterial populations growing on each media type. Distinct colonies, based on color, size, and morphological type, were selected for isolation and subsequent molecular identification. To ensure that pure cultures were obtained, the bacterial isolates were sub-cultured at least three times.

### 4.3.3 Identification of bacterial isolates

Isolated bacterial colonies were subjected to DNA extraction and partial 16S rRNA gene (the first 3 variable regions) polymerase chain reaction (PCR) amplification was performed using the 8F (5'-AGAGTTTGATCCTGGCTCAG-3') and 531R (5'-ACGCTTGCACCCTCCGTATT-3') primer set (Hirkala and Germida 2004), yielding an ~500 bp PCR product. The final concentrations of the reagents used for a 50 µl PCR reaction mixture were as follows: 1.0 µmol $l^{-1}$ each of the forward and reverse primers, 1.0 U *Taq* polymerase (Invitrogen, Carlsbad, CA, USA), 1.0 µmol $l^{-1}$ $MgCl_2$, 1.0 X PCR buffer (both provided with the *Taq* polymerase), and 4.0 µmol $l^{-1}$ of deoxyribonucleotide triphosphates (dNTPs). The thermal cycling profile was set according to Hirkala and Germida (2004). For sequencing, the PCR amplicons were purified using Qiagen's purification kit (Qiagen Sciences, Maryland, USA) according to the manufacturer's instructions. For identification and phylogenetic analysis, 16S rRNA gene sequences were compared to all type strains using seqmatch within the Ribosomal Database Project (RDP) database (Cole *et al.,* 2009). Sequence alignments were edited manually using the GeneDoc program v 2.7 (Nicholas and Nicholas 1997). Representative isolates from groups of different isolates having identical (100%) gene sequences were chosen (there were 59 genetically distinct isolates in total) for further phenotypic characterization. Phylogenetic trees of the aligned

unique sequences and the closest type strain sequences from the RDP database were constructed by the neighbor joining method (Saitou and Nei 1987) using MEGA5 with 1000 bootstrap replicates (Tamura *et al.,* 2011).

### 4.3.4 Phenotypic characterization of bacterial isolates

#### 4.3.4.1 Metal resistance and enzymatic profiling

An agar plate dilution method was employed to test each of the 59 different bacterial isolates for salt and metal/metalloid tolerance (Lim and Cooksey 1993). A 10 µl aliquot of a 1.0 X $10^8$ cells $ml^{-1}$ cell suspension was spotted, in duplicate, onto a series of 5% TSA plates amended with increasing concentrations of analytical grade metal salts: NaCl, $NiCl_2 \cdot 6H_2O$ (Analar, BDH, Ltd. Poole, England), $Na_2SeO_3$ (Alfa Aesar, Ward Hill, MA, USA), $Na_2HAsO_4 \cdot 7H_2O$ (Sigma-Aldrich, St Louis, MO, USA) and $NaAsO_2$ (J.T. Baker, Phillipsburg, NJ, USA). An appropriate incubation period necessary for conclusive determination of growth success and phenotype of each isolate was empirically determined by observation at 2, 5, 10 and 14 days. The plates were incubated at room temperature and growth inhibition was determined by comparison with the 5% TSA control plates. To test whether a correlation between resistance to metals and enzyme expression (De Souza *et al.,* 2007) existed, enzymatic activity assays for oxidase, catalase, amylase, nitrate reductase, gelatinase, urease, and proteinase were conducted for each distinct bacterial isolate. Standard media for enzymatic testing were prepared according to the Difco BD (MD, USA) instructions. The biochemical tests were carried out at room temperature and the incubation period was one week. The correlation analyses were conducted in R (version 2.8.1) (R Development Core Team, 2008).

#### 4.3.4.2 Metal transformation potential

The ability of bacterial isolates to mediate redox-transformations of metal elements was determined by culture using the following liquid media in 24 well microtiter plates: amorphous iron (Lovley 2006), sulphate (Postgate 1951), molybdenum (Shukor *et al.,* 2008), and 5% TSA amended media with 2.5 mmol $l^{-1}$ As (III) and 5 mmol $l^{-1}$ As (V). The biogeochemical potential of the bacterial isolates was determined visually, based on the appearance of a specific color corresponding to the reduction of arsenate to arsenite (yellow), arsenite to arsenate (brown), ferric to ferrous iron (black), sulphate to sulphide (black), or molybdate to molybdenum (blue). The redox state of arsenic was determined by flooding the media with 0.1 mol $l^{-1}$ of $AgNO_3$ (Simeonova *et al.,* 2004). Iron and sulphate enrichment broth were aseptically transferred into 24 well microtiter plates and inoculated with the bacterial isolates. The degree of oxygen requirement of each isolate was determined using thioglycollate broth and those isolates that did not grow in this type of medium were streaked onto 5% TSA media and incubated in an anaerobic glovebox with an atmosphere of 10% $CO_2$, 80% $O_2$-free $N_2$, and 10% $H_2$. All isolates were tested for arsenic and molybdenum redox-transformation potential under aerobic conditions and only facultative isolates were subjected to anaerobic growth on arsenic, iron, and sulphate enrichment media. Incubation periods for color development were determined empirically; 4 weeks for Fe (III) and $SO_4$ enrichment media, and 2 weeks for As (V), As (III) and Mo (VI) transformations. All tests were carried out in duplicate and the positive control organisms for the iron and sulfate reduction tests were *Geobacter metallireducens* (ATCC 53774) and *Desulfovibrio desulfuricans* (ATCC 29577), respectively.

### 4.3.5 DNA extraction from uranium tailings

The FastDNA SPIN kit (MP Biomedicals, Solon, OH, USA) for soil was used to extract DNA from the tailings core samples by following the supplier's recommended protocol with minor modification. Aliquots of 0.5 g tailings sediment from each of the 60 core samples were subjected to DNA extraction. Equivalent volumes of extracted DNA from individual tailings samples were then combined, resulting in three DNA pools representing composited material from the upper, middle or lower layers of the DTMF, hereafter referred to as the 0-20, 20-40 and 40-60 m pools.

### 4.3.6 Depth-dependent sequence-based analysis of tailings DNA

#### 4.3.6.1 Ion Torrent 16S rRNA gene sequencing

Ion Torrent sequencing and data processing were carried out using Torrent adapter A (forward) and adapter P1 (reverse) which were annealed to sequencing primers specific for the V5 region of the 16S rRNA gene. The forward primer also included a key tag and a multiplex identifier (MID). The sequence of these primers were F5'-**CCATCTCATCCCTGCGTG TCTCCGAC**TCAGMIDGATTAGATACCCTGGTAG and R5'-**CCTCTCTATGGGCAGTCGGTGAT**CCGTCAATTCCTTTRAGTTT, respectively, and the single underlined sequence represents the target region-specific primer, the double underlined sequence is the key tag, and the sequences in bold are the adapters. The MIDs used for each pooled DNA sample were as follows: ACGCT (0-20 m), AGACG (20-40 m), and AGCAC (40-60 m). PCR reactions were carried out in 50 µl volumes containing 2 µl of template DNA, 1.0 µmol $l^{-1}$ each primer, 1.0 U *Taq* polymerase (Invitrogen, Carlsbad, CA, USA), 1.0 µmol $l^{-1}$ $MgCl_2$, 1.0 X PCR buffer (both provided with the *Taq* polymerase), and 4.0 µmol $l^{-1}$ of deoxyribonucleotide triphosphates (dNTPs). Cycling conditions consisted of a 5 min denaturing

step at 95°C followed by 40 cycles of 30 s at 95°C, 30 s at 57°C, and 45 s at 72°C, and a final elongation step of 10 min at 72°C. The PCR amplicons were purified using Qiagen purification kit (Qiagen Sciences, Maryland, USA) according to the manufacturer's instructions and quantified using a NanoDrop spectrophotometer. Pooled, MID-tagged amplicon libraries were sequenced using an Ion Torrent Personal Genome Machine (Life Technologies, Carlsbad, CA) with a 314 chip at the Biotechnology Research Institute (Montreal, Quebec). Sequence data were processed using RDP pyrosequencing pipeline tools. The pipeline Initial Process Tool was used to trim and remove low quality sequences, and sequences shorter than 100 bp. Quality sequences were submitted to the RDP classifier with a bootstrap cutoff value of 50%. Unclassified DNA sequences were further examined using Basic Local Alignment Search Tool (BLAST) to confirm that they were the 16S rRNA-encoding gene. Once non-16S rRNA sequences were removed, Unifrac analysis was used to compare the three DNA libraries based on phylogenetic information obtained from the GreenGene core dataset (Hamady *et al.,* 2010).

#### 4.3.6.2 Cpn60 clone library sequencing

The cpn60 clone libraries were assembled according to Schellenberg et al. (2009) based on pooled DNA from the 0-20, 20-40 and 40-60 m regions of the DTMF. A total of 2800 white colonies were randomly picked and sequences were processed according to Schellenberg et al. (2009). Trimmed cpn60 sequences were submitted to RDP classifier previously trained on a set of cpn60 UT sequences which consisted of all type I chaperonin sequences.

### 4.3.7 Nucleotide sequence accession numbers

DNA sequences obtained in this study were submitted to the European molecular biology laboratory (EMBL) database. The accession numbers for the partial 16S rRNA gene sequences

are HE650716 to HE650774. The accession numbers for the cpn60 sequences are KC552251-KC553978.

## 4.4 Results

### 4.4.1 Taxonomic affiliation of cultured bacterial isolates

A total of 199 bacterial isolates were obtained, of which 51 and 148 were recovered under anaerobic and aerobic conditions, respectively. Analysis of partial 16S rRNA sequences revealed the presence of 59 unique bacterial isolates, of which 25 were affiliated with the phylum *Proteobacteria,* with 8, 9 and 8 isolates belonging to the *α-, β-,* and *γ-Proteobacteria,* respectively. Twenty-three isolates belonged to the *Actinobacteria*, 9 to the *Firmicutes,* and 2 to the *Bacteriodetes* (Figure 4.1**)**. The number of representative genera was found to be the highest for the *Proteobacteria* phylum (25 isolates) and lowest for the *Bacteriodetes* (2 isolates). *Proteobacteria* was the proportionately dominant phyla in the upper and middle zones of the DTMF and *Actinobacteria* was dominant in the lowest zone, respectively. Despite the fact that the majority of the unique isolates showed >97% sequence similarity to previously cultured type strain bacteria reported in the 16S rRNA database, 25% exhibited divergence of greater than 3%, indicating that they represented putatively novel species (Table 4.2) (Keswani and Whitman, 2001).

### 4.4.2 Characterization of unique bacterial isolates

#### 4.4.2.1 NaCl and metal/metalloid salt sensitivity

The majority of the 59 representative isolates showed tolerance to elevated NaCl and metal/metalloid salts concentrations (Figure 4.2). The resistance profiles varied significantly;

**Table 4.2 Isolates belonging to potentially novel species.**

| Distinct isolates | Accession number | Best 16S rRNA gene match | Family | % identity |
|---|---|---|---|---|
| **AET17H** | HE650749 | *Polaromonas vacuolata* 34-P | Comamonadaceae | 95 |
| **AER18D** | HE650759 | *Polaromonas vacuolata* 34-P | Comamonadaceae | 95 |
| **AER14F** | HE650747 | *Massilia niastensis* 5516S-1 | Sphingomonadaceae | 96 |
| **AER11A** | HE650757 | *Paenibacillus chondroitinus* DSMZ | Paenibacillaceae | 90 |
| **ANr04A** | HE650717 | *Alkalibacterium iburiense* M3 | Staphylococcaceae | 94 |
| **ANr55A** | HE650734 | *Bacillus akibai* 1139 | Bacillaceae | 94 |
| **ANr41/42** | HE650730 | *Bacillus circulans* T | Bacillaceae | 96 |
| **AER05A** | HE650729 | *Hymenobacter norwichensis* NS/50 | Bacteroidetes | 94 |
| **AER37C** | HE650737 | *Modestobacter versicolor* CP153-2 | Geodermatophilaceae | 96 |
| **AET51J** | HE650755 | *Georgenia muralis* 1A-C | Bogoriellaceae | 96 |
| **AET35A** | HE650763 | *Arthrobacter aurescens* DSM 20124 | Micrococcaceae | 96 |
| **AET51I** | HE650743 | *Leifsonia antarctica* SPC20 | Microbacteriaceae | 93 |
| **AET52A** | HE650745 | *Plantibacter flavus* P 297/02 | Staphylococcaceae | 96 |
| **AER22D** | HE650752 | *Yonghaparkia alkaliphila* KSL-113 | Microbacteriaceae | 96 |
| **AER22/23A** | HE650754 | *Pedobacter cryoconitis* A37 | Sphingobacteriaceae | 92 |

The16S rRNA gene sequences of bacterial isolates from the tailings were matched against the RDP database.

nickel and arsenite were inhibitory at relatively lower concentrations in comparison to arsenate and selenite. The overall toxicity of the metal ions was as follows: Ni (II) > As (III) > Se (IV) > As (V). Of the 59 cultures tested, 48% exhibited tolerance to 7% NaCl (w $v^{-1}$), 70% to 10 mmo $l^{-1}$ Se (IV), 73% to 100 mmol $l^{-1}$ As (V), 32% to 1.0 mmol $l^{-1}$ Ni (II), and 35% to 5.0 mmol $l^{-1}$ As (III). These concentrations corresponded to, or encompassed the range of, concentrations previously employed to discriminate metal/metalloid-resistant from metal/metalloid-sensitive bacteria (Burton *et al.,* 1987; Sabry *et al.,* 1997; Drewniak *et al.,* 2008).

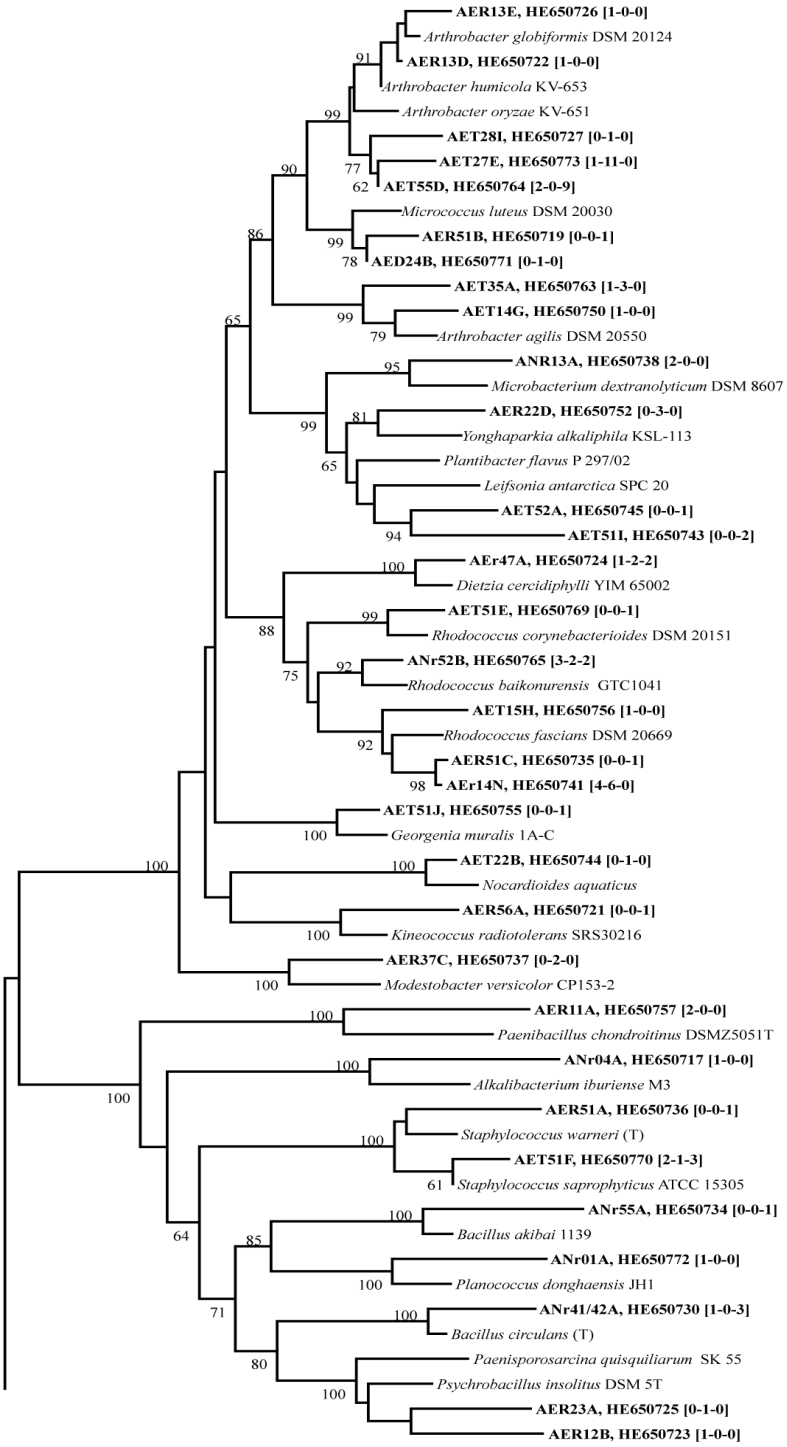


**Figure 4.1 Neighbour-joining phylogenetic tree of 59 distinct bacterial isolate sequences and reference 16S ribosomal sequences.**

The phylogenetic tree was devided into two panels for presentation puposes. The descriptive legend is provided next page.

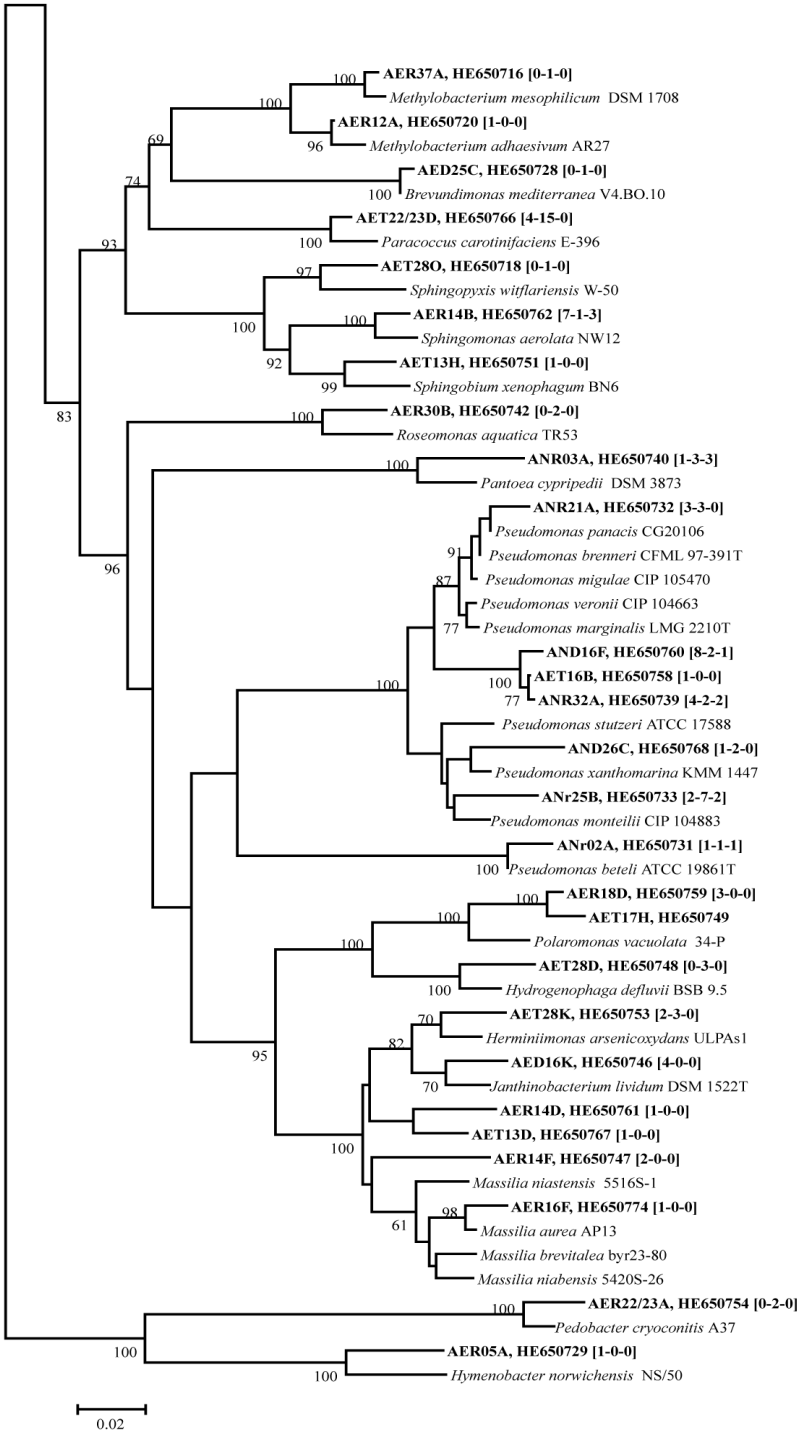


**Figure 4.1 Neighbour-joining phylogenetic tree of 59 distinct bacterial isolate sequences and reference 16S ribosomal sequences.** Sequences and their corresponding accession number of this study are shown in bold. Numbers in square brackets indicate the isolate's frequency of isolation in the tailings upper (0-20 m), middle (20-40 m) and lower (40-60 m) zones [upper-middle-lower]. Isolates were named according to atmospheric condition, media type, and depth of sample, as follows: AE (aerobic) or AN (anaerobic); R (R2A), r (R10), T (TSA), or D (DTA); number (sample depth), letter (isolate number).

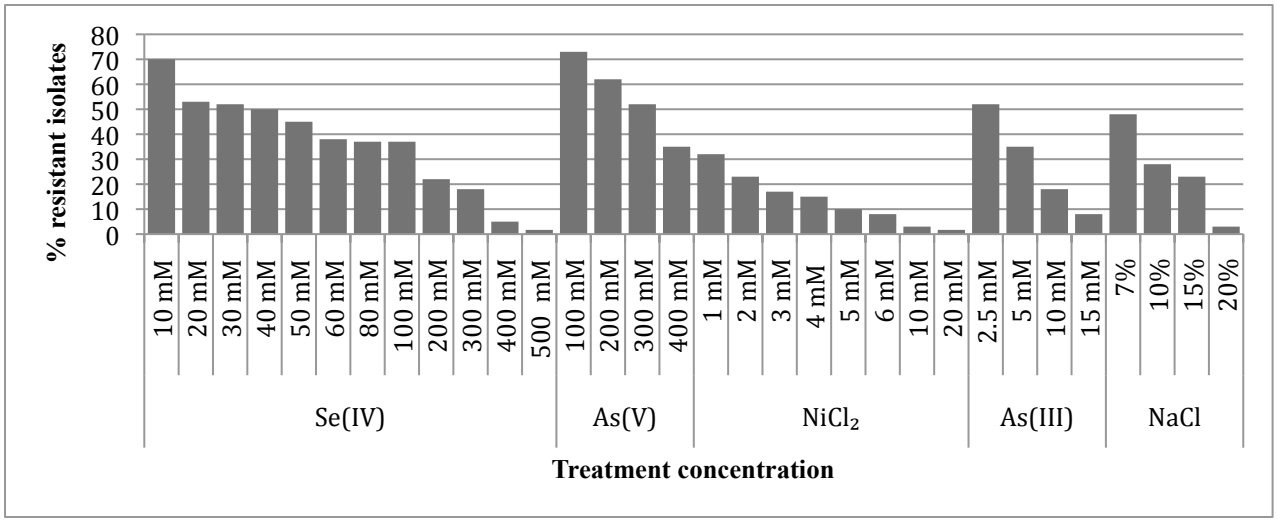


**Figure 4.2 Tolerance of the distinct bacterial isolates to different concentrations of salt and metal salts.**
Tolerance was based on the ability to grow on 5% TSA medium amended with increasing concentrations of analytical grade salts.

A high proportion of the tested strains were resistant to multiple metal ions: 14% of the tested isolates were tetra-, 31% were tri-, and 27% were dual-metal resistant. The multiple-metal resistant isolates predominantly belonged to the genera *Pseudomonas, Arthrobacter, Massilia, Micrococcus, Staphylococcus, Rhodococcus* and *Bacillus*. As the concentration of metal salts increased, the percentage of isolates capable of growth decreased; however, 15% of all bacterial isolates exhibited dual-metal hypertolerance (Table 4.3). These isolates not only showed tolerance to 300 mmol $l^{-1}$ Se (IV) and As (V) metalloids, but the majority could also grow at a relatively high NaCl concentration (15%). All dual-metal hypertolerant isolates demonstrated extreme tolerance to As (V) (400 mmol $l^{-1}$), and three isolates exhibited tolerance to Se (IV) (400 mmol $l^{-1}$). Furthermore, two isolates, which were closely related to *Rhodococcus fascians* (AET15H) and *Arthrobacter aurescens* (AET35A), showed tolerance to 20 mmol $l^{-1}$ Ni (II) and 500 mmol $l^{-1}$ Se (IV), respectively.

**Table 4.3 Salt tolerance of dual-metal hyper-tolerant bacterial isolates.**

| Name of the isolates | Closest match in RDP | % NaCl (w/v) |
|---|---|---|
| **AER51C** | *Rhodococcus fascians* | 15 |
| **AET51F** | *Staphylococcus saprophyticus* | 20 |
| **AET27E** | *Arthrobacter oryzae* | 7 |
| **AET15H** | *Rhodococcus fascians* | 15 |
| **AET35A*** | *Arthrobacter aurescens* | 15 |
| **AER22D*** | *Yonghaparkia alkaliphila* | 7 |
| **AET14G** | *Arthrobacter agilis* | 10 |
| **AER51B** | *Micrococcus luteus* | 15 |
| **AEr14N*** | *Rhodococcus fascians* | 15 |

Bacterial isolates were able to grow at a concentration of 300 mM Se (IV) and As (V).
* tolerant to 400 mM Se

#### 4.4.2.2 Correlation between enzyme activity profile and metal resistance

Enzymatic assay (i.e., catalase, oxidase, amylase, protease, gelatinase, urease and nitrate reductase) results were correlated to the metal ion resistance profiles of the distinct bacterial isolates, as conducted previously by De Souza et al. (2007). In general, bacterial isolates exhibiting multiple-metal resistance had a considerably wider range of enzymatic activities (Figure 4.3). A correlation coefficient ($R = 0.43$, $p < 0.05$) indicated that there was a moderate positive correlation between the two variables. Thus, multiple-metal resistant isolates tended to express a broader range of enzymatic potential than organisms that were resistant to fewer metals.

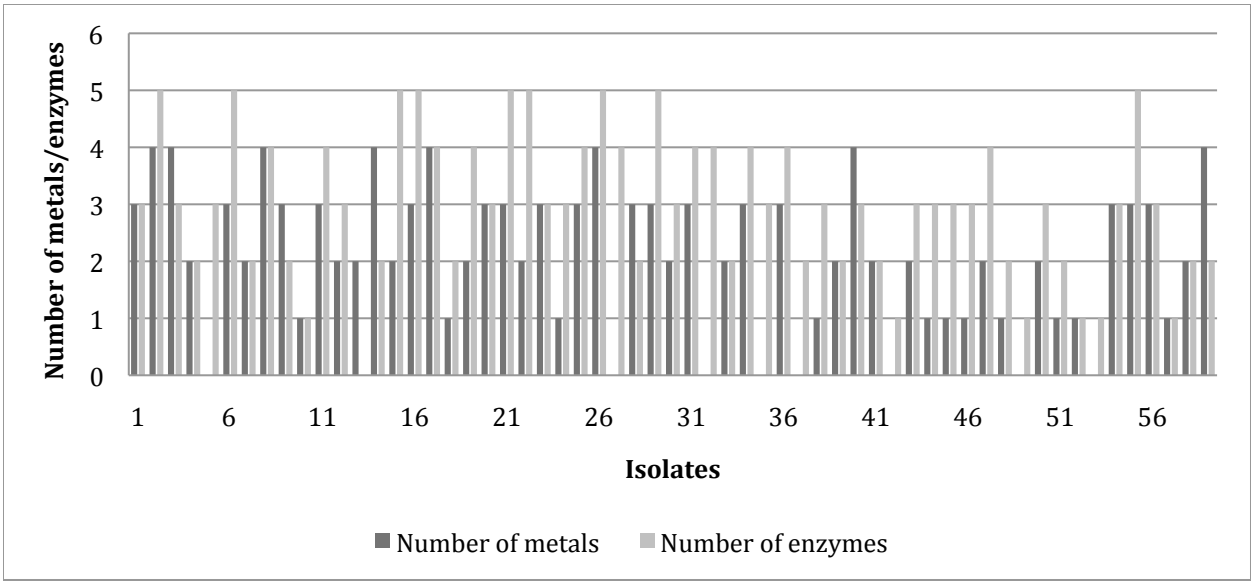


**Figure 4.3 Correlation between enzymes expressed and number of metals/metalloids to which bacterial isolates were resistant**.
Oxidase, catalase, amylase, nitrate reductase, gelatinase, urease, and proteinase enzymatic profile was correlated to Se (IV), As (V), Ni (II) and As (III) resistance.

#### 4.4.2.3 Metal redox-transformation potential

Seventeen isolates reduced amorphous iron and none of the isolates reduced sulfate, arsenate or oxidized arsenite under anaerobic conditions. The majority of the iron-reducing microorganisms were closely related to the genus *Pseudomonas* and the rest belonged to the genera *Pectobacterium, Microbacterium, Sphingomonas, Methylobacterium, Paenibacillus, Pedobacter* and *Janthinobacterium*. Furthermore, metal redox change was detected only for molybdate and arsenite under aerobic conditions, with twenty-two isolates reducing molybdate and seven isolates oxidizing arsenite to arsenate. Isolates that were able to oxidize arsenite were closely related to *Herminiimonas arsenicoxydans*, along with the genera *Arthrobacter, Micrococcus, Polaromonas, Massillia* and *Sphingomonas.*

### 4.4.3 Sequence analyses

To complement the culture-based methods, and to increase the sensitivity of detection of microbial diversity existing within the DTMF, two culture-independent techniques targeting two universal bacterial targets were employed. The same DNA template was used for both16S rRNA amplicon Ion Torrent sequencing and cpn60 clone library Sanger sequencing. A total of 21640 high-quality reads with an average length of 173 bp were retrieved following Ion Torrent sequencing, including 10169, 4152, and 7517 sequences corresponding to the 0-20, 20-40 and 40-60 m DNA libraries, respectively. From the clone library datasets, a total of 920, 952, 693 full-length cpn60 universal target reads were generated for the DNA extracted from the 0-20, 20-40 and 40-60 m zones, respectively. The combined data was classified into 415 genera representing 21 phyla. Furthermore, the two methods revealed slightly different taxonomic profiles, although the most abundant taxa in each dataset were from the same 8 phyla (Figure 4.4). Seven phyla (*Gemmatimonadetes*, *Chloroflexi*, *Deferribacteres*, *Deinococcus-Thermus, Verrucomicrobia*, *Aquificae*, *Thermotogae*) were detected only in the cpn60 libraries; whereas, 5 classified phyla (*Cyanobacteria/Chloroplast*, *Planctomycetes*, *Chlamydia, Fusobacteria, Tenericutes*) and one unclassified group were detected only by 16S rRNA sequencing.

The most prevalent phylum detected by both approaches was *Proteobacteria*. The relative abundance of this phylum varied between the two sequencing techniques, but exceeded 50% relative abundance in either case. The other major constituents of the sequence datasets included *Firmicutes*, *Actinobacteria*, and *Bacteroidetes* (Figure 4.4). Since the shared phyla of the two datasets included the most abundant taxa, the results were compared at the higher resolution of family and genus levels. A total of 151 families were detected of which 47% was

shared, 21% unique to the cpn60 clone libraries, and 32% unique to the 16S rRNA libraries (Figure 4.5).

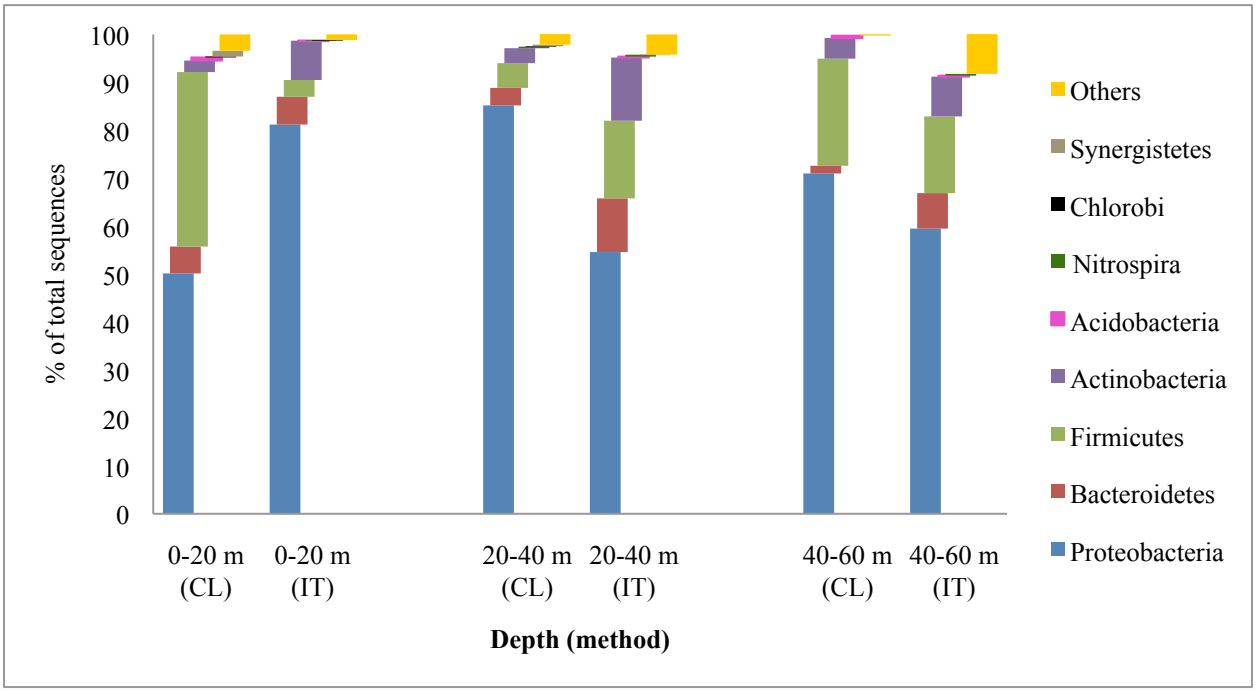


**Figure 4.4 Phylogenetic classifications of bacterial 16S rRNA and cpn60 universal gene sequences obtained by Ion Torrent and Sanger sequencing techniques.**
(CL= Clone library and IT= Ion Torrent).

It was remarkable to observe that only a relatively low percentage (13%) of the phylotypes were shared at the genus level, with 27% unique to the cpn60 clone library and 60% to the 16S rRNA method, respectively. Furthermore, the shared phylotypes were minor members of the bacterial community with relatively low frequency, except for *Rhodoccocus*, *Acidovorax*, *Oxalicitibacter*, *Polaromonas*, *Propionibacter*, *Pseudomonas*, *Variovorax*. At the fine scale analyses of the overlapped reads, Ion Torrent sequencing generally not only detected the

common phylotypes at higher frequency, but was also able to identify them in more samples in comparison with the cpn60 clone library.

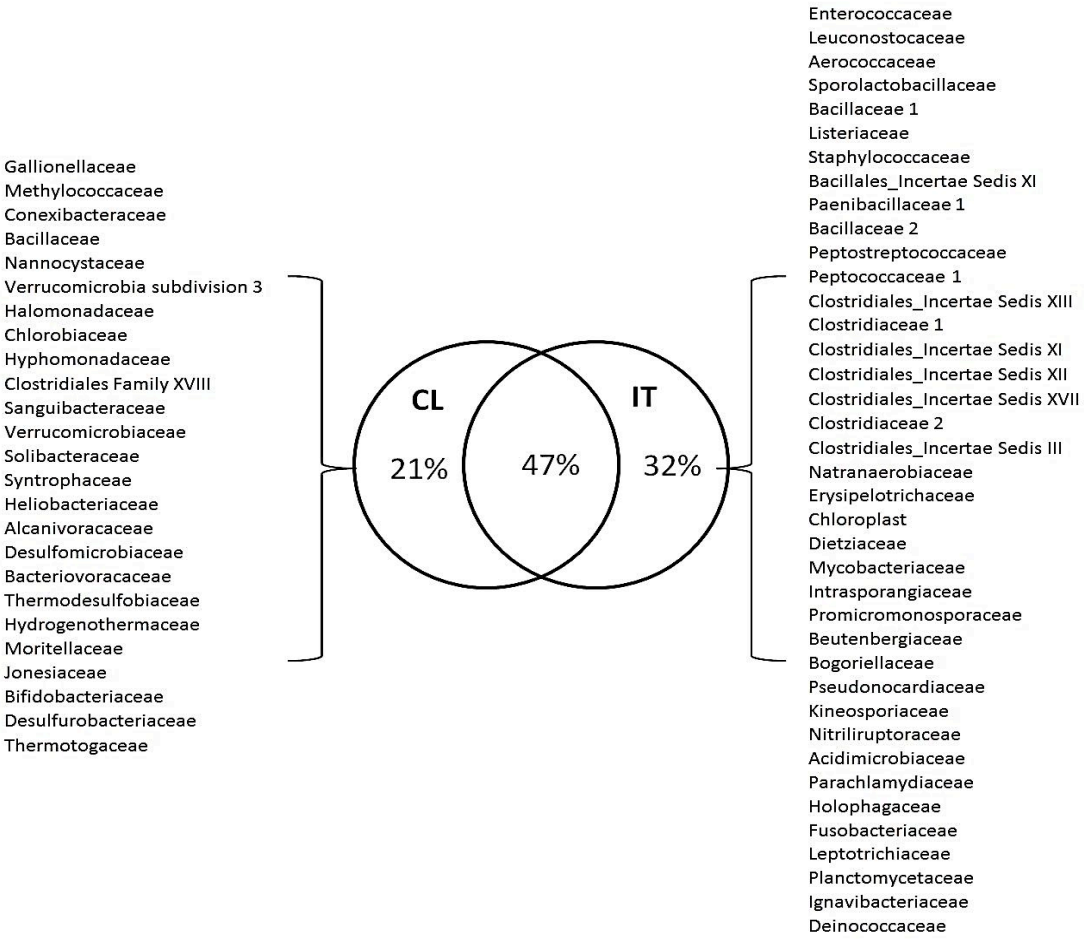


**Figure 4.5 Distribution of shared and unique bacterial taxa for the cpn60 clone library and 16S rRNA Ion Torrent sequencing.**
Analyses were performed on the combined datasets (CL= Clone library and IT= Ion Torrent).

### 4.4.4 Depth-dependent comparison of microbial community structure

Consistent with observations of culturable bacteria, sequence libraries from all three depths were largely dominated by *Proteobacteria*, *Firmicutes*, *Actinobacteria* and *Bacteroidetes*. Comparison of the phylogenetic composition of the 16S rRNA sequence libraries with Unifrac distance statistical analyses showed highly significant differences ($0.001 < p < 0.01$) between the

upper zones (0-20 m; 20-40 m) and lower zone (40-60 m) DNA libraries; whereas, the upper zone was significantly different ($0.01 < p < 0.05$) from the middle zone (Table 4.4).

**Table 4.4 Statistical significance (p-values) of differences among the bacterial communities from the three tailings zones using Unifrac distance analyses.**

| Ion torrent libraries of the tailings zone | 0-20 m | 20-40 m | 40-60 m |
|---|---|---|---|
| 0-20 m | | <0.05 | <0.01 |
| 20-40 m | | | <0.01 |

P-test significance was based on 500 permutation and P values were corrected for multiple comparison (Bonferroni correction).

### 4.4.5 Identified phylotypes with metal reducing potential

Taxonomic profiling by both sequencing mehods revealed the presence of bacterial groups that are well-documented in terms of biogeochemical potential for transforming elements that are abundant in the DTMF tailings and whose redox transformation may directly or indirectly influence mobilization of elements of concern (i.e., As, Se, Mo). Fifteen and 9 genera were captured that belong to recognized sulfate reducing and iron reducing bacterial groups, respectively. Four phylotypes, including *Ferruginibacter*, *Georgfuschia*, *Dethiobacter*, and *Albidiferax,* were detected consistently in all three pooled libraries with a maximum frequency reaching 0.9% in the lower zone (40-60 m).

## 4.5 Discussion

### 4.5.1 Resistance of isolates to metal/metalloid compounds

Elevated concentration of various heavy metals and oxyanions (Ni, Se, As, Mo) and high pH (10) dominate the DTMF environment. In general, the presence of heavy metals tends to inhibit bacterial activity and growth; therefore, microorganisms persisting in metal-contaminated

subsurface systems are likely to possess a high degree of genetic flexibility (Romero and Palacios, 1997) aiding in their adaptation to DTMF conditions. The positive correlation between bacterial potential activity and cultivability may imply that the specialized, readily cultivable microbiota play an important role in this unique ecosystem in terms of biogeochemical function (Ellis *et al.,* 2003). In the DTMF tailings, representatives from the *Proteobacteria*, *Actinobacteria*, and *Firmicutes* phyla were most frequently isolated by culture-based techniques. However, earlier studies have demonstrated that these phyla are, in general, the predominant culturable bacterial groups (Fredrickson *et al.,* 2004; Zhang *et al.,* 2007; Jose *et al.,* 2011) and thus they tend to be among the numerically most abundant taxa recovered at various contaminated sites (Akob *et al.,* 2006; Rastogi *et al.,* 2011).

It was somewhat remarkable that 69% of the DTMF isolates tested exhibited multiple-metal resistance. Other studies of multiple-metal resistance genes demonstrated the adaptive ability of a microbial community indigenous to mixed-contaminant waste sites (Sobecky and Comb 2004). There are three main microbial mechanisms of metal ion resistance: efflux, sequestration and redox modification (Ordonez *et al.,* 2005). Multiple-metal resistance may require a combination of these mechanisms. In the present study, we also found that 9 dual-hypertolerant bacterial isolates could grow in the presence of at least 300 mmol $l^{-1}$ of Se (IV) and As (V). The majority of these isolates were retrieved from the middle zone (20-40 m) of the tailings, which includes the interface between the McArthur River and Deilmann mine tailings. Selenium (IV) and As (V) are widespread in nature and therefore bacterial resistance would not be confined to contaminated areas. However, such a high level of tolerance to these elements is, based on the literature, rare (Drewniak *et al.,* 2008). In our study, isolates closely related to

*Rhodococcus fascians* and *Arthrobacter aurescens* exhibited hypertolerance to arsenic, selenium and nickel (Table 4.3).

Previous investigations have also reported exceptionally high levels of metal tolerance (hypertolerance) or multiple-metal resistance for bacterial isolates retrieved from contaminated environments; for example, *Arthrobacter* spp. from the Savannah River Site, South Carolina, and the Hanford Site, Washington, with resistance to Pb (II), Hg (II) and Cr (VI) (Benyehuda *et al.,* 2003), and a *Rhodococcus* sp. from a gold mine with tolerance to As (V) (Drewniak *et al.,* 2008). Members of the coryneform group are recognized for their high tolerance to elevated concentrations of As (V) (Ordonez *et al.,* 2005; Drewniak *et al.,* 2008); in addition, the arsenic resistance determinants of a *Corynebacterium glutamicum* strain have been fully elucidated (Ordonez *et al.,* 2005). However, little research has been conducted on the metal tolerance of *Arthrobacter* spp. (Benyehuda *et al.,* 2003). The *Arthrobacter* isolates recovered in the present study with demonstrated involvement in redox reactions could have biotechnological relevance because metal tolerance is also considered to be a prerequisite characteristic for bioremediation strategies. Microorganisms with potential to successfully bioremediate a pollutant must first survive in the presence of both target and non-target toxic metals (Haferburg *et al.,* 2007).

### 4.5.2 Correlation between enzyme activity profile and metal resistance

Previous studies on Antarctic bacterial isolates showed an inverse correlation between multiple metal resistant bacteria and enzymatic potential (De Souza *et al.,* 2007). Overall, their results demonstrated that the metal-resistant strains tended to have lower enzymatic potentials. In contrast, the DTMF isolates displayed a moderately positive correlation between multiple-metal resistance and enzymatic activity, suggesting that multiple-metal resistance did not compromise general, or overall, metabolic activity.

It was previously recognized that organic carbon tends to make heavy metals less bio-available (Kim *et al.,* 1999); therefore, bacterial isolates retrieved from environments with relatively high organic carbon content would tend to be metal sensitive and possess a wider range of enzyme profiles. Furthermore, it was previously observed that isolates from environments characterized by lower organic carbon concentrations exhibited multiple-metal resistance with lower enzymatic potential (Ordonez *et al.,* 2005). The DTMF tailings contain relatively high concentrations of numerous heavy metals and the solid-phase organic carbon concentrations may reach 0.9 %, a relatively high carbon content. It is thus speculated that the microbiota in the DTMF environment may not be required to sacrifice enzymatic functionality due to the abundance of both factors.

### 4.5.3 Metal redox reactions

Microbial iron reduction is a ubiquitous and well-documented process that may influence the geochemistry of subsurface settings. Phylogenetically diverse Fe (III)-reducing organisms have been isolated and described from various environments spanning a wide range of chemical and physical conditions (Webber *et al.,* 2006). The most common and comprehensively studied microorganisms that conserve energy to support growth from Fe(III) reduction belong to the *Geobacteriaceae* (genera: *Geobacter, Desulfuromonas, Desulfuromusa* and *Pelobacter, Acidobacteria* and *Shewanella* spp.) (Lovley, 2006; Webber *et al.,* 2006). Other iron-reducing bacterial groups have been previously reported; for example, *Pseudomonas* spp. (Nevin *et al.,* 2003). In a microcosm study conducted on high salinity, uranium-contaminated sediment samples, phylogenetic profiling demonstrated that microorganisms closely related to *Pseudomonas* species were involved in nitrate, followed by Fe (III) and U (VI), reduction (Nevin *et al.,* 2003).

In our study, the well-known iron reducing bacterial groups were not recovered because we did not use specific liquid media for them during initial culturing and isolation. However, our observation that the readily culturable bacterial members besides the well-known iron reducers exhibited reductive dissolution extends our understanding of the indigenous microbial community's biogeochemical potential and their potential effect on system stability. Furthermore, characterization of these organisms may allow the identification of physiological factors that may control the rate of iron reduction in this type of environment. Reductive dissolution of Fe on a large scale within the DTMF tailings would be a concern as this process could result in the release of adsorbed and co-precipitated As into the aqueous phase, with subsequent migration of this element into the environment.

The fact that none of the tailings bacteria isolated during this study were able to reduce arsenate under anaerobic or aerobic conditions suggests that arsenate did not serve as an electron acceptor during respiration and that whatever detoxification process is utilized by these organisms, it does not involve redox transformation to arsenite. However, in the case of the 7 isolates that were able to oxidize arsenite under aerobic conditions, oxidation was possibly due to a detoxification process rather than use of arsenite as an energy source (Oremland *et al.,* 2004). Several isolates have been reported to oxidize arsenite; for example, *Thiomonas* (Casiot *et al.,* 2003), *Pseudomonas* (Chang *et al.,* 2010), and *Polaromonas* (Osborne *et al.,* 2010). Bacterial conversion of As (III) to As (V) is also of considerable interest for bioremediation applications, as this process generates a less-toxic and less-soluble arsenic species (Oremland *et al.,* 2004). Microorganisms isolated from the DTMF with the ability to convert specific redox-sensitive elements to an insoluble state would thus have potential application in bioremediation. This is particularly true for bacterial isolates that are well-adapted to contaminated systems, such as

*Arthrobacter aurescens,* which exhibited extreme tolerance to As (V) (400 mmol $l^{-1}$) and Se (IV) (500 mmol $l^{-1}$), and may act to stabilize the DTMF tailings through conversion of As (III) to As (V).

### 4.5.4 Microbial diversity as estimated by sequencing based techniques

To minimize any potential biases of the 16S rRNA-based approach, techniques based on protein-encoding universal targets used in parallel with culture-based methods have been suggested (Donachie *et al.,* 2007; Na *et al.,* 2011; Roux *et al.,* 2011). Comparative studies have demonstrated that cpn60 fulfills the criteria of being an excellent molecular target and provides greater discriminatory power when closely related species are compared (Goh *et al.,* 1996; Hill *et al.,* 2005). In our study, the integration of these two molecular approaches led to the capture of greater bacterial diversity (21 phyla) relative to the use of either molecular technique employed alone. The complementary nature of these two sequencing methods targeting two different universal targets was further evidenced by the fact that at the family level, there was a relatively high fraction (47%) of taxa overlap; whereas, at higher taxonomic resolution only 13% overlap existed between the two datasets. A similar pattern has been observed in other comparative studies where 16S rRNA Sanger and pyrosequencing datasets were compared (Na *et al.,* 2011). The low number of bacterial taxa shared at the genus level can most likely be attributed to dataset size, amplification bias of "universal" PCR primers, as well as library construction method (clones vs. amplicon sequencing) (Schellenberg *et al.,* 2009; Roux *et al.,* 2011). Ion Torrent sequencing is a relatively new platform; however, reliability has recently been validated in a study that provided near-identical output as the 454 sequencing approach (Yergeau *et al.,* 2012). It is noteworthy that this study represents the first time that the RDP classifier has been used for cpn60 UT sequences. With an 80% cutoff value, the taxonomic identification of the

cpn60 sequences obtained with the trained classifier was in good agreement with the output of the wateredBlast.

### 4.5.5 Microbial diversity across depths and their biogeochemical potential

It has previously been demonstrated that concentrations of metals/metalloids could be considered as a strong determining factor of bacterial diversity at uranium-contaminated habitats (Fields *et al.,* 2005; Akob *et al.,* 2006). The significant difference in microbial diversity across the tailings depths can be primarily attributed to the difference in geochemical composition of the two ore bodies. In general, the concentration of the various elements (e.g., As, Ni) in the upper zone of the Deilmann solids are ~100X lower than in the deeper zones (Shaw *et al.,* 2011).

The major lineages (*Proteobacteria*, *Firmicutes, Actinobacteria*, and *Bacteroidetes*) captured by both molecular techniques were also detected by culturing. Only *Pectobacterium*, *Modestobacter*, *Georgenia*, *Planococcus*, *Paenisporosarcina*, *Hymenobacter*, *Kinococcus* were isolated, but not detected, by the culture-independent methods. The fact that the microbial diversity spectrum captured by the molecular techniques can be extended by the parallel application of culture-based methods is well-documented (Donachie *et al.,* 2007). It has previously been suggested that one of the potential biases relates to the difficulty in obtaining DNA template from bacterial groups with spore-forming ability (Donachie *et al.,* 2004).

Of particular importance is that the readily culturable bacterial isolates closely related to e.g., *Rhodococcus, Pseudomonas, Arthrobacter, Massilia, Micrococcus, Polaromonas, Hydrogenophaga,* and *Bacillus,* were also consistently observed at high frequency in the sequence datasets. In addition to relative high abundance and culturability, these microorganisms exhibited a high degree of tolerance to metals/metalloids or reducing/oxidizing capability. This

further suggests an important role of the abundant and readily culturable microorganisms in terms of their biogeochemical function in the DTMF system.

The most abundant lineages detected solely by sequence-based methods were also affiliated to *Proteobacteria* and *Firmicutes* that are known to survive harsh environments, such as extreme pH and heavily contaminated areas (Akob *et al.,* 2006). Less-abundant, but important, phylotypes that are closely related to well-known sulfate reducing and iron reducing bacteria were also identified. Representatives of sulfate reducing and iron reducing lineages included *Dethiobacter*, *Desulfovibrio*, *Desulfosporosinus*, *Desulfomicrobium,* and *Geobacter*, *Geoalkalibacter*, *Georgfuchsia*, *Ferruginibacter*, *Ralstonia*, respectively. These genera have been reported previously from uranium-, heavy metal- and hydrocarbon-contaminated sites (Sitte *et al.,* 2006; Zavarzina *et al.,* 2006; Rastogi *et al.,* 2011). Bioremediation studies have demonstrated that members of these genera may become numerically and functionally important when ferric- and sulphate-rich sediments are amended with various carbon sources, resulting in reductive dissolution (Vrionis *et al.,* 2005; Na *et al.,* 2011).

### 4.5.6 Conclusions

This is the first examination of microbial diversity and functional potential of culturable bacterial populations within high pH, metal-rich, low permeability mining-impacted environments such as the DTMF. High (and multi-) metal tolerance, as well as broad enzymatic potential, indicate that a significant proportion of the resident microorganisms are well-adapted to this unique environment. The fact that the uranium tailings support the growth of well-known iron reducing and sulfate reducing bacteria, along with detection of culturable bacterial populations that exhibit metal-reducing capability, indicates the potential for Fe and S biogeochemical cycling. Overall, the results of this study also emphasize the value of using

multiple approaches for the characterization of microbial functional and taxonomic diversity in complex ecological systems like the DTMF.

## 4.6 Connection to next study

Studies 1, 2, 3 demonstrated that the microbial communities in the water column, at the water-tailings interface, and within the tailings mass exhibit biogeochemical potential. The following study investigated the potential of bacterial flora native to the DTMF system to reduce environmental Eh as well as ferrihydrite in the DTMF system.

# 5 BIOGEOCHEMICAL IMPORTANCE OF THE BACTERIAL COMMUNITY IN URANIUM WASTE DEPOSITED AT KEY LAKE, NORTHERN SASKATCHEWAN

This chapter was submitted (June 10, 2015) to the journal of *Geomicrobiol J.* and it is under review. V.F. Bondici, G.D.W. Swerhone, J.J. Dynes, J.R. Lawrence, G.M. Wolfaardt, J. Warner, D.R. Korber Biogeochemical importance of the bacterial community in uranium waste deposited at Key Lake, northern Saskatchewan (manuscript ID number UGMB-2015-0118).

Author contributions

All authors participated in the design of the experiments and contributed to writing of the manuscript. Preparation of the initial draft of the manuscript, as well as all other data presented in this manuscript, are the work of the thesis author.

## 5.1 Abstract

The long-term stability of immobilized elements of concern in uranium tailings deposited in the Deilmann Tailings Management Facility (DTMF), northern Saskatchewan, is dependent upon maintenance of highly oxic conditions within the tailings mass. The main objective of this study was to investigate the effect of stimulating microbial activity on the redox potential and state of ferrihydrite, which are considered to be the primary controlling condition and mineral phase, respectively, within the tailings. To determine the potential for biologically mediated redox potential decrease and ferrihydrite reduction, a series of microcosm assays were performed. Non-sterile material from the DTMF tailings-water interface was inoculated with indigenous flora previously isolated from the tailings sediment and enriched with a carbon source (50 ppm tryptic soy broth) and incubated under continuous-flow or intermittent-flow conditions, and compared with an uninoculated, no-carbon control incubated under continuous-flow. Highly reducing conditions with redox potentials of less than -300 mV were detected after 2 days of incubation within the carbon-enriched tailings of microcosms receiving continuous-flow and less than -280 mV after 11 days of incubation within carbon-enriched tailings in microcosms receiving intermittent-flow. The lowest recorded Eh value of -545 mV was measured after 14 days in a carbon-enriched microcosm receiving intermittent flow. In contrast, the redox conditions in the continuously flowing control microcosm never dropped below -93 mV; thus, it was clear that microbial activity and available carbon lead to the observed reductions in microcosm Eh. The occurrence of low redox conditions was concomitant with the bulk chemical detection of Fe (II) in the effluent of carbon-enriched microcosms. Sites of microbial ferrihydrite reduction were also detected using scanning transmission X-ray microscope image analyses where Fe (II) species were observed in direct contact with bacterial

cells. Analysis of microbial diversity within the microcosms confirmed that microbes indigenous to the DTMF system have the potential to generate conditions amenable to the proliferation of sulphate and iron reducing bacteria, such as *Desulfosporosinus,* which was detected by Ion Torrent sequencing.

## 5.2 Introduction

Large quantities of uranium tailings waste are generated during uranium mining and processing. Uranium mine tailings are of environmental concern because they are radioactive and contain large quantities of highly toxic heavy metals which are released from the ore during the uranium leaching process (Abdelouas, 2006). The Deilmann Tailings Management Facility (DTMF) in northern Saskatchewan is an active deposition site for uranium tailings, and has been shown to contain elevated concentrations of contaminants such as As, Ni, Se and Mo (Moldovan *et al*., 2005; Shaw *et al*., 2011; Essilfie-Dughan *et al*., 2011). Ferrihydrite, the main secondary mineral phase in the tailings, is produced from the leached ore species and the reagents added during the neutralization process, plays a significant role in the sequestration and stability of these contaminants-in the DTMF tailings (Essilfie-Dughan *et al*., 2011; Essilfie-Dughan *et al*., 2012; Gomez *et al.*, 2013). The principal environmental concern is the possibility for long-term release of As from the in-pit tailings into the surrounding groundwater (Essilfie-Dughan *et al*., 2012). Therefore, factors influencing the stability of contaminant-bearing mineral phases (e.g., ferrihydrite) and other complexes within the DTMF uranium tailings are of great interest.

Managing metal-contaminated sites is a complex and challenging task thus, simple measurements of the numerical value of the concentration of a given contaminant is not sufficient to assess its potential escape and subsequent ecological risks (Chapman *et al*., 1999). It has long been recognized that redox potential (Eh) is a critical parameter in controlling the fate

or mobility of metal elements in subsurface sediments (Chuan *et al*., 1995). Studies have shown that microbial activity can influence this parameter because microorganisms can serve as biocatalysts for various redox reactions (Lensing *et al*., 1994; Calmano *et al*., 2003). For example, they are able to lower the redox potential of an environment through the oxidation of organic matter coupled with the reduction of dissolved oxygen and nitrate (Lovley and Chapelle, 1995).

Most strictly anaerobic bacteria require a low redox potential to grow and since aerobic heterotrophs and facultative anaerobes can lower the redox potential during growth these microorganisms may co-exist in various environmental settings (Straub and Schink, 2004). For example, it has been shown that ferrihydrite reduction by iron reducing bacteria can be stimulated by the activity of secondary bacterial species, which lower the Eh of the environment (Straub and Schink, 2004). According to equilibrium thermodynamics, as Eh decreases due to microbial activity, the redox equilibrium of other elements are shifted in favour of the reduced form (Lovley, 1991). Furthermore, microorganisms can also directly change the redox-state, hence the mobility of metal elements and metalloids (Lovley, 1991).

Dissimilatory iron reduction is considered an important process in both pristine and contaminated subsurface environments. Microbial metabolic pathways involve the coupled oxidation of various carbon sources, such as mono-aromatic compounds, to $CO_2$ or other metabolites, while Fe (III) serves as the sole electron acceptor (Lovley, 1994). In terms of reductive transformation, microbial reduction of ferrihydrite can be considered as a coupled biotic-abiotic process, where iron-reducing bacteria produce Fe (II) and which further catalyzes reductive dissolution of ferrihydrite, subsequently resulting in phase transformation (Hansel *et al*., 2003). The correlation between the development of reducing conditions and the simultaneous

presence of As (III) and Fe (II) has led to the well-accepted inference that reductive dissolution of arsenic-bearing iron(hydr)oxides results in the release of sorbed arsenic (Masscheleyn *et al*., 1991; Islam *et al*., 2004; Burnol *et al*., 2007; Sutton *et al*., 2009). It has previously been shown that arsenic can be released through reductive dissolution of ferrihydrite regardless of whether arsenic was adsorbed to, or co-precipitated with, ferrihydrite (Erbs *et al*., 2010).

Incubation batch experiments using arsenic-bearing ferrihydrite have shown that an increase in microbial growth results in an increase of Fe (II) and decrease of Eh with subsequent arsenic release (Masscheleyn *et al*., 1991; Islam *et al*., 2004). These types of correlation studies usually involve enrichment of arsenic-contaminated sediment with carbon sources and continuous measurement of Eh, Fe (II) and As (III). Quantitative measurements of Fe (II) or As (III) in batch-desorption and transport experiments using environmental samples does not always reflect microbial reduction of Fe (III) and release of Fe (II) or As (III) into the solution because these reduced elements can be sequestered temporally by the newly formed iron oxide phases or other solids such as clay minerals or aluminium oxides (Fredrickson *et al*., 1998; Dixit and Hering, 2003; Islam *et al*., 2005).

Bacterial communities form biofilms in almost all natural environments where they are present. Biofilms consist of bacterial cells and aggregates embedded in complex protective polymeric matrices of variable density with permeable water channels (Lawrence *et al*., 1991; Caldwell *et al*., 1992). Studies have shown that bacterial cells and extracellular polymeric substances (EPS), along with geochemical conditions created within biofilm matrices, are involved in the biogeochemical cycling of elements (Ferris *et al*., 1989; Haack and Warren, 2003; Dynes *et al*., 2006; Hunter *et al*., 2008). Therefore, to obtain a more accurate understanding of microbial effects on the redox state of elements of concern (EOCs), information

needs to be acquired at both the fine-scale as well as the bulk-system scale (Hunter *et al*., 2008). A substantial number of studies have investigated biofilm communities and their geochemical potential using various approaches (Brown *et al*., 1994; Lee *et al*., 2001; Geesey *et al*., 2008). From these works, the need for non-disruptive methods to delineate the association of intact microbial cells with geological elements, as well as speciation and quantitative mapping of metals, has consistently been emphasized (Neu *et al*., 2010).

To date, soft X-ray scanning microscopy (STXM) imaging and spectroscopy have been shown to be one of the most powerful methods for speciation-mapping of metals in the context of microbial biofilms (Lawrence *et al.,* 2003; Dynes *et al*., 2006; Hunter *et al*., 2008; Templeton and Knowles, 2009; Neu *et al*., 2010; Hitchcock *et al*., 2010). The primary objective of this study was to investigate the potential of bacterial flora native to the DTMF system to reduce environmental Eh and ferrihydrite, which are the primary controlling condition and mineral phase in the DTMF tailings, respectively. For this purpose, samples from the DTMF tailings-water interface were enriched (with indigenous flora previously isolated along with a carbon source) and incubated under continuous- and intermittent-flow conditions in microcosms. The control microcosm was gamma irradiated and no additional bacteria or carbon source were added. The *in situ* Eh change in the tailings samples was monitored throughout the incubation period using platinum wire microelectrodes, samples were analysed for microbial diversity using DNA sequencing methods and Fe (II) was detected and mapped within the tailings/biofilm using STXM.

## 5.3 Material and methods

### 5.3.1 Uranium tailings chemical analysis

Samples were obtained from the DTMF tailings-water interface as described by Khan *et al.* (2013). At the time of sampling the tailings samples were placed in glass bottles and filled with water obtained from the DTMF water column to eliminate air headspace. Samples were stored at 4°C in the dark until the microcosm experiment was initiated. Samples were subjected to inductively coupled plasma-mass spectrometry (ICP-MS) to characterize major chemical constituents. Before chemical analysis, samples were thoroughly dried and ground to a fine powder. The measurements were carried out using a Perkin Elmer Elan 5000 ICP-MS with the settings as previously described by Bondici *et al.* (2014).

### 5.3.2 Microcosm systems

To investigate microbially induced changes to redox and its subsequent influence on iron oxidation state within the DTMF tailings, microcosms (length = 10 cm, width =1 cm, height = 8 cm) were constructed from large glass microscopy slides (Ted Pella, Inc. CA, USA) and assembled using silicone sealant (Dow corning 3140, World Precision Instruments Inc., FL, USA). The microcosms received either a continuous or intermittent supply of DTMF water using a syringe pump system (WPI SP220iw Multi Syringe Infusion/Withdrawal Pump, WPI Inc. Sarasota, FL.). To prevent plugging of the outlet port, which was drilled at the bottom center of the front side of the microcosm, a polyethylene porous filter (Porex Technologies, Georgia, USA) was positioned at the bottom of each chamber. Eh microelectrodes were prepared in-house from platinum wire (Sigma-Aldrich, ON, CA) as described by Swerhone *et al.* (1999). To monitor the Eh over time the microelectrodes were inserted through the side of the microcosm chambers, with one probe located near the base of the tailings and a second probe positioned near the tailings-water interface. The depth difference between the two inserted microelectrodes

in the tailings column was approximately 2 cm. A reference electrode (2 mm, model SDR2; World Precision Instruments Inc., Sarasota, FL, USA) was positioned in the water above the tailings material The measured voltage was recorded using a data logger (Model 21X, Campbell Scientific Inc., Edmonton, AB) interfaced with an AM416 multiplexer (Campbell Scientific Inc.). The collected data were corrected to a standard hydrogen electrode using a correction factor of + 200 mV, which is generally used for a Ag/AgCl reference electrode in a saturated KCl solution.

Approximately 10 g of wet tailings material was placed into each microcosm and covered with 4 mL of non-sterile DTMF water. Microcosms receiving continuous flow were operated at a rate of 42 µl/h such that oxic DTMF water was introduced to the top of the chamber and drained from the bottom. In the case of microcosms receiving intermittent-flow , oxic DTMF water was added only periodically to replace water that was removed for analyses, thereby ensuring that the tailings material remained submerged at all times. Since the amount of uranium tailings available was limited, microcosm assays could only be carried out in duplicate, as follows: continuous-flow microcosm 1 and 2 (CF-M1 and CF-M2, respectively), intermittent-flow microcosm 1 and 2 (IF-M1 and IF-M2, respectively), and continuous-flow microcosm control (CF-MC). A control microcosm receiving intermittent-flow (IF-MC) failed during the course of the experiment, therefore no intermittent-flow information was available for comparison.

Components of the microcosm apparatus, including connectors, tubing and silica sand were sterilized by autoclaving. The interior surfaces of the microcosm chambers were rinsed 3X with 70% alcohol and air-dried in a biosafety cabinet. The tailings-sand mix used in the CF-MC microcosm (the control) was gamma irradiated at the Chemistry Department at University of Saskatchewan using a $Co^{60}$ source emitting 4.58 Gy/min. Ionizing radiation (IR) dosages of

between 5 and 12 kGy have previously been recommended for destruction of bacteria in soil samples with minimal chemical changes (Ostlung *et al*., 1989). Therefore, to avoid redox change and physicochemical perturbation in the control, the tailings-sand mixture was gamma irradiated for 30 hours for a total IR dose of 8.24 kGy. The DTMF water used for CF-MC microcosm was filter-sterilized using a 0.1 micron pore size filter. The remainder of non-irradiated (treatment) tailings-sand samples were distributed into the microcosm chambers and inoculated with the bacterial isolates.

Both continuous- and intermittent-flow microcosms were enriched one-time with additional carbon (trypticase soy broth; TSB), as follows. One ml of 0.75 g/L TSB was homogenously mixed into the tailings samples at the beginning of the experimental assay resulting in a final initial concentration of 50 ppm of additional nutrient. No TSB was added to the gamma-sterilized control microcosm, which was run under continuous-flow conditions. To ensure that water flowed evenly through the tailings material, the clay-like tailings was mixed with larger grain-sized sterile silica sand (~1 mm diameter) at a ratio of 65:35. To prevent plugging of the filter, a thin layer of silica sand was placed below the tailings-sand mix on top of the porous polyethylene filter. Clean sterile microscope slides were inserted vertically into the tailings-sand mix to provide a surface for microbial biofilm development within the tailings for subsequent analyses. A rubber gasket, used to cover the top of the microcosm chambers, was cast from Smooth-SilTM 940 pourable silicone rubber compound (Smooth-On, Inc., PA, USA). The microcosm assay was run for 40 days.

### 5.3.3 Microorganisms and inoculation

Pure cultures of five bacterial isolates previously recovered from DTMF tailings sediment (Bondici *et al*., 2013). were used as the enrichment inoculum. Based on the partial 16S

rRNA gene sequence analysis, performed using 8F and 531R (Hirkala and Germida, 2004) primers, the isolates were determined to be closely related to the following organisms: *Pectobacterium cypripedii* (97%)*, Pseudomonas brenneri* (99%), *Pseudomonas stutzeri* (98%), *Brevundimonas alba* (95%), and *Microbacterium dextranolyticum* (97%). These isolates were selected for use in the microcosm study based on having Fe (III) reducing capability and/or multiple metal/metalloid tolerance (Bondici *et al*., 2013).

Bacterial suspensions (~1.5 x $10^7$ cfu/ml) were prepared in the 1 ml TSB media (0.75 g/L) used for the enrichment and immediately mixed into the wet tailings-sand mixture within the microcosm, then immersed with DTMF water and the microcosm sealed with the top plate and the silicon gasket. To facilitate attachment of inoculated bacteria and adaptation of the inoculants and microorganisms present in the tailings to the conditions, all microcosms were allowed to acclimate for 14 h before flow was started. Bacterial cell counts in the effluent of each microcosm were monitored by culture-based methods. Plating was carried out in duplicate using 5% trypticase soy agar (TSA) (Difco media, Franklin Lakes, NJ) under aerobic conditions and enumerated after incubation for a week at room temperature (22 ± 2°C). Furthermore, effluent from each microcosm was periodically tested for the presence of the reduced form of iron using iron test strips (10004 EM Quant, Gibbstown, NJ, USA).

### 5.3.4 Ion Torrent 16S rRNA gene sequencing

To investigate changes in the microbial community structure, DNA extraction was carried out on the initial blended tailings material (prior to inoculation) at T=0 and after 40 days of incubation for all samples. The FastDNA SPIN kit (MP Biomedicals, Solon, OH) was used to extract DNA from the ~ 0.5 g tailings samples, in accordance with the manufacturer's instructions. Ion Torrent sequencing was carried out using a modified specific primer set (E786F

and U926R) (Baker *et al*., 2003) targeting the V5 region of the 16S rRNA gene. The forward primer also contained an additional sequence region, a key tag and a multiplex identifier (MID) specific to each replicate sample used on the Ion Torrent chip. The sequence of the forward and reverse primers were F5' CCATCTCATCCCTGCGTGTCTCCGACTCAGMIDGATTAGATACCCTGGTAG and R5'-CCTCTCTATGGGAGTCGGTGATCCGTCAATTCCTTTRAGTTT, respectively. The multiplex identifiers used for the DNA samples obtained from the tailings samples were as follow: TGATA (uninoculated tailings material); AGACG (CF-M1), AGCAC (CF-M2); ATCAG (IF-M1), ATATC (IF-M2) and ACGAG (CF-MC).

PCR amplification, Ion Torrent sequencing and data processing were carried out according to Bondici *et al.* (2013). PCR amplicon purification was performed using the Qiagen gel purification kit (Qiagen Sciences, Germantown, MD, USA). Pooled purified DNA products were sequenced using an Ion Torrent Personal Genome Machine (Life Technologies, Carlsbad, CA, USA) at the National Research Council (Montreal, Quebec, Canada). The RDP pipeline Initial Process Tool was employed to remove low-quality sequence data. The filter parameters were set to the default settings except the minimum read length was set to 75 bp. Taxonomic assignment of the quality sequence data was obtained through the RDP naïve Bayesian classifier algorithm with a bootstrap cut-off value of 50%, as recommended for sequences shorter than 250 bp.

### 5.3.5 Scanning Transmission X-ray Microscopy (STXM)

Biofilms grown on the glass microscope slides incubated within the tailings samples were removed by scraping and a ~1 µl volume of these samples was loaded onto X-ray-transparent $Si_3N_4$ windows (1 X 1 mm, thickness 100 nm on a 200 µm thick chip, 5 X 5 mm, Norcada Inc.,

Edmonton, Canada) under anaerobic conditions. Biofilm samples on $Si_3N_4$ windows were analyzed with STXM using the 10ID-1 beamline at the Canadian Light Source (CLS). Only samples from microcosms where the bulk liquid tested positive for the presence of Fe (II) were subjected to STXM analyses. Samples were transported to CLS in anaerobic GasPak pouches and kept under 1/6 atm of He during STXM analysis.

Transmitted X-ray data were collected at the 1s or 2p absorption edges (Dynes *et al.,* 2006). Stacks of absorption images were recorded using the 280-288.2 eV, 720-780 eV and 1315-1350 eV photon energy ranges for C, Fe, and As, respectively, for the same areas. To investigate Al and Mg distribution, image stacks were collected over the 1557 eV to 1589 eV and 1298 eV to 1326 eV energy ranges, respectively. The stack measurements for each element were executed with a 1 ms dwell time and with pixel sizes ranging from 40 to 100 nm. Images at specific energies were processed using the aXis2000 software package (http://unicorn.mcmaster.ca). To obtain absorption spectra the aligned image sequences were converted to optical density (ODs) using the transmitted flux through the sample and incident flux signal through areas on the window devoid of sample. Reference spectra were utilized to create the component maps of biomolecules and metal species (Lawrence *et al.,* 2003; Dynes *et al.,* 2006). Species of interest were mapped by fitting the stack to a linear combination of suitable reference spectra using Stack-fit (Dynes *et al*., 2006). Threshold masking of the obtained components maps was used to identify those pixels with large amounts of similar spectral characteristics from which the spectra were extracted. Identification and mapping of chemical components potentially present (e.g., for those elements without reference available) was carried out using principle component analysis (PCA) (Hitchcock *et al*., 2005).

## 5.4 Results

The tailings samples obtained from the DTMF interface and water from the water column covering the tailings (used as the aqueous phase in the microcosms) were subjected to ICP-MS analysis. The most abundant elements in the tailings were Ca, Mg, Al, and Fe. These elements were also found to be in the water samples, although at much lower concentrations (Table 5.1).

**Table 5.1 Total metal element concentrations (ppm) found in the tailings water and sediment.**

| Elements | Na | Mg | Al | Ca | V | Cr | Mn | Fe | As | Se | Mo | Pb | U |
|---|---|---|---|---|---|---|---|---|---|---|---|---|---|
| **Water** | 113 | 12 | 0.5 | 921 | 0.02 | 0 | 0.01 | 0.3 | 0.06 | 0.01 | 1.3 | 0.06 | 0.17 |
| **Tailings** | 643 | 14400 | 67302 | 97923 | 624 | 112 | 543 | 31415 | 832 | 15 | 76 | 4634 | 1169 |

Values are the average of duplicate ICP-MS measurements.

### 5.4.1 Redox potential development

Replicate microcosms containing DTMF uranium tailings were prepared to monitor the development of reducing conditions due to stimulated bacterial activity. All microcosms initially inoculated with bacterial isolates and enriched with an electron donor (a one-time addition of 50 ppm TSB), and irrespective of flow regime, developed highly reducing conditions within the tailings matrix, with Eh values dropping as low as -545 mV in IF-M1 (Figure 5.1B). The Eh values in CF-M1 and CF-M2 were -404 and -348 mV, respectively, by approximately the second day of incubation and thereafter stabilized between -267 and -386 mV over the remainder of the study (Figure 5.1A). In contrast, the control (CF-MC) remained highly oxic for 5 days, after which the Eh decreased to -93 mV and thereafter varied between -30 and +21 mV.

In microcosms receiving intermittent flow (IF-M1 and IF-M2), the Eh values fluctuated more widely in comparison to microcosms that received continuous flow (Figure 5.2B). For example, the Eh in IF-M2 dropped below -200 mV by the second day and then varied between -151 and -347 mV over the remaining incubation period (Figure 5.2B). The Eh in IF-M1 dropped

below 0 mV by the 9$^{th}$ day and then continued to decrease, reaching -545 mV by day 15. However, the Eh did not remain constant in microcosms that received intermittent flow, and in the case of IF-M1, it rose to slightly above 0 mV by day 20$^{th}$ (after receiving oxic water to replenish fluid levels) before decreasing again and generally re-stabilizing between -207 and -272 mV over the remainder study (Figure 5.1B). The color of the tailings sediment in IF-M1 started to turn black after approximately 21 days of incubation, with coloration initially appearing at the water-tailings interface and then subsequently at lower regions of the tailings matrix. Isolated black pockets of reduced tailings were also visible in IF-M1by the end of the incubation period. The Eh at the water-tailings interface in microcosms receiving continuously flowing liquid (CF-M1 and CF-M2) fluctuated for about 2 weeks and then was similar to that of the control; whereas, in microcosms, which periodically received oxic water (IF-M1 and IF-M2), the Eh fluctuated much more widely throughout the incubation period (Figure 5.2A, B).

### 5.4.2 Enumeration of bacteria in microcosm effluent

Bacterial numbers were monitored in the effluent from each microcosm. A similar decrease in bacterial cell number was measured from 7.0 to 5.8 $\log_{10}$ and 6.9 to 5.1 $\log_{10}$ CFU/ml in microcosms CF-M1 and CF-M2, respectively, that received a continous DTMF water flow rate of 42 µl/h. The bacterial cell counts in the effluents of microcosms receiving intermittent flow stayed relatively constant and within the range of 6 $\log_{10}$ (IF-M1) to 7 $\log_{10}$ (IF-M2) over the incubation period. Initially, no bacterial cells were detected in the control microcosm containing gamma-irradiated tailings and receiving continuous liquid flow; however, 4.6 $\log_{10}$ CFU/ml were detected in the effluent water after 10 days of incubation, with counts remaining in this range over the remainder of the incubation period.

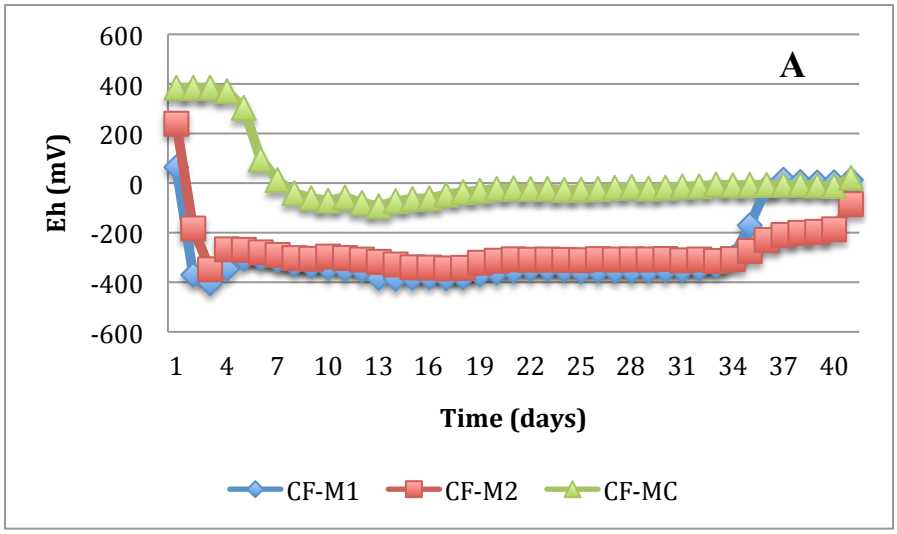


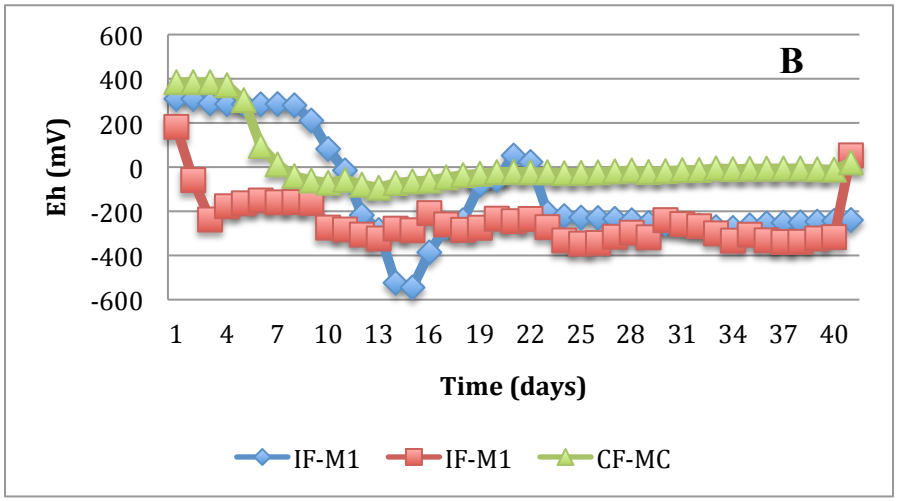


**Figure 5.1 Effect of continuous- (A) or intermittent-flow (B) on Eh measurements obtained from the bottom of microcosms containing uranium mine tailings over 40 days.**
Microcosms containing a mixture of tailings-sand and were enriched with a 5-member bacterial consortium and 1 ml of 0.75 g/L TSB as carbon source. An uninoculated control microcosm lacking nutrient enrichment was gamma-irradiated (8.24 kGy) and supplied with filter-sterilized DTMF water. Microcosms receiving continuous flow of DTMF water were run at a rate of 42 µL/h. Abbreviations used are as follows: CF-continuous flow; IF-intermittent flow, M-microcosm; C-control.

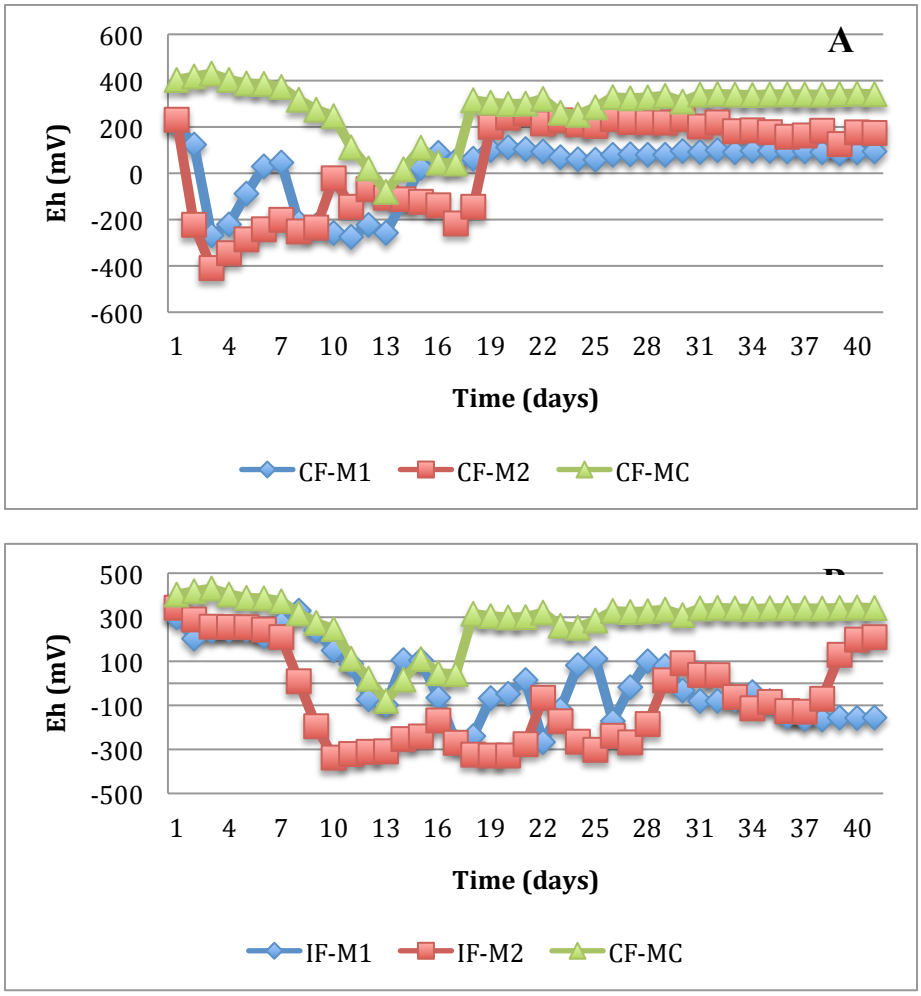


**Figure 5.2 Effect of continuous- (A) or intermittent-flow (B) on Eh measurements obtained from the upper region of microcosms containing uranium mine tailings over 40 days.** Microcosms containing a mixture of tailings and sand were enriched with a 5-member bacterial consortium and 1 ml of 0.75 g/L TSB as carbon source. An uninoculated control microcosm lacking nutrient enrichment was gamma-irradiated (8.24 kGy) and supplied with filter-sterilized DTMF water. Microcosms receiving continuous flow of DTMF water were run at a rate of 42 µ/L. Abbreviations used are as follows: CF-continuous flow; IF-intermittent flow; M-microcosm; C-control.

### 5.4.3 Microbial community composition

Bacterial 16S rRNA sequences were classified to the phylum level and shown to include proteobacterial classes (Figure 5.3). Sequence analyses revealed that bacterial community

composition was similar amongst the treatment replicates, as well as for the control microcosm, in terms of overall diversity, with the exception of IF-M1. Sequences affiliated with *Proteobacteria* accounted for greater than 50% of sequences in all libraries. DNA libraries from the unincoulated tailings material (T=0 day) and control microcosm (T=40 days) contained the highest proportion of *Proteobacteria*, with greater than 80% of total sequences affiliated with this phylum; whereas, the DNA library of microcosm IF-M1 at the same time had the lowest proportion of *Proteobacteria* (51%). The most prevalent *Proteobacterial* classes in all libraries were *β*-, *α*-, and γ-Proteobacteria. The second most-abundant phylum found in all microcosms was *Bacteroidetes,* except for IF-M1, where *Firmicutes* was the second most-abundant phylum with 43% of the total sequences. The relative higher frequency of *Firmicutes* in this particular microcosm was primarily due to the occurrence of sequences (~11000) closely related to *Desulfosporosinus*.

Despite the fact that *Pseudomonas*, *Brevundimonas*, *Microbacterium*, and *Pectobacterium* were used to inoculate all of the microcosms other than the control, these bacterial *spp.* were not the most abundant bacterial sequences recovered from the microcosms at the end of the study. In fact, sequences closely related to *Pseudomonas* and *Brevundimonas* occurred at lower, or similar frequencies, to those present in the unincoulated tailings material (T=0 day) and control microcosm (T=40 days). Furthermore, sequences closely related to *Microbacterium,* although low in number, were observed in all the treated microcosm replicates, but not the control. *Polaromonas,* along with *Hydrogenophaga* (both belonging to *Betaproteobacteria*), were the most abundant genera in the unioculated T=0 day tailings material and the control microcosm at the completion of the experiment. They were also most abundant,

along with sequences closely related to *Malikia,* in all the microcosms receiving continuous or intermittent flow.

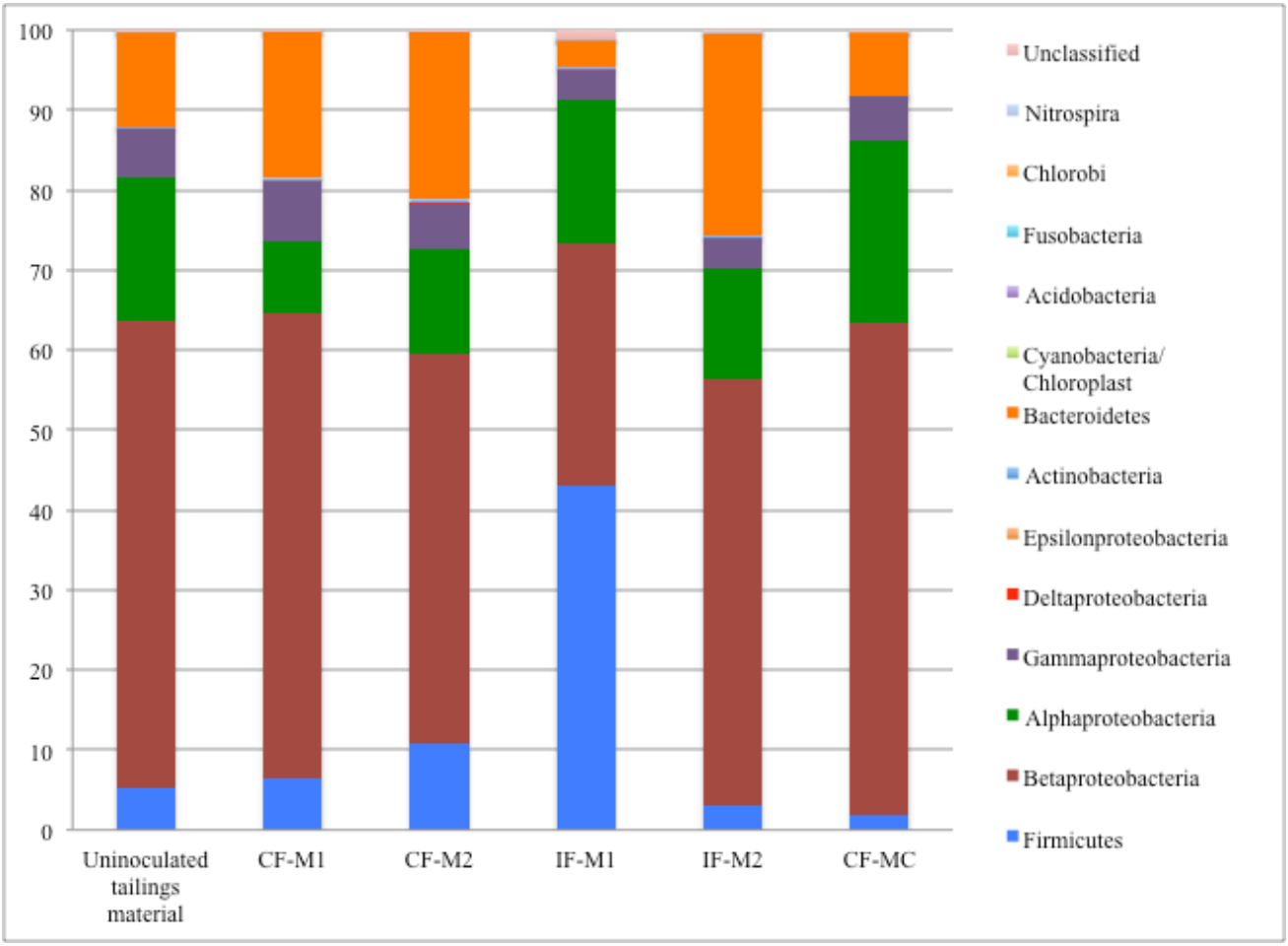


**Figure 5.3 Phylogenetic classification of bacterial 16S rRNA gene sequences obtained by Ion Torrent sequencing.**
Sequence libraries were generated for the following samples: unioculated tailings material (T=0 day) microcosm replicates receiving continuous flow (CF-M1, CF-M2), microcosm replicates receiving intermittent flow (IF-M1, IF-M2); control microcosm with continuous flow (CF-MC). Abbreviations used for naming are as follows: CF-continuous flow; IF-intermittent flow, M-microcosm; C-control.

### 5.4.4 Mapping elements of interest by STXM

Scanning transmission X-ray microscopy was used to detect, speciate and map the elements Fe, Al, Mg in the context of biofilms grown in microcosms containing uranium tailings from the DTMF. For STXM analysis, samples were selected from microcosms that showed relatively low Eh values and that had tested positive (using iron test strips) for the presence of reduced Fe in the bulk water. Since the Eh in IF-M1 (receiving intermittent flow) had dropped the most (-545 mV), an additional sample from this microcosm was examined using STXM. A sample from IF-M2 was also subjected to STXM analyses. Due to long times required for STXM data collection combined with limited beamtime access, along with the fact that the Eh measurements and bacterial composition were similar for replicate CF-M1 and CF-M2, only a sample from CF-M2 was analyzed with STXM.

The C 1s X-ray absorption spectra of bio-macromolecules (e.g., protein, lipids, polysaccharides) are unique thus, they can be differentiated and mapped in bacterial biofilms (Lawrence *et al*., 2003; Dynes *et al*., 2006). The C 1s absorption image scan shown in Figure 5.4A accordingly depicts the organic carbon distribution in the biofilm sample from IF-M1 microcosm wherein bacterial cell shapes are visible within the biofilm. Component maps for the major biomolecule (e.g., protein, lipid, and polysaccharide) are shown (Figures 5.4B1 – 5.4B3) along with a gray scale, which represents the quantitative thickness in nm of each specific type of biomolecule. Figure 5.4B4 displays a color-coded composite map with red, green and blue indicating protein, lipid and polysaccharide biomolecules, respectively. Distinct bacterial cells are apparent, and seen to be mainly composed of protein and lipid. Furthermore, the extracellular polymeric substances appear in association with the visible bacterial cells and consist of a mixture of the three biomolecules.

Spectra derived using threshold masking of the most intense pixels for each component are shown in Figure 5.5. The extracted protein spectrum is a good fit to the standard albumin spectrum, containing both the 1s→ π* C=C transition at 285.1 eV and the main transition 1s→ π* C=O at energy level 288.2 eV of the amide carbonyl bond (Lawrence *et al*., 2003). The lipid spectrum was in good agreement with the reference spectrum; however, an additional resonance peak at 285 eV in each extracted spectra is an indication of C double-bonds (Lawrence *et al*., 2003; Chen *et al*., 2014). This absorption region tends to vary since it depends on the degree of membrane lipid unsaturation (Hitchcock *et al*., 2009). It is well-documented that the K 2p and C 1s signals overlap; therefore, the visible resonance peaks at 297.2 eV and 299.8 eV indicate the presence of K (Hitchcock *et al*., 2009).

The distribution of Fe species was analyzed by recording Fe $L_{2,3}$-edge stacks for the same region examined at the C 1s edge. The oxidation state was defined from the shape of Fe 2p signal from the $L_3$-edge, which has two main resonance peaks with 708 eV being the strongest for Fe (II) and 709.8 eV for Fe (III) species (Dynes *et al*., 2006). Also, the L2-edge spectrum for Fe (II) species shows three peaks versus two peaks for Fe (III) species, and lower onset energy. To obtain the component map of both species, the Fe 2p image sequence was fitted to the ferric and ferrous chloride reference spectra (Figure 5.6A, B). Spectral comparison of the derived spectra to the reference Fe species indicated the presence of both oxidation states, Fe (II) and Fe (III), in the biofilm grown in IF-M1 (Figure 5.7). The most intense peak was at 709.8 eV, suggesting that both Fe species contained Fe (III) (Hitchcock *et al*., 2009). From the color-coded component map (Figure 5.6C) it is apparent that the two iron oxidation states tended to occur together within the biofilm matrix. However, Fe (II) is also visible without Fe (III) in close proximity to the bacterial cell (Figure 5.6D).

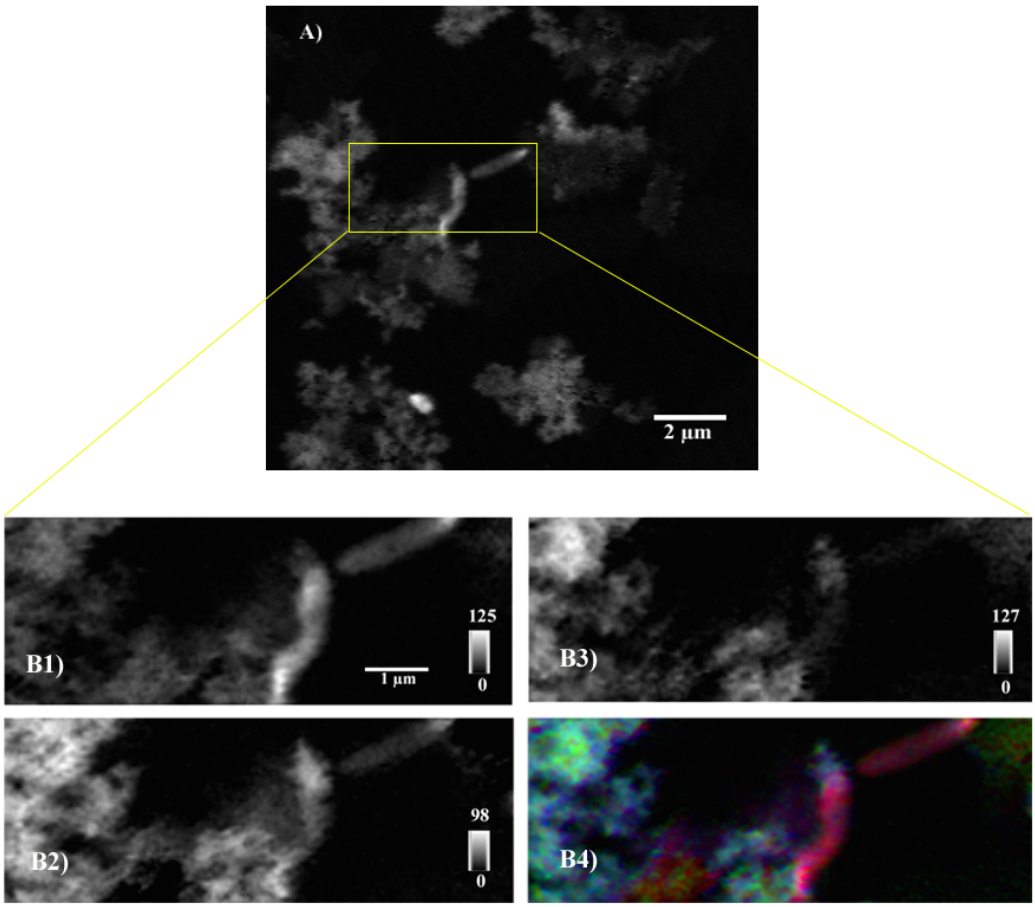


**Figure 5.4 Optical density and component map of carbon of the biofilm samples from microcosm IF-M1.**

**A)** Difference between optical density images at 288.2 and 282.0 eV of biofilm material from microcosm IF-M1. **B1 - B3**) the protein, polysaccharide and lipid component maps, respectively, derived by fitting C stack (128 images from 280 eV to 320 eV; 40 nm pixels, 1 ms per pixel) The gray scale indicates the thickness of each respective component in nanometers. **B4**) Color-coded composite map protein=red; lipid=green; polysaccharide=blue.

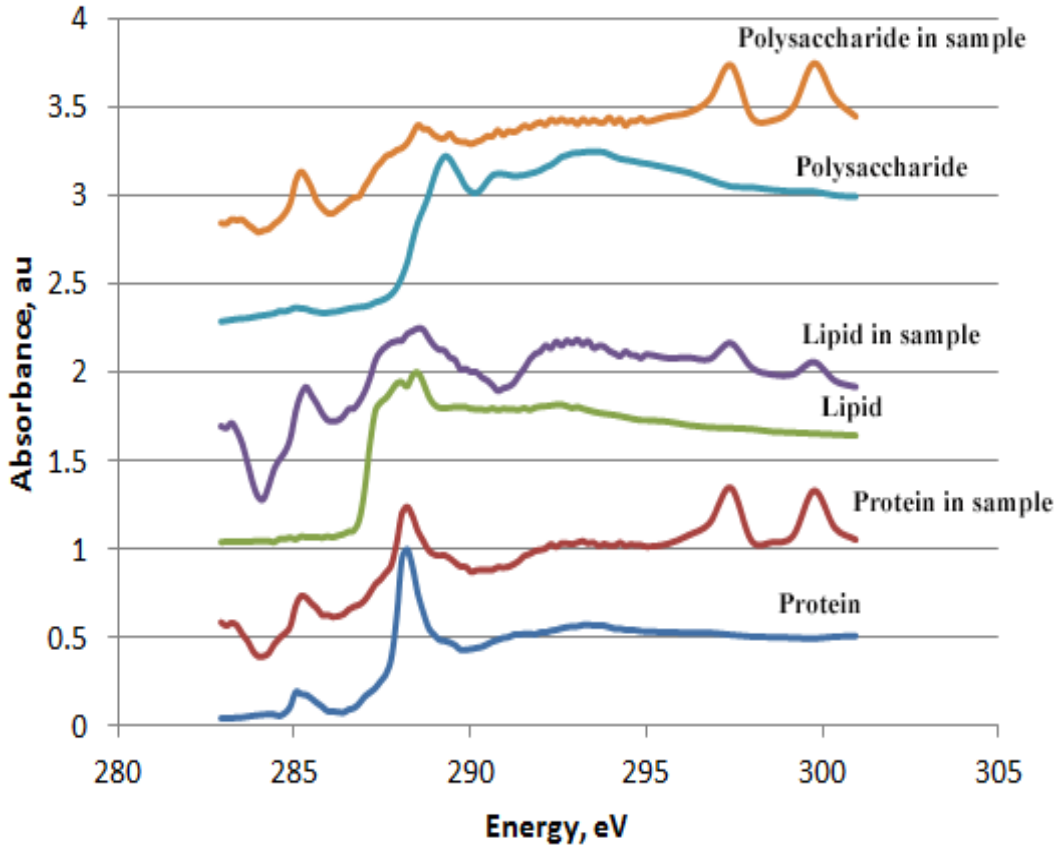


**Figure 5.5 The C K-edge spectra of protein, lipid and polysaccharide of the biofilm sample from microcosm IF-M1.**
Derived by threshold masking of high intensity pixels in the respective component map are shown and compared to the protein (albumin), lipid (1,2-dipalmitoyl-sn-glycero-3-phophocholine) and polysaccharide (xanthan gum) reference spectra.

The distribution of Mg and Al in biofilms was also investigated using principle component analysis (PCA). This approach allows the extraction of potential spectra and can indicate the number of chemical forms in which various elements may occur. The PCA maps (Supplemental data, Figure 9.3) indicated that there are, at a minimum, two different types of Mg and Al in the biofilm grown within the tailings sample of IF-M1. Comparison of the Mg and Al maps with the distribution of Fe species in the same region (Figure 5.6C) suggests that these components are co-localized. Furthermore, it is evident that Fe (II) and the most abundant form

of Mg and Al occur in similar areas. The distribution of carbon biomolecules and Fe species were mapped on a replicate sample from IF-M1. Component map analyses confirmed that all three biomolecules, protein, lipid and polysaccharide, occurred in the biofilm. Lipid thickness within the biofilm was the highest, with a value of 121 nm (Figure 5.8B), as measured in the previous IF-M1 sample (Figure 5.4B2). It was evident that the Fe (II) and Fe (III) (Figure 5.8E, F) followed the same pattern as the organic biomolecules, indicating the direct association of Fe with the bacterial biofilm.

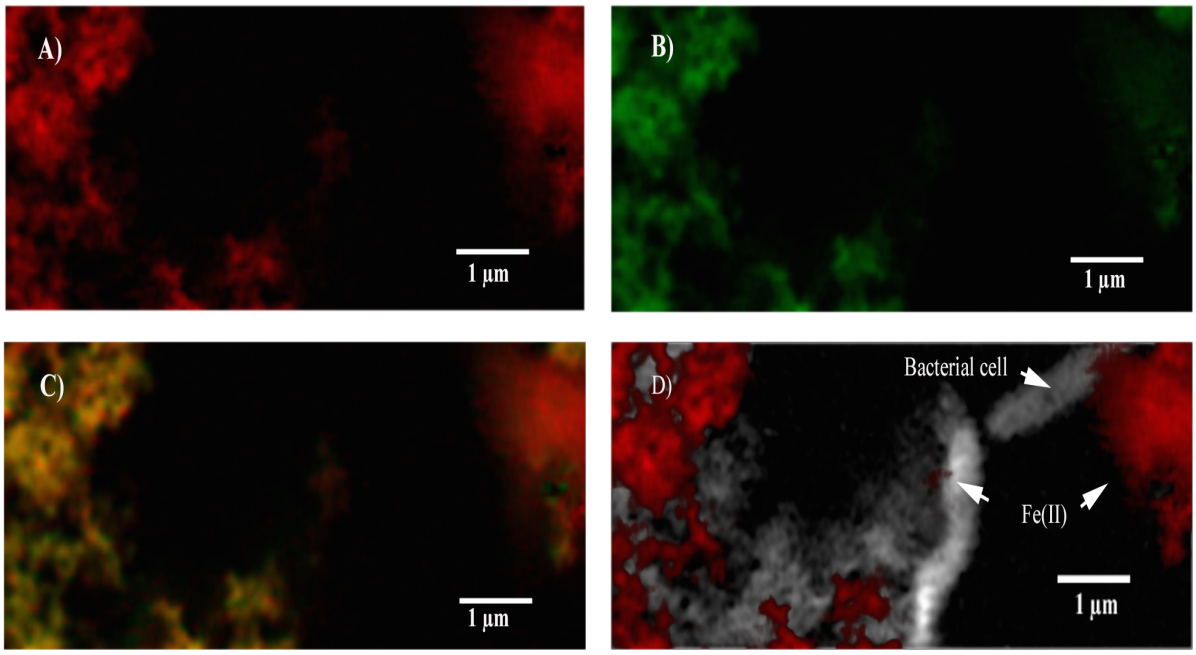


**Figure 5.6 Component maps of iron in the biofilm sample from IF-M1.**
**A**) Fe (II)-rich and **B**) Fe (III)-rich regions, derived by fitting image stack of Fe L2,3-edge (150 images from 695 to 735 eV, 1 ms per pixel, 40 nm) with the $FeCl_2 \cdot 4H_2O$, $FeCl_3 \cdot 6H_2O$ reference standards. **C**) Color-coded composite map (not rescaled) derived from Fe image sequence, Fe (II)=red and Fe (III)=green. **D**) Fe (II) was superimposed on the biological map (protein composite map).

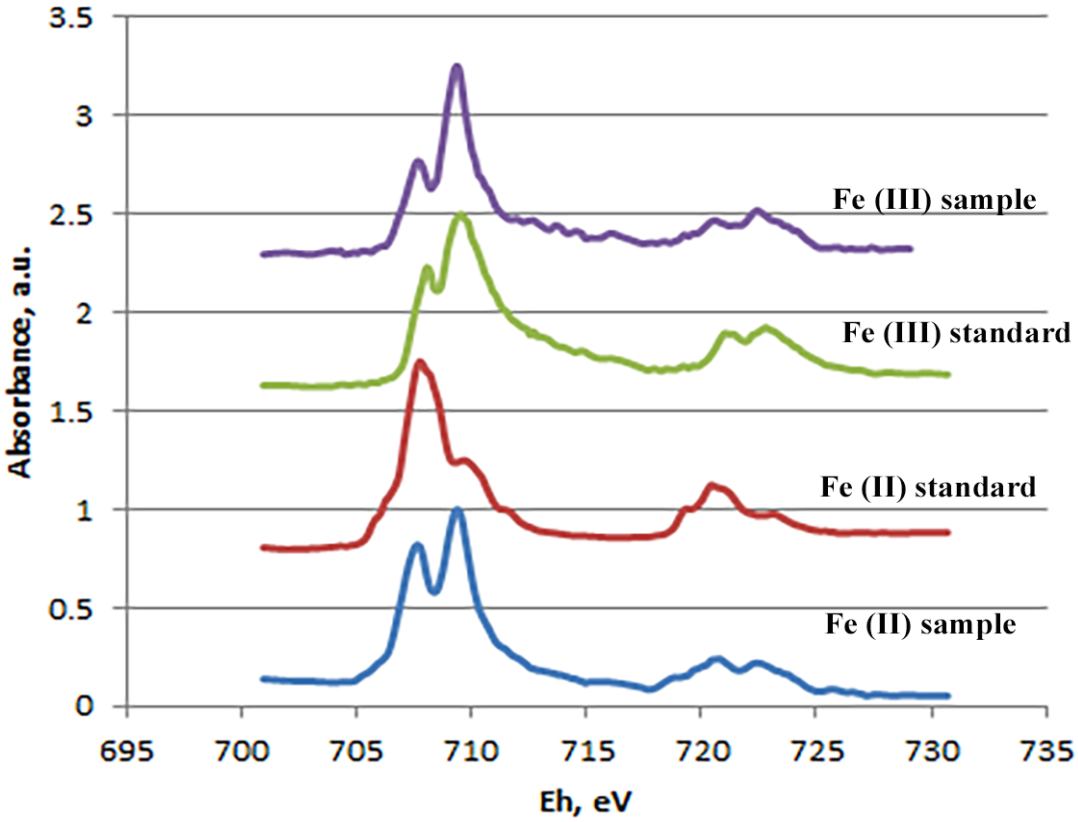


**Figure 5.7 The Fe 2p X-ray absorption spectra of $FeCl_2 \cdot 4H_2O$, $FeCl_3 \cdot 6H_2O$ standards and the Fe (II) and Fe (III) spectra derived by threshold masking of high intensity pixels in respective component map from the IF-M1 sample.**

For the IF-M1 sample, the oxidation state of iron was also quantified from the selected regions using curve fitting to the $FeCl_2 \cdot 4H_2O$, $FeCl_3 \cdot 6H_2O$ reference spectra. Curve fitting of the extracted Fe (II) further confirmed that the reduced Fe species was present in the mixed-valence form, constituted of 66% Fe (II) and 34% Fe (III) (F-test=232; M-correlation =0.89). Furthermore, curve fitting of the extracted Fe (III) showed that it consisted of 21% of Fe (II) and 79% Fe (III) (F-test=447; M=0.94). STXM analyses of samples from CF-M2 and IF-M2 microcosms showed a similar distribution of Fe species associated with biofilm bacteria as seen in samples from IF-M1 (Supplemental data, Figures 9.4 and 9.6). In general, Fe (II)-rich species

were associated with Fe (III); furthermore, in some regions, only Fe (II) species occurred in, or adjacent to, regions containing biofilm/bacterial cells (Supplemental data, Figure 9.4).

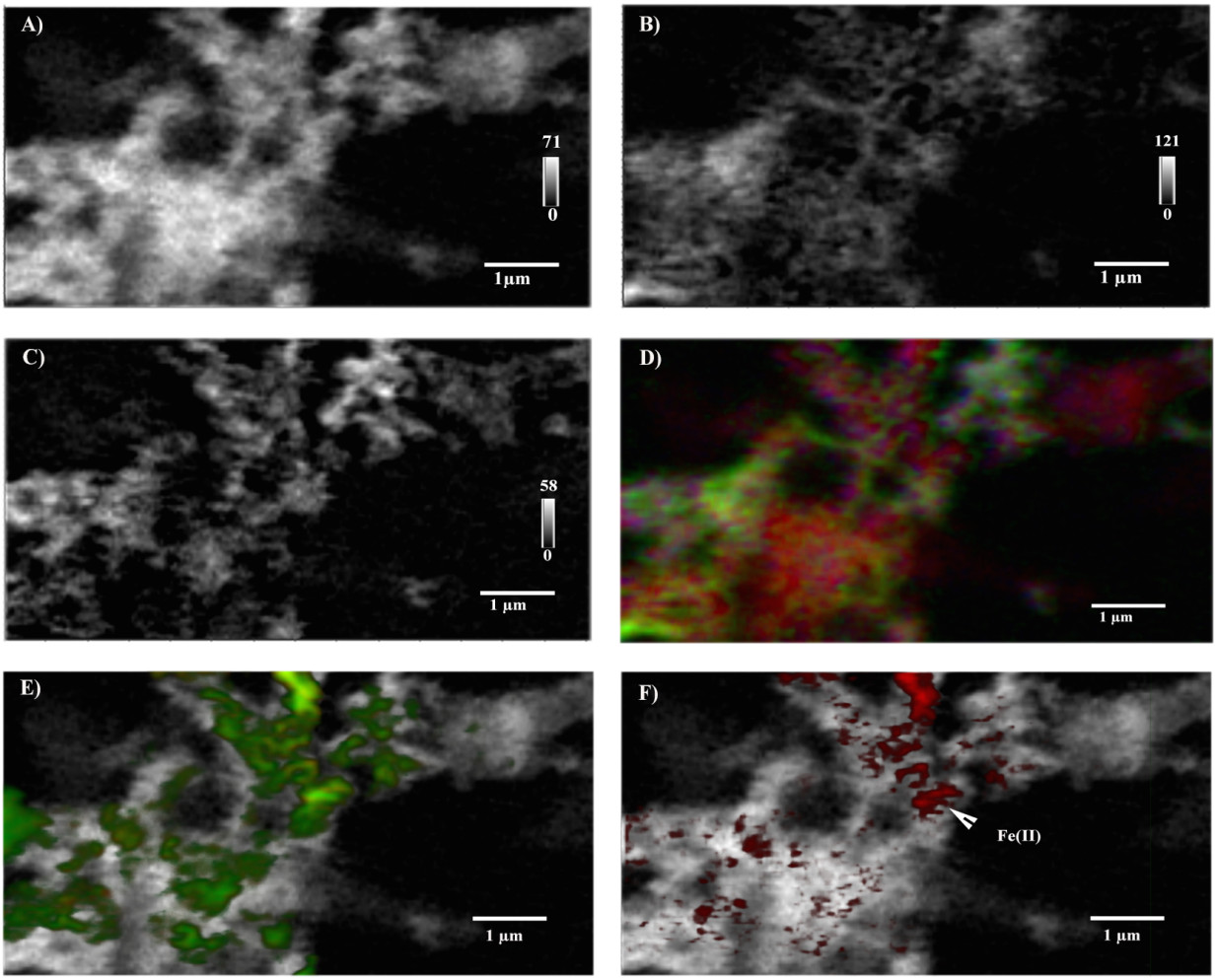


**Figure 5.8 Component maps of carbon and iron in the biofilm sample from IF-M1.** Protein (**A**), lipid (**B**) and polysaccharide (**C**) were derived by fitting an energy sequence of images (stack) of C (128 images from 280 eV to 320 eV; 40 nm pixels, 1 ms per pixel) using reference spectra from the IF-M1 microcosm sample. The gray scale indicates the thickness in nanometers. Color-coded composite map (**D**) protein=red; green= lipid; polysaccharide= blue. Color-coded composite maps (**E**) was derived from the Fe image stack (119 images from 700 eV to 721 eV; 50 nm pixels, 1 ms per pixel, Fe (II)=red and Fe (III)=green and superimposed on the biological map (protein component map). (**F**) represents Fe (II)=red superimposed on the biological map.

The Fe spectra of the sample from IF-M2 (Supplemental data, Figure 9.5) was similar to the spectra obtained from IF-M1 (Figure 6.7), and it was evident that the reduced form of iron occurred in mixed-valence form. However, it was also evident that in addition to the first peak that was characteristic of Fe (II), the third peak at 720 eV seemed to be more prominent than the fourth peak, which further confirmed the presence of Fe (II).

## 5.5 Discussion

In general, the main body of the DTMF is considered to be a diffusion-based system (Shaw *et al*., 2011); however, there exists the potential for non-diffusional processes to occur at the tailings-water interface due to advective (from porewater expulsion from the tailings body) and convective (due to local temperature gradients) processes. Thus, incorporating flow into our experimental system served to model these interfacial events with the intent of studying the potential biogeochemical impacts of the microbial community in this region. In general, the interfacial zone between the main DTMF body and the overlying water column is considered to be the key location for carbon source accumulation from the surrounding environment.

### 5.5.1 Chemical measurements

During the chemical leaching process of uranium, various elements are liberated from the ore (Donahue, 2000) and in general, these elements tend to vary in concentration depending on the initial composition of the ore and the extraction method used (Landa *et al*., 2004; Moldovan and Hendry, 2005). Our analyses of tailings from the tailings-water interface showed that Ca, Fe, Al, and Mg were the most abundant elements present in the tailings (Table 5.1). Previous geochemical analysis of McArthur tailings solids, which represents the upper layer of the DTMF tailings body, similarly showed that the concentration of these elements were relatively high. For example, values for Ca and Fe were 97,923 and 31,415 µg/g, respectively (Table 5.1), were

similar to those reported previously (Shaw *et al*., 2011).The elevated concentration of Ca is the result of neutralizing the raffinate with slaked lime ($Ca(OH)_2$). Other elements were also high in the tailings, as they become solubilized with uranium during the leaching step of the milling process (Shaw *et al*., 2011).

### 5.5.2 Redox potential change in tailings

Redox potential is considered a dominant factor governing the fate of metals/metalloids in mine tailings; therefore, processes that affect this parameter are of great interest (Chuan *et al*., 1995; Calmano *et al*., 2003). In our microcosm-based study, strong reducing conditions developed in the tailings matrix near the bottom of the treated microcosms over time in comparison to the control. The Eh in these regions tended to become reducing after only one day of immersion in DTMF water and remained reducing for more than 30 days, with the exception of the control microcosm and IF-M1 (Figure 5.1A, B). The Eh of the upper part of microcosms receiving continuous flow decreased after one day and thereafter fluctuated between reducing or oxic conditions for approximately 15 days, and thereafter gradually and slowly increased until the end of the experiment. In microcosms receiving intermittent flow, the Eh increased upon resupply of water, and then decreased again fairly rapidly, with Eh correlating with oxic-water resupply events until the end of the experiment. These types of changes in Eh at two distinct locations in the microcosms were likely caused by the presence of easily metabolizable organic carbon that was added at the beginning of the experiment along with oxygen supplied by the oxygenated DTMF water. The presence of organic carbon would have a stimulatory effect on microbial activity and, in general, specific microbial processes are determined by thermodynamic yields (Champ and Gulens, 1979), where oxygen yields the most energy to

support heterotrophic bacterial growth, followed by nitrate, oxidized manganese and ferric compounds (Lovley and Chapelle, 1995).

In an aerobic system where the $O_2/H_2O$ redox couple exists, the Eh usually ranges between +300 and +700 mV (DeLaune and Reddy, 2005). The microcosms in this study (other than the control) were enriched with an additional carbon source along with a heterotrophic bacterial consortium; hence, the relatively low Eh measured initially likely resulted from the rapid microbial utilization of readily available, dissolved organic carbon using molecular oxygen as the electron acceptor. The approximately 14 h incubation period of the submerged tailings without pumping (during inoculation) in the presence of this carbon material appears to have been sufficiently long to allow the adaptation and growth of a carbond-degrading, oxygen-utilizing, hence resulting in a rapid Eh decrease. The Eh of the control microcosm, lacking this supplemental carbon, remained oxic at both electrode locations for a longer period of time. Regardless of addition or infiltration of oxygenated water through the tailings in microcosms receiving continuous flow, the Eh continued to trend towards reducing conditions at the tailings-water interface with highly reducing conditions in the lower part of the microcosm. The measured redox change supports the contention that oxygen enhanced metabolic activity, primarily via the activity of heterotrophic bacteria in the presence of abundance of readily decomposable organic carbon (TSB), had occurred. A previous microcosm study reported a similar rapid transition from aerobic to reducing conditions, reaching -335 mV in under a 48 h time period (Catallo, 1999).

Sustained highly reducing conditions near the bottom of microcosms receiving continuous flow was presumably due to enhanced microbial activities, along with cycling of nutrients present in the biofilm matrix. The DTMF system initially receives a high concentration

of complex carbon-containing compounds (up to 0.9% w/w) discharged during the course of uranium milling processes; for example, amines in kerosene diluent are used for solvent extraction of uranium (Shaw *et al*., 2011). Previous column experiments examining the effect of percolated oxygenated water on soil dynamics have also demonstrated that despite a continuous supply of oxygen, the Eh of sediment decreased and reducing conditions persisted in soil samples receiving the highest amount of carbon source (Takai *et al*., 1974). In fact, these authors stated that supply of molecular oxygen stimulates microbial activity in soil sediments containing organic carbon resulting in a decrease of oxidation potential and increased formation of the reduced form of iron.

The Eh in the microcosms receiving intermittent flow fluctuated notably more than the microcosms receiving continuous flow. A sharp periodic increase in Eh was clearly the result of sudden, rapid re-supply of molecular oxygen through manual injection of oxygenated water. However, despite of these periodic perturbations, the most negative reducing conditions were measured at the bottom region of microcosm IF-M1. Depletion of $O_2$ in the absence of flow thus may have created more reducing conditions amenable for the proliferation of strictly anaerobic bacteria. This could have further contributed to a lowering of Eh.

A decrease in Eh was also measured in the control microcosm which received continuous flow, but to which no additional nutrients were added. The control, which was gamma-irradiated using the recommended irradiation dose of between 5 and 12 kGy (Ostlund *et al*., 1989) to obtain sterile sediment with a limited amount of chemical changes before initiation of the experiment, showed no bacterial growth initially. However, after an extended (10 day) incubation period, approximately $\log_{10} 4$ cells/mL bacteria were detected in the control microcosm effluent. Previous studies have also shown that bacterial activity may begin to rise in gamma radiation-

sterilized soil samples after 1 week of incubation (Tuominem *et al*., 1994) as a consequence of failure to achieve complete sterility of the soil matrix. It was suggested that free hydrogen and hydroxyl radicals cause complex carbohydrates to depolymerize, increasing the dissolved organic carbon concentration, resulting in enhanced recovery and growth of any bacterial survivors (Tuominem *et al*., 1994). In the present study, source of the microorganisms in the control microcosm was likely due to the incomplete killing by radiation (versus a contamination event) based on the biodiversity of survivors (see below).

### 5.5.3 Microbial diversity and their biogeochemical potential

The major lineages *Proteobacteria*, *Bacteroidetes* and *Firmicutes* detected in the uninoculated T=0 day tailings material and in all microcosm tailings after completion of the experiment were also found in the *in situ* DTMF tailings mass (Bondici *et al*., 2013) as well as the water column covering the DTMF tailings (Bondici *et al*., 2014). The most abundant bacterial classes within this phylum were *β*-, *α*-, and γ-Proteobacteria. The prevalence of these members corroborates earlier findings that reported similar dominant members in various subsurface settings, including radioactive waste repositories, heavy metal or hydrocarbon-contaminated sites (Radeva and Selenska-Pobell, 2005; Aburto *et al*., 2008; Fukuda *et al*., 2010; Rastogi *et al*., 2010).

A large number of sequences recovered from each microcosm, including the control microcosm and uninoculated T=0 day tailings material were affiliated with *Hydrogenophaga*, *Malikia*, *Polaromonas*, and *Acidovorax* within the *β*-Proteobacteria class. These members have also been identified as dominant microbial populations in a benzene-contaminated aquifer located below a petrochemical plant (Aburto *et al*., 2008), in hyper-alkaline leachate-affected soils (Burke *et al*., 2012) and BTEX (benzene, toluene, ethylbenzene, and xylenes) -impacted

aquifers (Aburto and Ball, 2009). *Hydrogenophaga* are facultative hydrogen-oxidizing bacteria (Willems *et al*., 1989) and it has previously been shown that *Hydrogenophaga* strains isolated from contaminated alkaline groundwater can degrade benzene and toluene as well as partially degrade xylenes (Fahy *et al*., 2008). *Malikia* species are strict aerobes and closely related to *Hydrogenophaga*. They have also been observed as members of active benzene degraders along with *Hydrogenophaga* species (Aburto and Ball, 2009). Clones closely related to *Polaromonas* aerobes have previously been detected along with strict-anaerobic benzene degraders in hydrocarbon-contaminated groundwater (Aburto *et al*., 2008). Furthermore, facultative denitrifiers, including *Acidovorax spp*., have previously been detected as the most-abundant species in an aerobic benzene-degrading microcosm (Fahy *et al*., 2006). These observations are highly relevant to the tailings environment, which receives significant additions of hydrocarbons in the form of kerosene as part of the urannium milling process.

The tailings-water interface zone has been identified as an important part of the water-sediment ecosystem, as it is a key location for the accumulation of any potential carbon sources that may promote microbial activity and proliferation (Novitsky, 1983; Landa *et al.,* 2004). The DTMF is an open system and can receive a variety of carbon sources from the surrounding environment; however, the most significant carbon compounds are those discharged into the tailings during the uranium milling process (Shaw *et al*., 2011). One of the most abundant carbon substrates deposited in the tailings is kerosene, a complex carbon compound that contains benzene, toluene, ethylbenzene and xylene (Dunlap and Beckman, 1988). Therefore, it is not surprising that the majority of the microbial community memebers in the tailings samples from the interface consisted of populations that can utilize benzene as carbon source.

Benzene can be readily degraded under aerobic conditions, firstly, because oxygen is a key element in benzene ring cleavage and secondly, since the utilization of oxygen as an electron acceptor yields more energy to benzene-degrading microorganisms (Aburto *et al*., 2009). However, benzene can also be degraded anaerobically using different ring cleavage mechanisms and alternate electron acceptors (Caldwell and Suflita, 2000; Aburto *et al*., 2009); for example, nitrate (Burland and Edwards, 1999), sulphate (Lovley *et al*., 1995), or iron (Lovley *et al*., 1994; Lovley, 1995).

The most prevalent sequences within the $\alpha$- and $\gamma$-Proteobacteria classes were closely related to *Brevundimonas* and *Pseudomonas*, respectively. Both were bacterial isolates used to inoculate the microcosms and they have previously been found in abundance in uranium-contaminated environments (North *et al*., 2004). *Pseudomonas* spp. are capable of degrading hydrocarbons (Fahy *et al*., 2006) and utilizing various electron acceptors, including Fe (III) (Nevin *et al*., 2003). In addition to aerobic and facultative bacterial species, strict anaerobes were also identified in the microbial community present in the uranium tailings microcosms. In general, few or no sequences affiliated with strict anaerobes were identified in the uninoculated T=0 day tailings material or the control. For example, sequences closely related to *Proteiniclasticum*, and *Fusibacter* were only abundant in treated (carbon and flow) microcosms. The latter bacterial species are thiosulfate-reducing bacteria and have been isolated from oil-producing wells (Ravot e*t al*., 1999).

Sequences closely related to *Desulfosporosinus* were most abundant in microcosm IF-M1 that received intermittent flow and had the lowest recorded redox potential (-545 mV). Since the number of recovered sequences for this species was low in other microcosms, including the uninoculated tailing, its high abundance in IF-M1 can be best explained by low redox conditions

enabling the proliferation of *Desulfosporosinus*. Sequence analyses of tailings samples from the DTMF tailings-water interface have shown that the predominant genera were *Proteiniclasticum* and *Desulfosporosinus* (Khan *et al*., 2013). *Desulfosporosinus* spp. are obligate anaerobic spore-forming autotrophs (Stackebrandt *et al*., 2003).

It is thus evident and not surprising that aerobic and anaerobic bacteria co-exist in the microcosms. Previous studies have also shown that strict aerobes and anaerobes, such as methanogens, may co-function together where aerobes consume molecular oxygen and decrease it to such a level that methanogens can proliferate (Gerrits and Gottschal, 1993). Furthermore, ferrihydrite reduction by strict anaerobic bacterial species can be stimulated by aerobic or facultative anaerobic bacteria (Straub and Schink, 2004). Aburto *et al*. (2009) presented possible explanations, which may have occurred in our microcosm, as to how a mixed aerobic and anaerobic bacterial community in contaminated groundwater can degrade benzene. It was stated that benzene degradation may occur in series where aerobic bacteria would open the benzene ring and remove molecular oxygen, and the anaerobes would thereafter utilize the resulting metabolites to reduce other available electron acceptors. Alternatively, aerobic and anaerobic processes could be occurring in different regions where localized anoxic conditions would develop.

The most prevalent identified bacterial species (e.g., *Hydrogenophaga*, *Malikia*, *Polaromonas*, *Acidovorax Brevundimonas* and *Pseudomonas*) affiliated with complex hydrocarbon degraders in all the microcosms, as well as in the uninoculated tailings material indicate that available carbon (e.g., kerosene) originally present in the tailings play an important role in shaping microbial diversity. However, the measured Eh differences between all the microcosms and the control implies that the additional carbon and the bacterial inoculants are

also important in enhancing microbial activity. Furthermore, detection of sequences closely related to strict anaerobes detected at higher frequency in the treated microcosms indicates that the enhanced overall microbial activity created favourable conditions for the appearance of these strict anaerobes.

### 5.5.4 Biogeochemical activity revealed by STXM

STXM analyses of biofilm material from 40-day microcosms were conducted in order to determine whether microbes indigenous to the DTMF tailings were capable of reducing ferrihydrite. Within the DTMF, ferrihydrite is the dominant mineral form responsible for complexation and retention of EOCs (Essilfie-Dughan *et al*., 2012; Essilfie-Dughan *et al*., 2013; Gomez *et al*, 2013). In the microcosms, not only was a significant decrease in Eh measured, but in microcosm effluents reduced Fe was also detected, indicating that the transformation of Fe (III) to Fe (II) occurred due to enhanced microbial activity. Both oxidation states of Fe were identified within microcosm biofilms observed with STXM, suggesting that bacteria utilize Fe (III) as electron acceptor or they create localized microenvironments within the biofilm with chemical conditions where iron was reduced (Hunter *et al*., 2008). From the organic and Fe component maps it was apparent that the occurrence of reduced Fe correlates with the organic components of the biofilm, with Fe (II) was typically observed in close proximity with distinct bacterial cells, indicating that oxidized iron possibly served as an electron acceptor for bacterial growth. However, in addition to direct enzymatic reduction through cellular attachment (Lloyd, 2003), iron can be reduced indirectly by reduced elements or chemical conditions that are produced by bacterial processes (Lovley and Philips, 1992; Li *et al*., 2007; Hunter *et al*., 2008).

Reduction of ferrihydrite by sulfate-reducing bacteria and biogenic sulphides could preferentially occur in microcosms having the highest abundance of DNA sequences closely

related to *Desulfosporosinus* (e.g., in microcosm IF-M1). It has previously been demonstrated that these bacterial species can reduce Fe (III) and sulphate enzymatically; furthermore, the formation of biogenic sulphides can aid in Fe (III) reduction (Senko *et al*., 2009; Bertel *et al*., 2011).

### 5.5.5 Microbially induced phase transformation of ferrihydrite

Bulk geochemical investigations of the DTMF tailings have previously shown that alkaline and oxic conditions exist throughout the deposited tailings body. Under these conditions, ferrihydrite is the main secondary phase that plays a significant role in the sequestration and stability of contaminants such as As, Ni, Mo, and Se (Shaw *et al*., 2011; Essilfie-Dughan *et al*., 2012). A recent research study by Gomez et al. (2013) has demonstrated that another important secondary mineral phase, Mg-Al/Fe containing-$SO_4$-$CO_3$ hydrotalcite, is also present and co-occurs with EOCs such as As and Ni. Since a conventional $H_2SO_4$ leaching process is used to extract uranium from the ore, the tailings contain substantial amount of $SO_4$ mainly in the form of gypsum, which is formed by the addition of slaked lime (Shaw *et al*., 2011).

The highly reducing redox potential and presence of Fe (II) (detected by iron test strips and STXM analyses) in our microcosms indicates that ferrihydrite potentially goes through phase transformation due to enhanced microbial activity. The stong reducing conditions measured in lower regions of microcosms containing supplemental nutrient strongly suggests that $O_2$ was removed in this region and that ferrihydrite or sulfate could equally serve as electron acceptors for microbial activity (Lovley and Chapelle, 1995). In our microcosm systems, the microbial communities that formed were dominated by bacterial species closely related to benzene degraders, which can utilize sulphate/iron as electron acceptors, as well as sulphate reducers (specifically seen in microcosm IF-M1). These microorganisms may serve as Fe (II) suppliers

and Fe (II), which can be produced directly or indirectly through bacterial processes, could potentially catalyze the reductive dissolution of ferrihydrite and subsequent phase transformations. Mapping and speciation of Fe using STXM analyses showed association of Fe (II) with Fe (III) and Mg-Al compounds in the context of microbial biofilm. This strongly indicates that proportions of biogenic Fe (II) detected in the microcosm effluent was potentially taken up by ferrihydrite and/or hydrotalcites. Reaction of Fe (II) with ferrihydrite may have resulted in more thermodynamically stable phases within the tailings. Reductive phase transformation of ferrihydrite is strongly dependent on the concentration of Fe (II) and similar phases can form under biotic and abiotic conditions (Zachara *et al*., 2002). In all microcosms other than the control, the highly reducing conditions created by enhanced bacterial activity is a clear indication that the biogenic Fe (II) supply was abundant, hence geothite and magnetite phases could potentially be formed (Hansel *et al*., 2003).

The appearance of black color in the IF-M1 tailings receiving intermittent flow could be attributed to the formation of magnetite. More magnetite could potentially have formed in this microcosm because in addition to microbial populations that can couple oxidation of complex carbon to Fe (III) reduction, sulphate reducing bacteria (which were abundant) could reduce Fe (III) directly or indirectly. Furthermore, the generated Fe (II) remained in the system rather than being removed through the effluent as in microcosms that received continuous flow.

### 5.5.6 Conclusions

This 40-day bench-scale microcosm assay provided insight into the potential for indigenous microbial activity to impact the redox conditions in the DTMF tailings. Since oxic conditions throughout the DTMF are essential for the stability of the contaminant-bearing mineral phases, (e.g., ferrihydrite), highly reducing conditions created due to stimulated

microbial activity directly confirms the importance and potential effect of the indigenous microorganisms on tailings stability. Microbial diversity detected in the microcosm tailings samples was clearly consistent with type of carbon source (e.g., kerosene, a complex-carbon compound that contains benzene, toluene, ethylbenzene and xylene) that potentially sustains the microbial community in the DTMF tailings. Furthermore, these studies have demonstrated that aerobic and facultative complex carbon degraders (e.g., benzene degraders) present in the tailings could potentially generate conditions necessary for the proliferation of iron- and sulphate-reducing bacteria which then could catalyze reductive dissolution of ferrihydrite, resulting in phase transformation and potential release of EOCs, such as As.

## 5.6 Connection to the next study

This study revealed that aerobic and anaerobic complex carbon degraders can potentially generate reducing conditions which can directly or indirectly influence the redox state of iron. A potentially novel species of the genus *Polaromonas* was consistently observed at high frequency at each site (water, interface and tailings body), as well as in the microcosm assay. To better understand the functional potential of this species, a full taxonomic characterization was undertaken which is described in the next study.

# 6 *POLAROMONAS DEILMANNI* SPP. NOV. ISOLATED FROM URANIUM MINE TAILINGS IN KEY LAKE, NORTHERN SASKATCHEWAN, CANADA

V F. Bondici, N.H. Khan, J.R. Lawrence, G.M. Wolfaardt and D.R. Korber for submission to the journal of *Int. J. Syst. Evol. Microbiol*.

Author contributions

All authors participated in the design of the experiments and contributed to writing of the manuscript. Preparation of the initial draft of the manuscript, as well as all other data presented in this manuscript, are the work of the thesis author and N.H. Khan.

## 6.1 Abstract

Two Gram-negative, non-motile, cocci, designated as AER18D-145 and AET17H-212, were isolated from uranium mine tailing sediments in Key Lake, Northern Saskatchewan, Canada. On the basis of 16S rRNA gene sequencing it was shown that the two isolates were members of the genus *Polaromonas* and shared >99 % sequence similarity to each other and 97 % to *Polaromonas vacuolata.* Phylogeny derived from the partial *trmE* gene and cpn60 and rpoA protein sequences further supported, although with greater distance, the 16S rRNA gene-derived affiliation. The major fatty acid content of both isolates were C16:0, C16:1, C18:0 and C18:1 consistent with other members of the genus *Polaromonas*. The G+C content of the genomic DNA of strains AER18D-145 and AET17H-212 were 59.3 and 59.2 mol%, respectively, also in keeping with the genus *Polaromonas*. On the basis of phenotypic and genotypic characteristics, the strains recovered from the Deilmann tailings management facility represent a novel species distinct from other known members of the genus *Polaromonas*, for which the name *Polaromonas deilmanni* is proposed

## 6.2 Introduction

Members of the genus *Polaromonas* thrive in extreme environments such as glacial ice and sub-glacial sediments. DNA sequence-based analyses have revealed the presence of *Polaromonas* phylotypes in glaciers, further supporting the fact that members of this genus are among the dominant bacteria inhabiting cold environments (Darcy *et al*., 2011). Recent studies have shown that *Polaromonas* species are also found in non-glacial, seasonally cold environments, and tend to exhibit high metabolic diversity; for example, they are able to oxidize $H_2$ (Sizova *et al*., 2007), arsenite (Osborne *et al*., 2012) and various organic compounds as their sole energy source (Mattes *et al*., 2008). The ability to utilize such a wide spectrum of energy

sources is thought to ensure the consumption of whatever substrate is available during transient warm periods (Darcy *et al*., 2011). Many isolates closely related to *Polaromonas* have previously been obtained and their metabolic potential investigated under various conditions; however, they have not been fully characterized nor identified to the species level (Foght *et al*., 2004; Osborne *et al*., 2012). The genus *Polaromonas* was first proposed by Irgens et al. (1996). Presently, the genus comprises seven species: the marine bacterium *P. vacuolata* (Irgens *et al*., 1996), *P. naphthalivorans* (Jeon *et al*., 2004) isolated from freshwater sediments, *P. aquatica* (Kampfer *et al*., 2006) isolated from tap water, *P. hydrogenivorans* (Sizova and Panikov, 2007) from Alaskan soil, *P. jejuensis* (Weon *et al*., 2008) from soil in Korea, and *P. glacialis* and *P. cryoconiti* (Margesin *et al*., 2012) which were most recently isolated from alpine glacier cryoconite. In the present study, two bacteria were isolated from uranium mine tailings, a high pH and metal-contaminated environment, and found to represent a novel species of the genus *Polaromonas*.

## 6.3 Materials and methods

Strains AET17H-212 and AER18D-145 were isolated aerobically from sediment samples collected at the 17 and 18 m depth (from the surface), respectively, from a uranium mine tailings management facility located at Key Lake, Northern Saskatchewan, Canada. During sample collection, the tailings temperature was 10°C and pH was close to 10. Approximately 0.2 g of tailings materials were re-suspended in 1.0 ml of sterile Tris-EDTA (TE) buffer of pH 8 and plated on four types of agar media, as described by Bondici et al. (2013). Two isolates, AER18D-145 and AET17H-212, were initially isolated on Reasoner's 2A (R2A) and 5% tryptic soy agar (TSA), respectively, under aerobic conditions after 3 weeks of incubation at 5°C (Bondici *et al*., 2013). Following isolation and subsequent sub-culturing of distinct colonies, the pure cultures were maintained in 5% TSB and 15% glycerol at -80° C.

The almost-complete 16S rRNA gene sequence was PCR-amplified using 8F (Amman *et al*., 1990) and 1492R (Embley *et al*., 1988) primer set. Reagent concentrations and thermal cycling used for PCR amplification were conducted in accordance with Bondici et al. (2013). To reliably resolve the phylogeny of these isolates, additional housekeeping genes, *cpn60* (Hill *et al*., 2005), *thdF* (GTP-binding, thiophene oxidation) and *rpoA* (RNA polymerase, alpha subunit) (Zeigler, 2003), were also targeted for sequencing. The *cpn60* gene sequence was amplified using H1594F (5'- CGC CAG GGT TTT CCC AGT CAC GAC GAC GTC GCC GGT GAC GGC ACC ACC AC-3') and H1595R (5'-AGC GGA TAA CAA TTT CAC ACA GGA CGA CGG TCG CCG AAG CCC GGG GCC TT-3') primer set (Sahin *et al*., 2010). The gene specific primer sequences also included the M13 sequencing primer sites (the underlined region). The *thdF* gene sequence was annotated as *trmE* within the available genome sequences; therefore, the *trmE* annotation is used throughout this manuscript. The trmE and rpoA primer sets were designed by manually searching for conserved regions of these genes within the aligned sequences. At the time of primer design, full genome sequences were only available for two *Polaromonas* strains (*Polaromonas sp.* JS666 and *Polaromonas naphthalenivorans* CJ2) in the NCBI/GenBank database. Properties and non-specific amplification of the designed primer set was tested using the online calculator, OligoCalc (Kibbe, 2007) and Primer-Blast (Ye *et al*., 2012). The designed primer sets for *trmE*- and *rpoA*-encoding genes were as follows: F'-5'-CGCCTGSCGCAAATCYTCC and R-5'- CSACYTACCTGCCGTTTCGCGA for *trmE* and F-5'-TGT CGC ACG GCG GCA AGA T and R-5'- GCA GTT TGC CGA ACG CAC CG for *rpoA*.

The PCR reaction mixture for each of the two primer sets consisted of 1 μl (50 μM) each of forward and reverse primers, 1 μl (200 μM) of dNTPs, 5 μL of 10 × PCR buffer, 5 μl $MgSO_4$

(20 mM), 1 U of HP Taq polymerase (UBI, Life Sciences, Saskatoon, SK), and 2 µl of genomic DNA (5-50 ng) and then adjusted to a final volume of 50 µl with sterile distilled water. The PCR cycle settings were as follows: an initial denaturation temperature of 95°C for 5 min followed by 35 cycles of 95°C for 1 min, annealing temperatures of 68°C for 45 sec (*trmE*); 59°C for 45 sec (*rpoA*), elongation at 72°C for 1 min (*trmE*); for 45 sec (*rpoA*) and a final extension of 72°C for 10 min. The expected amplicon size for *trmE* and *rpoA* were 1209 bp and 422 bp, respectively. Annealing temperatures were determined using temperature-gradient PCR until successful amplification of the desired product was obtained. The PCR cycle settings for *cpn60* was according to Sahin *et al*. (2010). Before sequencing, PCR products were gel-purified using the Qiagen purification kit (Qiagen Sciences, Germantown, MD, USA). DNA sequences obtained were assembled using the Staden package (Gap 4 and Pregap) (Bonfield *et al*., 1995). Taxonomic identification and clustering of 16S rRNA gene sequences was assigned based on similarities to all type strains within the Ribosomal Database Project (RDP release 10). Aligned sequences were downloaded from the RDP database, visualized and then edited manually using the GeneDoc program v 2.7 (Nicholas *et al*., 1997). A phylogenetic tree of the aligned sequences and their closest 16S rRNA gene matches was constructed by a neighbor joining method (Saitou and Nei, 1987) using MEGA v5 with 1000 bootstrap replicates (Tamura *et al*., 2011). Identification of protein coding genes was performed using Basic Local Alignment Search Tool (BLAST). The closest match sequences were downloaded from the NCBI/GenBank database. Phylogenetic analysis of the *cpn60* and *rpoA* housekeeping genes was carried out on the translated DNA sequence because of the high variation at the DNA-sequence level. The correct reading frame of the query sequences were obtained using the ExPaSy Bioinformatics Resource

Portal translate tool. Protein sequences were aligned using ClustalW and phylogenetic analyses were performed using the neighbour joining method (MEGA v5).

Analyses of fatty acid methyl esters from bacterial cell membranes were performed using gas liquid chromatography according to the instructions of the Microbial Identification System (MIDI) (Reed *et al*., 2000; Tan *et al*., 2011). Cellular morphologies of isolates AER18D-145 and AET17H-212 were directly determined using scanning electron microscopy (SEM) (Model Phillips 505-1983). SEM samples were prepared as follows: an appropriate concentration of cell suspension was obtained by serial dilution of log-phase cell cultures. Cells were initially fixed in 2.5% glutaraldehyde in buffer (0.1-0.2M phosphate, pH 6.8-7.2) at 4°C for 3 h, followed by repeated washing (3x) at 4°C for 30 min. Secondary fixation of the cells was performed in 1-2% osmium tetroxide in buffer at 4°C for 3 h. Cells were then repeatedly washed in distilled water (3x) for 30 min, after which cells were serially dehydrated for 20 min each in 25, 50, 75, 90 and 100% acetone at 4°C. Finally, cells were dried in a critical-point dryer using liquid $CO_2$ as the transition fluid. The dried samples were sputter-coated with gold under a vacuum and then examined with the SEM.

Gram staining and morphological determinations were also performed using the Difco Gram staining kit (BD, Franklin Lake, NJ, USA) according to the manufacturer's recommendations. Growth response under a range of different temperatures (from 4 to 40°C at 5°C increments), pH values (4.0 to 10.0 at 1.0 pH unit increments) and NaCl concentrations (0 to 10 % at 1% increments) were determined in R2A medium (in both broth and on semi-solid agar) over a two-week incubation period. Physiological and biochemical properties of isolates AER18D-145 and AET17H-212, including fermentation of carbon sources and enzymatic activities, were determined by using the API 20NE, API ID 32GN and API ZYM test kits

(Biomereux, Montreal, QC, Canada). The growth response in the presence of different antibiotics was tested using Sensititre$^{TM}$ CMV1AGNF plates (TREK Diagnostic Systems, England) that contained 15 different antibiotics at various concentrations distributed in 96 wells, as specified by the National Antimicrobial Resistance Monitoring System (NARMS). The test was carried out according to the instructions of the manufacturer. Both bacterial isolates could grow in the presence of 2.5 mM arsenite and two sets of degenerate primers were used for the amplification of approximately 500 bp of the gene that encoded the Mo-pterin subunit of *arsenite oxidase (aroA*) (Inskeep *et al*., 2007).

## 6.4 Results

Pairwise comparison of the 16S rRNA gene sequence showed that the two novel organisms were 99% similar to each other. Furthermore, the percent identity of these isolates to *Polaromonas* type strains present within the RDP database were as follows: 97 % to *P. vacuolata* 34-P and 96 % to *P. aquatica* CIP 108776, *P. naphthalenivorans* DSM, *P. hydrogenivorans* and *P. jejuensis* JS12-13. Furthermore, the two strains showed less than 96% sequence similarity with type strains other than *Polaromonas*. Thus, both strains formed a distinct cluster with other *Polaromonas* and were separated from other closely related genera by 100% bootstrap support (Figure 6.1). Maximum parsimony and maximum likelihood analyses both supported the position of the two strains amongst existing *Polaromonas* species. Sequence analyses of the other housekeeping genes also confirmed affiliation with *Polaromonas* spp*.,* but with more distant clustering (Figures 6.2, 6.3).

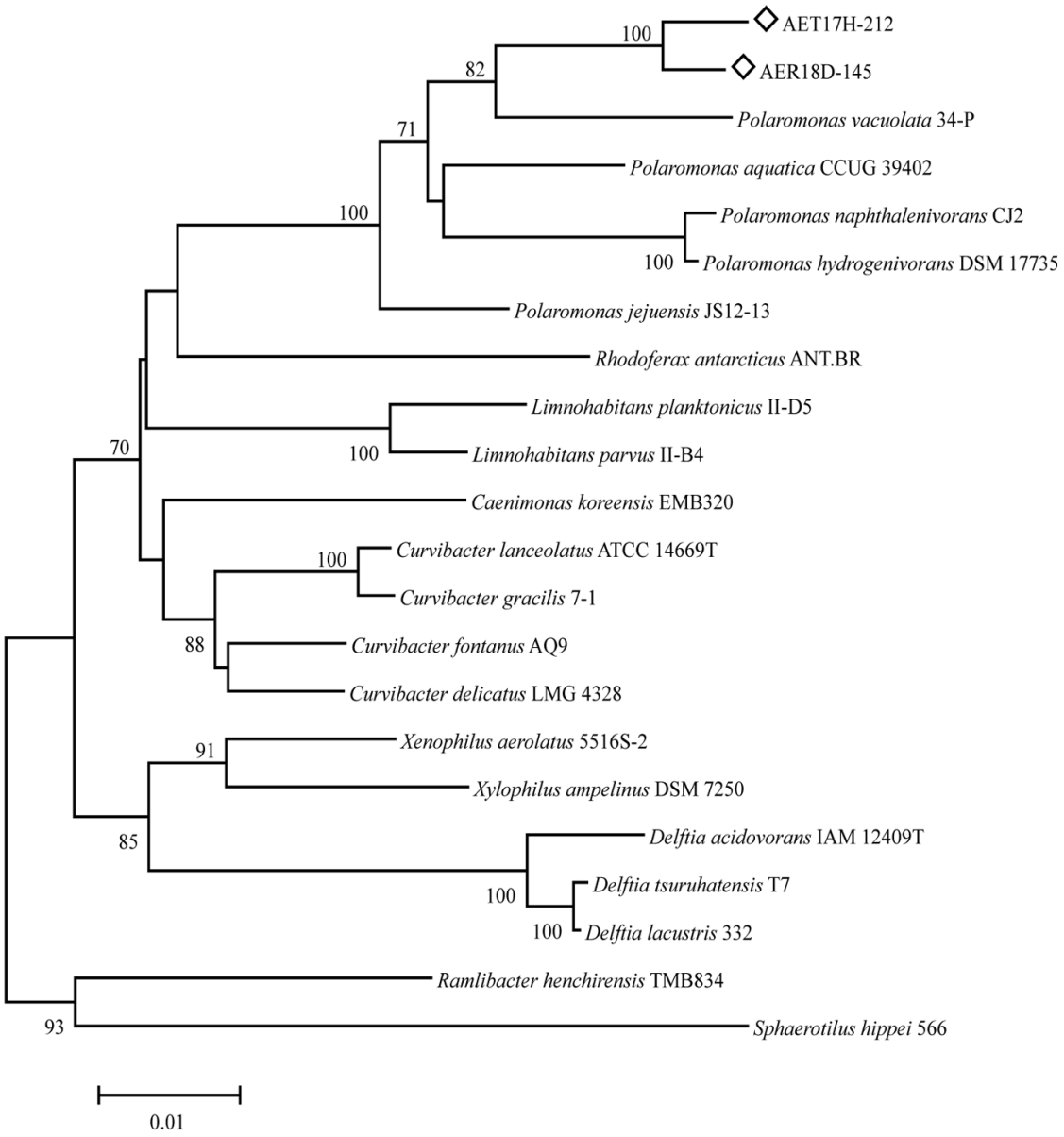


**Figure 6.1 Neighbour-joining phylogenetic tree based on 16S rRNA gene sequences showing the position of AER18D-145 and AET17H-212 isolates among type strains of closest related genera.**

Bootstrap values ≥ 60% (based on 1000 replications) are shown at the branch points. Bar represents 0.01 substitutions per nucleotide position.

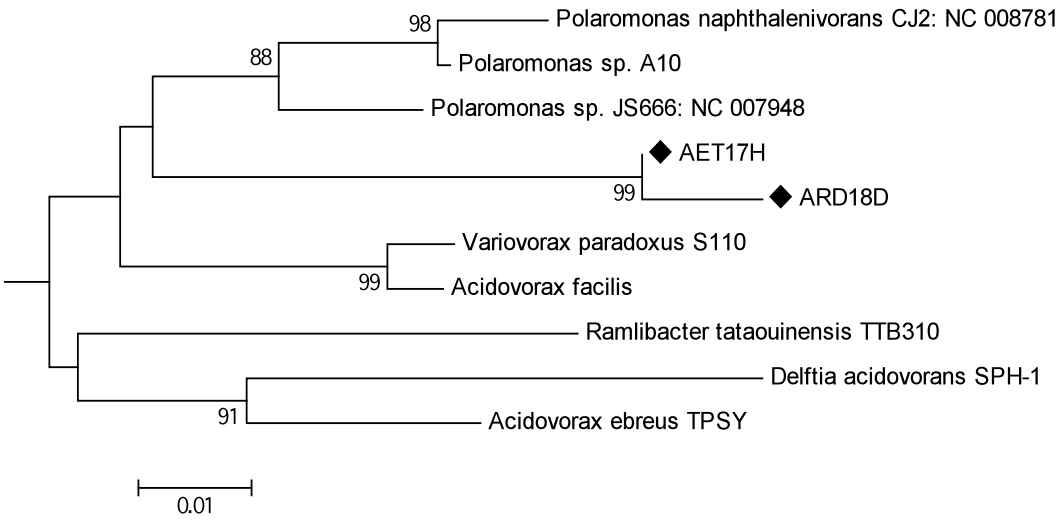


**Figure 6.2 Neighbour-joining phylogenetic tree based on cpn60 protein sequences showing the position of AER18D-145 and AET17H-212 isolates among type strains of closest related genera.**
Bootstrap values ≥ 60% (based on 1000 replications) are shown at the branch points. Bar represents 0.01 substitutions per nucleotide position. Sequences of non-type strain *Polaromonas* spp. were included into the analyses for the confirmation and clarity of the clustering.

Pairwise comparisons of sequence similarity between the housekeeping genes query sequences and the closest type strain, *P. naphthalenivorans* available in the database was also carried out. Based on *trmE* gene sequence comparison AET17H-212 and AER18D-145 isolates were 84% and 83% identical, respectively, to *P. naphthalenivorans*. Amplification of the *rpoA* partial gene sequence was only successful for AET17H-212 isolate. Due to high variation on DNA sequence level the rpoA protein sequence was used for the pairwise comparison, which showed that the AET17H-212 isolate was 93% identical to *P. naphthalenivorans.* Alternatively, based on the cpn60 protein sequences of AER18D-145 and AET17H-212, they were 58% and 59% identical, respectively, to *P. naphthalenivorans.*

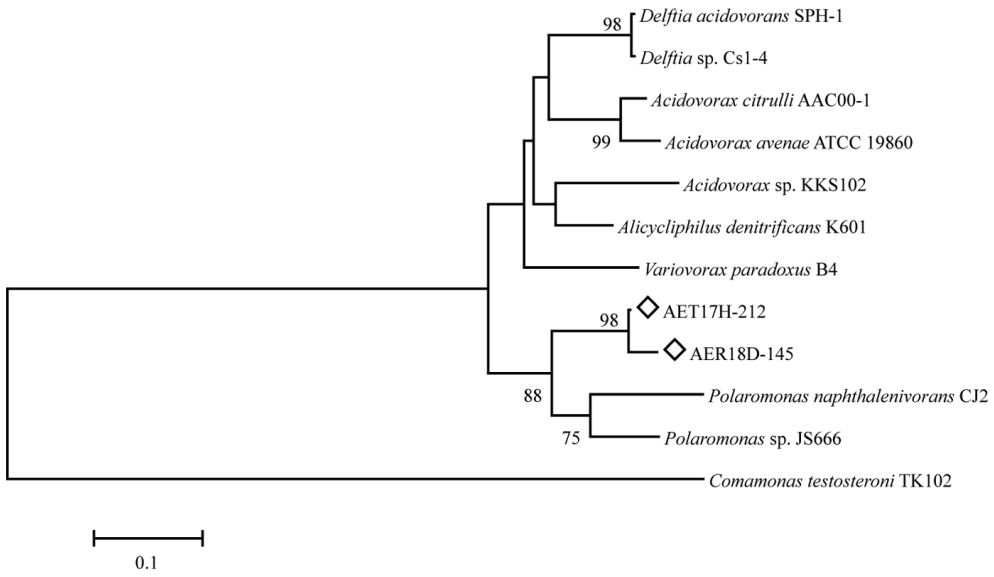


**Figure 6.3 Neighbour-joining phylogenetic tree based on based on *TrmE* gene sequences showing the position of AER18D-145 and AET17H-212 isolates among type strains of closest related genera.**

Bootstrap values ≥ 60% (based on 1000 replications) are shown at the branch points. Bar represents 0.1 substitutions per nucleotide position. Sequences of non-type strain *Polaromonas* spp. were included into the analyses for the confirmation and clarity of the clustering.

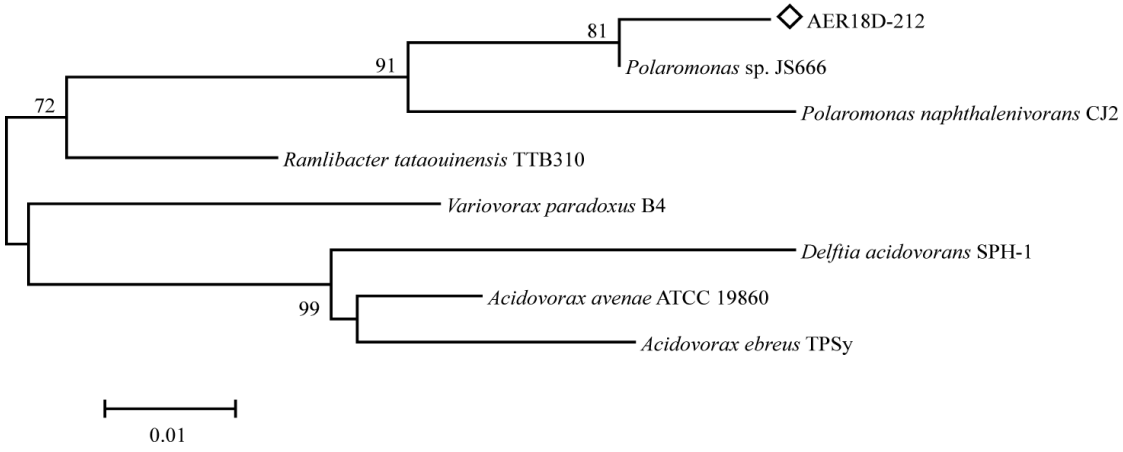


**Figure 6.4 Neighbour-joining phylogenetic tree based on based on rpoA protein sequences showing the position of AER18D-145 and AET17H-212 isolates among type strains of closest related genera.**

Bootstrap values ≥ 60% (based on 1000 replications) are shown at the branch points. Bar represents 0.01 substitutions per nucleotide position. Sequences of non-type strain *Polaromonas* spp. were included into the analyses for the confirmation and clarity of the clustering.

Whole cell fatty acid analyses showed that strains AER18D-145 and AET17H-212 were slightly different. The AER18D-145 cell membrane primarily contained C 16:0 (30.53%), C 16:1 (28.27%), C 18.0 (26.82%) and C 18:1 (14.38%) fatty acids. Membrane fatty acids for strain AET17H-212 mainly consisted of C 16:0 (35.9%), C 16:1 (49.1%), C 18:0 (4.80%) and C 18:1 (7.7%) units (Table 6.1).

The presence of higher amounts of C 16:0, C 16: 1 and C 18:1 confirmed that these isolates are members of the order Burkholderiales, more specifically belonging to the genus *Polaromonas* (Chen *et al*., 2012; Irgens *et al*., 1996; Sizova and Panikov, 2007; Kamfer *et al.*, 2006; Jeon *et al*., 2004). Strain AET17H-212 also contained minor amounts of C 14:0 and C 14:1 fatty acids. C 17:0 cyclo fatty acid (37.3%) was completely absent in our strains as well as in any other reported *Polaromonas* spp., except for *P. aquatica*. Other differences included the presence of a greater amount of C 18:0 fatty acids in AER18D-145 and AET17H-212 in comparison to other *Polaromonas* spp., furthermore, the absence of C 20:0 fatty acids, which have been reported for *P. hydrogenivorans* but was absent in our isolated strains. Lastly, some *Polaromonas* spp. possess C 8:0 3-OH, yet was absent in our strains. Despite existing differences, overall, the whole cell fatty acid profile demonstrates that both bacterial isolates are consistent with the genus *Polaromonas.*

Unique phenotypic characteristics of AER18D-145 and AET17H-212, relative to other *Polaromonas spp*., include the presence of nitrate reductase activity, coccoid cell morphology, a relatively larger cell size (2 × 2.8 μm), a wider range of pH tolerance and variable fatty acid composition.

**Table 6.1** Major fatty acid compositions of AER18D-145 and AET17H-212 and type strains of recognized *Polaromonas* species. Strains; **1**, AER18D-145 and **2**, AET17H-212 **3**, *P. jejuensis*; **4**, *P. aquatica*; **5**, *P. vacuolata*; **6**, *P. naphthalenivorans* **7**, *P. hydrogenivorans*; **8**, *P. glacialis* and **9**, *P. cryoconiti*.

| **Fatty Acids** | **1** | **2** | **3** | **4** | **5** | **6** | **7** | **8** | **9** |
|---|---|---|---|---|---|---|---|---|---|
| **C 8:0 3-OH** | - | - | 1.3 | - | 2.8 | 0.5 | - | - | - |
| **C 10:0 3-OH** | - | - | - | - | - | 2.5-2.9 | 2.9 | - | - |
| **C 12:0** | - | - | 2.9 | - | - | - | 1.9 | - | - |
| **C 14:0** | - | 0.51 | 0.6 | 1.1 | - | - | 1.4 | - | - |
| **C 14:1** | - | 0.47 | - | - | - | - | - | - | - |
| **C 16:0** | 30.53 | 35.9 | 28.4 | 35.9-37.2 | 17.0 | 19.6-22.2 | 22.6 - | 15.4 - | 28.0 - |
| **C 16:1** | 28.27 | 49.1 | 0.7 | 6.5-7.5 | 75.0 | 64.5-67 | 49.4 | 59.7 | 60.5 |
| **C 17:0** | - | - | 0.8 | 0.4 | 0.8 | 0-7.2 | - | - | - |
| **17:0 Cyclo** | - | - | - | 37.3 | - | - | - | - | - |
| **C 17:1** | - | - | 15.9 | 30.7 | 0.8 | 12.9 | 3.0 | - | - |
| **C 18:0** | 26.82 | 4.80 | 0.7 | 3.7-4.1 | - | - | 1.8 | - | - |
| **C 18:1** | 14.38 | 7.7 | 9.1 | 10.5-11.4 | 8.0 | 3.0-7.9 | 10.8 | 11.9 | - |
| **C 20:0** | - | - | - | - | - | - | 1.8 | - | - |

The 16S rRNA, along with *cpn60*, *trmE* and *rpoA*, and the biochemical comparative test data, demonstrated that these two bacterial isolates are unique among other available *Polaromonas* spp. The genetic and phenotypic data presented in this report clearly demonstrate that AER18D-145 and AET17H-212 strains, represent a novel species within the genus *Polaromonas*, for which the name *Polaromonas deilmanni* is proposed.

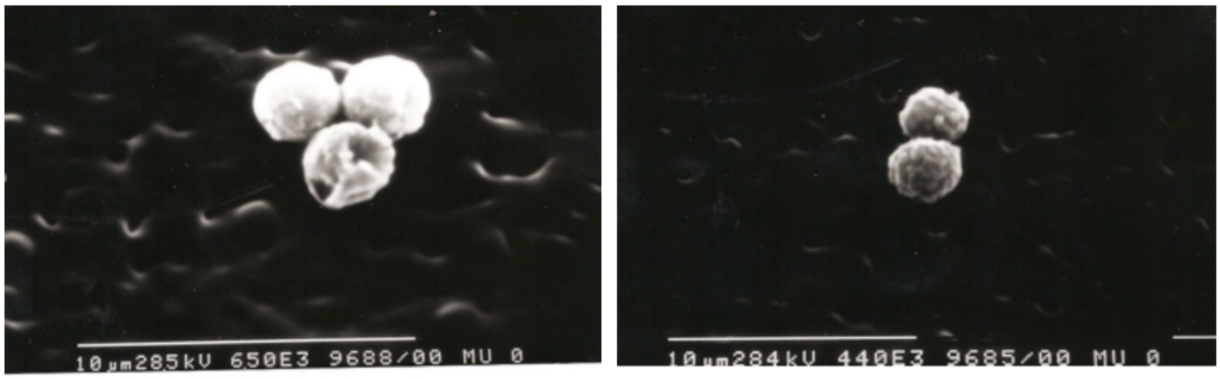


**Figure 6.5 Scanning electron micrograph showing the cell morphology.**
AER18D-145 (right) and AET17H-212 (left).

### 6.4.1 Description of *Polaromonas deilmanni* sp. nov.

*Polaromonas deilmanni sp*. nov. cells are aerobic, Gram-negative, non-motile, cocci (Figure 6.5) approximately 2.0 × 2.8 µm in size and found individually or in small clusters. Colonies that formed on R2A agar plates were pale yellow, but colorless on TSB agar plates. Growth occurred over 4-30°C (optimum 20-25°C), pH 3-9 (optimum 5 to 7) and 0 to 3% (w/v) NaCl. Both strains showed identical metabolic patterns, and were able to assimilate potassium nitrate, L-arginine, urea, L-ornithine, but not D-glucose, L-tryptophane, esculine citrate, gelatin, 4-nitrophenyl B-D galactopyranoside, L-arabinose, D-mannose, D-mannitol, N-acetyle-glucosamine, D-maltose, potassium gluconate, trisodium citrate, malic acid, L-arginine, L-lysine,

L-arabitol, galacturonic acid, potassium-5-ketogluconate, 5-bromo-3-indoxyl-nanonoate, sodium pyruvate, adonitol, palatinose, sodium malonate, D-sorbitol and trypsin (API 20NE and API ID 32GN). The two strains also exhibited the following enzyme activities: esterase, esterase lipase, alkaline phosphatase, lipase, leucine arylamidase, acid phosphatase, naphthol-AS-BI-phosphodrolase, L-aspartic acid arylamidase, oxidase, catalase and nitrate reductase (API ZYM) (Table 6.2). It is notable that, in general, information regarding substrate utilization and enzymatic potential of previously reported *Polaromonas* spp. is quite limited. The two isolates were negative for the following enzyme activities: N-acetyl-B-glucoseaminidase, B-galactocidase, A-glucocidase, A-galactocidase, gelatinase, amylase and protease (API ZYM). The AER18D-145 isolate was resistant to nalidixic acid, ceftiofur, sulfisoxazole, and trimethoprim/sulfamethoxazole , and AET17H-212 was susceptible for all the antiobiotics tested. No arsenite oxidase *(aroA*) gene was detected in either isolate. The predominant fatty acids were C 16:0, C 16:1, C 18:0 and C 18:1. The DNA G+C content of AER18D-145 and AET17H -212 were 59.3 and 59.2%, respective.

**Table 6.2 Differential characteristics of AER18D-145 and AET17H-212 and type strains of recognized *Polaromonas* species.** Strains; 1, AER18D-145 2, AET17H-212; 3, *P. jejuensis*; 4, *P. aquatica*; 5, *P. vacuolata*; 6, *P. naphthalenivorans* 7, *P. hydrogenivorans*; 8, *P. glacialis* and 9, *P. cryoconiti*. (ND = not determined).

| Characteristics | *Polaromonas* spp. | | | | | | | | |
|---|---|---|---|---|---|---|---|---|---|
| | **1** | **2** | **3** | **4** | **5** | **6** | **7** | **8** | **9** |
| Cell shape | Cocci | Cocci | Rods | Rods | Rods | Cocci | Cocci | Cocci | Short rod |
| Cell size (μm) | 2X2.8 | 2X2.8 | 0.6X1-3 | 1X 2 | 0.8X2-3 | 1-4 | 0.8 -2.8 | 0.7X0.9 | 0.8X1.2 |
| Flagella | - | - | - | + | + | - | - | - | - |
| Temperature range | 4-30 | 4-30 | 5-30 | 25-30 | 0-12 | 4-25 | 0-25 | 1-25 | 1-25 |
| NaCl range (%) | 0-3 | 0-3 | 0-1 | ND | 0-6 | ND | ND | 0-1 | <1 |
| pH | 3-9 | 3-9 | 5-9 | ND | 6-7 | 6-9 | 6-7 | 6-7 | 7 |
| Isolation source | Uranium tailing | Uranium tailing | Soil | Tap water | Seawater | Freshwater sediment | Soil over permafrost | Glacier cryoconite | Glacier cryoconite |
| Potassium nitrate | + | - | - | ND | ND | + | ND | | |
| Urea | + | + | + | - | + | + | ND | _ | _ |
| D-glucose | - | - | + | - | + | + | + | _ | _ |
| Potassium gluconate | - | + | + | _ | ND | + | _ | _ | |
| Trisodium citrate | - | - | + | - | - | + | _ | | |
| Malic acid | - | - | + | + | + | - | _ | _ | W |
| 5-bromo-3-indoxyl-nonanoate | - | + | - | ND | ND | + | ND | | |
| Sodium malonate | - | - | + | ND | ND | - | ND | | |
| N-acetyl-B-glucoseaminidase | - | - | - | ND | ND | ND | ND | _ | _ |
| B-galactocidase | - | - | + | ND | ND | ND | ND | _ | _ |
| Alpha-glucosidase | - | - | - | ND | ND | ND | ND | _ | _ |
| Alpha-galactocidase | - | - | - | _ | ND | W | _ | - | - |
| Esterase (C 4) | + | + | + | ND | ND | ND | ND | | |
| Esterase lipase (C 8) | + | + | + | ND | ND | ND | ND | | |
| Alkaline phosphatase | + | + | + | + | ND | _ | + | W | + |
| Lipase (C 14) | + | + | - | W | + | _ | W | W | + |
| Leucine arylamidase | + | + | + | ND | ND | ND | ND | + | + |
| Acid phosphatase | + | + | + | ND | ND | ND | ND | + | W |
| Naphthol-AS-BI-phosphohydrolase | + | + | weak | ND | ND | ND | ND | + | W |
| D-sorbitol | - | - | - | - | + | - | + | _ | _ |
| Trypsin | - | - | - | ND | | ND | ND | _ | _ |
| L-aspartic acid arylamidase | + | + | + | ND | ND | + | ND | | |
| Gelatinase | - | - | ND | ND | ND | + | ND | | |
| Amylase | - | - | W | W | - | _ | _ | W | - |
| Oxidase | + | + | + | + | + | + | + | + | + |
| Catalase | + | + | + | + | + | + | + | + | + |
| Protease | - | - | ND | ND | - | ND | ND | _ | _ |
| Nitrate reductase | + | + | - | _ | - | + | _ | + | + |
| GC content (mol %) | 59.3 | 59.2 | 63.7 | ND | 52.0 | 61.5 | 62.5 | 61.3 | 60.7 |

# 7 GENERAL DISCUSSION AND CONCLUSIONS

## 7.1 Discussion and limitations of these works

Microbial processes are important factors in determining the fate and transport of contaminants in various subsurface settings. In general, microbial metabolism or resistance mechanisms can change the redox state of metal or metalloid elements, resulting either in their immobilization or increased mobilization (Gadd, 2010). Microbial activity can also impact ferrihydrite phase transformation as well as absorption/co-precipitation capability when oxygen is consumed during microbial respiration and metabolism becomes shifted to anaerobic pathways. Under these conditions, electron donors oxidation can be coupled to Fe-oxide reduction, resulting in dissimilatory iron reduction (Lovley, 1991).

There is a large body of published material focusing on bioremediation of uranium-contaminated sediment and groundwater (Holmes *et al*., 2002; Vrionis *et al*., 2005; Akob *et al*., 2007), yet there are relatively few studies on the potential effect of microbial activity on the environmental behavior of contaminants associated with actual uranium tailings deposition sites (Wolfaardt *et al*., 2008; Rastogi *et al*., 2010; Islam *et al*., 2011). Furthermore, studies from uranium tailings in other regions of the world are of limited use in understanding microbial effects on tailings stability in northern Saskatchewan since the ore mined, the uranium extraction process and the geochemical controls of the tailings all tend to be unique,and when combined with environmental factors, makes correlations difficult.

This thesis research was undertaken to obtain early (e.g., within the first few decades after commissioning) insights into the potential geomicrobiological processes that might become important within the DTMF uranium tailings deposition site over extended periods of time, on

the order of thousands of years. The overall objective of this study was to characterize microbial diversity at three zones (the water column, water-tailings interface and tailings mass) of the DTMF, their potential functional roles, and their potential to alter the Eh and ferrihydrite, which are the primary controlling conditions and secondary phase, respectively within the DTMF tailings. To achieve these objectives, two molecular techniques (clone library construction and Ion Torrent sequencing), a range of conventional culture-based techniques, different metabolic assays addressing metabolic transformation and resistance to metals/metalloids, microscopic (CLSM) and spectroscopic (STXM) analyses, and bench-scale microcosm assays were executed.

My first study provided insight into biogeochemical potential of the microbial communities of biofilms grown *in situ* at four depths (at 13 m interval) in the water column overlying the DTMF uranium tailings. Chemical analyses of the biofilms grown at different depths revealed that Fe concentration accumulated in the biofilm in parallel with that of the dissolved Fe in the water column. Biofilm microbial diversity analyses using Ion Torrent next generation sequencing showed that biofilms developed at 13 m and 27 m in the water column had the highest microbial diversity in terms of number of genera detected, containing over 100 different microbial genera. Furthermore, the most abundant microbial populations were closely related to methylotrophs, as well as bacterial groups that are known to utilize complex hydrocarbons. Phylotypes closely related to iron reducing bacteria, (e.g., *Ralstonia*) were detected in low numbers in biofilms grown at all depths and bacterial groups that can use sulphate, thiosulphate or suphite as electron acceptor were found in biofilms from lower depths of the water column. Synchrotron-based analyses revealed the presence of reduced iron within biofilms grown at various depths. Accumulation of Fe as well as the presence of Fe (II) within the biofilm matrix surrounding bacterial cells has previously been detected and the effect of

microbes on the geochemical cycling of Fe has been recognized in various systems (Ferris *et al.*, 1989; Boult *et al*., 1997). The nature of microbial communities within biofilms indicates that complex hydrocarbons discharged into the tailings can potentially support microbial processes that involve Fe and S biogeochemical cycling in the water column covering the tailings mass. Investigation of the *in situ* grown biofilms also revealed that strict anaerobic conditions are not required for iron reduction in the DTMF system.

The number of coupons that could be installed in the DTMF for *in situ* biofilm development was limited to one site and one time period, limiting my ability to draw an overall conclusion as to whether the characteristic of biofilms, as well as microbial diversity, would vary spatially and temporarily within the DTMF water column. Characterization of biofilms developed at multiple sites and in different years and their correlation with physicochemical measurements of the water would confirm the likelihood of biofilms being an integrative indicator of system's chemistry. Furthermore, these types of temporal data would allow us to better understand and identify factors that can potentially influence biogeochemical processes within in the water column.

The tailings-water interface of a tailings system, in general, is considered a dynamic zone characterized by steep gradients of oxygen, a primary accumulation site for carbon source from the surrounding environment and a location where microbial abundance and activity could potentially be high. Therefore, the objective of the second study was to characterize microbial diversity and reductive metabolic processes at the water-tailings interface, the next zone of the DTMF, and to compare this tailings-impacted site to a nearby, unimpacted reference lake. The total bacterial cell counts in the DTMF interface was higher than the reference lake, and also higher than another tailings management site (Rabbit Lake) in the northern Saskatchewan region.

These elevated cell counts could be explained by the higher concentration of carbon present in the DTMF as a consequence of complex hydrocarbons (e.g., kerosene) used for uranium processing and carbon sources transported from the surrounding environment. *β- γ-Proteobacteria* and *Firmicutes* were proportionally the most abundant culturable bacterial taxa in the DTMF. These bacterial groups, in general, are resistant to unfavorable conditions, such as high concentration of heavy metals and are considered as complex hydrocarbon degraders (Bowers *et al*., 2009). Ion Torrent sequence analyses identified *Desulfosporosinus* as the most predominant genus from the *Firmicutes* in the DTMF. *Desulfosporsinus* spp. are strict anaerobes, capable of sufate/iron reduction and have previously been shown to dominate radionucleotide-contaminated subsurface sediments (Suzuki *et al*., 2002; Senko *et al*., 2009; Bertel *et al*., 2011). Comparative analyses of bacterial diversity in the DTMF and reference lake indicated that the tailings-water interface harboured a specialized group of bacteria potentially selected by physiochemical characteristics (e.g., high heavy metal concentration, alkaline pH) of the DTMF site. The results of this characterization signify biogeochemical potential, such as metal reduction, of the microbial communities that have been, and continue to be, incorporated into the tailings mass.

A limitation of this work was the lack of an understanding of the conditions required for the survival of sulfate reducing bacteria, such as *Desulfosporosinus*, that are native to this highly alkaline uranium waste management site. It was initially reflected by the difference in abundance of this microorganism as determined by culture-based methods and DNA sequence analysis. This kind of observation is not uncommon phenomena in microbial diversity studies; however, further efforts are required to understand factors influencing the culturability and viability of this microorganism. Isolation and characterization of *Desulfosporosinu*s spp. would help us to better

understand its potential to proliferate under the metal-rich and highly oxic conditions prevalent in the DTMF tailings, and more importantly, its potential to influence the system's biogeochemistry.

The objective of the third study was to describe the diversity and metabolic potential of microbial communities present in the low permeability DTMF tailings mass. Core sampling through the tailings vertical profile (~60 m thick) was conducted in order to isolate and characterize the microbes present. Bacterial isolates retrieved from the tailings were affiliated into four phyla: *Proteobacteria*, *Actinobacteria, Firmicutes* and *Bacteriodetes*. Similar phyla were detected in the DTMF water column and at the water-tailings interface using culture-based methods. The majority of the representative isolates exhibited tolerance to elevated metal and metalloid salts concentrations. A high proportion of the isolates were multiple-metal-resistant with some demonstrating extreme tolerance to As (V) and Se (IV). A correlation between enzyme activity profile and metal resistance showed that multiple-metal-resistant isolates tended to express a broader range of enzymatic potential than organisms resistant to fewer metals. Heterotrophs retrieved through conventional culturing techniques could reduce iron and molybdate, and oxidize arsenite.

Sequence-based analyses of three libraries representing composited DNA extracted from the upper, middle and lower regions of the DTMF captured 21 different phyla. The readily culturable bacterial isolates (e.g., *Pseudomonas*, *Arthrobacter*, *Massilia*, *Hydrogenophaga*, *Polaromonas*, *Bacillus*) which exhibited high degree of tolerance to metal/metalloids or reducing/oxidizing capabilities were also consistently detected in the sequenced DNA libraries. Microcosm studies have previously shown that *Pseudomonas* and *Massilia* spp. can reduce iron in uranium and heavy metal-contaminated sediment (Nevin *et al*., 2003; Hu *et al*., 2014).

Phylotypes closely related to well-characterized sulfate-, thiosulfate- and iron-reducing bacteria (e.g., *Desulfosporosinus*, *Dethiobacter*, *Geoalkalibacter*, *Ralstonia*, *Georgfuchsia*) were also detected, however at low frequencies. These genera have previously been observed at uranium-, heavy metal- and complex hydrocarbon-contaminated sites (Sitte *et al*., 2010; Rastogi *et al*., 2011). It is important to note that some members of iron reducers, such as *Geoalkalibacter*, *Georgfuchsia,* are strict anaerobes that are capable of linking aromatic compound degradation to Fe (III) reduction (Greene, *et al*., 2009; Weelink *et al*., 2009). Bioremediation studies of contaminated sites have previously shown that these bacterial groups could become numerically and functionally significant in response to carbon amendments, resulting in reductive dissolution (Vrionis *et al*., 2005). Characterization of microbial diversity using multiple approaches and functional potential of the culturable bacterial population strongly indicate that the DTMF tailings support the growth of a diverse microbial community consisting of microbial populations capable of redox metabolic processes that could become significant over extended period of times.

The major limitation of this study was the effect of pooling DNA extracted from 60 core samples into three major DNA libraries, a process carried out to decrease the overall cost of the analyses. Pooling reduced the number of samples, but at the same time could potentially mask, or dilute, members of the microbial community. Therefore, some bacterial populations could potentially be locally abundant, but these zones could be spatially rare, rendering them as low-frequency phylotypes in the pooled samples.

Microbial diversity in all three zones (water column, tailings-water interface and tailings body) was estimated based on the number of genera identified. Microbial communities were compared using UniFrac distance metric incorporating information on the phylogenetic distance

of comunities members. The average length of the amplified DNA sequence reads was approximately100 bp allowing only genus level identification; therefore taxonomic operational unit clustering was not utilized for ecological metrics calculation. Consequently, ecological metrics for microbial species richness, diversity and quantification, which have been widely used to understand structure, function and evolution of microbial communities (Haegeman *et al*., 2013), could not be applied in this study. Similarly, rarefaction curves are used to compare species richness between communities was not calculated. It has been previously pointed out that rare species affect estimation of species richness (Mao and Colwell, 2005). Shannon and Simpson diversity metrics, which are indices that combine richness and evenness, may also being used to quantify and compare microbial diversity (Haegeman *et al*., 2013). Longer DNA sequence reads would have enabled these more detailed ecological analyses to have been incorporated into my study.

The objective of the fourth study was to investigate the effect of stimulating microbial activity on the redox potential of the tailings as well as on the state of ferrihydrite, which are the primary controlling condition and mineral phase, respectively, within the tailings. A series of microcosm assays were performed where samples from the tailings-water interface of the tailings deposition site were inoculated with indigenous flora previously isolated from the tailings sediment, enriched with nutrients (50 ppm tryptic soy broth), and incubated under continuously flowing or intermittently flowing conditions, and compared with an uninoculated, no-carbon continuously flowing control. Highly reducing conditions with redox potentials of less than -300 mV were detected within the enriched tailings microcosms. In contrast, the redox conditions in the no-carbon control microcosm never dropped below -93 mV; thus, it was clear that carbon-enhanced microbial activity drove the Eh conditions to become highly reducing. The occurrence

of highly reducing redox conditions was concomitant with the detection of Fe (II) in the effluent of carbon-enriched microcosms.

STXM analyses also revealed the presence of reduced iron, typically observed in close proximity to distinct bacterial cells, indicating that oxidized iron possibly served as an electron acceptor during microbial processes. The most abundant identified phylotypes present within all microcosms were complex carbon degraders (e.g., *Hydrogenophaga*, *Malikia*, *Polaromonas*, *Acidovorax*, *Brevundimonas* and *Pseudomonas*). These microorganisms were abundant in the water column as well as in the tailings mass, which suggests that the carbon source (e.g., kerosene) originally present in the tailings plays an important role favouring complex hydrocarbon degraders. The presence of reduced iron and strictly anaerobic bacteria in all the treated microcosms strongly indicate that the complex hydrocarbon degrading heterotrophs, indigenous to the DTMF tailings, have the potential to couple metabolic processes to iron reduction and can potentially create (highly reducing) conditions amenable to the growth of strict anaerobic bacteria, such as sulphate- and iron-reducing bacteria. Similar studies have shown that the activity (e.g., iron reduction) and growth of strictly anaerobic bacteria can be stimulated by aerobic or facultative heterotrophs (Straub and Schink *et al*., 2004; Aburto *et al*., 2009).

Thus, the microcosm study revealed that a heterotrophic bacterial community native to the DTMF tailings could create highly reducing conditions within the tailings favourable for the proliferation of strict anaerobic sulfate reducing bacteria. The relatively high heterotrophic bacterial cell counts (reaching $2.2 \times 10^8$ cfu/g wet tailings) detected at some depths within the tailings body strongly indicate that heterotrophic biogeochemical processes primarily induced by available carbon can occur within the DTMF tailings.

One of the limitations of the microcosm assay was the limited amount of tailings that was available for the assay, which prevented extensive biological or technical experimental replication. The microcosm effluent was subjected to periodic culturing and chemical testing for reduced form of iron; however, chemical and DNA sequence analyses of the tailings samples at various time points would have helped us to define the exact conditions that supported *Desulfosporosinus* spp proliferation. More tailings material would have aided in conducting these analyses. Furthermore, monitoring ferrihydrite phase transformation using X-ray diffraction, as well as Micro-Raman spectroscopic analyses, would have confirmed secondary phase formation due to microbial processes. Furthermore, to monitor arsenic redox species present within the effluent in timely manner would have been very useful to confirm fate of arsenic during ferrihydrite reductive dissolution within the tailings.

A significant proportion of the heterotrophic bacteria retrieved from the DTMF were potentially novel species. In order to better understand their potential function, two of these isolates, which were consistently recovered at high frequencies in the DTMF, were subjected to full taxonomic characterization. One of the limitations of this study was that the genus *Polaromonas* is comprised of only seven species and that the general information regarding substrate utilization and enzymatic potential of previously reported *Polaromonas* spp. is quite limited. Furthermore, the whole genome sequence was available only for two species; therefore, targeting and amplification of housekeeping genes was difficult and for some genes, unsuccessful. In addition, selection of consensus region for primer annealing becomes less effective when only two sequences are available for the sequence alignment. From the characterization work, it was found that both isolates were affiliated with the genus *Polaromonas*. Complete genome sequencing of these isolates would have provided more

evidence to support taxonomic affiliation. Furthermore, identification of catabolic genes would further aid in the understanding and prediction of metabolic function of these microorganisms within the DTMF.

## 7.2 Conclusions and future prospects

(based on a conceptual ordering of the thesis "arranged from water to interface to tailings body")

1. Biofilms in the water column overlying the DTMF tailings mass are key components that reflect the water chemistry, type of carbon utilized for bacterial growth, and biogeochemical processes.
2. Iron is reduced likely due to microbial processes in distinct microenvironments within biofilm aggregates that can grow in the DTMF water column.
3. Tailings-water interface harbors a distinct microbial community in comparison to a nearby reference lake.
4. Abundance of *Desulfosporosinus* at the tailings-water interface strongly indicates the potential for reductive metabolic processes, such as sulfate or iron reduction, to occur at the interface zone.
5. The DTMF tailings support the growth of a diverse microbial community.
6. Microbial diversity changed with depth within the tailings body and could primarily be attributed to the difference of geochemical composition of the ore material utilized for uranium extraction.
7. Readily culturable heterotrophs, also observed in high frequency in the sequence libraries, exhibited a high-degree of metal resistance as well as the ability to redox-

transform metal elements. This strongly suggests that the microbial community present in the DTMF has the potential to influence the long-term geochemistry of the tailings.

8. Iron- and sulfate-reducing bacteria were detected in low frequencies within the DTMF tailings body.
9. Heterotrophic bacterial communities native to the DTMF are capable of creating highly reducing conditions amenable to the growth of strict anaerobic sulfate reducing bacteria; therefore, metabolic processes by the heterotrophs could become increasingly important over extended period of time.
10. The isolates selected for taxonomic characterization are novel species.

The DTMF tailings are rich in iron and sulfate, and in terms of microbial diversity, it was initially presumed that the well-known iron and sulphate reducing bacteria would be abundant in this system. My research studies at this site revealed that the microbial communities present in the DTMF mainly consisted of complex hydrocarbon degraders and the well-characterized sulphate/iron reducers that, in general, were low in frequency except at the tailings-water interface where phylotypes closely related to *Desulfosporosinus* were shown to be abundant. Furthermore, members of these bacterial groups have the potential to directly or indirectly cause reductive dissolution of iron, thereby influencing the long-term geochemistry of the tailings.

At the same time, these initial investigations have generated many more hypotheses that should be followed up in future studies. For example, the fact that phylotypes closely related to *Desulfosporosinus* were low in number throughout the tailings body strongly suggests that the interface may have only temporarily served as a favourable location for the proliferation of these strict anaerobic bacteria and that conditions become more inhibitory (i.e., highly oxic) for these organisms as they are incorporated within the tailings mass. This would not be surprising

because the tailings-water zone is the primary site for carbon source accumulation from the surrounding environment, possibly resulting in activated heterotrophic bacterial activity creating local reducing environment suitable for the proliferation of sulfate reducing bacteria. Alternatively, another hypothesis is that dissimilatory sulfate reducing bacteria proliferate at the tailings-water interface and could become only temporarily inhibited as they are integrated into the tailings. Members of this bacterial group are spore-forming obligate anaerobes and have the potential to survive and then proliferate when the conditions become favourable. The microcosm assays indicated that by enhancing heterotrophic bacterial activity, *Desulfosporosinus* spp. can become more abundant. Furthermore, the relatively high heterotrophic bacterial cell counts (reaching 2.2 X $10^8$ cfu/g wet tailings) detected at some depths could establish reducing conditions similar to those observed in the bench-scale microcosm assays. Therefore, it is not unlikely that there are already zones, or such zones would develop with time, where these microorganisms become abundant within the tailings body, as demonstrated in my microcosm assay. Such niches throughout the tailings body could be spatially rare, and the local chemical measurability (e.g., reducing condition) or visual characteristic (e.g., black color, which is an indication of biogenic magnetite formation) difficult to detect, because these potential geochemical changes could be buffered by the large tailings mass.

In order to delineate fate of sulfate reducing bacteria and their biogeochemical effect within the tailings body, this microbial population must be re-identified within *in situ* samples, isolated and then subjected to controlled conditions prevalent in the tailings mass. Growth, metabolism and biogeochemical processes of these microorganisms should be investigated within the tailings in the absence, as well as in the context, of other native microbial flora. Growth of *Desulfosporsinus* spp. could be monitored by using culture-based method

(enrichment/selective media) and real time PCR, targeting specific functional genes. Active microorganisms that may potentially take part in biogeochemical processes of interest could be monitored through, RNA-based sequence libraries construction. Direct comparison of the DNA data derived from the total genomic and from RNA sequence data could provide insight into whether the most abundant microbial species correspond with the active microbial population potentially involved in the biogeochemical processes. These sequence-based examinations may allow us to identify *Desulfosporosinus* ssp. and other active microorganisms with targetable specific functions, such as Fe (III) reduction. To detect biogeochemical processes, such as phase transformations, X-ray diffraction as well as Micro-Raman spectroscopic analyses, could be carried out on initial and final (microbially reacted) solids.

Overall, from my research studies it can be concluded that bacterial communities native to the DTMF have the potential to introduce redox changes within the tailings system; however, a major challenge still remains to extrapolate an estimate of their overall contribution to biogeochemical processes within the tailings. There is still a need to identify the group of hydrocarbon degraders that can most effectively utilize the site-relevant carbon sources and relate it to biogeochemical processes. Of particular interest would be kerosene (complex hydrocarbon used during uranium extraction) in the fresh tailings, water column, and aged tailings, from the DTMF in relation to iron reductive dissolution rates under conditions of interest to the DTMF (e.g., temperature, pH, liable carbon supply). Stable isotope probing (SIP) is a powerful method for characterizing microbial activity (Chen and Murrel, 2010). In order to identify the microbial populations, including the less-abundant species, that utilize kerosene as carbon source, samples containing complex *in situ* microbial community could be exposed to $^{13}C$

labeled kerosene combined with large-scale sequencing of the isotope containing DNA sequence fraction.

My thesis research project and the proposed research directions would serve as an excellent opportunity to develop models of biogeochemical potential that could be coupled with geochemical models for a more accurate prediction of long-term stability of the DTMF.

# 8 REFERENCES


Abdelouas, A. (2006) Uranium Mill Tailings: Geochemistry, mineralogy, and environmental impact. *Elements* 2, 335-341.

Aburto, A. and Ball, A.S (2009) Bacterial population dynamics and separation of active degraders by stable isotope probing during benzene degradation in BTEX-impacted aquifer. *Rev. Int. Contam. Ambient.* 25, 147-156.

Aburto, A., Fahy, A., Coulon, F., Lethbridge, G., Timmis, K.N., Ball, A.S. and McGenity, T.J. (2009) Mixed aerobic and anaerobic microbial communities in benzene-contaminated groundwater. *J. Appl. Microbiol*. 106, 317-328.

Akob, D.M., Mills, H.J. and Kostka, J.E. (2007) Metabolically active microbial communities in uranium-contaminated subsurface sediments. *FEMS Microbiol. Ecol.* 59, 95-107.

Al-Hashimi, A., Evans, G. J. and Cox, B. (1996) Aspects of the permanent storage of uranium tailings. *Water Air and Soil Poll.* 88, 83-92

Amann, R.I., Binder, B.J., Olson, R.J., Chilsholm, S.W., Devereux, R. and Stahl, D.A. (1990). Combination of 16S rRNA –targeted oligonucleotide probes with flow cytometry for analyzing mixed microbial populations. *Appl. Environ. Microbiol.* 56,1919-1925.

Amann, R.I., Ludwig, W. and Schleifer, K.H. (1995) Phylogenetic identification and *in situ* detection of individual microbial cells without cultivation. *Microbiol. Rev*. 1, 143-169.

Ancion, P-Y., Lear, G., Dopheide, A. and Gillian, D.L. (2013) Metal concentrations in stream biofilm and sediments and their potential to explain biofilm microbial community structure. *Environ. Pollut.* 173, 117-124.

Anderson, R.T., Vrionis, H.A., Ortiz-Bernad, I., Resch, C.T., Long, P.E., Dayvault, R., Karp, K., Marutzky, S. *et al*. (2003) Stimulating the *in situ* activity of *Geobacter* species to remove uranium from the groundwater of a uranium-contaminated aquifer. *Appl. Environ. Microbiol.* 69, 5884-5891.

Azam, S., Khaled, S.M., Kotzer, T. and Mittal, H.K. (2014) Geotechnical performance of a uranium tailings containment facility at Key Lake, Saskatchewan. *Int. J. Min. Reclam. Environ*. 28, 103-117.

Aziz, H. A, Adlan, M.N. and Ariffin, K.S. (2008) Heavy metals (Cd, Pb, Zn, Ni, Cu, and Cr (III)) removal from water in Malaysia: Post treatment by high quality limestone. *Bioresor. Technol.* 99, 1578-1583.

Baker, G.C., Smith, J.J. and Cowan, D.A. (2003) Review and re-analysis of domain-specific 16S primers. *J. Microbiol. Methods* 55, 541-555.

Beelen, T.P.M., Shi, W., Morrison, G.R., van Garderen, H.F., Browne, M.T., van Santen, R.A. and Pantos, E. (1997) Scanning transmission X-ray Microscopy: A new method for the investigation of aggregation in silica. *J. Colloid. Interface. Sci.* 185, 217-227.

Behrens, S., Kappler, S. and Obst, M. (2012) Linking environmental processes to the *in situ* functioning of microorganism by high-resolution secondary ion mass spectrometry (NanoSIMS) and scanning transmission X-ray microscopy (STXM). *Environ. Microbiol*. 14, 2851-2869.

Benedetto, J.S., de Almeida, S.K., Gomes, H.A., Vazoller, R.F. and Ladeira, A.C.Q. (2005) Monitoring of sulfate-reducing bacteria in acid water from uranium mines. *Miner. Eng*.18, 1341-1343.

Benyehuda, G., Coombs, J., Ward, P.L., Balkwill, D. and Barkary, T. (2003) Metal resistance among aerobic chemoheterotrophic bacteria from the deep terrestrial subsurface. *Can. J. Microbiol*. 49, 151-156.

Bertel, D., Peck, J., Quick, T.J. and Senko, J.M. (2011) Iron transformation induced by an acid-tolerant *Desulfosporosinus* species. *Appl. Environ. Microbiol*. 78, 81-88.

Bethke, C.M., Sanford, R.A., Kirk, M.F., Jin, Q. and Flynn, T.M. (2011) The thermodynamic ladder in geomicrobiology. *Am. J. Sci.* 311, 183-210.

Binning, G., Rohrer, H., Gerber, C., Weibel, E. (1982) Surface studies by scanning tunnelling microscopy. *Phys. Rev. Lett.* 49, 57-61.

Bondici, V.F., Khan, N.H., Swerhone, G.D.W., Dynes, J.J., Lawrence, J.R., Yergeau, E., Wolfaardt, G.M., Warner, J. and D.R. Korber. (2014) Biogeochemical activity in microbial biofilms obtained from uranium mine tailings covering water *J. Appl. Microbiol.* 117, 1074-1094.

Bondici, V.F., Lawrence, J.R., Khan, N.H., Hill, J.E., Yergeau, E., Wolfaardt, G.M., Warner, J. and D.R. Korber. (2013) Microbial communities in low permeability, high pH uranium mine tailings: characterization and potential effects. *J. Appl. Microbiol.* 114, 1671-1686.

Bonfield, J.K., Smith, K.F. and Staden, R. (1995) A new DNA sequence assembly program. *Nucleic Acids Res.* 23, 4992–4999.

Borch, T., Masue, Y., Kukkadapu, R.K. and Fendorf, S. (2007) Phosphate imposed limitations on biological reduction and alteration of ferrihydrite. *Environ. Sci. Technol*. 41, 166-172.

Boult, S., Johnson, N. and Curtis, C. (1997) Recognition of a biofilm at the sediment–water interface of an acid mine drainage-contaminated stream, and its role in controlling iron flux. *Hydrol. Process* 11, 391- 399.

Bowers, K.J., Mesbah, N.M. and J. Wiegel. 2009. Biodiversity of poly extremophilic *Bacteria*: Does combining the extremes of high salt, alkaline pH and elevated temperature approach a physico-chemical boundary for life? *Saline Syst.* 5, 1-8.

Brannon, J.M. (1987) Fixation, transformation and mobilization of arsenic in sediments. *Environ. Sci. Technol*. 21, 450-459.

Brown, D.A., Kamineni, D.C., Sawicki, J.A. and Beveridge, T.J. (1994) Minerals associated with biofilms occurring on exposed rock in a granitic underground research laboratory. *Appl. Environ. Microbiol.* 60, 3182-3191.

Burke, I.T., Mortimer, R.J.G., Palaniyandi, S., Whittleston, R.A., Lockwood, C.L., Ashley, D.J. and Stewart, D.I. (2012) Biogeochemical reduction processes in a hyper-alkaline leachate affected soil profile. *Geomicrobiol. J.* 29, 769-779.

Burkhardt, E.M., Akob, D.M., Bischoff, S., Sitte, S., Kostka, J.O., Banerjee, D., Scheinost, A.C. and Kusel, K. (2010) Impact of biostimulated redox processes on metal dynamics in an iron-rich creek soil of a former uranium mining area. *Environ. Sci. Technol.* 44, 177–183.

Burland, S.M. and Edwards, E.A. (1999) Anaerobic benzene biodegradation linked to nitrate reduction. *Appl. Environ. Microbiol.* 65, 529-533.

Burnol, A., Garrido, F., Baranger, P., Joulian, C., Dictor, M-C., Bodénan, F., Morin, G. and Charlet, L. (2007) Decoupling of arsenic and iron release from ferrihydrite suspension under reducing conditions: a biogeochemical model. *Geochem. Transact.* 8, 1-18.

Burton, G. A. Jr., Giddings, T.H., DeBrine, P. and Fall, R. (1987) High incidence of selenite-resistant bacteria from a site polluted with selenium. *Appl. Environ. Microbiol.* 53, 185-188.

Caldwell, D.E., Korber D.R. and Lawrence, J.R. (1992) Imaging of bacterial cells by fluorescence exclusion using scanning confocal laser microscopy. *J. Microbiol. Methods* 15: 249-261.

Caldwell, M.E. and Suflita, J.M. (2000) Detection of phenol and benzoate as intermediates of anaerobic benzene biodegradation under terminal electron-accepting conditions. *Environ. Sci. Technol.* 34, 1216-1220.

Calmano, W., Hong, J. and Forstner, U. (2003) Heavy metals in contaminated sediments affected by pH and redox potential. *Water Sci. Technol.* 28, 223-235.

Cameco Corporation. (2009) Mining: uranium operations; Saskatoon, Saskatchewan.

Cameco Corporation. (2011) Mining: uranium operations; Saskatoon, Saskatchewan.

Cameco, Key Lake extension project. Project description: Safety, health environment and quality (2010).

Cameco, Key Lake Operation-Deilmann Tailings Management Facility tailings investigation and monitor well construction (2009).

Camus, H., Little, R., Acton, D., Aguero, A., Chambers, D., Chamney, L., Daroussin, J.L., Droppo, J., Ferry, C., Gnanapragasam, E., Hallam, C., Horyna, J., Lush, D., Stammose, D., Takahashi, T., Toro, L. and Yu, C. (1998) Long-term contaminant migration and impacts from uranium mill tailings. *J. Environ. Radioact.* 42, 289-304.

Cardenas, E., Wu, W.M., Leigh, M.B., Carley, J., Carroll, S., Gentry, T., Luo, J., Watson, D., Gu, B., Vogel-Ginder, M., Kitanidis, K.P., et al. (2008) Micorbial communities in contaminated sediments, associated with bioremediation of uranium submicromolar levels. *Appl. Environ. Microbiol.* 75, 3718-3729.

Case, R.J., Boucher, Y., Dahllof, I., Holmstrom, C., Doolittle, W.F. and Kjelleberg, S. (2007) Use of 16S r RNA and *rpoB* genes as molecular markers for microbial ecology studies. *Appl. Environ. Microbiol.* 73, 278-288.

Casiot, C., Morin, G., Juillot, F., Bruneel, O., Personne, J.C., Leblanc, M., Duquesne, K., Bonnefoy, V. and Elbaz-Poulichet, F. (2003) Bacterial immobilization and oxidation of arsenic in acid mine drainage (Carnoules creek, France). *Water Res.* 37, 2929-2936.

Catallo, W.J. (1999) Hourly and daily variation of sediments redox potential in tidal wetland sediments. U.S. geological survey, Biological Resource Division Biological Science Report USGS/BRD/BSR-1999-0001, pp.1-10.

Chabalala, S. and Chirwa E.M.N. (2010) Removal of uranium(VI) under aerobic and anaerobic conditions using an indigenous mine consortium. *Miner. Eng.* 23, 526–53.

Chaban, B., Links, M.G., Paramel Jayaprakash, T., Wagner, E.C., Bourque, D.K. et al. (2014) Characterization of the vaginal microbiota of healthy Canadian women through the menstrual cycle. Microbiome 2, 1-12.

Chakraborty, R., O'Connor, S.M., Chan, E. and Coates, J.D. (2005) Anaerobic degradation of benzene, toluene, ethylbenzene, and xylene, compounds by *Dechloromonas* strain RBC. *Appl. Environ. Microbiol.* 71, 8649-8655.

Champ, D.R., Gulens, J., and Jakson, R.E. (1979). Oxidation-reduction sequences in ground water flow systems. *Can. J. Earth. Sci.* 16, 12-23.

Chang, J-S., Yoon, I-H., Lee, J-H., Kim, K-R., An, J. and Kim, K-W. (2010) Arsenic detoxification potential of *aox* genes in arsenite-oxidizing bacteria isolated form natural and constructed wetlands in the Republic of Korea. *Environ. Geochem. Health* 32, 95-105.

Chao, T.T. and Theobald, P.K. (1976) The significance of secondary iron and manganese oxides in geochemical exploration. *Econ. Geol.* 71, 1560-1569.

Chatain, V., Bayard, R., Sanchez, F., Moszkowicz, P. and Gourdon R. (2005) Effect of indigenous bacterial activity on arsenic mobilization under anaerobic conditions. *Environ. Int.* 31, 221-226.

Chen, C., Dynes, J.J., Wang, J., Karunakaran, C. and Sparks, D.L. (2014) Soft X-ray spectromicroscopy study of mineral-organic matter associations in pasture soil clay fractions. *Environ. Sci. Technol.* 40, 6678-6686.

Chen, W.M., Cho, N.T., Yang, S.H., Arun, A.B., Young, C.C. and Sheu, S.Y. (2012) *Aquabacterium limnoticum* sp. nov., isolated from a freshwater spring. *Int. J. Syst. Bacteriol.* 62, 698-704.

Chen, Y. and Murrel, J.C. (2010) When metagenomics meets stable-isotope probing: progress and perspectives. *Trends Microbiol.* 18, 157-163.

Chistoserdova, L. (2011) Methylotrophy in a lake: from metagenomics to single organism physiology. *Appl. Environ. Microbiol*. 77, 4705-4711.

Cho, K., Zholi, A., Frabutt, D., Flood, M., Floyd, D. and Tiquia, S.M. (2012) Linking bacterial diversity and geochemistry of uranium-contaminated groundwater. *Environ. Technol.* 33, 1629–1640.

Choudhary, S. and Sar, P. (2009) Characterization of a metal resistant *Pseudomonas* sp. isolated from uranium mine for its potential in heavy meta ($Ni^{+2}$, $Co^{+2}$, and $Cd^{+2}$) sequestration. *Bioresour. Technol.* 100, 2482-2492.

Chuan, M.C, Shu, G.Y. and Liu, J.C. (1995) Solubility of heavy metals in a contaminated soil: effects of redox potential and pH. *Water Air Soil Pollu.* 90, 543-556.

Claxton, N.S., Fellers, T.J. and Davidson, M.W. (2005) *Laser scanning confocal microscopy*, Department of Optical Microscopy and Digital Imaging, National High Magnetic Field Laboratory, Florida State University, (http://www.olympusfluoview.com/theory/LSCMIntro.pdf)

Cole, J.R., Wang, Q., Cardenas, E., Fish, J., Chai, B., Farris, R.J., Kulam-Syed-Mohideen, A.S., McGarrell, D.M., Marsh, T., Garrity, G.M. and Tiedje, J.M. (2009) The Ribosomal Database Project: improved alignments and new tools for rRNA analysis. *Nucleic Acids Res.* 37 (Database issue): D141-D145; doi: 10.1093/nar/gkn879.

Costerton, J.W. and Lewandowski, Z. (1995) Microbial biofilms. *Annu. Rev. Microbiol.* 49, 711-45.

Costerton, J.W., Lewandowski, Z., Debeer, D., Caldwell, D.E., Korber, D.R. and James, G. (1994) Biofilms, the customized microniche. *J. Bacteriol*. 176, 2137-2142.

Cramer, S.P. and Hodgson, K.O. (1979) X-ray absorption spectroscopy: a new structural method and its applications to bioinorganic. *Prog. Inorg. Chem*. 25, 1-39.

Dahllof, I., Baillie, H. and Kjelleberg, S. (2000) *rpoB*-based microbial community analysis avoids limitations inherent in 16S rRNA gene intraspecies heterogeneity. *Appl. Environ. Microbiol*. 66, 3376-3380.

Darcy, J.L., Lynch, R.C., King, A.J., Robeson, M.S. and Schmidt, S.K. (2011) Global distribution of *Polaromonas* phylotypes-evidence for highly successful dispersal capacity. *PLoS One* 6, e23742.

Davey, M.E. and O'toole, G.A. (2000) Microbial biofilms: from ecology to molecular genetics. *Microbiol. Mol. Bio. Rev.* 64, 847-67.

Davis, K.E.R., Joseph, S.J. and Janssen, P.H. (2005) Effects of growth medium, inoculum size and incubation time on culturability and isolation of soil bacteria. *Appl. Environ. Microbiol.* 71, 826-834.

De Souza, M.J., Loka Bharathi, P.A., Nair, S. and Chandramohan, D. (2007) "Trade-off" in Antarctic bacteria: limnetic psychrotrophs concede multiple enzyme expression for multiple metal resistance. *Biomet.* 20, 821-828.

Decho, A.W. (1990) Microbial exopolymer secretions in ocean environments: their role(s) in food webs and marine processes. *Oceanogr. Mar. Biol. Annu. Rev*. 28, 73-153.

Decho, A.W. (2000) Microbial biofilms in intertidal systems: an overview. *Continent. Shelf Research* 20, 1257-1273.

Delaune, R.D. and Reddy, K.R. (2005) Redox potential. In encyclopedia of soils in the environment. D. Hillel (ed). Academic Press. pp. 336-371.

Dhal, P.K. and Sar, P. (2014) Microbial communities in uranium mine tailings and mine water sediment from Jaduguda U mine, India: A culture independent analysis. *J. Environ. Health.* 49, 694-709.

Dhal, P.K., Islam, E., Kazy, S.K. and Sar, P. (2011) Culture-independent molecular analysis of bacterial diversity in uranium-ore/-mine waste-contaminated and non-contaminated sites from uranium mines. *Biotech*. 1, 261-272.

Dib, J.R., Annika, W., Neumann, A., Ordonez, O., Estevez , M.C., and Farias, M.E. (2009) Isolation of bacteria from remote high altitude Andean Lakes able to grow in the presence of antibiotics. *Recent Patents Anti-Infective Drug Discov.* 4, 66-76.

Dixit, S. and Hering, J.G. (2003) Comparison of arsenic(V) and arsenic(III) sorption onto iron oxide minerals: implication for arsenic mobility. *Environ. Sci. Technol*. 37, 4182-4189.

Donachie, S.P, Foster, J.S. and. Brown, M.V. (2007) Culture clash: challenging the dogma of microbial diversity. *ISME* 1, 97-102.

Donachie, S.P., Hou, S., Lee, K.S., Riley, C.W., Pikina, A., Belisle, C., Kempe, S., Gregory, T.S., Bossuyt, A., Boerema, J., Liu, J., Freitas, T.A., Malahoff, A. and Alam, M. (2003) The Hawaiian Archipelago: A microbial diversity hotspot. *Microb. Ecol.* 48, 509-520.

Donahue, R., Hendry, M.J. and Landine, P. (2000) Distribution of arsenic and nickel in uranium mill tailings, Rabbit Lake, Saskatchewan, Canada. *Appl. Geochem.* 15, 1097-1119.

Dong, D., Nelson, Y.M., Lion, L.W., Shuler, M.L. and Ghiorse, W.C. (2000) Adsorption of Pb and Cd onto metal oxides and organic material in natural surface coatings as determined by selective extractions: new evidence for the importance of Mn and Fe oxides. *Water Res.* 34, 427-436.

Drewniak, L., Styczek, A., Majder-Lopatka, M. and Sklodowska, A. (2008) Bacteria, hypertolerance to arsenic in the rocks on an ancient gold mine, and their potential role in dissemination of arsenic pollution. *Environ. Pollut.* 156, 1069-1074.

Duckworth, A.W., Grant, W.D., Jones, B.E. and van Steenbergen, R. (1996) Phylogenetic diversity of soda lake alkaliphiles. *FEMS Microbiol. Ecol.* 19, 181–191.

Dughan-Essilfie, J., Pickering, I.J., Hendry, M.J., George, G.N. and Kotzer, T. (2011) Molybdenum speciation in uranium mine tailings using X-ray absorption spectroscopy. *Environ. Sci. Technol.* 45, 455-460.

Dunlap, L. and Beckmann, D. (1988) Soluble hydrocarbon analysis from kerosene/diesel. Proceedings of the Conference on Petroleum hydrocarbons and Organic Chemicals in Groundwater: Prevention Detection and Restoration. Dublin, Ohio: National Water Well Association.

Dynes, J.J., Tyliszcsak, T., Araki, T., Lawrence, J.R., Swerhone, G.D.W., Leppard, G.G. and Hitchcock, A.P. (2006) Speciation and quantitative mapping of metal species in microbial biofilms using Scanning Transmission X-ray Microscopy. *Environ. Sci. Technol.* 40, 1556-1565.

Eggleton, R.A. and Fitzpatrick, R.W. (1988) New data and a revised structural model for ferrihydrite. *Clays and Clay Minerals*. 36, 111-124.

Ellis, R.J., Morgan, P., Weightman, A.J. and Fry, J.C. (2003) Cultivation-dependent and –independent approaches for determining bacterial diversity in heavy-metal-contaminated soil. *Appl. Environ. Microbiol.* 69, 3223-3230.

Embley, T.M., Smida, J. and Stackebrandt, E. (1998). Reverse-trasncriptase sequencing of 16S ribosomal RNA from *Faenia rectivirgula*, *Pseudonocardia hermophila* and *Saccharopolyspora hirsute*, 3 wall type actynomycetes which lack mycolic acids. *J. Gen. Microbiol.* 134, 961-966.

Erbs, J.J., Berquo, T.S., Reinsch, B.C., Lowry, G.L., Banerjee, S.K. and Penn, R.L. (2010) Reductive dissolution of arsenic-bearing ferrihydrite. *Geochim. Cosmochim. Act.* 74, 3382-3395.

Essilfie-Dughan, J., Hendry, J., Warner, J. and Kotzer, T. (2012) Microscale mineralogical characterization of As, Fe, and Ni in uranium mine tailings. *Geochim. Cosmochim. Acta* 96, 336–352

Essilfie-Dughan, J., Pickering, I. J., Hendry, M. J., George, G. N., Kotzer, T. (2011) Molybdenum speciation in uranium mine tailings using X-ray absorption spectroscopy. *Environ. Sci. Technol.* 45, 455−460.

Fahy, A., Ball, A.S., Lethbridge, G., Timmis, K.N. and McGenity, T.J. (2008) Isolation of alkali-tolerant benzene-degrading bacteria from a contaminated aquifer. *Lett. Appl. Microbiol.* 47, 60-66.

Ferris, F.G., Schultze, S., Witten, T.C., Fyfe, W.S and Beveridge T.J. (1989) Metal interaction with microbial biofilms in acidic and neutral pH environment. *Appl. Environ. Microbiol.* 55, 1249-1257.

Fettus, G.H. and McKinzie, M.G. (2012) Nuclear fuel's dirty beginnings: Environmental damage and public health risks from uranium mining in the American west. Natural Resources Defense Council p.1-104.

Fields, M.W., Yan, T., Rhee, S-K., Carroll, S.L., Jardine, P. M., Watson, D.B., Criddle, C.S. and Zhou, J. (2005) Impacts on microbial communities and cultivable isolates from groundwater contaminated with high levels of nitric acid-uranium waste. *FEMS Microbiol. Ecol.* 53, 417-428.

Fierer, N. and Lennon, J.T. (2011) The generation and maintenance of diversity in microbial communities. *Am. J. Bot.* 98, 439-448.

Flemming, H.C. and Wingender, J. (2010) The biofilm matrix. *Nat. Rev. Microbiol.* 8, 623-632.

Foght, J., Aislabie, J., Turner, S., Brown, C.E., Ryburn. J et al. (2004) Culturable bacteria in subglacial sediments and ice from two southern hemisphere glaciers. *Microb. Ecol.* 47, 329–340.

Francis, A.J. (1990) Microbial dissolution and stabilization of toxic metals and radionuclides in mixed wastes. Birkhauser Verlag, CH-4010, Basel/Switzerland, *Experientia* 46, 840-851.

Fredrickson, J.K., Zachara, J.M., Balkwill, D.L., Kennedy, D., Li, S-mei.W., Kostandarithes, H.M., Daly, M.J., Romine, M.F. and Brockman, F.J. (2004) Geomicrobiology of high-level

nuclear waste contaminated vadose sediments at the Hanford site, Washington State. *Appl. Environ. Microbiol.* 70, 4230-4241.

Fredrickson, J.K., Zachara, J.M., Kennedy, D.W., Dong, H., Onstott, T.C., Hinman, N.W. and Li, S-m. (1998) Biogenic iron mineralization accompanying the dissimilatory reduction of hydrous ferric oxide by a groundwater bacterium. *Geochim. Cosmochim. Act*. 62, 3239–3257.

Fukuda, A., Hagiwara, H., Ishimura, T., Kouduka, M., Ioka, S., Amano, Y., Tsunogai, U., Suzuki, Y. and Mizuno, T. (2010) Geomicrobiological properties of ultra-deep granitic groundwater from the Mizunami Underground Research Laboratory (MIU) central Japan. *Microb. Ecol.* 60, 214-225.

Gadd, G.M. (2010) Metals, minerals and microbes: geomicrobiology and bioremediation. *Microbiol.* 156, 609–64 3.

Gavrilescu, M., Pavel, L.V. and Cretescu, I. (2009) Characterization and remediation of soils contaminated with uranium. *J. Hazard Mater* 163, 475-510.

Geesey, G.G., Borch, T. and Reardon, C.L. (2008) Resolving biogeochemical phenomena at high special resolution through electron mincroscopy. *Geobiol.* 6, 263-269.

George, G.N. and Pickering, I.J. (2007) X-ray absorption spectroscopy in biology and chemistry. Brilliant light in life and material sciences. Tsakanov,V., Wiedemann, H. Eds. Springer: Dordrecht, The Netherlands, 2007. Page 97-119.

Gerritse, J. and Gottschal, J.C. (1993) Two-memberred mixed cultures of methagenomic and aerobic bacteria in $O_2$-limited chemostats. *J. Gen. Microbiol*. 139, 1853-1860.

Glenn, T.C. (2011) Field guide to next-generation DNA sequencers. *Mol. Ecol. Resour.* 11, 759-769.

Goh, S.H., Potter, S., Wood, J.O., Hemmingsen, S.M., Reynolds, R.P. and Chow. A.W. (1996) HSP60 gene sequences as universal targets for microbial species identification: studies with coagulase-negative staphylococci. *J. Clin. Microbiol.* 34, 818-823.

Goldstein, I.J. and Hayes, C.E. (1978) The lectins: carbohydrate-binding proteins of plants and animals. *Adv. Carbohydr. Chem. Biochem.* 35, 127-340.

Gomez, M.A., Hendry, M.J., Elouatik, S., Elssifie-Dogan, J. and Paikaray, S. (2014) $Fe(II)_{(aq)}$ uptake of Mg(II)-Al(III)/Fe(III)-$SO_4$/$CO_3$ HTLCs under alkaline conditions: adsorption and solid state transformation mechanisms *RSC Adv.* 4, 54973-54988..

Gomez, M.A., Hendry, M.J., Koshinsky, J., Essilfie-Dughan, J. and Chen, J. (2013) Mineralogical controls on aluminum and magnesium in uranium mill tailings: Key Lake, Saskatchewan, Canada. *Environ. Sci. Technol*. 47, 7883-7891.

Gow, J.A. and Mills, F.H. (1984) Pragmatic criteria to distinguish psychrophiles and psychrotrophs in ecological systems. *Appl. Environ. Microbiol.* 47, 213-215.

Haack, E.A and Warren, L.A (2003) Biofilm hydrous manganese oxyhydroxides and metal dynamics in acid rock drainage. *Environ. Sci. Technol*. 37, 4138-4147.

Haegeman, B., Hamelin, J., Moriarty, J., Neal, P., Dushoff, J. and Weitz, J.S. (2013) Robust estimation of microbial diversity in theory and in practice. *ISME J.* 7, 1092-1101.

Haferburg, G., Merten, D., Buchel, G. and Kothe, E. (2007) Biosorption of metal and salt tolerant microbial isolates from a former uranium mining area. Their impact on changes in rare earth element patterns in acid mine drainage. *J. Basic Microbiol.* 47, 474-484.

Hamady, M., Lozupone, C. and Knight, R. (2010) Fast UniFrac: facilitating high-throughput phylogenetic analyses of microbial communities including analysis of pyrosequencing and PhyloChip data. *ISME* 4, 17–27.

Hamzaoui, A., Mgaidi, A., Megriche, A. and El Maaoui, M. (2002) Kinetic study of goethite from ferrihydrite in alkaline medium. *Ind. Eng. Chem. Res.* 41, 5226-5231.

Handelsman, J., Rondon, M.R., Brady, S.F., Clardy, J. and Goodman, R.M. (1998) Molecular biological access to the chemistry of unknown soil microbes: a new frontier for natural products. *Chem. Biol.* 5, 245-249.

Hansel, C.M., Benner, S.G., Neiss, J., Dohnalkova, A., Kukkadapu, R.K. and Fendorf, S. (2003) Secondary mineralization pathways induced by dissimilatory iron reduction of ferrihydrite under advective flow. *Geochim. Cosmochim. Act*. 67, 2977–2992.

Hazen, C.T., Rocha, A.M. and Techtmann, M.S. (2013) Advances in monitoring environmental microbes. *Curr. Opin. Biotech*. 24, 526-533.

Herbell, M. and Fenforf, S. (2006) Biogeochemical processes controlling the speciation and transport of arsenic within iron coated sands. *Chem. Geol.* 228, 16-31.

Herlihy, A.T. and Mills, A.L. (1985) Sulfate reduction in freshwater sediments receiving acid mine drainage. *Appl. Environ. Microbiol.* 49, 179-186.

Hill, J.E., Goh, S.H., Money, D.M., Doyle, M., Li, A., Crosby, L.W., Links, M., Leung, A., Chan, D. and Hemmingsen, S.M. (2005) Characterization of vaginal microflora of healthy, nonpregnant women by *chaperonin-60* sequence-based methods. *A. J. Obst. Gyn*. 193, 682-692.

Hill, J.E., Penny, S.L., Crowel, K.G., Goh, S.H. and Hemingsen, S.M. (2004) cpnDB: a chaperonin sequence database. *Genome. Res.* 14, 1669-1675.

Hirkala, D.L.M. and Germida, J.J. (2004) Field and soil microcosm studies on the survival and conjugation of *Pseudomonas putida* strain bearing a recombination plasmid, pADPTel. *Can. J. Microbiol.* 50, 595-604.

Hirsch, P.R., Mauchline, T.H. and Clark, I.M. (2010) Culture-independent molecular techniques for soil microbial ecology. *S. Biol. Biochem.* 42, 878-887.

Hitchcock A.P. (2008) aXis2000 is written in Interactive Data Language (IDL) and available free for non-commercial use. Available at http://unicorn.mcmaster.ca/aXis2000.html.

Hitchcock, A.P., Dynes, J.J., Lawrence, J.R., Obst, M., Swerhone, G.D.W., Korber, D.R., and Leppard. G.G. (2009) Soft X-ray spectromicroscopy of nickel sorption in a natural river biofilm. *Geobiol*. 7, 432-453.

Hitchcock, A.P., Morin, C., Zhang, X., Araki, T., Dynes, J., Stover, H., Brash, J., Lawrence, J.R and Leppard, G.G. (2005) Soft X-ray spectromiscroscopy of biological and synthetic polymer systems. *J. Electron. Spectrosc. Relat. Phenom.* 144-147, 259-269.

Hitchcock, A.P., Obst, M., Wang, J., Lu, Y. and Tyliszczak, T. (2012) Advances in the detection of As in environmental samples using low energy X-ray fluorescence in a scanning transmission X-ray microscope: Arsenic immobilization by an Fe(II)oxidizing freshwater bacteria. *Environ Sci Technol* 5, 2821-2829.

Hongoh, Y., Yuzawa, H., Ohkuma, M., Kudo, T. (2003) Evaluation of primers and PCR conditions for the analysis of 16S rRNA genes from natural environment. *FEMS Microbiol. Let.* 221, 299-304.

Hua, X., Dong, D., Ding, X., Yang, F., Jiang, X. and Guo, Z. (2013) Pb and Cd binding to natural freshwater biofilms developed at different pH: the important role of culture pH. *Environ. Sci. Pollut. Res.* 20, 413-420.

Hunter, R.C., Hitchcock, A.P., Dynes, J.J., Obst, M., Beveridge, T.J. (2008) Mapping the speciation of iron in *Pseudomonas aeruginosa* biofilms using Scanning Transmission X-ray Microscopy. *Environ. Sci. Technol.* 42, 8766-8772.

IAEA (International Atomic Energy Agency) (1997) Planning for environmental restoration of uranium mining and milling sites in central and Eastern Europe. IAEA-TECDOC-982, Vienna.IAEA (International Atomic Energy Agency) (2004) The long term stabilization of Uranium mill tailings IAEA-TECDOC-1403, Vienna.

Inskeep, W.P., Macur, R.E., Hamamura, N., Warelow, T.P., Ward, S.A. and Santini, J.M. (2007) Detection, diversity and expression of aerobic bacterial arsenite oxidase genes. *Environ. Microbiol.* 9, 934-943.

Irgens, R.L., Gosink, J. J. and Staley, J.T. (1996) *Polaromonas vacuolata* gen. nov., sp. nov., a psychrophilic, marine, gas vacuolate bacterium from Antarctica. *Int. J. Syst. Bacteriol.* 46, 822–826.

Irisawa, T. and Okada, S. (2009) *Lactobacillus sucicola* sp. nov., a motile lactic acid bacterium isolated from oak tree (*Quercus* sp.) sap. *Int. J. Syst. Evol. Microbiol.* 59, 2662-2665.

Islam, E. and Sar, P. (2011) Culture-dependent and -independent molecular analysis of the bacterial community within uranium ore. *J. Basic Microbiol*. 51, 372–384.

Islam, E., Dhal, P.K., Kazy, S.K. and Sar, P. (2011) Molecular analysis of bacterial communities in uranium ores and surrounding soils from Banduhurand open cast uranium mine, India: A comparative study. *J. Environ. Sci. Health Part A* 46, 271-280.

Islam, F.S., Gault, A.G., Boothman, C., Polya, D.A., Charnock, J.M., Chatterjee, D. and Lloyd, J.R. (2004) Role of metal-reducing bacteria in arsenic release from Bengal delta sediments. *Nat.* 430, 68-71.

Jacobsen, C., Wirick, S., Flynn, G. and Zimba, C. (2000) Soft X-ray spectroscopy from image sequences with sub-100 nm special resolution. *J. Microsc.* 197, 173-184.

Jain, D.K. (1995) Evaluation of semisolid Postgate's B medium for enumerating sulfate-reducing bacteria. *J. Microbiol. Methods* 22, 27-38.

Jambor, J.L. and Dutrizac, J.E. (1998) Occurence and constitution of natural synthetic ferrihydrite a widespread iron oxyhydroxide. *Chem. Rev.* 98, 2549-2586.

Janda, J.M. and Abbott, S.L. (2007) 16S rRNA gene sequencing for bacterial identification in the diagnostic laboratory: pluses, perils, and pitfalls. *J. Clin. Microbiol.* 45, 2761-2764.

Jang, A., Kim, S.M., Kim, S.Y., Lee, S.G. and Kim, I.S. (2001) Effect of heavy metals (Cu, Pb and Ni) on the compositions of EPS in biofilms. *Water Sci. Technol.* 43, 41-48.

Jechalke, S., Franchini, A.G., Bastida, F., Bombach, P., Rosell, M., Seifert, J., von Bergen, M., Vogt, C. and Richnow, H.H. (2013) Analysis of structure, function, and activity of a benzene-degrading microbial community. *FEMS Microbiol. Ecol.* 85, 14-26.

Jenner, G.A., Longerich, H.P., Jackson, S.E. and Fryer, B.J. (1990) ICP-MS-a powerful tool for high-precision trace-element analysis in earth sciences: Evidence from analysis of selected U.S.G.S. reference samples. *Chem. Geol.* 83, 133-148.

Jeon, C.O., Park, W., Ghiorse, W.C. and Madsen, E.L. (2004) *Polaromonas naphthalenivorans* sp. nov., a naphthalene-degrading bacterium from naphthalene-contaminated sediment. *Int. J. Syst. Evol. Microbiol.* 54, 93–97.

Johansson, G.A., Tyliszczak, T., Mitchell, G.E., Keefe, M.H. and Hitchcock, A.P. (2007) Three-dimensional chemical mapping by scanning transmission X-ray spectromicroscopy. *J. Synchrotron Rad.* 14, 395-402.

Jones, B.E., Grant, W.D., Duckworth, A.W. and Owenson, G.G. (1998) Microbial diversity of soda lakes. *Extremophiles* 2, 191-200.

Jones, S.T., Newton, R.J. and McMahon, K.D. (2009) Evidence for structuring of bacterial community composition by organic carbon source in temperate lakes. *Environ. Microbiol.* 11, 2463-2472.

Jose, J., Giridhar, R., Anas, A., Loka Bharathi, P.A. and Nair, S. (2011) Heavy metal pollution exerts reduction/adaptation in the diversity and enzyme expression profile of heterotrophic bacteria in Cochin estuary, India. *Environ. Pollut.* 159, 2775-2780.

Jourabchi, P., Cappellen, P.V. and Regnier, P. (2005) Quantitative interpretation of pH distribution in aquatic sediments: a reaction-transport modeling approach. *Am. J. Sci.* 305, 919-956.

Kampfer, P., Busse, H.J. and Falsen, E. (2006) *Polaromonas* aquatica sp. nov., isolated from tap water. *Int. J. Syst. Evol. Microbiol.* 56, 605–608.

Kawai, J. (2000) Absorption technique in X-ray spectrometry. Encyclopedia of analytical chemistry. Ed. Meyers, Page, 13288-13315.

Keswani, J. and Whitman,W.B. (2001) Relationship of 16S rRNA sequence similarity to DNA hybridization in prokaryotes. *Int. J. Syst. Evol. Microbiol.* 51, 667-678.

Khan, N.H., Bondici, V.F., Medihala, P.G, Lawrence, J.R, Wolfaardt, G.M., Warner, J. and Korber, D.R. (2013) Bacterial diversity and composition of an alkaline uranium mine tailings-water interface. *J. Microbiol.* 51, 558-69.

Kibbe, W.R. (2007) OligoCalc: an online oligonucleotide properties calculator. Nucleic Acids Research 35, Web server issue W43-W46. doi:10.1093/nar/gkm234

Kieber, R.J., Zhou, X. and Mopper, K. (1990) Formation of carbonyl compounds from UV-induced photodegradation of humic substances in natural waters: fate of riverine carbon in the sea. *Limnol. Oceanogr.* 35, 1503-1515.

Kim, S.D., Huizhong, M., Allen, H.E. and Cha, D.K. (1999) Influence of dissolved organic matter on the toxicity of copper to *Ceriodaphnia dubia*: Effect of complexation kinetics. *Environ. Toxicol. Chem.* 18, 2433-2437.

Kimura, M. (1980) A simple method for estimating evolutionary rates of base substitutions through comparative studies of nucleotide sequences. *J. Mol. Evol.* 16, 111-120.

Kraft, T. and Macy, J.M. (1998) Purification and characterization of the respiratory arsenate reductase of Crysiogenes arsenates. *Eur. J. Biochem.* 255, 647-653.

Kwok, A.Y., Su, S.C., Reynolds, R.P., Bay, S.J., Av-Gay, Y., Dovichi, N.J. and Chow, A.W. (1999) Species identification and phylogenetic relationships based on partial HSP60 gene sequences within the genus *Staphylococcus*. *Int. J. Syst. Bact.* 49, 1181-1192.

Landa, E.R. (2004) Uranium mill tailings: nuclear waste and natural laboratory for geochemical and radioecological investigations. *J. Environ. Radioact*. 77, 1-27.

Landa, E.R., Phillips, E.J.P. and Lovley, D.R. (2001) Release of $^{226}$Ra from uranium mill tailings by microbial Fe (III) reduction. *Appl. Geochem.* 6, 647-652

Lawrence, J.R., Chenier, M.R., Roy, R., Beaumier, D., Fortin, N., Swerhone, G.D.W., Neu, T.R. and Greer, C.W. (2004) Microscale and molecular assessment of impacts of nickel, nutrients, oxygen level on structure and function of river biofilm communities. *Appl. Environ. Microbiol.* 70, 4326-4339.

Lawrence, J.R., Korber, D.R., Hoyle, J.W., Costerton, J.W. and Caldwell, D.E. (1991) Optical sectioning of microbial biofilms. *J. Bacteriol.* 173, 6558-6567.

Lawrence, J.R., Swerhone, G.D.W., Dynes, J.J., Korber, D.R. and Hitchcock, A.P. (2014) Soft X-ray spectromicroscopy for speciation, quantification and nano-eco-toxicology of nanomaterials. *J. Microscop*. 00, 1-18.

Lawrence, J.R., Swerhone, G.D.W., Leppard, G.G., Araki, T., Zhang, X., West, M.M. and Hitchcock, A.P. (2003) Scanning Transmission X-ray, Laser scanning, and transmission electron microscopy mapping of the exopolymeric matrix of microbial biofilms. *Appl. Environ. Microbiol.* 69, 5543-5554.

Lear, G., Song, B., Gault, A.G., Polya, D.A. and Lloyd, J.R. (2007) Molecular analysis of arsenate-reducing bacteria within Cambodian sediments following amendment with acetate. *Appl. Environ. Microbiol.* 73, 1041-1048.

Lee, J-U. and Beveridge, T.J. (2001) Interaction between iron and Pseudomonas aeruginosa biofilms attached to Sepharose surface. *Chem. Geol.* 180, 67-80.

Lee, K., Kim, K.W. and Kim, S.K. (2009) Geochemical and microbial effects on the mobilization of arsenic in mine tailings soil. Environ. Geochem. Health 32, 32-44.

Lembre, P., Lorentz, C. and Martino, P.D. (2012) Exopolysaccharides of the biofilm matrix: A complex biophysical world. http://dx.doi.org/10.5772/51213

Lensing, H.J., Vogt, M. and Herrling, B. (1994) Modelling of biologically mediated redox processes in the subsurface. *J. Hydrol.*159, 125-143.

Ley, R.E., Turnbaugh, P.J., Klein, S. and Gordon, J.T. (2006) Microbial ecology: Human gut microbes associated with obesity. *Nature.* 444, 1022-1023.

Li, Y-L., Vali, H., Yang, J., Phelps, T.J. and Zhang, C.L. (2006) Reduction of iron oxides enhanced by a sulfate-reducing bacterium and biogenic $H_2S$. *Geomicrobiol. J.* 23, 103-117.

Lim, C. K. and Cooksey, D.A. (1993) Characterization of chromosomal homologs of the plasmid-borne copper resistance operon of *Pseudomonas syringae. J. Bacteriol.* 175, 4492-4498.

Lin, B., Hyacinthe, C., Bonneville, S., Braster, M., Van Cappellen, P., Wilfred F.M. and Roling, W.F. (2007) Phylogenetic and physiological diversity of dissimilatory ferric iron reducers in sediments of the polluted Scheldt estuary, Northwest Europe. *Environ. Microbiol*. 9, 1956–1968

Links, M.G., Dumonceaux, T.J., Hemmingsen, S.M. and Hill, J.E. (2012) The chaperonin-60 universal target is a barcode for bacteria that enables *de novo* assembly of metagenomic sequence data. *PLoS One* 7, 49755e.

Liu, L., Li, Y., Li, S., Hu, N., He, Y., Pong, R., Lin, D., Lu, L. and Law, M. (2012) Comparison of next-generation sequencing systems. *J. Biomed. Biotech.* doi:10.1155/2012/251364

Liu, W-T., Marsh, T.L., Cheng, H. and Forney, L.J. (1997) Characterization of microbial diversity by determining terminal restriction fragment polymorphisms of genes encoding 16S rRNA. *Appl. Environ. Microbiol*. 63, 4516-4522.

Lloyd, J.R. (2003) Microbial reduction of metals and radionuclides. *FEMS Microbiol. Rev.* 27, 411-425.

Lloyd, J.R. and Gadd, G.M. (2011) The geomicrobiology of radionuclides. *Geomicrobiol. J.* 28, 383–386.

Longerich, H.P., Jenner, G.A., Fryer, B.J. and Jakson, S.E. (1990) Inductively coupled plasma-mass spectrometric analysis of geological samples: a critical evaluation based on case studies. *Chem. Geol.* 83, 105-118.

Lottermoser, B. Mine wastes: Characterization, treatment and environmental impacts. (2007) Springer-Verlag Berlin Heidelberg. 2nd ed., pp. 327-328.

Lovley D.R. (2006) Dissimilatory Fe(III)- and Mn(IV)- reducing prokaryotes. *Prokaryotes* 2, 635-658.

Lovley, D.R and Philips, E.J. (1992) Reduction of uranium by *Desulfovibrio desulfuricans*. *Appl. Environ. Microbiol.* 58, 850-856.

Lovley, D.R. (1995) Bioremediation of organic and metal contaminants with dissimilatory metal reduction. *J. Indust. Microbiol.* 14, 85-89.

Lovley, D.R. and Chapelle, F.H. (1995) Deep subsurface microbial processes. *Rev. Geoph*. 33, 365-381.

Lovley, D.R. and Phillips E.J.P.(1992) Reduction of uranium by *Desulfovibrio desulfuricans*. *Appl. Environ. Microbiol.* 58, 850–856.

Lovley, D.R., Coats, J.D., Woodward, J.C. and Phillips, E.J.P (1995) Benzene oxidation coupled to sulphate reduction. *Appl. Environ. Microbiol.* 61, 953-958.

Lovley, D.R., Phillips, E.J.P., Gorby, Y.A. and Landa, E. (1991) Microbial reduction of uranium. *Nat*. 350, 413–416.

Lovley, D.R., Ueki, T., Zhang, T., Malvankar, N.S., Shrestha, P.M., Flanagan, K.A., Aklujkar, M., Butler, J.E., Giloteaux, L., Rotaru, A.E. et al. (2011) Geobacter: the microbe electric's physiology, ecology, and practical applications. *Adv. Microbiol. Physiol.* 59, 1-100.

Lovley, D.R., Widman, P.K., Woodward, J.C. and Phillips, E.J. (1993) Reduction of uranium by cytochrome C3 of *Desulfovibrio vulgaris*. *Appl. Environ. Microbiol.* 59, 3572–3576.

Lovley, D.R., Woodward, J.C. and Chapelle, F.H. (1994) Stimulated anoxic biodegradation of aromatic hydrocarbons using Fe(III) ligands. *Nat.* 370, 128-131.

Ma,Y., Xue, Y., Grant, W.D., Collins, N.C., Duckworth, A.W., van Steenbergen, R.P. and . Jones, B.E. (2004) *Alkalimonas amylolytica* gen. nov., sp. nov., and *Alkalimonas delamerensis* gen. nov., sp. nov., novel alkaliphilic bacteria from soda lakes in China and East Africa. *Extremophiles* 8, 193–200 .

MacLean, L.C.W., Beauchemin, S., and Rasmussen, P.E. (2010) Application of synchrotron X-ray techniques for the determination of metal speciation in (house) dust particles. In Urban Airborne Particulate Matter: Origins, Chemistry, Fate and Health Impacts.Wiseman, C. L. S., Zereini, F., Eds.,Springer-Verlag, Berlin, p. 193-216.

Mao, C.X. and Colwell, R.K. (2005) Estimation of species richness: Mixture models, the role of rare species, and inferential challenges. *Ecology* 86, 1143-1153.

Marco, P.D., Pacheco, C.C., Figueiredo, A.R. and Moradas-Ferreira, P. (2004) Novel pollutant-resistant methylotrophic bacteria for use in bioremediation. *FEMS Microbiol. Lett.* 234, 75-80.

Margesin, R., Sproer, C., Zhang, D.C. and Busse, H.J. (2012). *Polaromonas glacialis* sp. nov. and *Polaromonas cryoconiti* sp. nov., isolated from alpine glacier cryoconite. *Int. J. Syst. Evol. Microbiol*. 62, 2662-2668.

Masscheleyn, P.H., Delaune, R.D and Patrick, W.H. Jr. (1991) Effect of redox potential and pH on arsenic speciation and solubility in a contaminated soil. *Environ. Sci. Technol.* 25, 1414-1419.

Mattes, T.E., Alexander, A.K., Richardson, P.M., Munk, A.C., Han, C.S., Stothard, P. and Coleman, N.V. (2008) The genome of *Polaromonas* sp. Strain JS666: insights inot the evolution of hydrocarbon- and xenobiotic-degrading bacterium, and features of revelance to biotechnology. *Appl. Environ. Microbiol.* 74, 6405-16.

McFeters, G.A., Yu, F.P., Pyle, B.H., and Stewart, P.S. (1995) Physiological methods to study biofilm disinfection. *J. Indust. Microbiol*. 15, 333-338.

Mellmann, A., Harmsen, D., Cummings, C.A., Zentz, E.B., Leopold, S.R., Rico, A., Prior, K., Szczepanowski, R., Ji, Y., Zhang, W., McLaughlin, S.F. et al. (2011) Prospective genomic characterization of the german enterohemorrhagic *Escherichia coli* O104:H4 outbreak by rapid next generation sequencing technology. *PLoS ONE* 6, e22751

Meng, X., Korfiatis, G.P., Jing, C. and Christodoulatos, C. (2001) Redox transformation of arsenic and iron in water treatment sludge during aging and TCLP extraction. *Environ. Sci. Technol.* 35, 3476-3481.

Mergeay, M., Monchy, S., Vallaeys, T., Auquier, V., Benotmane, A., Bertin, P., Taghavi, S., Dunn, J., van der Lelie, D., Wattiez, R. (2003) *Ralstonia metallidurans*, a bacterium specifically adapted to toxic metals: towards a catalogue of metal-responsive genes. *FEMS Microbiol. Rev*. 27, 385-410.

Miller, C.L., Landa, E.R. and Updegraff, D.M. (1987) Ecological aspects of microorganisms inhabiting uranium mill tailings. *Microb. Ecol.* 14, 141-155.

Mills, A.L., Bell, P.E. and Herlihy, A.T. (1989) Microbes, sediments, and acidified waters: the importance of biological buffering. Microbial interactions in acid stressed aquatic ecosystems. CRC Press, Inc., Boca Raton, Fla., ed. *In* S.S. Rao. p.1-19.

MineWatch Canada (2014) Catastrophic tailings spills at Mount Polley mine. http://www.miningwatch.ca/blog/catastrophic-tailings-spill-mount-polley-mine.

Mitsui, H., Gorlach, K., Lee, H-jin., Hattori, R. and Hattori, T. (1997) Incubation time and media requirements of culturable bacteria from different phylogenetic groups. *J. Microbiol. Methods* 30, 103-110.

Mohapatra, B.R., Dinardo, O., Gould, W.D., Koren, D.W. (2010) Biochemical and genomic facets on the dissimilatory reduction of radionuclides by microorganisms. *Miner. Eng.* 23, 591-599.

Moldovan, B.J., Jiang, D.T. and Hendry, M.J. (2003) Mineralogical characterization of arsenic in uranium mine tailings precipitated from iron-rich hydrometallurgical solutions. *Environ. Sci Technol.* 37, 873– 879

Moldovan, B.J., Jiang, D.T. and Hendry, M.J. (2005) Characterization and quantifying controls on arsenic solubility over a pH range of 1-11 in uranium mill-scale experiment. *Environ. Sci. Technol.* 39, 4913-4.

Moreels, D., Crosson, G., Garafola, C., Monteleone, D., Taghavi, S., Fitts, J.P. and Van der Lelie, D. (2008) Microbial community dynamics in uranium contaminated subsurface sediments under biostimulated conditions with high nitrate and nickel pressure. *Environ. Sci. Pollut. Res. Intern.* 15, 481-491.

Morin, G. and Calas, G. (2006) Arsenic in soils, mine tailings and former industrial sites. *Elements* 2, 97-101.

Mudd, G.M. (2000) Remediation of uranium mill tailings wastes in Australia. Contaminated site remediation; From source zones to ecosystems. In Proceedings 2000 CSRC, Melbourne, Australia, 4-8 December 2000, 777-784.

Muehe, E.M., Scheer, L., Daus, B. and Kappler, A. (2013) Fate of arsenic during microbial reduction of biogenic versus abiogenic As-Fe(III)-mineral coprecipitates. *Environ. Sci. Technol.* 47, 8297-8307.

Muscatello, J.R., Belknap, A. M. and Janz, D.M. (2008) Accumulation of selenium in aquatic systems downstream of uranium mining operation in northern Saskatchewan, Canada. *Environ. Pollut.* 156, 387-393.

Muyzer, G. (1999) DGGE/TGGE a method for identifying genes from natural ecosystems. *Curr. Opin. Microbiol.* 2, 317-322.

Na, H., Kim, O.S., Yoon, S.H., Kim, Y. and Chun, J. (2011) Comparative approach to capture bacterial diversity of coastal waters. *J. Microbiol*. 49, 729-740.

Natural Resources Canada (2004) Energy sector – Uranium/nuclear energy: Tailings management.

Natural Resources Canada (2006) Canada's uranium production and nuclear power. Nuclear Issue Briefing, Paper No. 3. Ottawa, Ontario, Canada.

Neu, R.T., Manz, B., Volke, F., Dynes, J.J., Hitchcock, A.P. and Lawrence, J.R. (2010) Advanced imaging techniques for assessment of structure composition and function in biofilm systems. *FEMS Microbiol. Ecol.* 72, 1-21.

Neu, T., Swerhone, G.D. and Lawrence, J.R. (2001) Assessment of lectin-binding analysis for *in situ* detection of glycoconjugates in biofilm systems. *Microbiol.* 147, 299-313.

Neu, T.R. and Lawrence, J.R (2014) Advanced techniques for the *in situ* analysis of the of the biofilm matrix (structure, composition, dynamics) by means of laser microscopy. Donelli G (ed) Microbial biofilms: Methods and protocols. Vol. 1147, Springer, New York, p. 43-64.

Neu, T.R., Manz, B., Volke, F., Dynes, J.J., Hitchcock, A.P. and Lawrence, J.R. (2010) Advanced imaging techniques for assessment of structure, composition and function in biofilm systems. *FEMS Microbiol. Ecol*. 72, 1-21.

Nevin, K. and Lovley D. (2002) Mechanisms for Fe(III) oxide reduction in sedimentary environments. *Geomicrobiol. J.* 19, 141-159.

Nevin, K.P., Finneran, K.T. and Lovley, D.R. (2003) Microorganisms associated with uranium bioremediation in high-salinity subsurface sediment. *Appl. Environ. Microbiol.* 69, 3672-3675.

Nguyen, H. L., Cao, B., Mishra, B., Boyanovm, M.I., Kenneth, M.K., Fredrickson, J.K. and Beyenal, H. (2012) Microscale geochemical gradients in Hanford 300 area sediment biofilms and influence of uranium. *Water Res.* 46, 227-334.

Nicholas, K.B. and Jr. Nicholas, H.B. (1997) GeneDoc: a tool for editing and annotating multiple sequence alignments. Distributed by the author. www.psc.edu./biomed/genedoc.

Nielsen, M.B., Kjeldsen, K.U. and Ingvorsen, K. (2006) *Desulfitibacter alkalitolerans* gen. nov., sp. nov., an anaerobic, alkalitolerant, sulfite-reducing bacterium isolated from a district heating plant. *Int. J. Syst. Evol. Microbiol*. 56, 2831-2836.

Nies, H.D. (1999) Microbial heavy-metal resistance. *Appl. Microbiol. Biotechnol.* 51, 730-750.

North, N.N., Dollhopf, S.L., Petrie, L., Istok, J.D., Balkwill, D.L. and Kostka, J.E. (2004) Change in bacterial community structure during in situ biostimulation of subsurface sediment cocontaminated with uranium and nitrate. *Appl. Environ. Microbiol.* 70, 4911-4920.

Novitsky, J.A. (1983) Microbial activity at the sediment-water interface in Halifax Harbor, Canada. *Appl. Environ. Microbiol.* 45,1761-1766.

Obst, M., Wang, J. and Hitchcock, A.P. (2009) Soft X-ray spectro-tomography study of cyanobacterial biomineral nucleation. *Geobiol*. 7, 577-591.

Ordonez, E., Letek, M., Valbuena, N., Gil, J.A. and Mateos L.M. (2005) Analysis of genes involved in arsenic resistance in *Corynebacterium glutamicum* ATCC 13032. *Appl. Environ. Microbiol.* 71, 6206-6215.

Oremlad, R.S., Capone, D.G., Stolz, J.F. and Fuhrman, J. (2005) Whither or wither geomicrobiology in the era of 'community metagenomics'. *Nat. Rev*. 3, 572-578.

Oremland, R.S., Stolz, J.F. and Hollibaugh, J.T. (2004) The microbial arsenic cycle in Mono Lake, California. *FEMS Microbiol. Ecol.* 48, 15-27.

Osborne, T.H., Heath, M.D., Martin, A.C., Pankowski, J.A., Hudson-Edwards, K.A. and Santinin, J.M. (2012). Cold-adapted arsenite oxidase from a psychrotolerant *Polaromonas* species. *Metallomics* 5, 318-324.

Osborne, T.M., Jamieson, H.E., Hudson-Edwards, K.A., Nordstrom, D.K., Walker, S.R., Ward, S.A. and Santini, J.M. (2010) Microbial oxidation of arsenite in a subarctic environment: diversity of arsenite oxidase genes and identification of a psychrotolerant arsenite oxidiser. *BMC Microbiol.* 10, 205-513.

Ostlund, P., Carman, R. and Edvardsson, U.G. and Hallstadius, L. (1989) Sterilization of sediments by ionizing radiation. *Appl. Geochem.* 4, 99-103.

Palmer, J.P. Jr. and Sternberg, C. (1999) Modern microscopy in biofilm research: confocal microscopy and other approaches. *Environ. Biotechnol*. 10, 263-268.

Palmisano, A. and Hazen, T. (2003) Bioremediation of metals and radionuclides: what it is and how it works. ed. 2., *LBNL* 42595.

Penner-Hahn, J.E. (1999) X-ray absorption spectroscopy in coordination chemistry. *Coord. Chem. Rev.* 190-192, 1101-1123.

Petrie, L., North, N.N., Dollhopf, S.L., Balkwill, D.L. and Kostka, J.E. (2003) Enumeration and characterization of Iron (III)-reducing microbial communities from acidic subsurface sediments contaminated with uranium (IV). *Appl. Environ. Microbiol.* 69, 467-7479.

Pierce, M.L. and Moore, B.C. (1981) Adsorption of arsenite and arsenate on amorphous iron hydroxide. *Water Res.* 16, 1247-1253.

Pierre, G., Graber, M., Rafiliposon, B.A., Dupuy, C., Orvain, F., De Grignis, M. and Maugard, T. (2012) Biochemical composition and changes of extracellular polysaccharides (2003) produced during microphytobenthic biofilm development (Marennes-Oleron, France). *Microb. Ecol.* 62, 157-69.

Podda, F., Zuddas, P., Minacci, A., Pepi, M. and Baldi, F. (2000) Heavy metal coprecipitaion with hydrozincite $Zn_5(CO3)_2(OH)_6$ from mine waters caused by photosynthetic microorganisms. *Appl. Environ. Microbiol.* 66, 5092-5098.

Postgate, J.R. (1951) The reduction of sulphur compounds by *Desulphovibrio desulphuricans*. *J. Gen. Microbiol.* 5, 725-738.

Pyle, G.G., Swanson, S.M. and Lehmkuhl, D.M. (2002) Toxicity of uranium mine receiving waters to early life stage fathead minnows (Pimephales promelas) in the laboratory. *Environ. Pollut.* 116, 243-255.

Radeva, G. and Selenska-Pobell, S. (2005) Bacterial diversity in water samples from uranium wastes as demonstrated by 16S r DNA and ribosomal intergenic space amplification retrieval. *Can. J. Microbiol.* 51, 910-923

Rastogi, G., Barua, S., Sani, R.K. and Peyton, B.M. (2011) Investigation of microbial populations in the extremely metal-contaminated Coeur d' Alene River sediments. *Microb. Ecol.* 62, 1-13.

Rastogi, G., Osman, S., Vaishmpayan, P.A., Andersen, G.L., Stetler, L.D. and Sani, R.K. (2010) Microbial diversity in uranium mining-impacted soils as revealed by high-density 16S microarray and clone library. *Microb. Ecol*. 59, 94-108.

Ravot, G., Magot, M., Fardeau, M.L., Patel, B.K., Thomas, P., Garcia, J.L. and Olivier, B. (1999) *Fusibacter paucivorans* gen. nov., sp. nov., an anaerobic, thiosulfate-reducing bacterium from an oil-producing well. *Int. J. Syst. Bacteriol.* 49, 1141-1147.

Reed, D.W., Schafer, U.A. and Covello, P.S. (2000) Characterization of the *Brassica napus* extraplastidial linoleate desaturase by expression in *Saccharomyces cerevisiae*. *Plant. Physiol.* 122, 715–720.

Richardson, D.J. (2000) Bacterial respiration: a flexible process for a changing environment. *Microbiol.* 146, 551–571

Riesenfeld, C.S., Schloss, P.D. and Handelsman, J. (2004) Metagenomics: genomic analysis of microbial communities. *Annu. Rev. Genet.* 38, 525-552.

Robinson, C.J., Bohannan, B.J.. and Young, V.B. (2010) From structure to function: the ecology of host-associated microbial communities. *Microbiol. Mol. Biol*. 74, 453-476.

Romero, D. and Palacios, R. (1997) Gene amplification and genomic plasticity in prokaryotes. *Ann. Rev. Genet.* 31, 91-111.

Rothberg, J.M. and Leamon, J.H. (2008) The development and impact of 454 sequencing. *Nature Biotechnol.* 25, 1117-1124.

Rothberg, J.M., Hinz, W., Rearick, T.M., Schultz, J., Mileski, W., Davey, M., Leamon, J.H., Johnson, K., Milgrew, M.J. el al. (2011) An integrated semiconductor device enabling non-optical genome sequencing. *Nature* 475, 348-352.

Roux, S., Enault, F., Bronner, G. and Debroas, D. (2011) Comparison of 16S rRNA and protein-coding genes as molecular markers for assessing microbial diversity (Bacteria and Archaea) in ecosystems. FEMS *Microbiol. Ecol.* 78, 617-628.

Sabry, S.A., Ghozlan, H.A. and Abou-Zeid, D.M. (1997) Metal tolerance and antibiotic resistance patterns of a bacterial population isolated from seawater. *J. Appl. Microbiol.* 82, 245-252.

Sahin, N., Gonzalez, J.M., Iizuka, T. and Hill, J.E. (2010) Characterization of two aerobic ultramicrobacteria isolated from urban soil and description of *Oxalicibacterium solurbis* sp. nov. *FEMS Microbiol. Lett.* 307, 25-29.

Saitou, N. and Nei, M. (1987) The neighbor-joining method: a new method for reconstructing phylogenetic trees. *Mol. Biol. Evol.* 4, 406-425.

Salipante, S., Kawashima, T., Rosenthal, C., Hoogestraat, D.R., Cummings, L.A., Sengupta, D.J., Harkins, T.T., Cookson, T.B. and Hoffman, N.G. (2014) Performance comparison of Illumina and Ion Torrent next-generation sequencing platforms for 16S rRNA-based bacterial community profiling. *Appl. Environ. Microbiol.* 80, 7583-7591.

Saskatchewan Mining Association. (2010 ) Saskatchewan Mining Association Fact Sheet, SMA, Regina, SK, Canada.

Schellenberg, J., Links, M.G., Hill, J.E., Dumonceaux, T.J., Peters, G.A., Tyler, S., Ball, T.B., Severini, A. and Plummer, F.A. (2009) Pyrosequencing of the chaperonin-60 universal target as a tool for determining microbial community composition. *Appl. Environ. Microbiol.* 75, 2889-2898.

Schellenberg, J., Links, M.G., Hill, J.E., Hemmingsen, S.M., Peters, G.A., Dumonceaux, T.J. (2011) Pyrosequencing of chaperonin-60 (cpn60) amplicons as a means of determining microbial community composition. *Methods Mol. Biol*. 733, 143-158.

Schmidt, M., Prieme, A. and Stougaard, P. (2006) Bacterial diversity in permanently cold and alkaline ikaite columns from Greenland. *Extremophiles* 10, 551-562.

Schwertmann, U. and Taylor, R.M. (1989) Iron oxides. In minerals in soil environments, J.B. Dixon and S.B. vol.1, ed. 2 p. 379-438.

Selenska-Pobell, S. (2002) Diversity and activity of bacteria in uranium waste piles, *In*: M.J. Keith-Roach and F.R. Livens (eds.), Interactions of microorganisms with radionuclides*,* Oxford, UK, Elsevier Sciences Ltd., pp. 225-254.

Selenska-Pobell, S., Kampf, G., Hemming, K., Radeva, G. and Satchanska, G (2001) Bacterial diversity in soil samples from two uranium waste piles as determined by rep-APD, RISA and 16S rDNA retrieval. *Anton. Van Leeuwen.* 79, 149–161.

Senko, J.M., Zhang, G., McDonough, J.T., Bruns, M.A. and Burgos, W.D. (2009) Metal reduction at low pH by a *Desulfosporosinus* species: implications for the biological treatment of acid mine drainage. *Geomicrobiol. J.* 26, 71-82.

Sevcik, M. (2003) Report, Uranium Tailings in Kyrgyzstan: Catalyst for cooperation and confidence building. The Nonproliferation Rev., Spring 2003, p.147-154.

Shaw, S.A., Hendry, M.J., Essilfie-Dughan, J., Kotzer, T. and Wallschlager, D. (2011) Distribution, characterization, and geochemical controls of elements of concern in uranium mine tailings, Key Lake, Saskatchewan, Canada. *Appl. Geochem*. 26, 2044-2056.

Shelobolina, E.S., O'Neill, K., Finneran, K.T., Hayes, L.A. and Lovley, D.R. (2003) Potential for *in situ* bioremediation of a low-pH, high-nitrate uranium-contaminated groundwater. *Soil Sediment Contami.* 12, 865-884.

Shokralla, S., Spall, J.L., Gibson, J.F. and Hajibabaei, M. (2012) Next generation sequencing technologies for environmental DNA research. *Mol. Ecol*. 21, 1794-1805.

Shukor, M.Y., Habib, S.H., Rahman, M.F, Jirangon, H., Abdullah, M.P., Shamaan, N.A. and Syed. M.A. (2008) Hexavalent molybdenum reduction to molybdenum blue by *S. marcescens* strain Dr. Y6. *Appl. Biochem. Biotechnol.* 149, 33-43.

Simeonova, D.D., Lievremont, D., Lagarde, F., Muller, D.A., Groudeva, V.I. and Lett, M.C. (2004) Microplate screening assay for the detection of arsenite-oxidizing and arsenate-reducing bacteria. *FEMS Microbiol. Lett.* 237, 249-253.

Simon, C. and Daniel, R. (2011) Metagenomic analyses: past and future trends. *App. Environ. Microbiol*. 77, 1153-1161.

Singleton, R. Jr. (1993) The sulfate-reducing bacteria: an overview, *In:* J.M. Odom and R. Singleton (eds.), The sulfate-reducing bacteria: contemporary perspectives. Springer Verlag, Inc., New York, pp. 1-20.

Siqueira, J.F. Jr., Fouad, A.F. and Rocas, I.N. (2012) Pyrosequencing as a tool for better understanding of human microbiomes. *J. Oral Microbiol.* 4, 10743 - DOI: 10.3402/jom.v4i0.10743.

Sitte, J., Akob, D.M., Kaufmann, C., Finster, K., Banerjee, D., Burkhardt, E.M., Kostka, J.E., Scheinost, A.C., Buchel, G. and Kusel, K. (2010) Microbial links between sulfate reduction and metal retention in uranium- and heavy metal-contaminated soil. *Appl. Environ. Microbiol.* 76, 3143–3152

Sizova, M. and Panikov, N. (2007). *Polaromonas hydrogenivorans* sp. nov., a psychrotolerant hydrogen-oxidizing bacterium from Alaskan soil. *Int. J. Syst. Evol. Microbiol.* 57, 616–619.

Smedley, P.L. and Kinniburgh, D.G. (2002) A review of the source, behaviour and distribution of arsenic in natural waters. *Appl. Geochem.* 17, 517-568.

Sobecky, P.A. and Coombs, J.M. (2009) Horizontal gene transfer in metal and radionuclide contaminated soils. *Methods Mol. Biol.* 532, 455-472.

Somot, S., Pagel, M. and Thiry, J. (1997) Speciation of radium in uranium mill tailings from Ecarpière (Vendée, France). *Comptes Rendus de l'Académie des Sciences, Paris* 325, 111-118

Sorokin, D.Y., Banciu, H., van Loosdrecht, M. and Kuenen, J.G. (2003) Growth physiology and competitive interaction of obligately chemolithoautotrophic, haloalkaliphilic, sulphur-oxidizing bacteria from soda lakes. *Extremophiles* 7, 195–203.

Spring, S. and Rosenzweig, F. (2006) The genera *Desulfitobacterium* and *Desulfosporosinus*: taxonomy. The Prokaryotes. Springer: Berlin, Heidelberg, p. 771–786.

Stackebrandt, E., Schumann, P., Schüler, E. and Hippe, H. (2003) Reclassification of *Desulfotomaculum auripigmentum* as *Desulfosporosinus auripigmenti* corrig., comb. nov. *Int. J. Syst. Evol. Microbiol.* 53, 1439–1443.

Stefanova, V., Kmetov, V. and Canals, A. (2003) Application of internal standardization in ICP-QMS through discrete sample introduction methodologies. *J. Anal. Atom Spectrom.* 18, 1171-1174.

Stolz, F.J., Basu, P., Santini, J.M. and Oremland, R.S. (2006) Arsenic and selenium in microbial metabolism. *Annu. Rev. Microbiol.* 60, 107-130.

Strathmann, M., Wingender, J. and Flemming, H.C. (2002) Application of fluorescently labeled lectins for the visualization and biochemical characterization of polysaccharides in biofilms of *Pseudomonas aeruginosa*. *J. Microbiol. Meth.* 50, 237-248.

Straub, K.L. and Schink, B. (2004) Ferrihydrite reduction by *Geobacter* species is stimulated by secondary bacteria. *Arch. Microbiol.* 182, 175-181.

Stumm.,W. and Sulzberger, B. (1992) The cycling of iron in natural environments: Considerations based on laboratory studies of heterogeneous redox processes. Geochimica Vol. 56. Pergamon Press Ltd. p. 3233-3257.

Sutton, N.B., Kraan, G.M., Loosdrecht, M.C., Muyzer, G., Bruining, J., Schotting, R.J. (2009) Characterization of geochemical constituents and bacterial populations associated with As mobilization in deep and shallow tube wells in Bangladesh. *Water Res*. 43, 1720-1730.

Suzuki, Y. and Suko T. (2006) Geomicrobiological factors that control uranium mobility in the environment: Update on recent advances in the bioremediation of uranium-contaminated sites. *J. Miner. Petro. Sci.* 101, 299-307.

Suzuki, Y., Kelly, S.D., Kemner, K.M. and Banfield, J.F. (2002) Nanometre-sized products of uranium bioreduction. *Nat.* 419, 134. doi:10.1038/419134a

Swash, P.M. and Monhemius, A.J. (1995) Synthesis, characterisation and solubility testing of solids in the Ca-Fe-AsO4 system. Presented at the Sudbury '95, Conference on Mining and the Environment, Sudbury, ON, Canada, 1995.

Swerhone, G.D.W., Lawrence, J.R., Ruchards, J.G. and Hendry, M.J. (1999) Construction and testing of a durable platinum wire Eh electrode for in situ redox measurements in the subsurface. *Ground Water Monit. R*. 19, 132-136.

Takai, Y., Wada, H., Kagawa, H. and Kobo, K. (1974) Microbial mechanism of effects of water percolation on Eh, iron, and nitrogen transformation in the submerged paddy soils. *Soil. Sci. Plant. Nutr*. 20, 33-45.

Tamaki, S. and Frankenberger W.T.Jr. (1992) Environmental biochemistry of arsenic. *Rev. Environ. Contam. Toxicol.* 124, 79-110

Tamura, K., Peterson, D., Peterson, N., Stecher, G., Nei, M. and Kumar, S. (2011) MEGA5: Molecular Evolutionary Genetics Analysis using Maximum Likelihood, Evolutionary Distance, and Maximum Parsimony Methods. *Mol. Biol. Evol.* 28, 2731-2739.

Tan, L., Meesapyodsuk, D. and Qiu, X. (2011) Molecular analysis of Δ6 desaturase and Δ6 elongase from *Conidiobolus obscurus* in the biosynthesis of eicosatetraenoic acid, a ω3 fatty acid with nutraceutical potentials. *Appl. Environ. Microbiol*. 90, 591-60.

Tazaki, K. (2000) Formation of banded iron-manganese structures by natural microbial communities. *Clays Clay Miner.* 48, 511–520.

Templeton, A. and Knowles E. (2009) Microbial transformations of minerals and metals: Recent Advances in Geomicrobiology Derived from Synchtron-Based X-Ray Spectroscopy and X-Ray Microscopy. *Annu. Rev. Earth Planet. Sci*. 37, 367-391.

Thomas, T., Gilbert, J. and Meyer, F. (2012) Metagenomics- a guide from sampling to data analysis. *Microb. Info. Experim.* 2, 3-15.

Thompson, P.A., Kurias, J. and Mihok, S. (2005) Derivation and use of sediment quality guidelines for ecological risk assessment of metals and radionuclides released to the environment from uranium mining and milling activities in Canada. *Environ. Monit. Assess.* 110, 71-85.

Toner, B., Fakra, S., Villalobos, M., Warwick, T. and Sposito, G. (2005) Spatially resolved characterization of biogenic manganese oxides production within bacterial biofilm. *Appl. Environ. Microbiol.* 71, 1300-1310.

Toner, B., Manceau, A., Marcus, M.A., Millet, D.B. and Sposito, G. (2005) Zinc sorption by a bacterial biofilm. *Environ. Sci. Technol.* 39, 8288-8294.

Tufano, K.J. and Fendorf, S. (2008) Confounding impacts of iron reduction on arsenic. *Environ. Sci. Technol.* 42, 4777-4783.

Tuominen, L., Kairesalo, T. and Hartikainen, H. (1994) Comparison of methods for inhibiting bacterial activity in sediment. *Appl. Environ. Microbiol.* 60, 3454-3457.

Tyson, G.W., Chapman, J., Hugenholtz, P., Allen, E.E., Ram, J.R., Richardson, P.M., Solovyev, V.V., Rubin, E.M., Rokhsar, D.S. and Banfield, J.F. (2004) Community structure and metabolism through reconstruction of microbial genomes from the environment. *Nature* 428, 37-43.

Van Geen, A., Rose, J., Thoral, S., Garnier, J.M., Zheng, Y. and Bottero, J.Y. (2004) Decoupling of As and Fe release to Bangladesh groundwater under reducing conditions. Part II: evidence from sediment incubations. *Geochem. Cosmochim. Acta.* 69, 3475-3486.

Vatsurina, A., Badrutdinova, D., Schumann, P., Spring, S.M. and Vainshtein, M. (2008) *Desulfosporosinus hippei* sp. nov., a mesophilic sulfate-reducing bacterium isolated from permafrost. *Int. J. Syst. Evol. Microbiol.* 58, 1228-1232.

Vaxevanidou, K., Papassiopi, N. and Paspaliari, I. (2008) Removal of heavy metals and arsenic from contaminated soils using bioremediation and chelant extraction techniques. *Chemosph.*70, 1329-1337.

Verbeke, T.J., Sparling, R., Hill, J.E., Links, M.G., Levin, D. et al. (2011) Predicting relatedness of bacterial genomes using the chaperonin-60 universal target (cpn60 UT): application to *Thermoanaerobacter* species. *Syst. Appl. Microbiol*. 34, 171-179.

Vrionis, H.A., Anderson, R.T., Ortiz-Bernad, I., O'Neill, K.R., Resch, C.T., Peacock, A.D., Dayvault, R., White, D.C. *et al.* (2005) Microbiological and geochemical heterogeneity in an in situ uranium bioremediation field site. *Appl. Environ. Microbiol.* 71, 6308–6318.

Waggit, P. (1994) A review of worldwide practices for disposal of uranium mill tailings. Thechnical memorandum 48. Australian Government Publishing service Canberra. pp.1-52.

Wagner, D. 2008. Microbial communities and processes in arctic permafrost environments. *In*: P. Dion and S.N. Chandra (ed.), Microbiology of extreme soils. Soil Biology. vol. 13. Springer, Berlin. pp.133-154.

Warren, L.A. and Haack, E.A. (2001) Biogeochemical controls on metal behavior in freshwater environments. *Earth-Sci. Rev.* 54, 261-320.

Waychunas, G.A., Rea, B.A., Fuller, C.C. and Davis, J.A. (1993). Surface chemistry of ferrihydrite: Part1. EXAFS studies of the geometry of coprecipitated adsorbed arsenate. *Geochim. Cosmochim. Acta.* 56, 2251-2269.

Weber, K.A., Achenbach, L.A. and Coates, J.D. (2006) Microorganisms pumping iron: anaerobic microbial iron oxidation and reduction. *Nature Rev. Microbiol.* 4, 752-764.

Weisburg, W.G., Barns, S.M., Pelletier, D.A. and Lane, D.J. (1991) 16S Ribosomal DNA amplification for phylogenentic study. *J. Bacteriol.* 173, 697-703.

Weon, H.Y., Yoo, S.H., Hong, S.B., Kwon, S.W., Stackebrandt, E., Go, S.J. and Koo, B.S. (2008). *Polaromonas jejuensis* sp. nov., isolated from soil in Korea. *Int. J. Syst. Evol. Microbiol.* 58, 1525-1528.

Whiteley, A.S., Jenkins, S., Waite, I., Kresoje, N., Payne, H., Mullan, B., Allcock, R. and O'Donnel, A. (2012) Microbial 16S rRNA Ion Tag and community metagenome sequencing using Ion Torrent (PGM) platform. *J. Microbiol. Meth.* 91, 80-88.

Wilkin, R.T. (2008) Contaminant attenuation processes at mine sites. *Mine. Water Environ.* 27, 251-258.

Willems, A., Busse, J., Goor, M., Pot, B., Falsen, E., Jantzen, E., Hoste, B., Gillis, M., Kersters, K., Auling, G. and De Ley, J. (1989) *Hydrogenophaga*, a new genus of hydrogen-oxidizing bacteria that includes *Hydrogenophaga flava* comb. nov. (formerly *Pseudomonas flava*), *Hydrogenophaga palleronii* (formerly *Pseudomonas pseudoflava* and "*Pseudomonas carboxydoflava*") and *Hydorgenophaga taeniospiralis* (Formerly *Pseudomonas taeniospiralis*). *Int. J. Syst. Bacteriol.* 39, 319-333.

Williams, K.H., Bargar, J.R., Lloyd, J.R., and Lovley, D.R. (2013) Bioremediation of uranium-contaminated groundwater: a systems approach to subsurface biogeochemistry. *Curr. Opin. Biotech.* 24, 489–497.

Wolfaardt, G.M., Hendry, M.J. and Korber, D.R. (2008) Microbial distribution and diversity in saturated high pH, uranium mine tailings, Saskatchewan, Canada. *Can. J. Microbiol.* 54, 932-940.

Wolfaardt, G.M., Lawrence, J.R., Robarts, R.D. and Caldwell, D.E. (1998) *In situ* characterization of biofilm exopolymers involved in the accumulation of chloride organics. *Microb. Ecol*. 35, 213-223.

Wozniak, D.J., Wyckoff, T.J.O., Starkey, M., Keyser, R., Azadi, P., O'Toole, G.A. and Parsek, M.R. (2003) Alginate is not a significant component of the extracellular polysaccharide matrix of PA14 and PAO1 *Pseudomonas aeruginosa* biofilms. *Proceedings of the National Academy of Science* 100, 7907-7912.

Xu, M., Wu, W.M., Wu, L., He, Z., van Nostrand, J.D., Deng,Y., Luo, J., Carley, J., Matthew Ginder-Vogel, M., Gentry, T.J., Gu, B., Watson, D., Jardine, P.M., Marsh, T.L., Tiedje, J.M., Hazen, T., Criddle, C.S., and Zhou, J. (2010) Responses of microbial community functional structures to pilot-scale uranium in situ bioremediation. *ISME* 4, 1060–1070.

Yang, S., Ngwenya, B.T., Butler, I.B., Kurlanda, H. and Elphick, S.C. (2013) Coupled interactions between metals and bacterial biofilms in porous media: implications for bioflm stability, fluid flow and metal transport. *Chem. Geol.* 338, 20-29.

Ye, J., Coulouris, G., Zaretskaya, I., Cutcutache, I., Rozen, S. and Madden, T. (2012) Primer-Blast: A tool to design target-specific primers for polymerase chain reaction. *Bioinformatics* 13,134.

Yergeau, E., Lawrence, J.R., Sanschagrin, S., Roy, J.L., Swerhone, G.D., Korber, D.R. and Greer, C.W. (2013) Aerobic biofilms grown from Athabasca watershed sediments are inhibited by increasing concentrations of bituminous compounds. *Appl. Environ. Microbiol.* 79, 7398-7412.

Yergeau, E., Lawrence, J.R., Sanschagrin, S., Waiser, M.J., Korber, D.R. and Greer, C.W. (2012) Next-generation sequencing of microbial communities in the Athabasca river and its tributaries in relation to oil sands mining activities. *Appl. Environ. Microbiol.* 78, 7626-7637.

Zachara, J.M., Kukkadapu, R.K., Fredickson, J.K., Gorby, Y.A. (2002) Biomineralization of poorly crystalline Fe (III) oxides by dissimilatory metal reducing bacteria (DMRB). *Geomicrobiol. J.* 19, 179-202.

Zavarzina, D.G., Kolganova, T.V., Bulygina, E.S., Kostrikina, N.A., Turova T.P. and Zavarzin, G.A. (2006) *Geoalkalibacter ferrihydriticus*gen. nov. sp. nov., the first alkaliphilic representative of the family *Geobacteraceae*, isolated from a Soda Lake. *Microbiol.* 75, 775-785.

Zeigler, D.R. (2003). Gene sequences useful for predicting relatedness of whole genomes in bacteria. *Int. J. Syst. Evol. Microbiol.* 53,1893-1900.

Zhang, H.B., Yang, M.X., Shi, W., Zheng, Y., Sha, T. and Zhao, Z.W. (2007) Bacterial diversity in mine tailings compared by cultivation and cultivation-independent methods and their resistance to lead and cadmium. *Microb. Ecol.* 54, 705-712.

Zinder, S.H and Salyers, A.A. (2001) Microbial ecology - new directions, new importance. In Bergey's Manual of Systematic Bacteriology. Ed. Boone, D.R., Castenholz, R.W., Garrity, G.M. ed. 2. *Springer*. Vol.1, pp. 101-110.

# 1 Supplemental data

## Table 1.1 Chemical characterization of the water column covering the DTMF.

| Depth (m) | pH | Bicarbonate | Carbonate | Chloride | Specific conductivity | Sum of ions | Nitrate | Calcium | Magnesium | Potassium | Sodium | Sulfate |
|---|---|---|---|---|---|---|---|---|---|---|---|---|
| 1 | 6.54 | 5 | <1 | 12 | 1560 | 1280 | 21 | 325 | 17 | 8.9 | 24 | 890 |
| 6 | 6.41 | 5 | <1 | 12 | 1560 | 1290 | 21 | 328 | 17 | 8.9 | 24 | 900 |
| 11 | 6.19 | 2 | <1 | 13 | 1620 | 1330 | 22 | 335 | 16 | 9.1 | 23 | 930 |
| 16 | 6.46 | 7 | <1 | 14 | 1690 | 1390 | 22 | 358 | 15 | 9.6 | 24 | 960 |
| 21 | 7.08 | 15 | <1 | 17 | 1800 | 1540 | 22 | 395 | 14 | 11 | 27 | 1060 |
| 26 | 6.91 | 15 | <1 | 16 | 1750 | 1470 | 22 | 377 | 15 | 10 | 25 | 1010 |
| 31 | 8.01 | 28 | <1 | 23 | 1970 | 1720 | 18 | 433 | 13 | 14 | 38 | 1170 |
| 36 | 8.98 | 7 | 22 | 40 | 2450 | 2240 | 2.4 | 536 | 12 | 23 | 85 | 1510 |
| 41 | 9.44 | <1 | 36 | 55 | 2790 | 2560 | 1.1 | 541 | 8.3 | 31 | 188 | 1700 |

| Aluminum | Arsenic | Barium | Cobalt | Copper | Iron | Lead | Manganese | Molybdenum | Nickel | Selenium | Uranium | Vanadium | Zinc |
|---|---|---|---|---|---|---|---|---|---|---|---|---|---|
| 0.061 | 18 | 0.028 | 0.5 | 0.095 | 0.0027 | 0.0025 | 1.71 | 0.628 | 2.51 | 0.0079 | 283 | 0.0005 | 0.42 |
| 0.058 | 18 | 0.028 | 0.5 | 0.095 | 0.0025 | 0.0024 | 1.73 | 0.631 | 2.52 | 0.0081 | 276 | 0.0005 | 0.42 |
| 0.23 | 17 | 0.027 | 0.48 | 0.09 | 0.0046 | 0.0039 | 1.68 | 0.666 | 2.36 | 0.0084 | 277 | 0.0008 | 0.39 |
| 0.11 | 16 | 0.027 | 0.44 | 0.065 | 0.0025 | 0.0022 | 1.54 | 0.738 | 2.17 | 0.0085 | 272 | 0.0011 | 0.33 |
| 0.025 | 18 | 0.03 | 0.27 | 0.022 | 0.006 | 0.0007 | 1.12 | 0.933 | 1.42 | 0.01 | 267 | 0.0025 | 0.17 |
| 0.054 | 19 | 0.029 | 0.33 | 0.045 | 0.0047 | 0.0036 | 1.28 | 0.866 | 1.71 | 0.0097 | 259 | 0.0021 | 0.25 |
| 0.14 | 31 | 0.033 | 0.12 | 0.004 | 0.0049 | 0.0013 | 0.69 | 1.25 | 0.703 | 0.01 | 243 | 0.0059 | 0.024 |
| 1.04 | 48 | 0.045 | 0.0073 | 0.0009 | 0.0052 | 0.0017 | 0.11 | 2.22 | 0.08 | 0.012 | 143 | 0.016 | 0.0063 |
| 1.34 | 77 | 0.039 | 0.004 | 0.0007 | 0.0041 | 0.0026 | 0.016 | 3.6 | 0.048 | 0.019 | 63 | 0.036 | 0.0023 |

Measurements were carried out at the time (August, 2011) of biofilm coupon removal. The table is divided into two panels for presentation purposes. Total concentrations of the elements are as mg $L^{-1}$ except for U and As, μg $L^{-1}$. Specific conductivity unit is μS/cm.

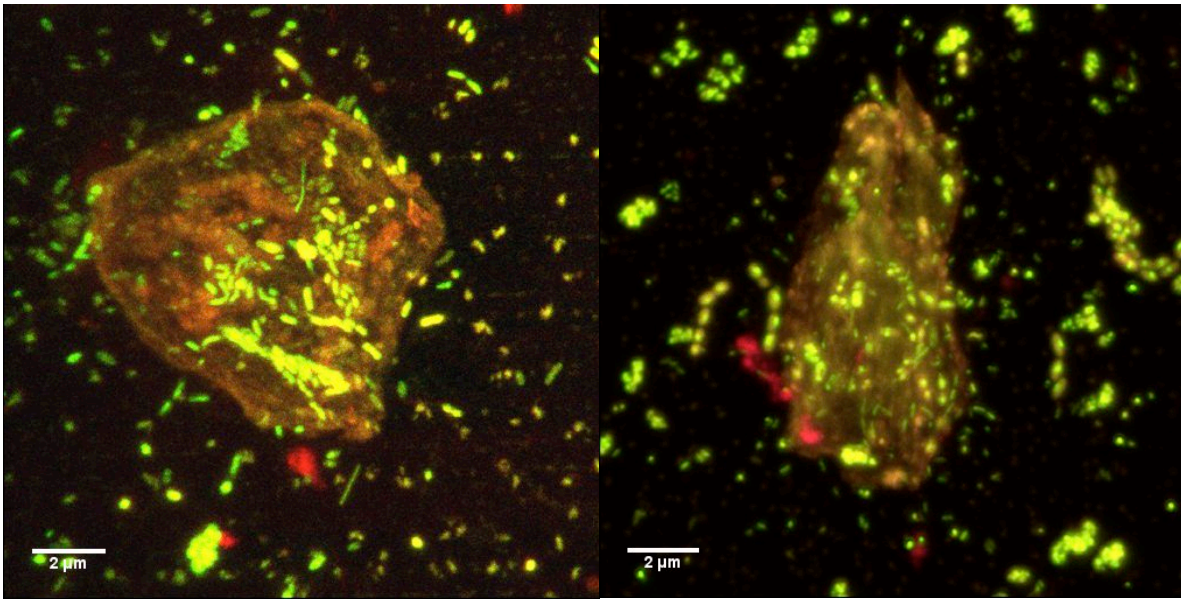


**Figure 9.1 Confocal scanning laser microscope image to indicate bacterial cell attachment onto tailings particles.**
Bacterial cell within the biofilm samples grown at the tailings-water interface was treated with Syto 9.

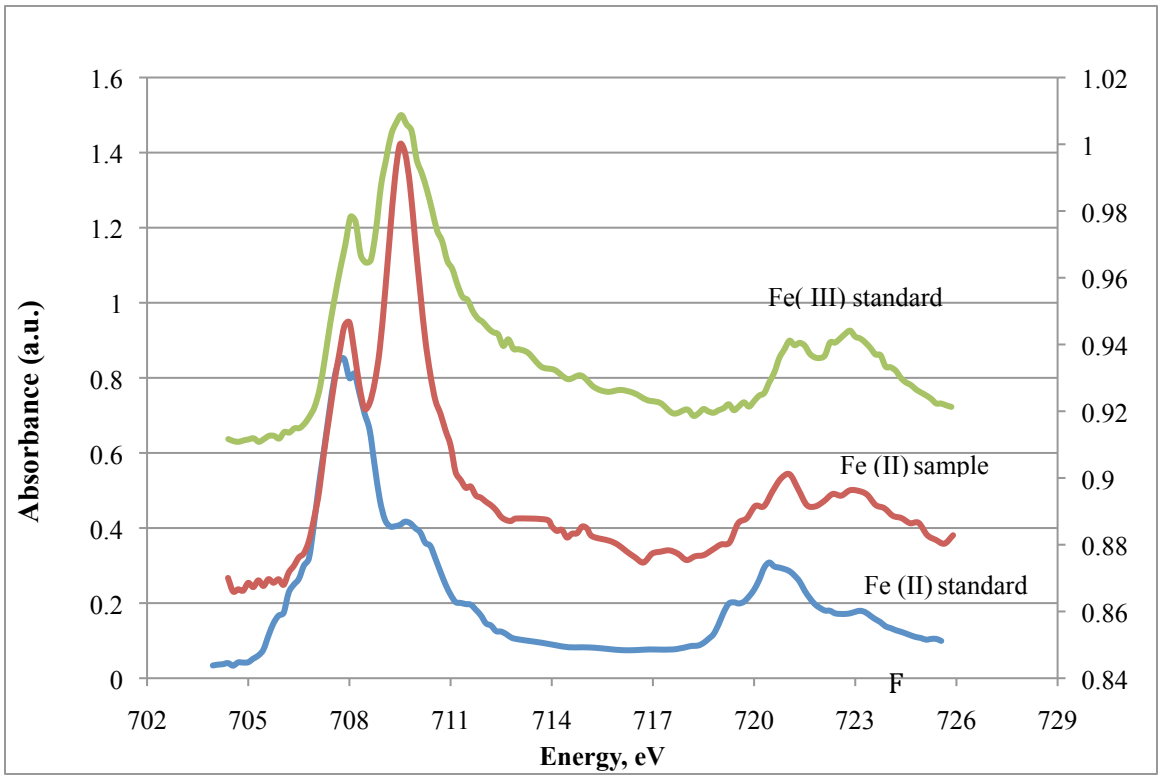


**Figure 9.2 Fe 2p X-ray absorption spectra of $FeCl_2 \bullet 4H_2O$, Fe $Cl_3 \bullet 6H_2O$ standards and Fe (II) rich location in the biofilm sample grown at 1 m depth.**

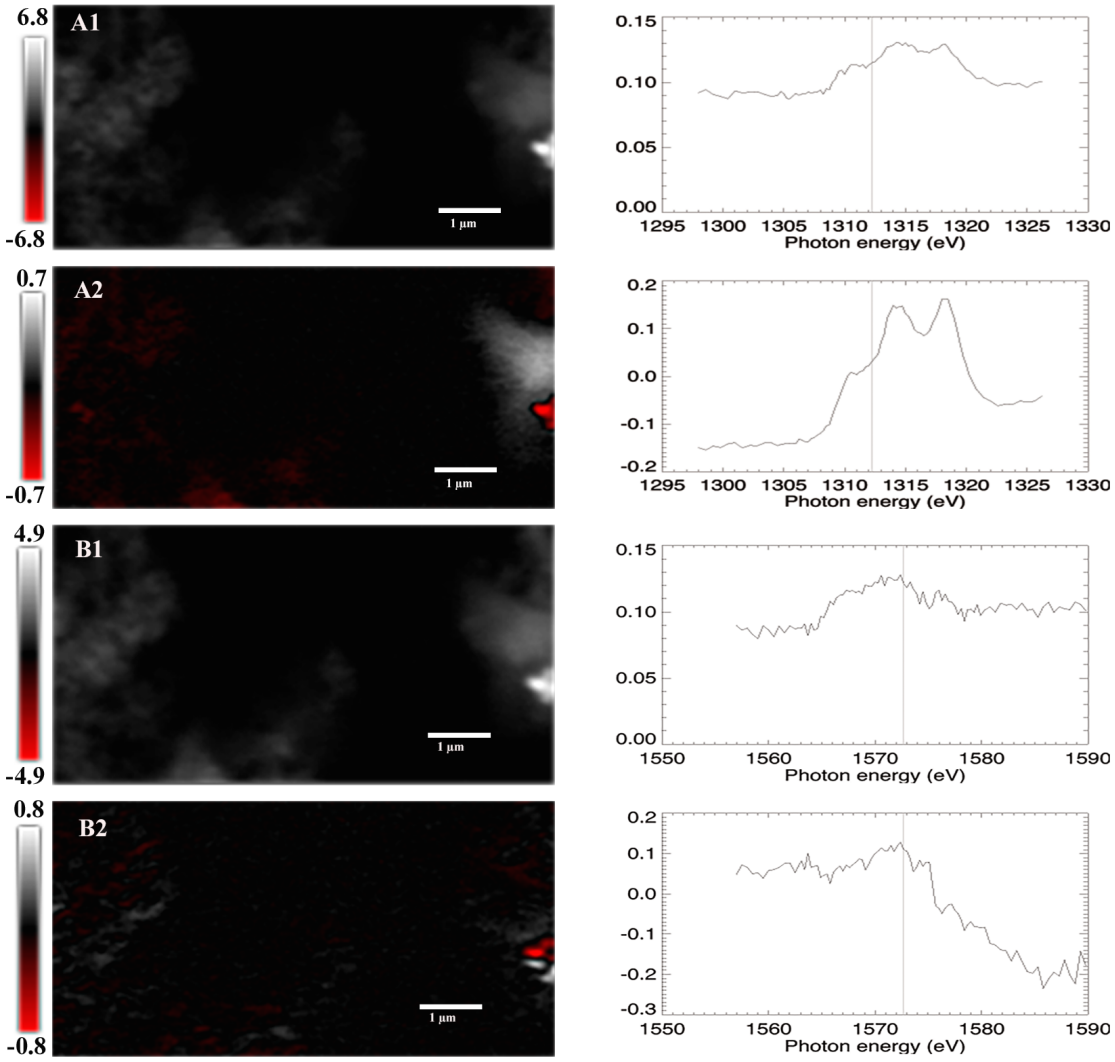


**Figure 9.3 Principle component analyses of energy sequence images (stack) of Mg and Al in a biofilm sample from IF-M1.**

The Mg image stack in (A1, 2) is comprised of 84 images from 1298 eV to 1326 eV, 1 ms per pixel, and 40 nm resolution. The Al stack (B1, 2) is comprised of 89 images from 1557 eV to 1589 eV, 1 ms per pixel and 40 nm resolution. A1 and A2 represent the distribution of Mg and its corresponding potential forms and B1 and B2 represent the distribution of Al forms.

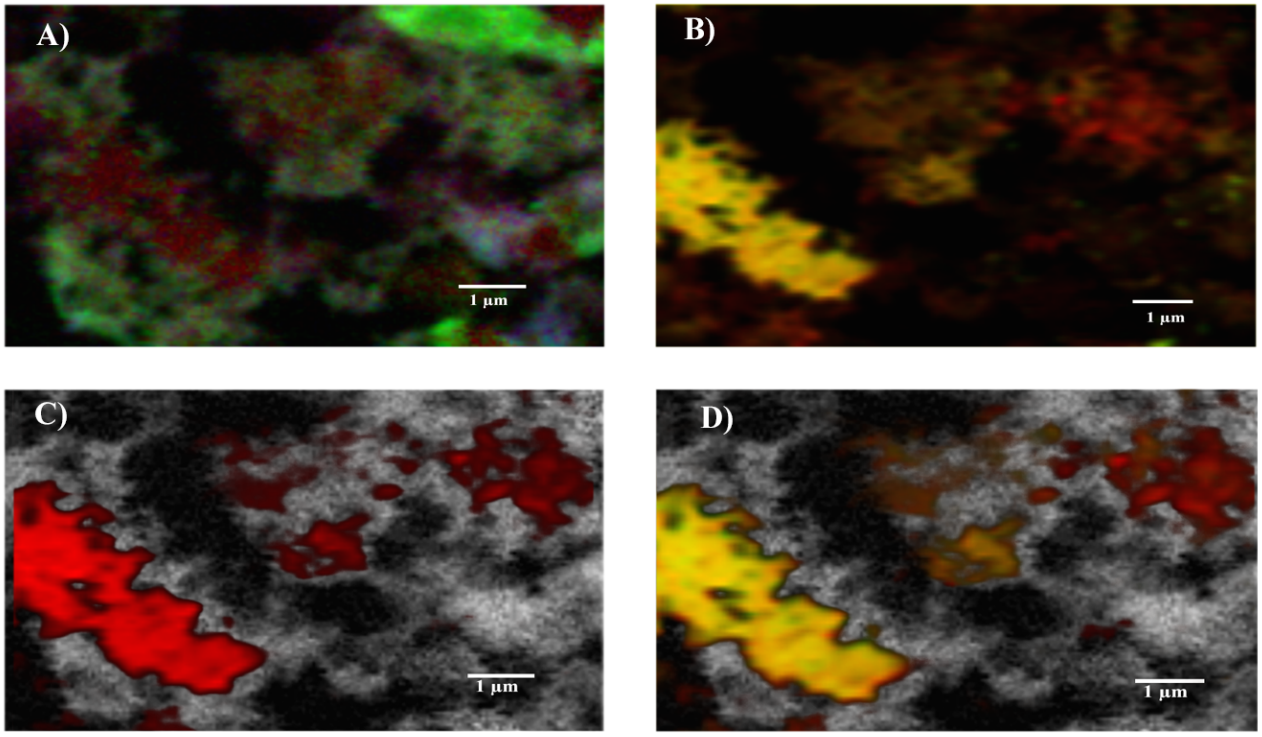


**Figure 9.4 Color-coded composite map of carbon and iron in biofilm samples from IF-M2.** Maps were derived by fitting an energy sequence of images (128 images from 280 to 320 eV, 1 ms per pixel) of C (carbon), protein=red; lipid=green; polysaccharide= blue. B) color-coded composite map derived from Fe image stack (139 images from 699 to 730 eV, 1 ms per pixel) , Fe (II)=red and Fe (III)=green. C) Fe (II)=red superimposed on the biological map (protein composite map). D) Fe color-coded composite map superimposed on the biological map (protein composite map).

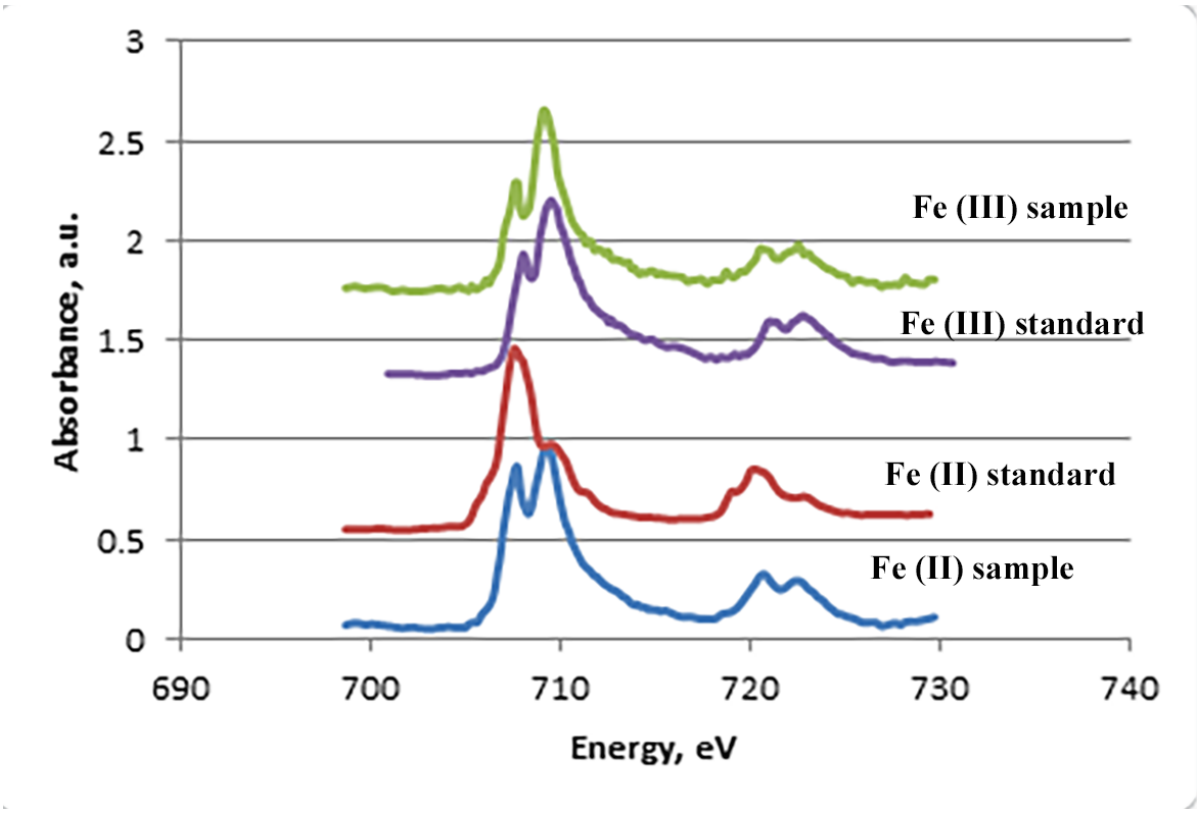


**Figure 9.5 The Fe 2p X-ray absorption spectra of $FeCl_2 \cdot 4H_2O$, $FeCl_3 \cdot 6H_2O$ standards and extracted Fe (II) and Fe (III) spectra of samples from IF-M2.**

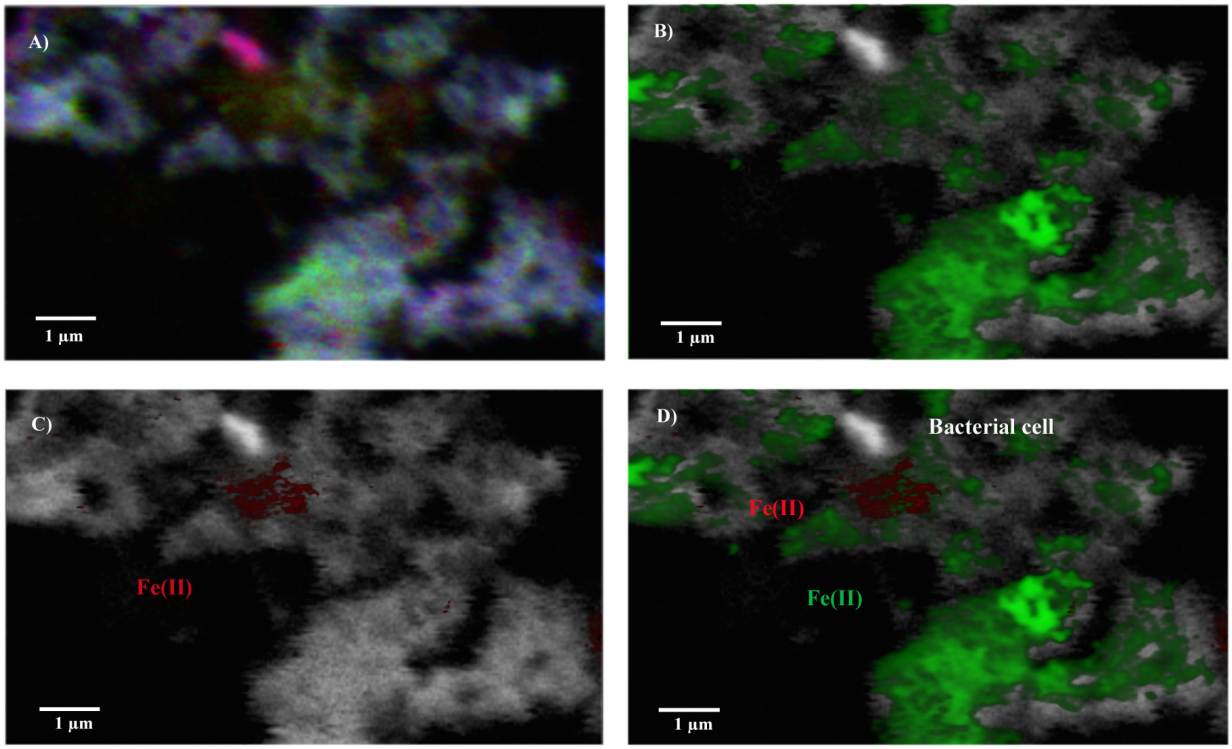


**Figure 9.6 Color-coded composite map of carbon and iron in biofilm samples from CF-M2.** Maps were derived by fitting an energy sequence of images (103 images from 280 to 320 eV; 1 ms per pixel) of C (carbon), protein=red; lipid=green; polysaccharide= blue. B) Fe (III)=green superimposed on the biological map (protein composite map). C) Fe (II)=red composite map superimposed on the biological map (protein composite map). D) color-coded composite map derived from Fe image stack (96 images from 700 to 726 eV, 1 ms per pixel) Fe(II)=red and Fe(III)=green superimposed on the biological map (protein composite map).